UNIVERSITY OF SOUTHAMPTON

FACULTY OF ENGINEERING, SCIENCE & MATHEMATICS

SCHOOL OF CHEMISTRY

Novel Antibiotics From DNA Adenine Methyltransferase Inhibitors

by

Michael David Maynard-Smith

Thesis for the degree of Doctor of Philosophy

September 2009

UNIVERSITY OF SOUTHAMPTON

ABSTRACT

FACULTY OF ENGINEERING, SCIENCE AND MATHEMATICS

SCHOOL OF CHEMISTRY

Doctor of Philosophy

Novel Antibiotics From DNA Adenine Methyltransferase Inhibitors

by Michael David Maynard-Smith

DNA adenine methylation plays a role in several core bacterial processes, including DNA mismatch repair, the timing of DNA replication and gene expression. The dependence of bacterial virulence on the activity of Dam, an adenine methyltransferase, makes it an attractive target for novel antibiotics. Dam from *Yersinia pestis*, the plague causing bacteria, was expressed and purified by nickel affinity chromatography. A plasmid containing the methylation sensitive restriction endonuclease *dpnI* gene was assembled. DpnI was expressed and purified by nickel affinity chromatography. A *Y. pestis* Dam activity assay, which relied on the sensitivity of DpnI to DNA methylation, was developed. This continuous fluorescence based assay was used to determine several kinetic parameters of the enzyme. The assay was validated for use in a high throughput 96-well format and used to screen a library of one thousand compounds for *Y. pestis* Dam inhibitors. Several compounds of interest were identified. These compounds were synthesised, re-tested for activity against Dam, counter-screened against the restriction endonuclease DpnI and assayed for an ability to bind DNA. A plasmid encoding Dam from the hyperthermophile *Pyrococcus horikoshii* was assembled. Wild type *P. horikoshii* Dam was expressed and purified by nickel affinity chromatography. The resultant Dam was contaminated by a product of mis-initiation of translation at an internal methionine codon. Site directed mutagenesis was undertaken to replace the problematic codon in the *dam* gene. Mutant *P. horikoshii* Dam was expressed and purified by nickel affinity chromatography. This hyperthermophilic enzyme was used in the development of a direct and continuous fluorescence based assay for Dam activity. Several kinetic parameters of *P. horikoshii* Dam were determined with the direct assay.

Contents

List of figures

List of tables

List of schemes

List of equations

DECLARATION OF AUTHORSHIP

I, Michael David Maynard-Smith, declare that the thesis entitled 'Novel Antibiotics From DNA Adenine Methyltransferase Inhibitors' and the work presented in it are my own. I confirm that:

- This work was done wholly or mainly while in candidature for a research degree at the University of Southampton.

- Where any part of this thesis has previously been submitted for a degree or any other qualification at this University or any other institution this has clearly been stated.

- Where I have consulted the published work of others, the source is always given. With the exception of such quotations, this thesis is entirely my own work.

- I have acknowledged all main sources of help.

- Where the thesis is based on work done jointly with others, I have made clear exactly what was done by others and what I have contributed myself.

- Parts of this work have been published as:

Wood, R. J., Maynard-Smith, M. D., Robinson, V. L., Oyston, P. C., Titball, R. W., and Roach, P. L. (2007) *PLoS ONE* **2**, e801

Wood, R. J., Mckelvie, J. C., Maynard-Smith, M. D. and Roach, P. L. (2010) *Nucleic Acids Res* **38**, e107

Signed:

Date: September 2009

Acknowledgements

I thank those here mentioned for their contributions towards this work: Project students Claire Williams, Danielle Coomber and Alexandra Stares for their work on the expression and purification of *P. horikoshii* Dam and Montse Shelbourne for her work on the synthesis of potential Dam inhibitors. PhD student Jenny McKelvie for her work on the expression and purification of *P. horikoshii* Dam, Lightcycler experiments and advice. Dr Rohan Ranasinghe for helpful discussions. Dr Robert Wood for his initial work on the *Y. pestis* Dam assay, advice and support in the laboratory and input into many aspects of the project. John Langley and Julie Herniman for the mass spectrometry service and Joan Street and Neil Wells for the NMR service. I also thank those members of the Roach group past and present who have provided me with friendship and support.

I thank Dr. Peter Roach for his supervision during my PhD and help with the writing of this thesis. I am grateful for his enthusiasm and honest, sometimes painfully honest, assessment of my experiments and reports over the past few years. I am also grateful to him for letting me work on what continues to be a very exciting project. I thank Professor Tom Brown for his advice and expertise which has been so helpful and for the high quality oligonucleotides which atdbio have provided. I thank the EPSRC for the PhD funding they have provided.

I would also like to thank my parents, grandparents and wife Rebekah for the support and encouragement that they have given me during my PhD.

Abbreviations

AdoHcy	-	*S*-adenosylhomocysteine
AdoMet	-	*S*-adenosylmethionine
Afu	-	*Archaeolobus fulgidis*
AGE	-	Agarose gel electrophoresis
APS	-	Ammonium persulfate
Arb	-	Arbitrary
BINAP	-	2,2'-bis(diphenylphosphino)-1,1'-binapthyl
bp	-	Base pairs
BSA	-	Bovine serum albumin
Dam	-	DNA adenine methyltransferase
DNA	-	Deoxyribonucleic acid
DTT	-	Dithiothreitol
E. coli	-	*Escherichia coli*
EDTA	-	Ethylenediaminetetraacetic acid
FEP	-	Fluorescence equilibrium perturbation
FRET	-	Förster resonance energy transfer
His	-	Histidine
kDa	-	Kilo Daltons
MDR	-	Multi-drug resistant
MOPS	-	3-(N-Morpholino)propanesulfonic acid
MTase	-	Methyltransferase
NEB	-	New England Biolabs
PCR	-	Polymerase chain reaction
Pfu	-	*Pyrococcus furiosus*
P. horikoshii	-	*Pyrococcus horikoshii*
PMSF	-	Phenylmethylsulfonyl fluoride
PVDF	-	Polyvinylidene fluoride
REase	-	Restriction endonuclease
Rf	-	Retention factor
RFU	-	Relative fluorescence unit
R/M	-	Restriction / modification

SDS-PAGE	-	Sodium dodecyl sulphate polyacrylamide gel electrophoresis
S. typhimuirium	-	Salmonella typhimurium
Taq	-	*Thermus aquaticus*
TEMED	-	N,N,N',N'-Tetramethylethylenediamine
Tris	-	Tris(hydroxymethyl)aminomethane
UDG	-	Uracil-DNA glycosylase
UV	-	Ultraviolet
V. cholerae	-	*Vibrio cholerae*
Xantphos	-	4,5-bis(diphenylphosphino)-9,9-dimethylxanthene
Y. enterocolitica	-	*Yersinia enterocolitica*
Ype	-	*Yersinia pestis*
Y. pestis	-	*Yersinia pestis*
Y. pseudotuberculosis	-	*Yersinia pseudotuberculosis*

Note: Numbering scheme for DNA bases

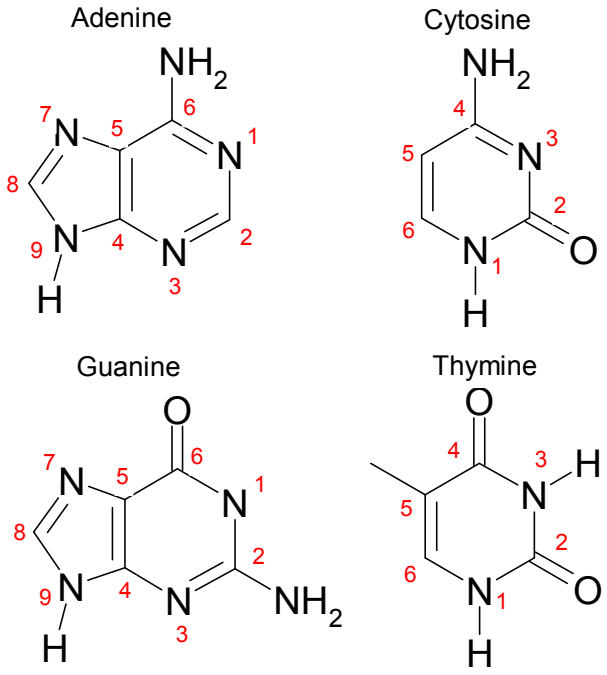

Chapter 1:- Introduction

1.1 DNA methylation and the role of the Dam MTase in bacteria

DNA methyltransferases add extra epigenetic information to DNA by catalysing the transfer of a methyl group from *S*-adenosyl-*L*-methionine to adenine or cytosine bases. Three modifications can be carried out by these methyltransferases (Figure 1.1). Cytosine can be modified at the C5 or N4 positions and adenine at N6 (1,2).

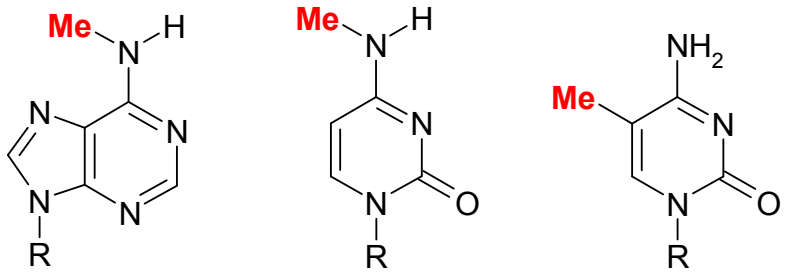

Figure 1.1 The three bases found in DNA which result from methyltransferase activity. N6-methyladenine, N4-methylcytosine and C5-methylcytosine are shown respectively.

All of these sites are in the major groove of B-form DNA, the region where enzymes can most effectively use hydrogen bonding and hydrophobic interactions to recognise the DNA sequence and base modifications (Figure 1.2) (1,3).

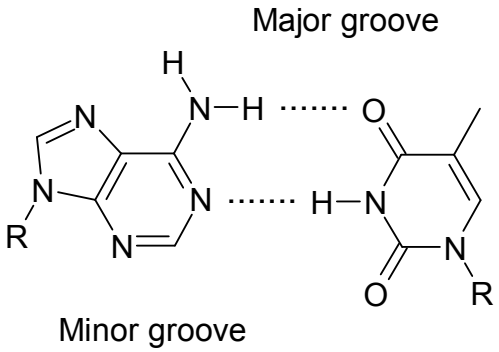

Figure 1.2 An A-T base pair with major and minor groove positions displayed.

Adenine methylation also destabilises DNA and resultant conformational changes to the double helix are recognised by some enzymes (4,5).

DNA adenine methylation is used by some organisms within each of the domains of life, bacteria, archaea and eukaryotes. Within the kingdom animalia, a subdivision of the eukaryotic domain, adenine methylation is absent. Animals instead use methylation of the C5 position of cytosine (1,3,6-8).

Many known adenine MTases form part of a R/M system that allows bacteria to differentiate between self and foreign DNA, whilst others belonging to phage are used to counter this bacterial defence (9). The bacterial 'Dam' MTases, which have similar biochemical properties to the type II MTases from R/M systems, do not have a partner restriction enzyme (1,10). The majority of adenine methyltransferases can be categorised as α, β or γ according to the arrangement of their structural domains (Table 1.1) (11-15). The Dam MTases of *E. coli* and *Y. pestis* are in the α family and methylate adenine in the palindromic sequence GATC (Figure 1.3). The AdoMet binding and catalytic regions contain the conserved amino acid motifs FXGXG and DPPY respectively.

Family	***Arrangement of structural domains (N to C terminus)***		
α	**AdoMet binding region**	**Target recognition region**	**Catalytic region**
β	**Catalytic region**	**Target recognition region**	**AdoMet binding region**
γ	**AdoMet binding region**	**Catalytic region**	**Target recognition region**

Table 1.1 Arrangements of domains for the major groups of N6-adenine MTases.

Adenine methylation is thought to require distortion of the double helix with rotation of the target base about the phosphodiester backbone into the enzyme active site. DNA base flipping has been demonstrated for the HhaI cytosine and M.EcoDam adenine methyltransferases and is also used by other types of DNA-manipulating enzyme

(Figure 1.3) (13,16,17). It has been proposed that base flipping may provide a universal mechanism by which DNA methyltransferases access their target bases (13).

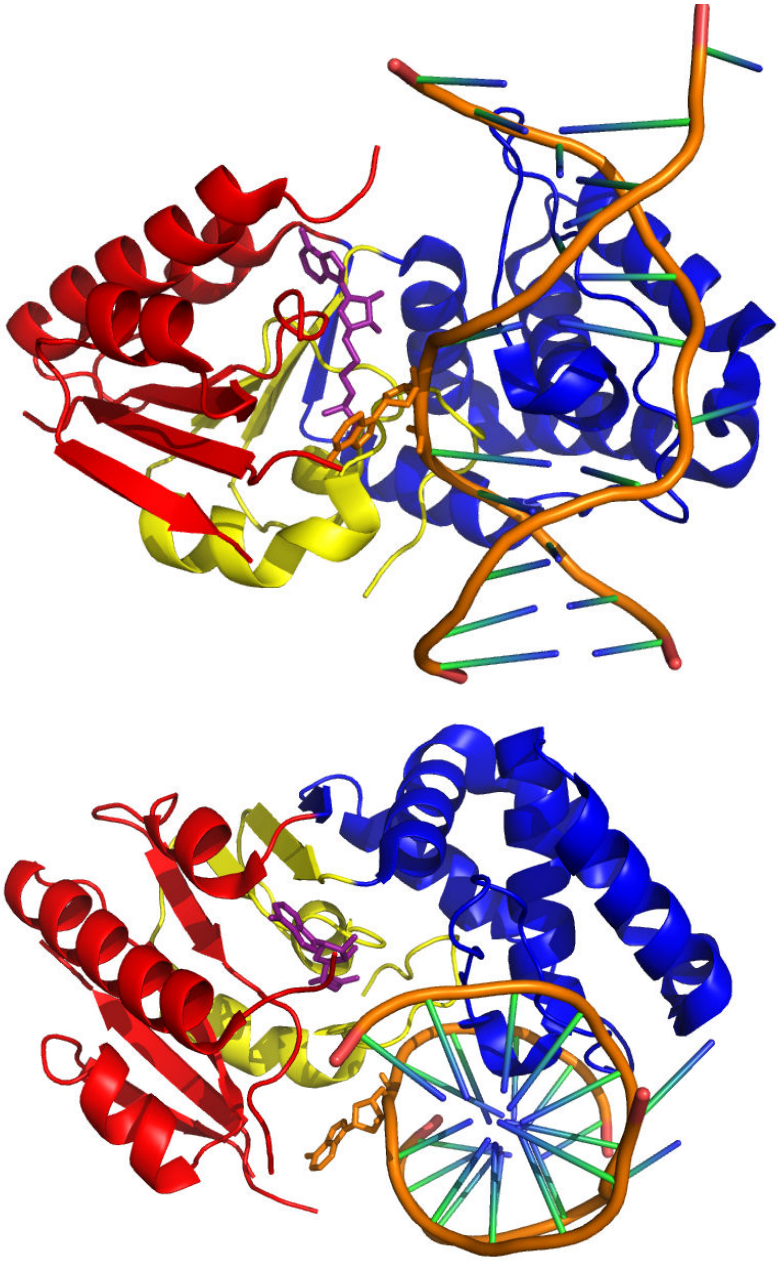

Figure 1.3 X-ray crystal structure of *E. coli* Dam bound to DNA and AdoHcy (purple) shown from two different angles (17). The AdoMet binding region (yellow) can be seen in the centre, harbouring AdoHcy. The target recognition region (blue) can be seen on the right, in close contact with the DNA. The target adenine base (orange) in the DNA is flipped out towards the catalytic region (red).

The lifetime of a DNA base pair is typically in the range of 1-500 ms (1). For an A-T base pair there will be natural periods when the adenine base is partially flipped out of

the double helix. It is believed that M.EcoDam encourages this flipping through the contacts it makes with the DNA backbone and the stabilisation it provides to the adenine base in the flipped conformation via its conserved DPPY motif. Base flipping is therefore promoted by a combination of active and passive means (18).

Methyl transfer to the exocyclic nitrogen of adenine proceeds directly, in an S_N2 reaction without a covalently bound enzyme substrate intermediate (Figure 1.4) (19). The DPPY motif, conserved in the catalytic region of the *E. coli* and *Y. pestis* Dam MTases, helps to negatively polarise the N6 position of the target adenine base, facilitating the nucleophilic attack. Specifically, it is the side chain of the aspartic acid residue and the main chain carbonyl of the first proline residue in the motif which accomplish this via their hydrogen bonds to the amino group. The tyrosine residue of the DPPY motif packs against the target adenine constraining its mobility. It also provides some stabilisation of the cationic transition state through interaction with its π-electrons (1,3). Once released from the enzyme, the methylated adenine can form a normal Watson / Crick base pair with the adjacent thymine base.

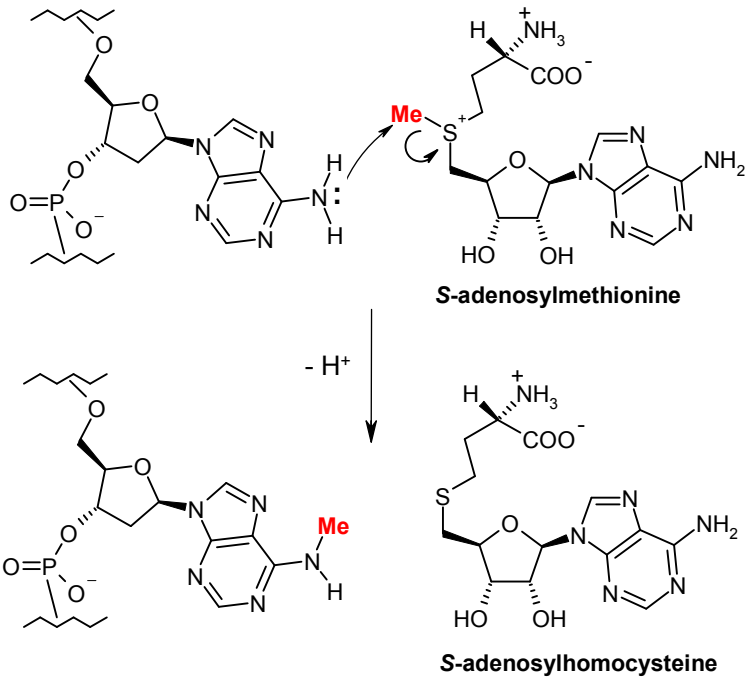

Figure 1.4 Methyl transfer from AdoMet to the exocyclic nitrogen of adenine. The target base is flipped out of the double helix into the enzyme active site. Transfer of the methyl group proceeds via an S_N2 reaction in which AdoMet is converted into AdoHcy.

The order of substrate binding by *E. coli* Dam appears dependant upon experimental conditions. There are literature reports which provide evidence for a DNA first and an AdoMet first order of binding (20,21). Likewise some experiments have shown Dam to be processive whilst others have pointed to a distributive mode of action (20-22). Differences in measured processivity are attributable to the 2-3 bp adjacent to the GATC recognition sequences used in the studies, which affect Dam behaviour (23). In order to effectively participate in DNA repair and gene regulation Dam is required to act both processively and distributively. To efficiently methylate the majority of the 20,000 GATC sites in the *E. coli* genome enzyme processivity is thought to be essential (24). It has been shown that *E. coli* Dam will meet a GATC site ~3000 times following binding to λ-DNA before it dissociates. Since this is a one dimensional random walk along the DNA many GATC sites will be visited on more than one occasion and so this corresponds to methylation of 55 sites prior to dissociation (20). It is likely that *in vivo* the number of sites processively methylated will be lower than this due to displacement of Dam by other DNA binding proteins. By contrast, GATC sites in the *pap* promoter are flanked by sequences which ensure low processivity. This allows differential methylation of the sites which forms the basis of the control mechanism for pilus expression (25). CcrM and M.SssI are two other solitary MTases and have both been shown to act processively (26,27). In contrast, MTases which are part of a R/M system act distributively since this confers maximum protection against invading phage DNA (28,29).

Dam methylation plays a role in several core bacterial processes, including DNA mismatch repair, the timing of DNA replication and gene expression (30-38). Several important *E. coli* genes, the *Yersinia* outer proteins and at least 20 genes in *Salmonella typhimurium* are under its control (39-41). These are described in more detail in the 'Dam and bacterial pathogenesis' section.

During DNA replication the status of GATC sites in the *E. coli* genome changes from fully to hemi-methylated. This is because replication is semi-conservative and adenine introduced into the new DNA strand is unmethylated. In *E. coli* there are an estimated 130 molecules of Dam which re-methylate the hemi-methylated DNA (42). Plasmid DNA can be re-methylated within two to four seconds but chromosomal DNA in slow growing cells requires about a minute (42-44). During this short interval, replication

errors in the nascent strand are repaired. Methylation, or its absence, is the marker which allows the cell's repair apparatus to differentiate between the template and nascent strand. Alteration of Dam activity in bacteria causes an increased rate of spontaneous mutation (45,46). Mutants lacking *dam* and some other genes encoding enzymes involved in DNA repair, for example *recA, B, C, J, ruv* and *lexA*, are not viable (47).

One region of the DNA which keeps its hemi-methylated status for longer is the origin of replication, which has an abundance of GATC sites. Control of the methylation status of these sites is central to the bacterial mechanism for timing DNA replication. The regulatory protein SeqA binds to the hemi-methylated origin of replication and sequesters it, delaying re-methylation. Since hemi-methylated origins of replication are inactive this limits DNA replication to once per cell cycle (48).

Control of genes coding for the Pap pilus proteins in *E. coli* is an example of transcriptional regulation associated with Dam methylation (39,48-50). Conditions within the cell just after DNA replication determine if Dam is able to methylate GATC sites proximal to or distal from the promoter region of the gene operon. The establishment of a methylation pattern locks *pap* operon transcription in the on or off position until the DNA is again replicated. Expression of these *E. coli* pyelonephritis-associated-pilus proteins is an important virulence determinant in urinary tract infections (51).

1.2 Dam and bacterial pathogenesis

Evidence for a relationship between microbial virulence and Dam activity exists for several disease causing bacteria (Table 1.2). In some, including certain *Y. pseudotuberculosis* strains, *Y. enterocolitica* and *V. cholerae*, the *dam* gene is essential for viability (40,52). In others, including *Y. pseudotuberculosis strains, S. typhimurium* and *Y. pestis*, *dam* deficient bacteria are viable but show reductions in virulence of 1 million-fold, 10,000-fold and > 2300-fold respectively (41,53,54). Attenuation was determined for these mutants by comparing the median lethal dose in mice to that of the wild type bacteria.

Altered Dam activity is not universally linked to bacterial attenuation as there are literature examples where this is not the case (55,56). In *E. coli*, whilst there is a demonstrated link between Dam activity and the regulation of *pap* genes known to be required for virulence, there have been no *in vivo* demonstrations of this link. There is however a report that a *dam* deficient mutant of enterohaemorrhagic *E. coli* showed increased adherence to mammalian cells in *vitro* and was capable of colonisation of the mammalian intestine (56).

Alteration of Dam activity in bacteria can also have other problematic consequences. Reduction of Dam activity in enterohaemorrhagic *E. coli* can lead to induction of prophages and an accompanied production of Shiga toxin (57). Shiga toxin invades mammalian cells and attacks ribosomal RNA in a manner similar to ricin toxin (58,59). Both toxins possess RNA *N*-glycosidase activity and remove an adenine base from position 4324 in the 28S ribosomal RNA of eukaryotes, thus inhibiting protein synthesis.

Where there is a link between Dam activity and bacterial virulence there are several possible mechanisms by which the attenuation may be brought about.

In *Salmonella*, many genes with a possible role in virulence are under the control of Dam. It has been shown that 20 genes which are preferentially expressed by *Salmonella in vivo* (mouse) are repressed by active Dam (41). These included four genes, *spvB*, *pmrB*, *mgtA* and *entF*, which have been implicated in virulence. The *spvB* gene encodes an ADP-ribosyltransferase and facilitates growth at sites of systemic infection (60). Gene *pmrB* is involved in resistance of antibacterial peptides and *mgtA* and *entF* are involved in magnesium and iron transport respectively. In their recent review, Marinus and Casadesus list five defects which have been observed in *Salmonella dam* mutants and trace the underlying causes (34). Firstly, murine studies have shown that *dam* mutants have a reduced ability to interact with intestinal epithelial cells (61). The cause is believed to be the inefficient activation of genes, including *hilA*, *hilC*, *invF*, *sipB*, *sipC*, *sicA* and *prgH*, in *S. enterica* pathogenicity island I (SPI-I) (34,62). SPI-I is not activated because of lower levels of transcriptional activator HilD. Expression of this protein appears to be posttranscriptionally and therefore indirectly regulated by Dam

(34). A possible mechanism for this regulation is through the effect of adenine methylation on the production of small non-coding RNA or antisense RNA molecules (34). Secondly, *Salmonella dam* mutants have reduced motility. This is thought to be because of altered expression of flagellar proteins such as *fliC* and *fliD* which interferes with the orderly process of flagellar assembly (62). Thirdly, *Salmonella dam* mutants have an unstable envelope which allows proteins to leak from the cells (63). Envelope instability has been linked to impaired binding of Tol and PAL envelope proteins to the peptidoglycan cell wall and decreased transcription of the gene encoding Braun lipoprotein. The exact mechanism by which the Tol / PAL to peptidoglycan binding process is impaired is not known. Fourthly, fimbrial proteins such as StdA are ectopically expressed in *dam* mutants of *Salmonella* which may stimulate a host immune response (34,64,65). Fifthly, *dam* mutants are more susceptible to bile salts (66). Since bile salts have a detergent activity this property of *dam* mutants is likely linked to their envelope instability (34). Prieto and co-workers have also shown that bile salts induce the SOS response and increase the rate of DNA mutation in *Salmonella* (67). These observations are consistent with a view that bile salts damage *Salmonella* DNA. It has been found that *dam* mutants also lacking the MutHLS methyl-directed mismatch repair system are less sensitive to bile salts. It is thought that in *dam* negative strains, the damage done by bile salts can lead to MutHLS-induced strand breaks as the DNA has no methyl groups to direct the repair process (67).

Pathogenic Bacterium	***Resultant Disease***
Section A	
Actinobacillus actinomycetecomitans (68)	Periodontal infection
Aeromonas hydrophila (69)	Gastrointestinal infection
Bordetella pertussis (70)	Respiratory infection (whooping cough)
‡*Escherichia coli* (51)	Gastrointestinal / urinary tract infections
Klebsiella pneumoniae (71)	Pneumonia
Haemophilus influenzae (72)	Bacteraemia, pneumonia, meningitis
Neisseria meningitides (73)	Meningitis
Pasteurella multocida (46)	Cutaneous infection
Salmonella typhimurium (41,74)	Gastrointestinal infection
Vibrio cholerae (40)	Gastrointestinal infection (cholera)
Yersinia pestis (53,54)	Bubonic and pneumonic plague
Yersinia enterocolitica (52)	Gastrointestinal infection
Yersinia pseudotuberculosis (40) (75)	Gastrointestinal infection
Section B	
# *Shigella flexneri* (55)	Gastrointestinal infection
† *Brucella abortus* (76)	Brucellosis

Table 1.2 Section A: Bacteria whose pathogenicity is linked to Dam activity. Section B: Other pathogenic bacteria of interest. # *Shigella flexneri* showed no significant link between virulence and Dam activity. † *Brucella abortus* virulence is linked to the CcrM adenine methyltransferase. ‡ *E. coli dam* mutants may or may not be attenuated in urinary tract infections, in gastrointestinal infection no attenuation was observed.

In an attenuated *Yersinia pestis dam* mutant it was found that 129 genes had altered expression when compared to the wild type strain. There were 53 genes with reduced expression, none of which were known virulence determinants. Attenuation of *Y. pestis dam* mutants has therefore been attributed to an increased visibility to the immune system caused by the altered gene expression patterns (54).

The precise effects of deleting the *dam* gene vary between bacteria, but the frequent link between its activity and bacterial virulence, coupled with the fact that mammalian cells

exploit cytosine and not adenine methylation, make it an attractive target for novel antibacterial compounds (41,77).

1.3 *Yersinia pestis* and the need for novel antibiotics

Plague has afflicted humans for thousands of years, the earliest record may be the outbreak of 'tumours' amongst the Philistines described in the Old Testament book of Samuel. Three pandemics have occurred since then. First was the Justinian Plague of A.D. 542 which originated in the Egyptian port of Pelusium and spread throughout Europe and the Middle East. Second was the 14th century 'Black Death' or 'Great Mortality', originating in Asia, it spread throughout the entirety of Eurasia. Between 1347 and 1351 a third of the European population, an estimated 24 million people, were killed by the disease (78). The causative agent of plague was identified as the bacillus *Yersinia pestis* by Alexander Yersin during the third pandemic which began in Hong-Kong at the end of the 19th century (Figure 1.5) (79). *Yersinia pseudotuberculosis*, a genetically similar bacteria of the same genus had been identified a decade earlier (80,81). Some have argued that the 14th century outbreak was not due to *Y. pestis* but this minority view is undermined by the presence of *Y. pestis* DNA in the tooth pulp of bodies from 14th century 'catastrophe graves' in southern France (78,82,83).

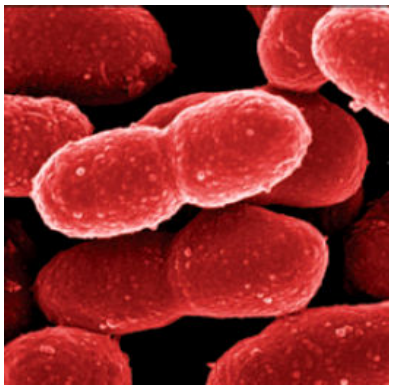

Figure 1.5 A scanning electron micrograph of *Y. pestis* bacteria (84).

Bubonic plague is the most common form of the disease and causes swollen lymph glands, fever, headache and extreme exhaustion. If untreated 50-60 % of bubonic plague victims will die whilst the pneumonic and septacaemic forms are almost always fatal

(85). Standard treatments include the use of streptomycin or gentamicin and have brought this mortality rate down to below 14 % (86).

Plague has not been eradicated in modern times and each year thousands of cases are reported to the World Health Organization (85). Under the right conditions large plague outbreaks still occur. An example is the spike in the number of cases in Asia at the time of the Vietnam War (Figure 1.6).

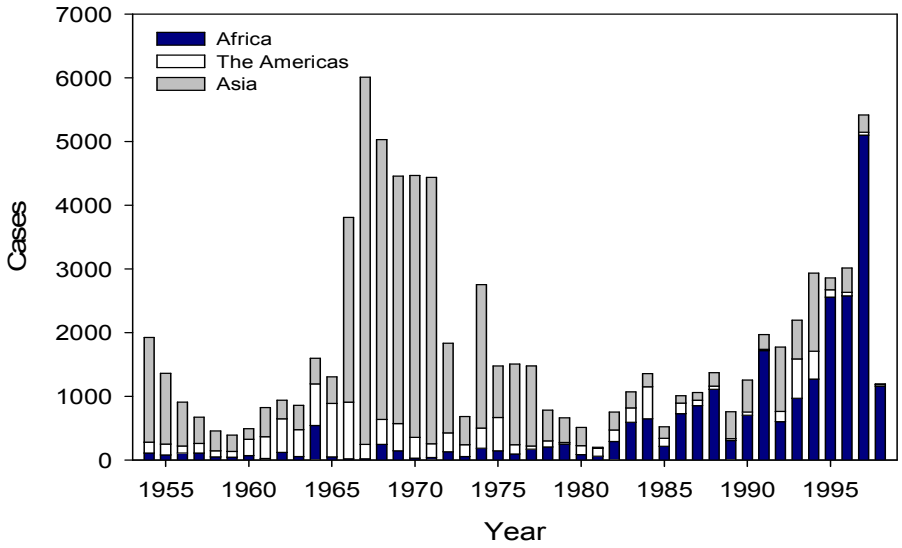

Figure 1.6 Cases of plague reported to the World Health Organisation between 1954 and 1998.

Y. pestis isolates from sufferers are normally susceptible to the antibiotics commonly used against gram-negative bacteria. However, in 1995 *Y. pestis* from a patient in Madagascar was observed to be multi-drug resistant, with decreased susceptibility to chloramphenicol, streptomycin, tetracycline, ampicillin, kanamycin, spectinomycin and minocycline (87). A second strain with resistance to streptomycin was isolated from a patient in another Madagascan district the same year (88). Resistance genes in the MDR-*Y. pestis* were present on a plasmid which could be transferred between bacteria by conjugation (87). Worryingly, there is a large reservoir of such plasmids distributed in MDR zoonotic pathogens associated with agriculture. This increases the chance that such plasmids will again be spread to *Y. pestis* in the future (89). It is the use of antibiotics in animal feed that has made livestock a fertile arena for the selection and maintenance of antibiotic resistance genes (90,91).

The naturally occurring drug resistant plague cases highlight the need to develop new antibacterial agents against *Y. pestis*, but there is another equally strong motivation. *Y. pestis*, possibly modified with antibiotic resistance genes, could be released deliberately as a biological warfare agent (92). This happened during World War II when the Japanese army dropped *Y. pestis* harbouring fleas in China with the aim of causing a plague outbreak. More recently, in the 1970s, the Soviet Union is believed to have weaponised the bacterium (86,93). Today, as a result of internationally accepted conventions banning the use of biological weapons, it seems to be assumed that a deliberate release of plague would most likely be by bio-terrorists (94). Several factors make *Y. pestis* a good candidate for such purposes. Firstly, it is prevalent in nature throughout the world and so could be isolated and grown in a laboratory (82). Secondly, aerosol dispersion could cause the more deadly pneumonic plague, which could then be spread from person to person (86). Thirdly, the dose of *Y. pestis* needed to cause infection is low, between 100 and 500 bacteria (95).

Besides plague a number of other important diseases could potentially be treated with Dam inhibitors and some are worth exploring in greater detail (Table 1.2). *Vibrio cholerae* is responsible for cholera, a disease currently in its seventh pandemic. In 1992 a new epidemic strain, O139, emerged and more recently MDR forms of this strain have been identified (85). Interestingly, this resistance was mediated by a plasmid very similar to the one responsible for the 1995 MDR-*Y. pestis* case in Madagascar (96). Problematic levels of drug resistance have also been observed in uropathogenic *E. coli* and MDR-*Salmonella typhimurium* DT104, which is widespread in cattle throughout the UK and has spread to humans through the food chain (97-99).

1.4 Existent DNA adenine methyltransferase assays

To identify and study Dam inhibitors a good assay, which can be used for high throughput screening and kinetic analysis, is required.

Common assay strategies, suitable for measuring turnover by adenine MTases, can be broadly divided into three types: 1) measurement of the addition of radiolabelled methyl groups onto DNA from [methyl-^{3}H/^{14}C]-AdoMet, 2) measurement of the conversion of

AdoMet to AdoHcy, 3) measurement of the susceptibility of a DNA substrate to cleavage by a restriction enzyme (Figure 1.7).

MTase activity has also been measured by MALDI-TOF mass spectrometry in a multi-step assay (100). A common method used to study MTase DNA interaction, but not turnover, involves 2-aminopurine, a base analogue displaying increased fluorescence when removed from the stacking environment of double helical DNA (101-104). Other methods, used solely for studying C5-cytosine MTases and their products include those based on bisulfite treatment or trapping of the covalent MTase DNA intermediate (105-108). Under certain conditions sodium bisulfite reacts with unmethylated cytosine bases and causes their deamination, thus converting them into uracil bases (105-107). DNA can then be amplified by PCR and sequenced. Only cytosines methylated in the original DNA strand will still appear as cytosines in the sequenced strand.

The first strategy is frequently used to study both adenine and cytosine MTase activity. Methyl groups are transferred by the MTase from [methyl-^{3}H/^{14}C]-AdoMet onto DNA which is the separated from unreacted [methyl-^{3}H/^{14}C]-AdoMet in a purification step. The incorporation of radioactive methyl groups can then be quantitatively determined. Purification procedures vary and can involve binding and washing the DNA on a filter paper (10,109), TLC (110), column chromatography (111) or an affinity tag on the DNA substrate (112). Such assay methods can be time consuming, insensitive to low levels of methylation and do not give real-time data. M.EcoRV adenine MTase activity has been measured with this strategy, employed in a microplate format that exploits biotin-avidin binding (112). Samples containing biotinylated oligonucleotide substrate were taken from MTase assays and added to avidin coated wells. The wells were then washed, the bound DNA released by enzymatic degradation and the radioactivity analysed by liquid scintillation counting. This format does overcome some disadvantages, for example allowing higher throughput, improved sensitivity and the potential for automation. Despite this it is still a multi-step, discontinuous assay with the inherent risks of radioactive materials.

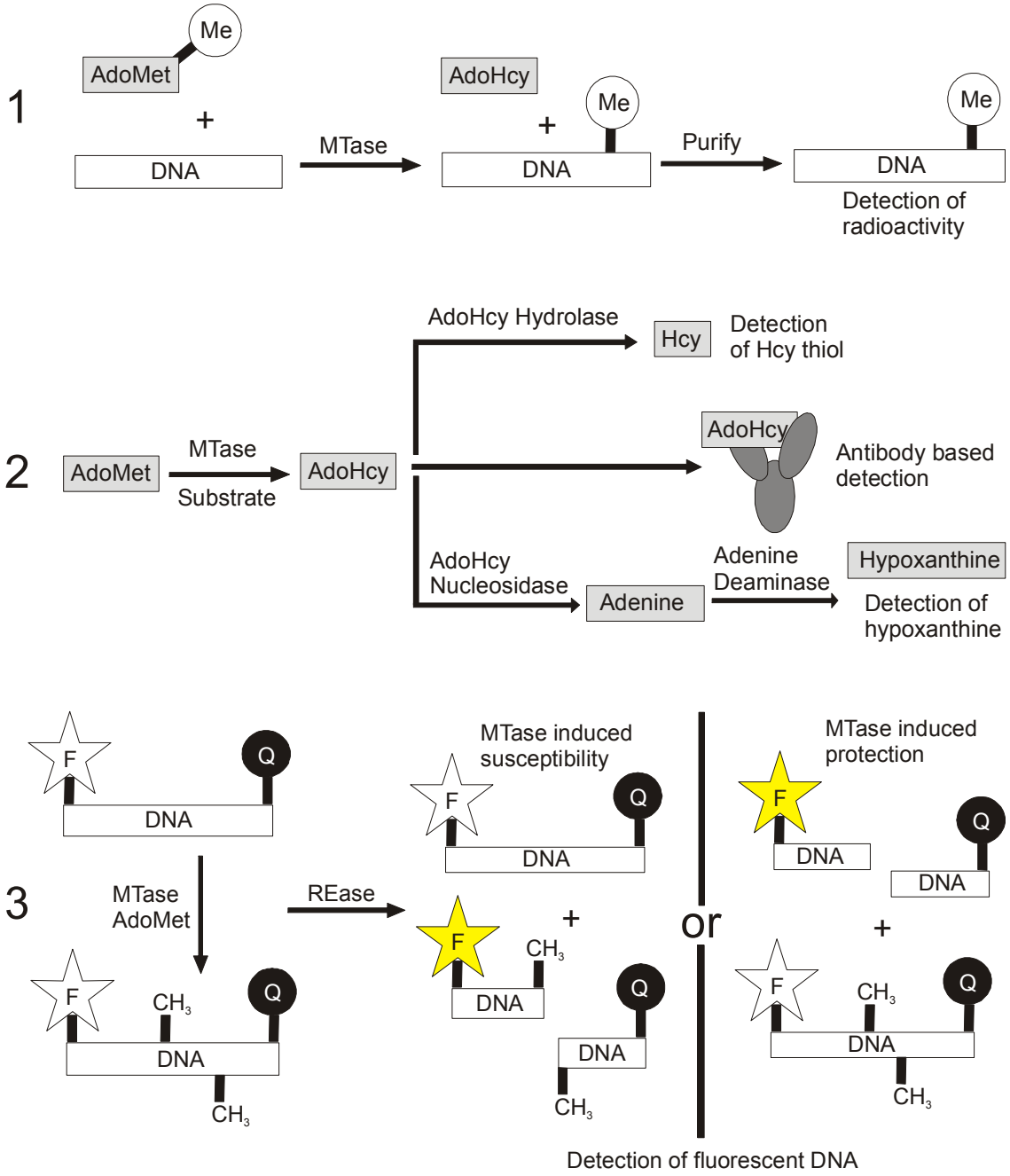

Figure 1.7 Common assay strategies suitable for measurement of adenine MTase activity: 1) measurement of the addition of radioactive methyl groups onto DNA. 2) measurement of the formation of AdoHcy. 3) measurement of the susceptibility of a DNA substrate to cleavage by a REase.

The second strategy, measuring AdoHcy production, was developed as a general way to assay AdoMet-dependent MTases. One such assay, demonstrated with salicylic acid carboxyl MTase, relies on two additional enzymes in solution to convert AdoHcy to

homocysteine. This thiol containing molecule is then quantified colourimetrically with Ellman's reagent (Figure 1.8) (113). Radioactive substrates are dispensed with and end product inhibition by AdoHcy prevented. The assay is however discontinuous and complex, with two enzymatic and one chemical step needed for signal generation. Sensitivity is also low, it has been estimated that only changes in AdoHcy concentration of over 4 μM could be resolved with the assay. This value is based on the typical sensitivity of instruments used to make the necessary absorbance measurements (113).

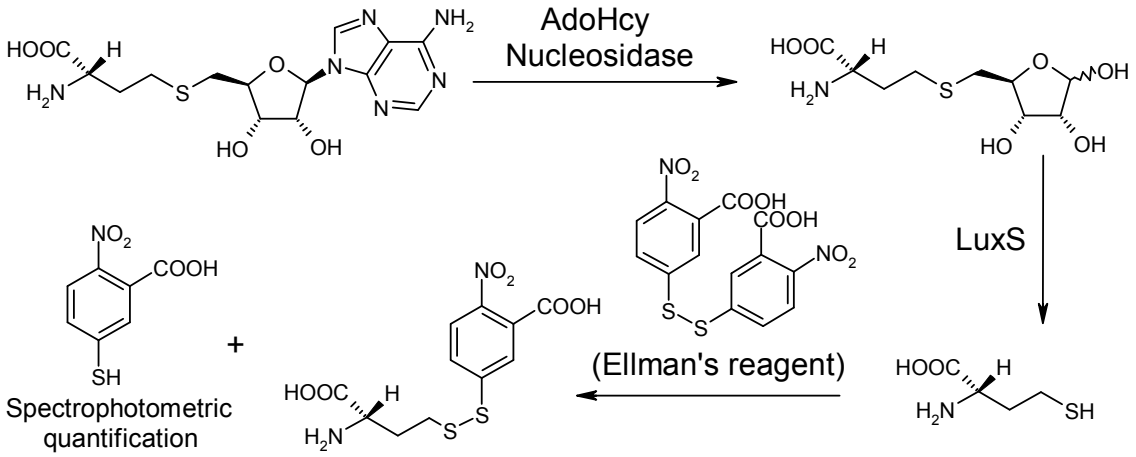

Figure 1.8 The principle of Hendrick's assay for methyltransferase activity. AdoHcy nucleosidase converts Adohcy into *S*-ribosylhomocysteine. Homocysteine is produced from *S*-ribosylhomocysteine by the enzyme LuxS. Homocysteine reacts with 5, 5'-dithiobis-(2-nitrobenzoic acid) (Ellman's reagent) to yield 2-nitro-5-thiobenzoate which can be quantified spectrophotometrically.

Subsequent improvements have simplified the assay to need just one coupling enzyme, *S*-adenosylhomocysteine hydrolase, and increased the sensitivity four fold with the use of a thiol activated fluorescent reporter molecule (Figure 1.9) (114).

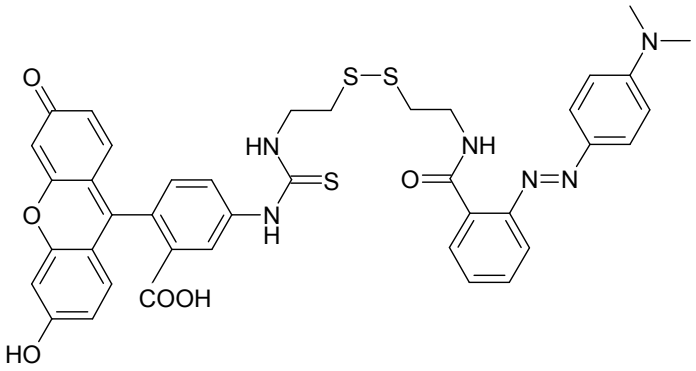

Figure 1.9 A thiol activated reporter molecule containing a FRET pair, fluorescein and methyl red, linked by a disulfide bond. Reaction with AdoHcy breaks the disulfide bond and leads to an increase in fluorescein fluorescence.

A continuous variant of this strategy has also been developed in which two enzymes convert the adenine in AdoHcy into hypoxanthine, a process associated with a decrease in absorbance at 265 nm (Figure 1.7) (115). This assay suffers from low sensitivity which would be accentuated against a background containing DNA which absorbs strongly at ~265 nm. A similar absorbance based assay has been used to measure the conversion of AdoHcy into *S*-inosylhomocysteine by a non-specific deaminase from Aspergillus oryzae (116). In this assay a decrease in absorbance of 0.1, over a path length of 1 cm, required a change in AdoHcy concentration of 11.6 μM. This concentration of a short oligonucleotide substrate would have produced a background absorbance of approximately 1. Such absorbance based assays therefore produce a signal which is approximately 10 % of the background. A different variation of the strategy relies on competition between AdoHcy produced by the MTase and a tracer AdoHcy-fluorescein conjugate for AdoHcy specific antibodies. MTase generated AdoHcy displaces the tracer AdoHcy-fluorescein conjugate from the antibodies, resulting in a measurable decrease in fluorescence polarisation (117). This antibody method improves sensitivity and can still be carried out in microplate format. It is however discontinuous and a way to terminate MTase activity, without affecting subsequent AdoHcy antibody interactions, is required. High AdoMet concentrations have also been shown to interfere with results. This interference is due to the slight affinity of AdoMet, which is structurally similar to AdoHcy, for the antibodies.

Strategy three often involves an oligonucleotide, labelled with a fluorphore and quencher, that is rendered susceptible to or protected from a restriction endonuclease by the action of a DNA MTase (118). Cleavage by the REase separates the fluorophore and quencher giving rise to a fluorescence increase. This protection assay format has been used to screen large compound libraries for Dam inhibitors and an ELISA based variant to study cytosine and other adenine MTases (77,119). Such methods are discontinuous, involving multiple steps but do avoid radioactive substrates, are highly sensitive and can be used for a variety of methyltransferases, even without cognate restriction enzymes. More recently, methylation induced REase susceptibility has formed the basis of a sensitive, continuous, coupled enzyme assay for Dam activity (120). This relied on the ability of DpnI to preferentially cut the Dam recognition sequence GATC when fully methylated (121,122). REases specific for m6A / m4C / m5C containing DNA are rarer than those whose activity is blocked by methylation. Consequentially, whilst being good for studying Dam, such continuous assays may be unsuitable for other important MTases. Despite this, as REases with new recognition sequences and methylation sensitivities are found, the scope of these continuous assays will increase. A recently introduced methylation sensitive restriction enzyme is GlaI. This enzyme has permitted the development of a robust continuous assay for the important cytosine MTase Dnmt1 (123,124). In the assay Dnmt1 adds one extra methyl group to an oligonucleotide producing a tetramethylated sequence that is recognised and cleaved by GlaI.

1.5 DNA adenine methyltransferase inhibitors

As with all antibiotics the current adenine MTase inhibitors, none of which are in clinical use, can be divided into two types, natural and synthetic.

Known natural adenine MTase inhibitors include the by-product of methylation *S*-adenosylhomocysteine and sinefungin, a molecule isolated from *Streptomyces griseolus* (Figure 1.10, Figure 1.11) (125).The K_i for these two molecules measured with the EcoRI adenine MTase was 10 μM and 9 nM respectively (109). Both of the compounds are analogues of the *S*-adenosylmethionine substrate and target its binding pocket. As a consequence they inhibit a broad range of MTases. Sinefungin in particular has toxic effects in mammals making it unsuitable for clinical use (77).

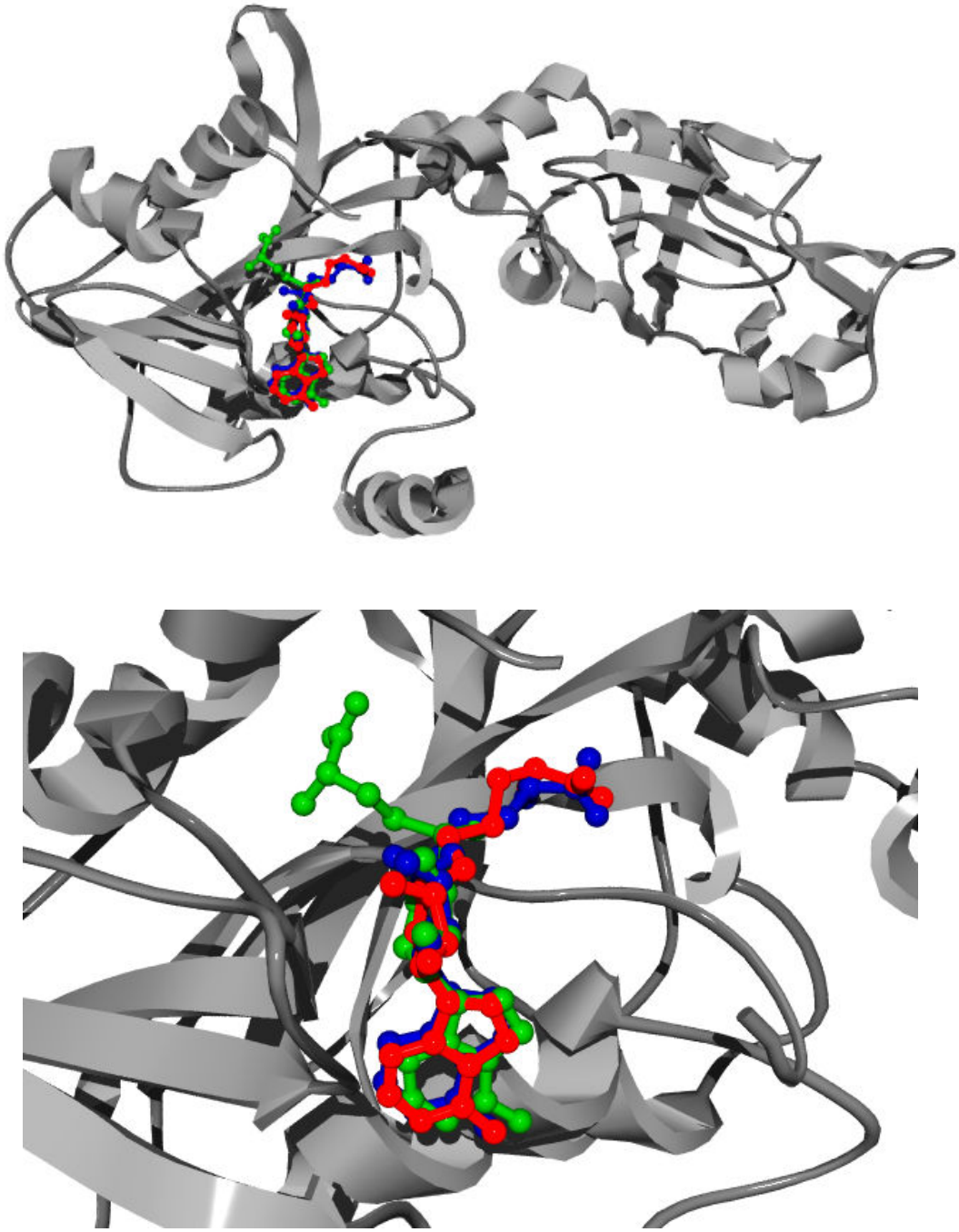

Figure 1.10 A composite of three X-ray crystal structures showing the orientation of AdoMet (green), AdoHcy (red) and sinefungin (blue) in the active site of the M.TaqI adenine methyltransferase (126). The whole enzyme and a close up of the Adomet binding pocket are shown in the upper and lower panels respectively.

There are reports of other synthetic *S*-adenosylhomocysteine analogues which can inhibit and activate DNA MTases but they too appear to be non-specific (127) (Figure 1.11).

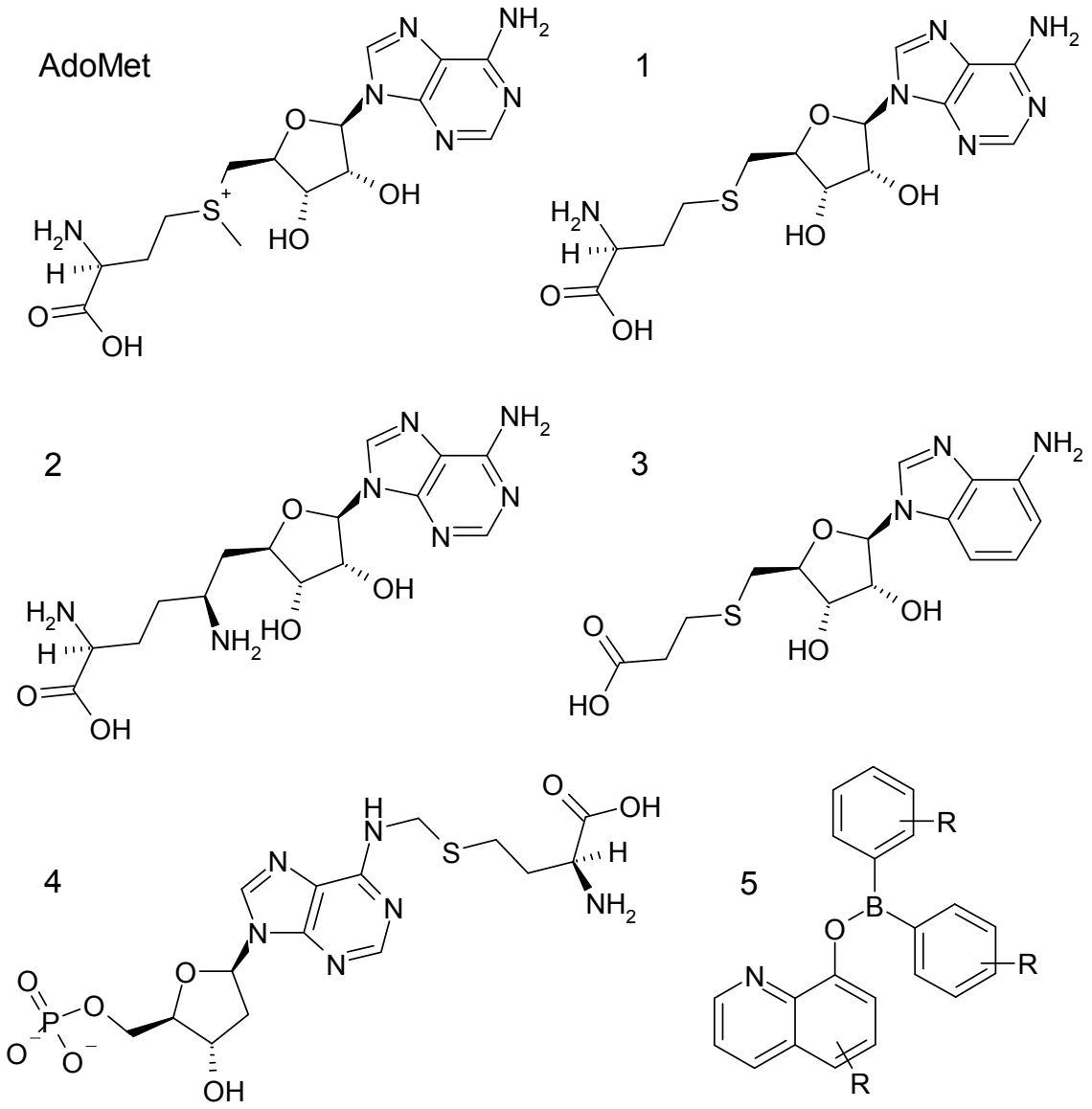

Figure 1.11 Compounds which interact with adenine methyltransferases: **AdoMet**, the natural substrate; **1**, (AdoHcy) the by-product of methylation and a known inhibitor; **2**, (sinefungin) a known inhibitor; **3**, (5'-S-(Propionic acid)5'-deoxy-9-(1'-β-D-ribofuranosyl)1,3-dideaza adenine) an apparent MTase activator (127); **4**, one of the bi-substrate inhibitors with a preference for adenine MTases designed by Benkovic and co-workers (128); **5**, core structure of the borinic ester, adenine MTase specific, inhibitors developed by Benkovic and co-workers (129).

To try and achieve selectivity, Benkovic and co-workers produced a number of rationally designed bi-substrate mimics. These incorporated a deoxyadenosine nucleotide with amino and carboxylic acid groups tethered onto the N6 position via a sulphur atom (compound 4, Figure 1.11). The deoxyadenosine was designed to mimic

the target adenine base in DNA whilst the amino and carboxylic groups sat in the AdoMet binding pocket. Such molecules were selective for the adenine MTase CcrM over the cytosine MTase HhaI (128). Benkovic's group went on to create and screen a combinatorial library of molecules based on this lead structure and identified borinic esters as potent Dam inhibitors (129) (compound 5, Figure 1.11).

Using a high throughput screening approach on a diverse compound library Mashoon and co-workers identified five novel classes of Dam inhibitor (Figure 1.12). These classes displayed a variety of inhibition modalities and several examples from each were found to be selective for Dam over Dnmt1, a cytosine MTase found in mammals (77).

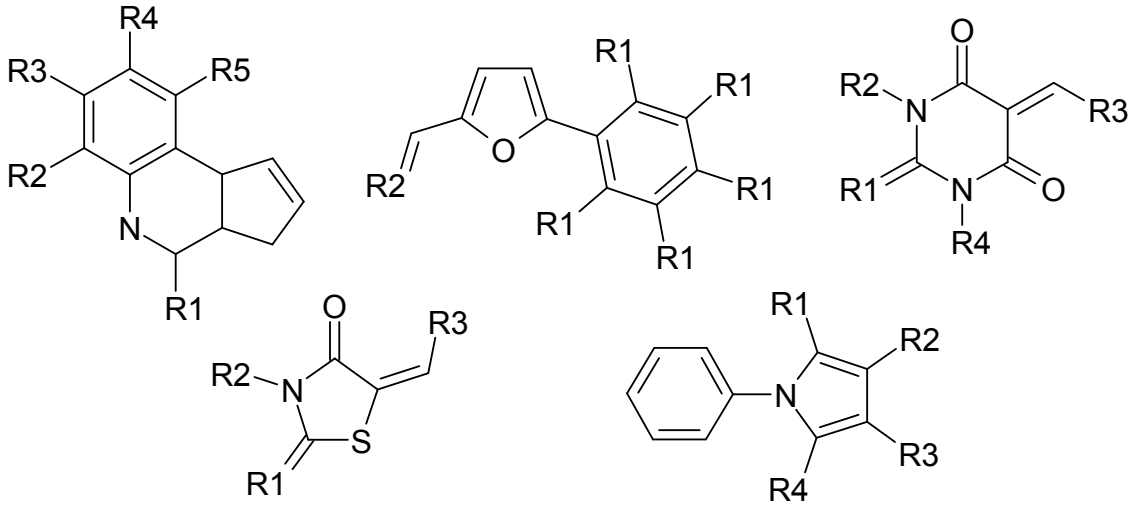

Figure 1.12 The five classes of Dam inhibitor identified by Mashoon and co-workers.

1.6 Summary and conclusions

Novel antibacterials effective against *Y. pestis* are required. Thousands of cases of plague occur annually and multi-drug resistant strains have been observed. *Y. pestis* could potentially be used as a biological weapon due to its availability, infectivity and high fatality rate.

Dam is an adenine methyltransferase with a key regulatory role in bacteria. *Y. pestis* Dam represents an attractive target for novel antibiotics because of its proven link to

virulence, absence in humans and wider distribution in other pathogenic gram-negative bacteria.

There exist a number of assays which could be used to monitor Dam activity but many rely on radioactivity and none are truly real-time. To facilitate the identification and characterisation of *Y. pestis* Dam inhibitors, the first requirement is a new Dam assay, amenable to high throughput screening and in depth kinetic analysis. The development of this assay and its application to finding and characterising new Dam inhibitors has been the focus of my research within the Roach group.

1.7 References

1. Dryden, D. T. F. (1999) Bacterial DNA Methyltransferases. In: Cheng, X., and Blumenthal, R. M. (eds). *S-Adenosylmethionine-Dependent Methyltransferases: Structures and Functions*, World Scientific, Singapore, New Jersey, London, Hong Kong
2. Dunn, D. B., and Smith, J. D. (1958) *Biochem J* **68**, 627-636
3. Jeltsch, A. (2002) *Chembiochem* **3**, 275-293
4. Guo, Q., Lu, M., and Kallenbach, N. R. (1995) *Biochemistry* **34**, 16359-16364
5. Bae, S. H., Cheong, H. K., Cheong, C., Kang, S. H., Hwang, D. S., and Choi, B. S. (2003) *J Biol Chem* **278**, 45987-45993
6. Bheemanaik, S., Reddy, Y. V. R., and Rao, D. N. (2006) *Biochem J* **399**, 177-190
7. Koike, H., Katsushi, Y., Tsuyoshi, K., Tomoko, Y., Shin-ichi, M., Lester, C., and Masashi, S. (2005) *Proc Jpn Acad Ser B Phys Biol Sci* **81**, 278-290
8. Hattman, S. (2005) *Biochemistry (Mosc)* **70**, 550-558
9. Tock, M. R., and Dryden, D. T. F. (2005) *Curr Opin Microbiol* **8**, 466-472
10. Geier, G. E., and Modrich, P. (1979) *J Biol Chem* **254**, 1408-1413
11. Tran, P. H., Korszun, Z. R., Cerritelli, S., Springhorn, S. S., and Lacks, S. A. (1998) *Structure* **6**, 1563-1575
12. Malone, T., Blumenthal, R. M., and Cheng, X. (1995) *J Mol Biol* **253**, 618-632
13. Cheng, X., and Roberts, R. J. (2001) *Nucleic Acids Res* **29**, 3784-3795
14. Jeltsch, A. (1999) *J Mol Evol* **49**, 161-164
15. Guyot, J. B., Grassi, J., Hahn, U., and Guschlbauer, W. (1993) *Nucleic Acids Res* **21**, 3183-3190
16. O'Gara, M., Klimasauskas, S., Roberts, R. J., and Cheng, X. (1996) *J Mol Biol* **261**, 634-645
17. Horton, J. R., Liebert, K., Bekes, M., Jeltsch, A., and Cheng, X. (2006) *J Mol Biol* **358**, 559-570
18. Liebert, K., Hermann, A., Schlickenrieder, M., and Jeltsch, A. (2004) *J Mol Biol* **341**, 443-454
19. Pogolotti, A. L., Jr., Ono, A., Subramaniam, R., and Santi, D. V. (1988) *J Biol Chem* **263**, 7461-7464
20. Urig, S., Gowher, H., Hermann, A., Beck, C., Fatemi, M., Humeny, A., and Jeltsch, A. (2002) *J Mol Biol* **319**, 1085-1096
21. Mashhoon, N., Carroll, M., Pruss, C., Eberhard, J., Ishikawa, S., Estabrook, R. A., and Reich, N. (2004) *J Biol Chem* **279**, 52075-52081
22. Zinoviev, V. V., Evdokimov, A. A., Malygin, E. G., Schlagman, S. L., and Hattman, S. (2003) *J Biol Chem* **278**, 7829-7833
23. Bergerat, A., Kriebardis, A., and Guschlbauer, W. (1989) *J Biol Chem* **264**, 4064-4070
24. Coffin, S. R., and Reich, N. O. (2009) *J Biol Chem* **284**, 18390-18400
25. Peterson, S. N., and Reich, N. O. (2006) *J Mol Biol* **355**, 459-472
26. Berdis, A. J., Lee, I., Coward, J. K., Stephens, C., Wright, R., Shapiro, L., and Benkovic, S. J. (1998) *Proc. Natl. Acad. Sci* **95**, 2874-2879
27. Renbaum, P., and Razin, A. (1992) *FEBS Lett* **313**, 243-247
28. Surby, M. A., and Reich, N. O. (1996) *Biochemistry* **35**, 2201-2208
29. Surby, M. A., and Reich, N. O. (1996) *Biochemistry* **35**, 2209-2217
30. Modrich, P. (1989) *J Biol Chem* **264**, 6597-6600

31. Au, K. G., Welsh, K., and Modrich, P. (1992) *J Biol Chem* **267**, 12142-12148
32. Lobner-Olesen, A., Marinus, M. G., and Hansen, F. G. (2003) *Proc. Natl. Acad. Sci* **100**, 4672-4677
33. Lobner-Olesen, A., Skovgaard, O., and Marinus, M. G. (2005) *Curr Opin Microbiol* **8**, 154-160
34. Marinus, M. G., and Casadesus, J. (2009) *FEMS Microbiol Rev* **33**, 488-503
35. Barras, F., and Marinus, M. G. (1989) *Trends Genet* **5**, 139-143
36. Low, D. A., Weyand, N. J., and Mahan, M. J. (2001) *Infect Immun* **69**, 7197-7204
37. Casadesus, J., and Low, D. (2006) *Microbiol Mol Biol Rev* **70**, 830-856
38. Bakker, A., and Smith, D. W. (1989) *J Bacteriol* **171**, 5738-5742
39. Hernday, A. D., Braaten, B. A., and Low, D. A. (2003) *Mol Cell* **12**, 947-957
40. Julio, S. M., Heithoff, D. M., Provenzano, D., Klose, K. E., Sinsheimer, R. L., Low, D. A., and Mahan, M. J. (2001) *Infect Immun* **69**, 7610-7615
41. Heithoff, D. M., Sinsheimer, R. L., Low, D. A., and Mahan, M. J. (1999) *Science* **284**, 967-970
42. Boye, E., Marinus, M. G., and Lobnerolesen, A. (1992) *J Bacteriol* **174**, 1682-1685
43. Stancheva, I., Koller, T., and Sogo, J. M. (1999) *Embo J* **18**, 6542-6551
44. Campbell, J. L., and Kleckner, N. (1988) *Gene* **74**, 189-190
45. Marinus, M. G., Poteete, A., and Arraj, J. A. (1984) *Gene* **28**, 123-125
46. Chen, L., Paulsen, D. B., Scruggs, D. W., Banes, M. M., Reeks, B. Y., and Lawrence, M. L. (2003) *Microbiology* **149**, 2283-2290
47. Peterson, K. R., and Mount, D. W. (1993) *J Bacteriol* **175**, 7505-7508
48. Low, D. A., and Casadesus, J. (2008) *Curr Opin Microbiol* **11**, 106-112
49. Baga, M., Goransson, M., Normark, S., and Uhlin, B. E. (1985) *Embo J* **4**, 3887-3893
50. van der Woude, M., Braaten, B., and Low, D. (1996) *Trends Microbiol* **4**, 5-9
51. Hale, W. B., van der Woude, M. W., Braaten, B. A., and Low, D. A. (1998) *Mol Genet Metab* **65**, 191-196
52. Falker, S., Schmidt, M. A., and Heusipp, G. (2005) *Microbiology-Sgm* **151**, 2291-2299
53. Taylor, V. L., Titball, R. W., and Oyston, P. C. (2005) *Microbiology* **151**, 1919-1926
54. Robinson, V. L., Oyston, P. C., and Titball, R. W. (2005) *FEMS Microbiol Lett* **252**, 251-256
55. Honma, Y., Fernandez, R. E., and Maurelli, A. T. (2004) *Microbiology* **150**, 1073-1078
56. Campellone, K. G., Roe, A. J., Lobner-Olesen, A., Murphy, K. C., Magoun, L., Brady, M. J., Donohue-Rolfe, A., Tzipori, S., Gally, D. L., Leong, J. M., and Marinus, M. G. (2007) *Mol Microbiol* **63**, 1468-1481
57. Murphy, K. C., Ritchie, J. M., Waldor, M. K., Lobner-Olesen, A., and Marinus, M. G. (2008) *J Bacteriol* **190**, 438-441
58. Saxena, S. K., O'Brien, A. D., and Ackerman, E. J. (1989) *J Biol Chem* **264**, 596-601
59. Sandvig, K. (2001) *Toxicon* **39**, 1629-1635
60. Otto, H., Tezcan-Merdol, D., Girisch, R., Haag, F., Rhen, M., and Koch-Nolte, F. (2000) *Mol Microbiol* **37**, 1106-1115
61. Garcia-Del Portillo, F., Pucciarelli, M. G., and Casadesus, J. (1999) *PNAS* **96**, 11578-11583

62. Balbontin, R., Rowley, G., Pucciarelli, M. G., Lopez-Garrido, J., Wormstone, Y., Lucchini, S., Garcia-Del Portillo, F., Hinton, J. C., and Casadesus, J. (2006) *J Bacteriol* **188**, 8160-8168
63. Pucciarelli, M. G., Prieto, A. I., Casadesus, J., and Garcia-del Portillo, F. (2002) *Microbiology* **148**, 1171-1182
64. Alonso, A., Pucciarelli, M. G., Figueroa-Bossi, N., and Garcia-del Portillo, F. (2005) *J Bacteriol* **187**, 7901-7911
65. Jakomin, M., Chessa, D., Baumler, A. J., and Casadesus, J. (2008) *J Bacteriol* **190**, 7406-7413
66. Heithoff, D. M., Enioutina, E. Y., Daynes, R. A., Sinsheimer, R. L., Low, D. A., and Mahan, M. J. (2001) *Infect Immun* **69**, 6725-6730
67. Prieto, A. I., Ramos-Morales, F., and Casadesus, J. (2004) *Genetics* **168**, 1787-1794
68. Wu, H., Lippmann, J. E., Oza, J. P., Zeng, M., Fives-Taylor, P., and Reich, N. O. (2006) *Oral Microbiol Immunol* **21**, 238-244
69. Erova, T. E., Fadl, A. A., Sha, J., Khajanchi, B. K., Pillai, L. L., Kozlova, E. V., and Chopra, A. K. (2006) *Infect Immun* **74**, 5763-5772
70. Goldman, S., Navon, Y., and Fish, F. (1987) *Microb Pathog* **2**, 327-338
71. Mehling, J. S., Lavender, H., and Clegg, S. (2007) *FEMS Microbiol Lett* **268**, 187-193
72. Watson, M. E., Jarisch, J., and Smith, A. L. (2004) *Mol Microbiol* **53**, 651-664
73. Bucci, C., Lavitola, A., Salvatore, P., Del Giudice, L., Massardo, D. R., Bruni, C. B., and Alifano, P. (1999) *Mol Cell* **3**, 435-445
74. Oza, J. P., Yeh, J. B., and Reich, N. O. (2005) *FEMS Microbiol Lett* **245**, 53-59
75. Julio, S. M., Heithoff, D. M., Sinsheimer, R. L., Low, D. A., and Mahan, M. J. (2002) *Infect Immun* **70**, 1006-1009
76. Robertson, G. T., Reisenauer, A., Wright, R., Jensen, R. B., Jensen, A., Shapiro, L., and Roop, R. M. (2000) *J Bacteriol* **182**, 3482-3489
77. Mashhoon, N., Pruss, C., Carroll, M., Johnson, P. H., and Reich, N. O. (2006) *J Biomol Screen* **11**, 497-510
78. Kelly, J. (2005) *The Great Mortality*, Fourth Estate, London, New York
79. Yersin, A. (1894) *Annals de Institut Pasteur* 662-667
80. Achtman, M., Zurth, K., Morelli, G., Torrea, G., Guiyoule, A., and Carniel, E. (1999) *PNAS* **96**, 14043-14048
81. Malassez, L., and Vignal, W. (1884) *Arch Physiol Norm Pathol* **3**, 81-105
82. Stenseth, N. C., Atshabar, B. B., Begon, M., Belmain, S. R., Bertherat, E., Carniel, E., Gage, K. L., Leirs, H., and Rahalison, L. (2008) *PLoS Med* **5**, e3
83. Raoult, D., Aboudharam, G., Crubezy, E., Larrouy, G., Ludes, B., and Drancourt, M. (2000) *PNAS* **97**, 12800-12803
84. DeLeo, F. R., and Hinnebusch, B. J. (2005) *Nat Med* **11**, 927-928
85. Anker, M., and Schaaf, D. (2000) *WHO Report on Global Surveillance of Epidemic-prone Infectious Diseases*, World Health Organization, Geneva
86. Inglesby, T. V., Dennis, D. T., Henderson, D. A., Bartlett, J. G., Ascher, M. S., Eitzen, E., Fine, A. D., Friedlander, A. M., Hauer, J., Koerner, J. F., Layton, M., McDade, J., Osterholm, M. T., O'Toole, T., Parker, G., Perl, T. M., Russell, P. K., Schoch-Spana, M., and Tonat, K. (2000) *JAMA-J. Am. Med. Assoc.* **283**, 2281-2290
87. Galimand, M., Guiyoule, A., Gerbaud, G., Rasoamanana, B., Chanteau, S., Carniel, E., and Courvalin, P. (1997) *N Engl J Med* **337**, 677-680

88. Guiyoule, A., Gerbaud, G., Buchrieser, C., Galimand, M., Rahalison, L., Chanteau, S., Courvalin, P., and Carniel, E. (2001) *Emerg Infect Dis* **7**, 43-48
89. Welch, T. J., Fricke, W. F., McDermott, P. F., White, D. G., Rosso, M. L., Rasko, D. A., Mammel, M. K., Eppinger, M., Rosovitz, M. J., Wagner, D., Rahalison, L., Leclerc, J. E., Hinshaw, J. M., Lindler, L. E., Cebula, T. A., Carniel, E., and Ravel, J. (2007) *PLoS ONE* **2**, e309
90. Walsh, C. (2003) *Antibiotics*, ASM Press, Washington D.C.
91. Witte, W. (1998) *Science* **279**, 996-997
92. Greenfield, R. A., and Bronze, M. S. (2003) *Drug Discov Today* **8**, 881-888
93. McGovern, T. W., and Friedlander, A. M. (1997) Plague. In: Zajtchuk, R., and Bellamy, R. F. (eds). *Medical Aspects of Chemical and Biological Warfare*, Office of The Surgeon General, Department of the Army, United States of America, Bethesda
94. Health_Protection_Agency. (2008) *Deliberate Release of Plague: Information for the Public. Available at* http://www.hpa.org.uk/webw/HPAweb&HPAwebStandard/HPAweb_C/1203084387130?p=1191942145702
95. Health_Protection_Agency. (2008) *Available at* http://www.hpa.org.uk/web/HPAweb&HPAwebStandard/HPAweb_C/1204100442192
96. Pan, J. C., Ye, R., Wang, H. Q., Xiang, H. Q., Zhang, W., Yu, X. F., Meng, D. M., and He, Z. S. (2008) *Antimicrob Agents Chemother* **52**, 3829-3836
97. Gupta, K., Hooton, T. M., and Stamm, W. E. (2001) *Ann Intern Med* **135**, 41-50
98. Manges, A. R., Johnson, J. R., Foxman, B., O'Bryan, T. T., Fullerton, K. E., and Riley, L. W. (2001) *N Engl J Med* **345**, 1007-1013
99. Threlfall, E. J. (2000) *J Antimicrob Chemother* **46**, 7-10
100. Humeny, A., Beck, C., Becker, C. M., and Jeltsch, A. (2003) *Anal Biochem* **313**, 160-166
101. Allan, B. W., and Reich, N. O. (1996) *Biochemistry* **35**, 14757-14762
102. Allan, B. W., Beechem, J. M., Lindstrom, W. M., and Reich, N. O. (1998) *J Biol Chem* **273**, 2368-2373
103. Holz, B., Klimasauskas, S., Serva, S., and Weinhold, E. (1998) *Nucleic Acids Res* **26**, 1076-1083
104. Ward, D. C., Reich, E., and Stryer, L. (1969) *J Biol Chem* **244**, 1228-1237
105. Luo, J., Zheng, W., Wang, Y., Wu, Z., Bai, Y., and Lu, Z. (2009) *Anal Biochem* **387**, 143-149
106. Clark, S. J., Harrison, J., Paul, C. L., and Frommer, M. (1994) *Nucleic Acids Res* **22**, 2990-2997
107. Frommer, M., McDonald, L. E., Millar, D. S., Collis, C. M., Watt, F., Grigg, G. W., Molloy, P. L., and Paul, C. L. (1992) *PNAS* **89**, 1827-1831
108. Frauer, C., and Leonhardt, H. (2009) *Nucleic Acids Res* **37**, e22
109. Reich, N. O., and Mashhoon, N. (1990) *J Biol Chem* **265**, 8966-8970
110. Jeltsch, A., Friedrich, T., and Roth, M. (1998) *J Mol Biol* **275**, 747-758
111. Kim, B. Y., Kwon, O. S., Joo, S. A., Park, J. A., Heo, K. Y., Kim, M. S., and Ahn, J. S. (2004) *Anal Biochem* **326**, 21-24
112. Roth, M., and Jeltsch, A. (2000) *Biol Chem* **381**, 269-272
113. Hendricks, C. L., Ross, J. R., Pichersky, E., Noel, J. P., and Zhou, Z. S. (2004) *Anal Biochem* **326**, 100-105
114. Wang, C., Leffler, S., Thompson, D. H., and Hrycyna, C. A. (2005) *Biochem Biophys Res Commun* **331**, 351-356

115. Dorgan, K. M., Wooderchak, W. L., Wynn, D. P., Karschner, E. L., Alfaro, J. F., Cui, Y., Zhou, Z. S., and Hevel, J. M. (2006) *Anal Biochem* **350**, 249-255
116. Schlenk, F., and Zydek, C. R. (1968) *Biochem Biophys Res Commun* **31**, 427-432
117. Graves, T. L., Zhang, Y., and Scott, J. E. (2008) *Anal Biochem* **373**, 296-306
118. Biggins, J. B., Prudent, J. R., Marshall, D. J., Ruppen, M., and Thorson, J. S. (2000) *Proc. Natl. Acad. Sci* **97**, 13537-13542
119. Woo, Y. H., Rajagopalan, P. T., and Benkovic, S. J. (2005) *Anal Biochem* **340**, 336-340
120. Li, J., Yan, H., Wang, K., Tan, W., and Zhou, X. (2007) *Anal Chem* **79**, 1050-1056
121. Lacks, S., and Greenberg, B. (1975) *J Biol Chem* **250**, 4060-4066
122. Lacks, S., and Greenberg, B. (1977) *J Mol Biol* **114**, 153-168
123. Wood, R. J., McKelvie, J. C., Maynard-Smith, M. D., and Roach, P. L. (2010) *Nucleic Acids Res* **38**, e107
124. Tarasova, G. V., Nayakshina, T. N., and Degtyarev, S. K. (2008) *BMC Mol Biol* **9**, 7
125. Hamil, R. L., and Hoehn, M. M. (1973) *J Antibiot (Tokyo)* **26**, 463-465
126. Schluckebier, G., Kozak, M., Bleimling, N., Weinhold, E., and Saenger, W. (1997) *J Mol Biol* **265**, 56-67
127. Kumar, R., Srivastava, R., Singh, R. K., Surolia, A., and Rao, D. N. (2008) *Bioorg Med Chem* **16**, 2276-2285
128. Wahnon, D. C., Shier, V. K., and Benkovic, S. J. (2001) *J Am Chem Soc* **123**, 976-977
129. Benkovic, S. J., Baker, S. J., Alley, M. R. K., Woo, Y. H., Zhang, Y. K., Akama, T., Mao, W. M., Baboval, J., Rajagopalan, P. T. R., Wall, M., Kahng, L. S., Tavassoli, A., and Shapiro, L. (2005) *J Med Chem* **48**, 7468-7476

Chapter 2:- Development of an assay for *Y. pestis* Dam activity

2.1 Introduction

Hairpin oligonucleotides possessing adjacent fluorophore and quencher pairs have been used to assay the activity of restriction enzymes such as BamHI (1). When the fluorophore and quencher are attached to an oligonucleotide the pair are held in close proximity. Overlap of the fluorophore emission and quencher absorbance spectra allows Förster resonance energy transfer (FRET) to occur, decreasing the observed fluorophore fluorescence (Figure 2.1). Since the efficiency of this process is inversely proportional to the sixth power with respect to distance, restriction enzyme activity separating the FRET pair restores the fluorophore fluorescence (2,3).

Restriction enzyme DpnI is often used to identify the methylation status of DNA because it recognises and cuts palindromic GATC sequences only when the adenine on both of the strands is methylated (4,5). The aim was to combine the discriminatory ability of DpnI with the use of a hairpin oligonucleotide to produce a continuous coupled enzyme assay for Dam activity. Methylation of a fluorescently labelled hairpin oligonucleotide by *Y. pestis* Dam would result in its recognition and restriction by DpnI, with an associated fluorescence increase. At the time development of our assay began, Li and co-workers had yet to publish their work on a similar assay and our research took no intellectual inspiration from theirs (6). As will be demonstrated in this and subsequent chapters the assay which we developed was actually superior to Li's because of one small but crucial difference.

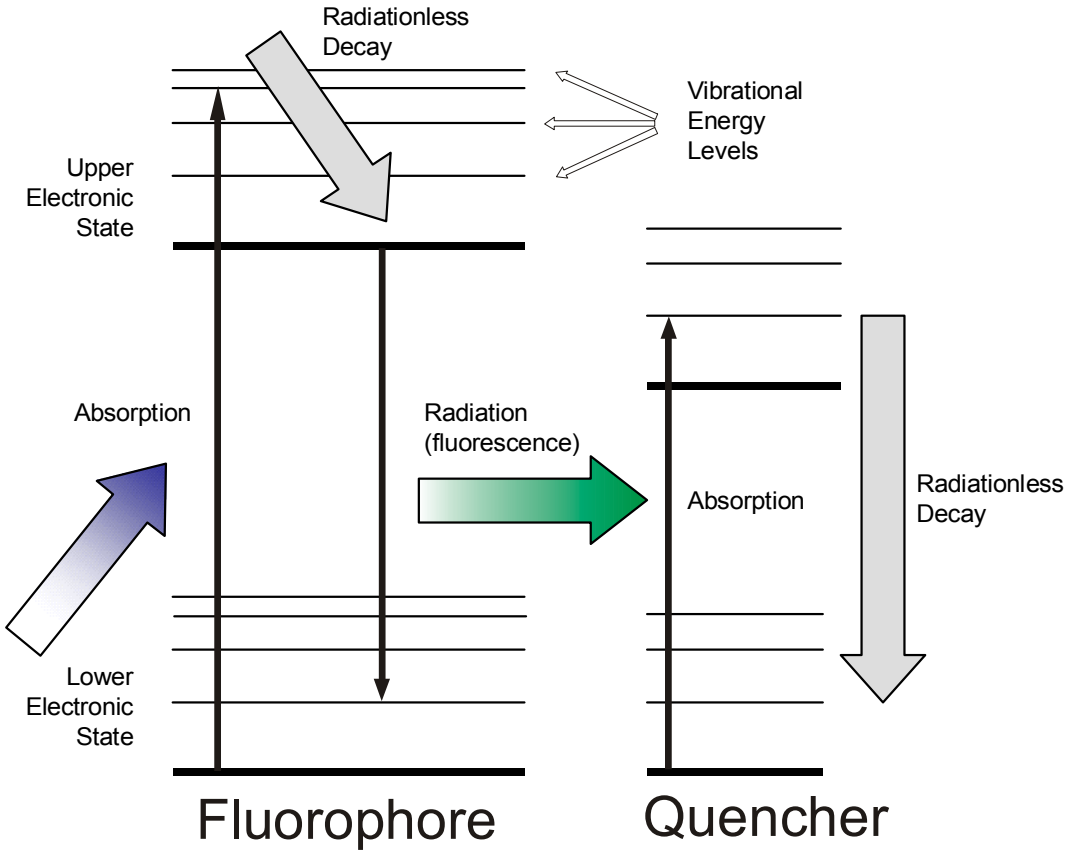

Figure 2.1 Förster Resonance Energy Transfer: The fluorophore absorbs electromagnetic radiation and is taken into an excited electronic state. The excited molecule loses energy through collisions with surrounding molecules and descends to the lowest vibrational level of the excited electronic state. The fluorophore returns to the lower electronic state, emitting excess energy as electromagnetic radiation. A nearby quencher molecule absorbs this radiation and is taken into an excited electronic state. The quencher returns to the ground electronic state, transferring the excess energy into the surrounding molecules in a radiationless manner.

Plasmid pRJW421307, which contained the *Y. pestis* Dam gene under the control of an arabinose inducible promoter, had been created by Dr R. J. Wood and used to express active *Y. pestis* Dam. It was considered worthwhile to re-test expression in several different *E. coli* strains harbouring the plasmid. DpnI from a commercial source was used for initial assay development but later it was more economical to prepare recombinant DpnI from an expression system. Construction of a DpnI expression plasmid, identification of a good expression strain and optimisation of the purification were therefore undertaken.

This chapter describes the cloning, expression and purification of the two enzymes *Y. pestis* Dam and DpnI, and the stages in the development of a fluorescent real-time coupled enzyme assay for Dam activity. Maps of the expression plasmids, including pRJW421307 produced by Dr. R. Wood, may be found in appendix A.

2.2 Cloning, expression and purification of enzymes for use in the assay

2.2.1 Expression of *Y. pestis* Dam

The expression of N-terminally-His_6-tagged *Y. pestis* Dam, abbreviated His_6-M.YpeDam (7), from pRJW421307 was investigated in *E. coli* strains BL21 (DE3), JM110 and GM215 (Table 2.1). Cultures of each strain were grown in 100 ml of 2YT media and the absorbance at 600 nm monitored over time. When the absorbance at 600 nm reached 0.6, protein expression was induced with arabinose and the protein content of cells analysed by SDS-PAGE every hour for four hours thereafter.

The cultures of BL21 (DE3) and GM215 grew unremarkably up to an absorbance of 0.6 at 600 nm in approximately 2 hours (Figure 2.2, upper and lower graphs). Strain JM110 took longer, with three hours passing before an absorbance of 0.6 was reached (Figure 2.2, middle graph). Induction of Dam expression in strain BL21 (DE3) curtailed growth significantly. Strain GM215 showed some reduction in growth, but only 2 hours after induction. Growth of strain JM110 appeared unaffected by the addition of the arabinose inducer.

Strain	***Genotype***	***Comments***
BL21 (DE3) (8),(9)	*F-, ompT, hsdSB(rB-, mB-), dcm, gal, λ(DE3)*	Dcm –ve. Generally used as an expression host. Deficient in lon and ompT proteases
GM33 (10),(11)	*F-, LAM-, IN(rrnD-rrnE)1, dam-3, sup-85*	Dam –ve strain. Colonies and cell pellet greasy in appearance. Difficult to collect by centrifugation.
GM48 (10)	*F-, thr-1, araC14, leuB6(Am), fhuA31, lacY1, tsx-78, glnV44(AS), galK2(Oc), galT22, LAM-, dcm-6, dam-3, thi-1*	Dam and Dcm –ve strain.
GM124	*F-, lacZ118(Oc), rpsL275(strR), dam-4*	Dam –ve strain. Streptomycin resistant.
GM161	F-, *thr-1*, *leuB6*(Am), *fhuA21*, *lacY1*, *glnV44*(AS), *LAM-*, *dam-4*, *thi-1*, *hsdS1*	Dam –ve strain.
GM215 (12)	*F-, rna-1, LAM-, dam-3, thi-1, end-1*	Dam –ve strain. Lacks endonuclease I and RNase I.
GM2929 (derived from GM2163)	*F-, araC14, leuB6(Am), fhuA13, lacY1, tsx-78, glnV44(AS), galK2(Oc), galT22, LAM-, mcrA0, dcm-6, hisG4(Oc), rfbC1, rpsL136(strR), dam-13::Tn9, xylA5, mtl-1, recF143, thi-1, mcrB9999, hsdR2*	Dam –ve strain. Chloramphenicol resistant. Streptomycin resistant.
JM110 (13)	*rpsL (StrR,) thr, leu, thi-1, lacY, galK, galT, ara, tonA, tsx, dam, dcm, supE44, Δ(lac-proAB), [F′ traD36 proAB lacIqZΔM15]*	Dam and Dcm –ve. Streptomycin resistant.
TOP10 (Genotype same as DH10B (14))	*F-, mcrA, Δ(mrr-hsdRMS-mcrBC), φ80lacZΔM15, ΔlacX74, recA1, araD139, Δ(ara-leu) 7697, galU, galK, rpsL(StrR), endA1, nupG λ-*	High transformation efficiency, used for the maintenance of plasmids. Streptomycin resistant.

Table 2.1 *E. coli* strain genotypes. Strains beginning ‘GM’ were originally produced by Professor Martin. G. Marinus.

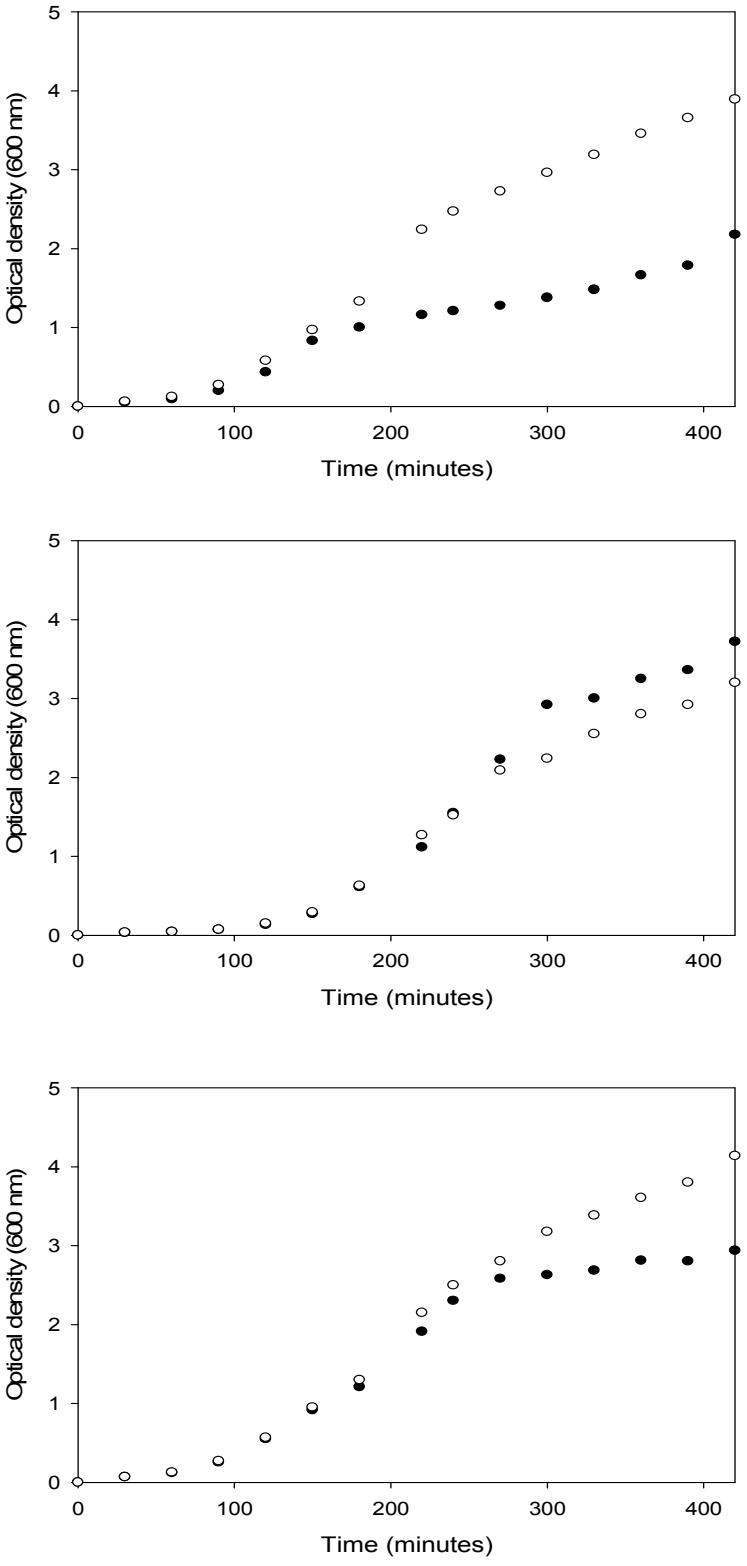

Figure 2.2 Growth curves of induced (●) and uninduced (○) cultures of *E. coli* strains BL21 (DE3) (upper graph), JM110 (middle graph) and GM215 (lower graph) harbouring plasmid pRJW421307. A time-course of the absorbance of the cultures at 600 nm is shown.

SDS-PAGE analysis suggested that there was probably low level *Y. pestis* Dam expression in all of the cell strains tested (Figure 2.3, Figure 2.4, Figure 2.5). An extra protein, with the expected molecular weight of *Y. pestis* Dam, 32,118 Da, was seen in every induced sample of BL21 (DE3) (Figure 2.3). In JM110, expression was also faintly observed 1-3 hours after induction but beyond this time it was difficult to judge Dam levels (Figure 2.4).

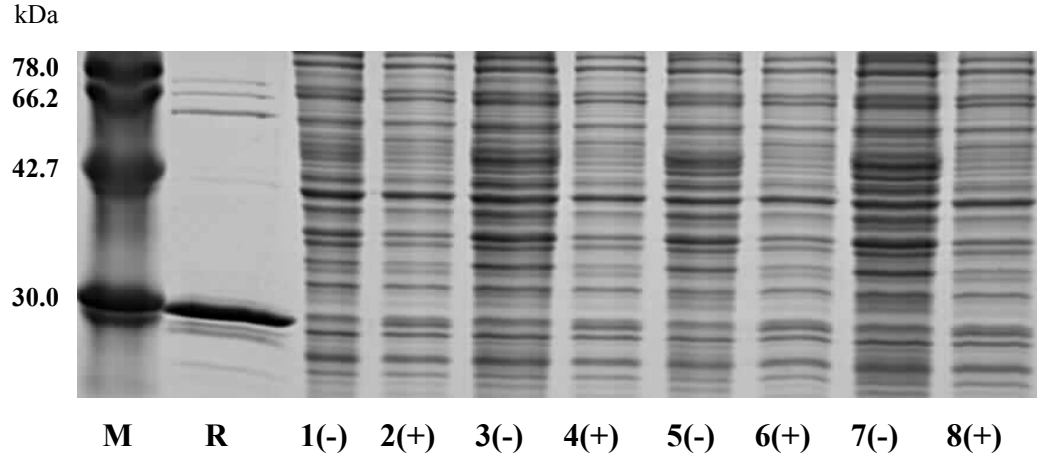

Figure 2.3 15 % SDS-PAGE analysis of Dam expression in strain BL21 (Dam +). M = Marker, R = Dam reference, Lanes 1, 3, 5 and 7 = lysate from uninduced cultures at 1, 2, 3 and 4 hours respectively, Lanes 2, 4, 6 and 8 = lysate from induced cultures at 1, 2, 3 and 4 hours after induction.

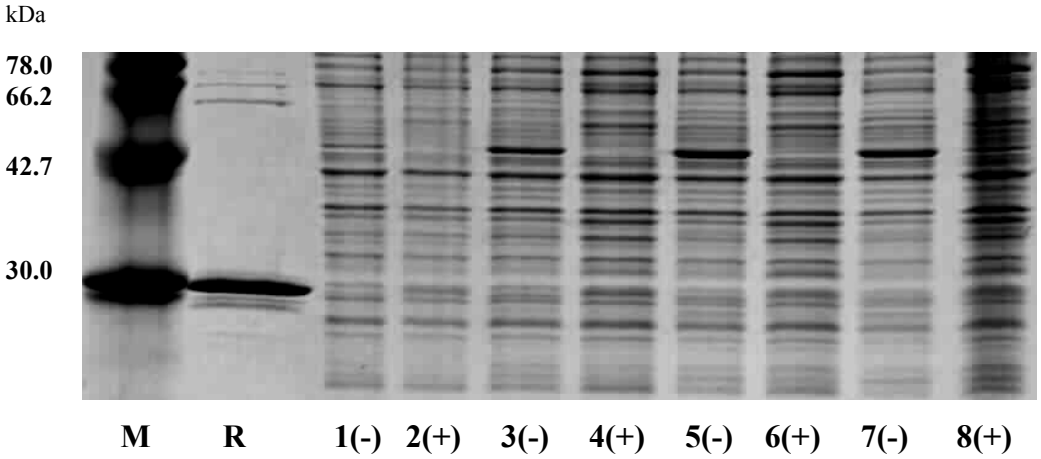

Figure 2.4 15 % SDS-PAGE analysis of Dam expression in strain JM110 (Dam -). M = Marker, R = Dam reference, Lanes 1, 3, 5 and 7 = lysate from uninduced cultures at 1, 2, 3 and 4 hours respectively, Lanes 2, 4, 6 and 8 = lysate from induced cultures at 1, 2, 3 and 4 hours after induction.

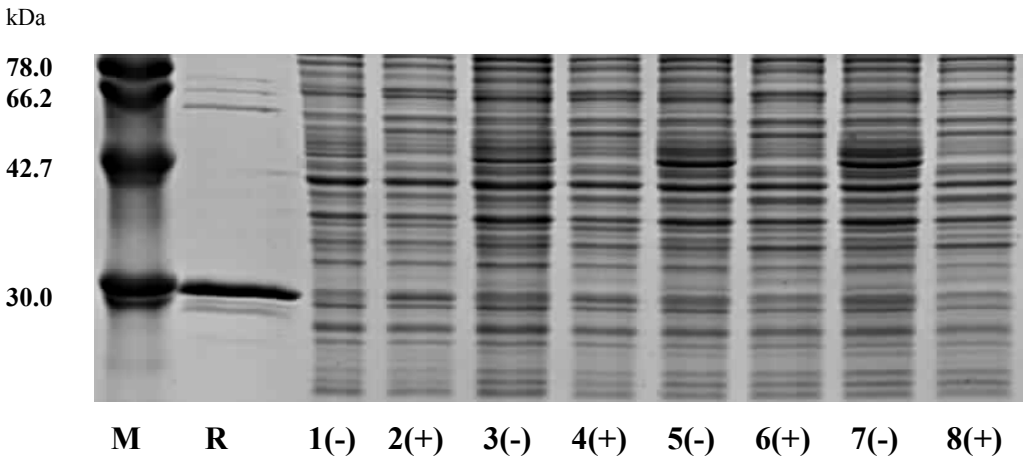

Figure 2.5 15 % SDS-PAGE analysis of Dam expression in strain GM215 (Dam -). M = Marker, R = Dam reference, Lanes 1, 3, 5 and 7 = lysate from uninduced cultures at 1, 2, 3 and 4 hours respectively, Lanes 2, 4, 6 and 8 = lysate from induced cultures at 1, 2, 3 and 4 hours after induction.

With strain GM215, the 32 kDa protein band was clearly more intense after 1 hour in the induced culture sample. Between 3 and 4 hours post induction this protein band reduced in intensity, which may indicate degradation of the protein.

E. coli strain GM215 was chosen to express *Y. pestis* Dam on a large scale. GM215 grew significantly better than BL21 (DE3) and was chosen over JM110 because, whilst there was evidence of protein expression in both strains, GM215 was *endA* negative. Herman and Modrich reported endonuclease A contaminating *E. coli* Dam they purified from GM31 (15). Endonuclease A can digest oligonucleotides over 7 bp long and so could have adversely affected assay development (16,17).

Large scale expression of *Y. pestis* Dam was carried out in 5 L cultures of *E. coli* GM215 harbouring plasmid pRJW421307. Typically such growths yielded 20 g of cell paste from which Dam could be purified by nickel affinity chromatography. A purification using 10 g of cell paste normally yielded 1.5 mg of protein. *Y. pestis* Dam prepared in this manner was estimated to be > 95 % pure based on SDS-PAGE analysis (Figure 2.6). Protein was dialysed for two half hour periods into storage buffer containing 20 % glycerol and kept in frozen aliquots at a concentration of 0.2 mg ml $^{-1}$.

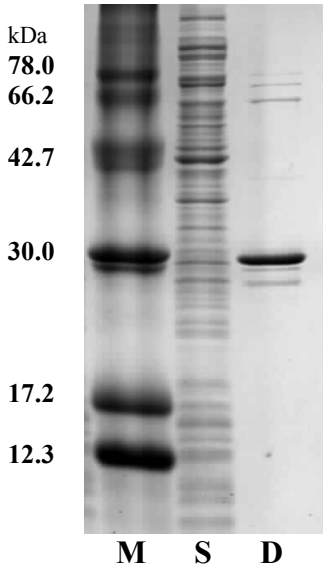

Figure 2.6 15 % SDS-PAGE analysis of N-terminally His-tagged *Y. pestis* Dam purified from GM215. M = Marker, S = Supernatant, D = Dam.

2.2.2 Subcloning, expression and purification of restriction enzyme DpnI

2.2.2.1 Harvesting of DpnI gene template DNA

DNA encoding the DpnI restriction endonuclease was kindly provided by Professor Sanford Lacks of Brookhaven National Laboratory in the form of a plasmid, pLS251, harboured in lyophilised *E. coli* GM 33 bacteria (5). The bacteria were recovered by re-suspension in liquid growth media and plating out onto solid ampicillin-containing media. Plasmid was isolated from overnight cultures of the bacteria grown from single colonies, and subjected to analytical digestion (Figure 2.7)

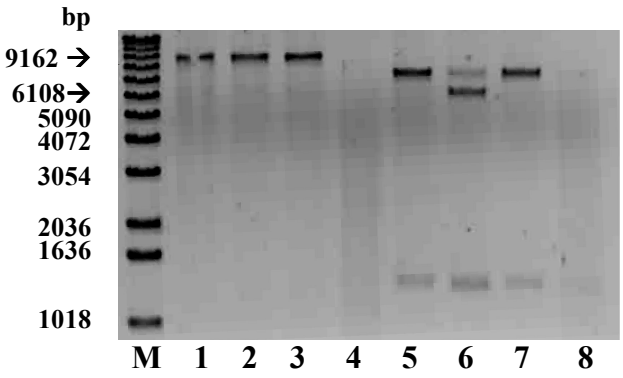

Figure 2.7 1 % AGE analysis of digested plasmid extracted from cultures of GM33 harbouring plasmid pLS251 (8.7 kbp). Lane M = DNA ladder. Lanes 1-4 show plasmid from four colonies linearised with BamHI, expected size = 8700 bp. Lanes 5-8 show plasmid from the same four colonies, in the same order, digested with NcoI, expected sizes = 7500 and 1200 bp (5).

Only plasmid isolated from colonies 1 and 3 produced DNA fragments consistent with pLS251 upon digestion.

2.2.2.2 Subcloning of the *dpnI* gene

Plasmid isolated from colony 1 was used as template DNA in PCR reactions to amplify the *dpnI* gene with primers DpnIf and DpnIr (Table 2.2).

Primer	*Sequence 5' to 3'*
DpnIf	CCCCCCATGGAATTACACTTTAATTTAGAATTAGTA
DpnIr	CCCC***CTCGAG***TCATAATTTCCGATACTTTCC

Table 2.2 Sequences of the forward (DpnIf) and reverse (DpnIr) primers used to amplify the DpnI gene. The NcoI and XhoI restriction sites are shown underlined and in bold italics respectively.

Analysis of the PCR reactions by agarose gel electrophoresis revealed that DNA of the expected length had been synthesised (Figure 2.8).

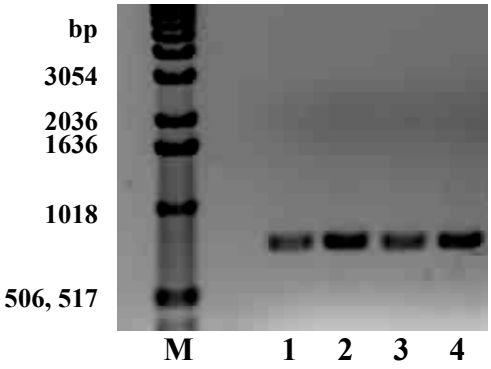

Figure 2.8 1 % AGE analysis of PCR reactions to amplify the *dpnI* gene. Lane M = DNA ladder. Lanes 1-4 = PCR reactions containing 1, 10, 100 and 1000 fold diluted template respectively, expected size = 781 bp.

The purified *dpnI* gene was digested with restriction enzymes XhoI and NcoI to produce sticky ends. A vector, with complementary sticky ends and an ampicillin resistance marker, was made by digestion of plasmid pMK171, a pBad derivative, with the same enzymes. This vector also encoded a His_6-tag which would be appended onto the start of the *dpnI* gene. Both gene and vector were purified by gel electrophoresis before analysis by 1 % AGE (Figure 2.9).

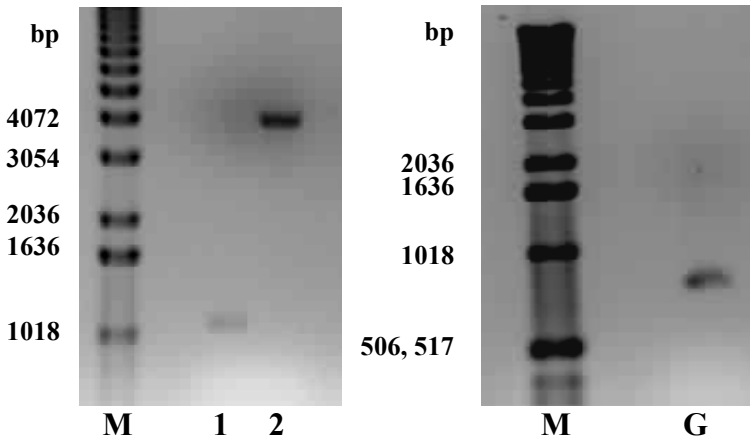

Figure 2.9 (Left) 1 % AGE analysis of NcoI and XhoI doubly digested, gel purified, fragments of plasmid pMK171. Lane M = DNA ladder, 1 = insert, 2 = vector, expected size = 4015. (Right) 1 % AGE analysis of NcoI and XhoI doubly digested, gel purified *dpnI* gene, expected size = 767 bp.

Vector and *dpnI* gene DNA appeared as single bands of the expected sizes. These DNA fragments were therefore joined in ligation reactions which were used to transform

aliquots of chemically competent *E. coli* GM2929. Transformants were cultured overnight on solid, ampicillin-containing growth media.

Selected colonies were screened by PCR to confirm that they possessed a copy of the *dpnI* gene. Of the fourteen colonies screened, nine gave a correctly sized fragment in the PCR reaction (Figure 2.10).

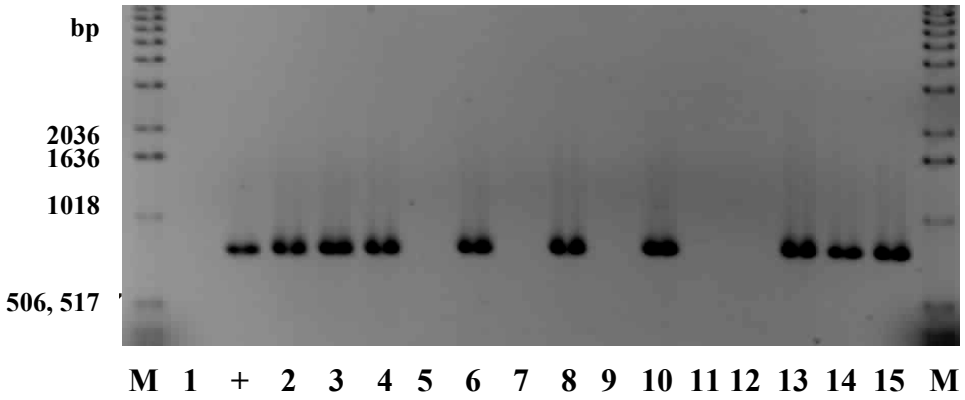

Figure 2.10 1 % AGE analysis of colony PCR screen for the *dpnI* gene. Lane M = DNA Ladder. 1 = negative control (*E. coli* GM2929 transformed with pMK171). + = positive control (pLS251). Lanes 2 – 15 = Colonies transformed with ligation mixture.

Plasmid harvested from overnight growths of the same colonies was subjected to digestion by XhoI or a combination of XhoI and NcoI. Analysis of the digests by AGE gave results consistent with the PCR screen (Figure 2.11). The nine colonies which had yielded a PCR product with the DpnI primers also harboured a plasmid of the expected size, 4782 bp, which contained an anticipated 767 bp insert delimited by XhoI and NcoI restriction sites. This new DpnI expression plasmid was named pMMS495859. Colonies which had yielded no PCR product all contained an unexpectedly large plasmid of over 8000 bp.

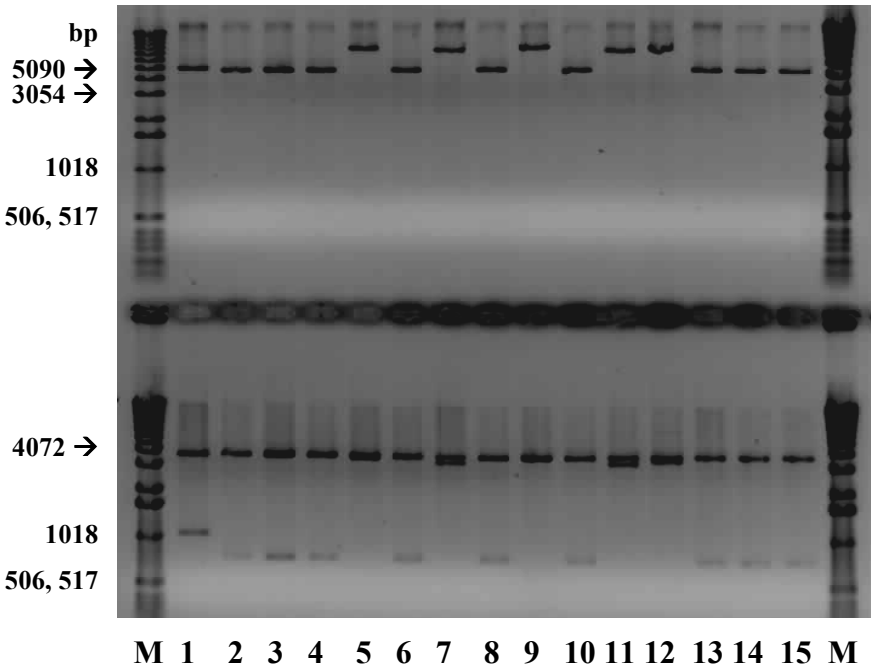

Figure 2.11 1 % AGE analysis of plasmid extracted from transformants. Lane M = DNA Ladder. Upper lanes 1 – 15 show plasmid isolated from transformants 1 – 15 (as labelled in figure 2.9) linearised with XhoI. Lower lanes 1 – 15 show plasmid from the same transformants digested with NcoI and XhoI.

2.2.2.3 Expression and purification of His_6-DpnI

Expression studies were carried out on colonies 2, 3, 6 and 14 which contained plasmid pMMS495859. Cultures derived from the respective colonies were grown to an absorbance of 0.6 at 600 nm and induced with arabinose. Protein content of the cells was analysed by SDS-PAGE 1 and 2 hours post induction and compared with that of GM2929 harbouring pBad HisA as a negative control (Figure 2.12).

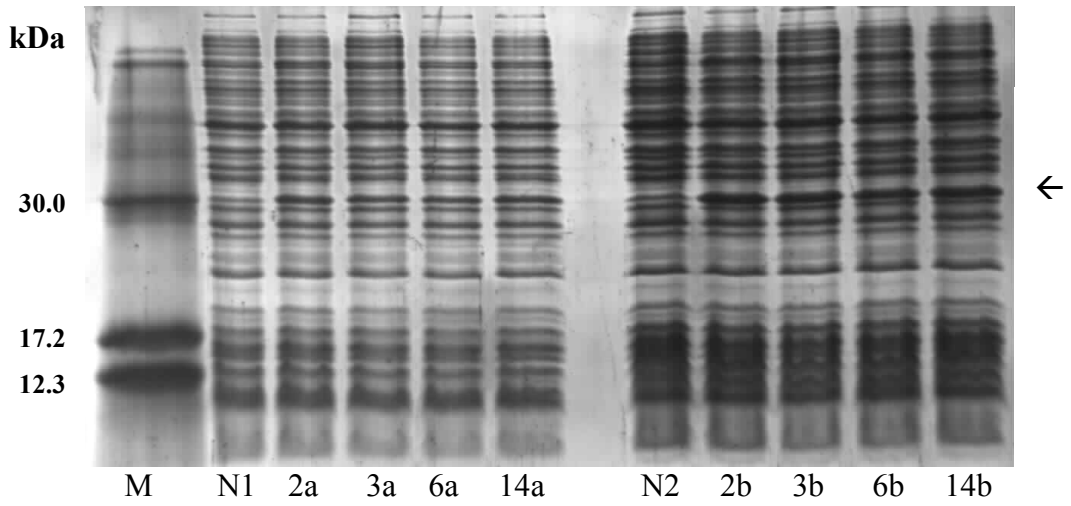

Figure 2.12 15 % SDS-PAGE analysis of DpnI expression in GM2929. M = molecular weight marker. N1 = negative control (*E. coli* GM2929 containing a pBad plasmid without the DpnI gene one hour after induction). 2a-14a = protein from growths of colonies 2, 3, 6 and 14 one hour after induction. N2 = negative control (two hours after induction). 2b-14b = protein from growths of colonies 2, 3, 6 and 14 two hours after induction.

After 1 hour, significantly more protein with the molecular weight of DpnI, 30,810 Da, was being expressed in the *E. coli* GM2929 containing pMMS495859 (Figure 2.12, black arrow). After 2 hours the amount of this protein of interest had continued to increase.

It was concluded that DpnI was probably being produced and so a large scale expression and purification using strain GM2929 were undertaken. A 5 L culture grown at 27 °C for 3 hours after induction yielded 23 g of cell paste. Two purifications were carried out with this cell paste by nickel affinity column chromatography (Figure 2.13, Figure 2.14).

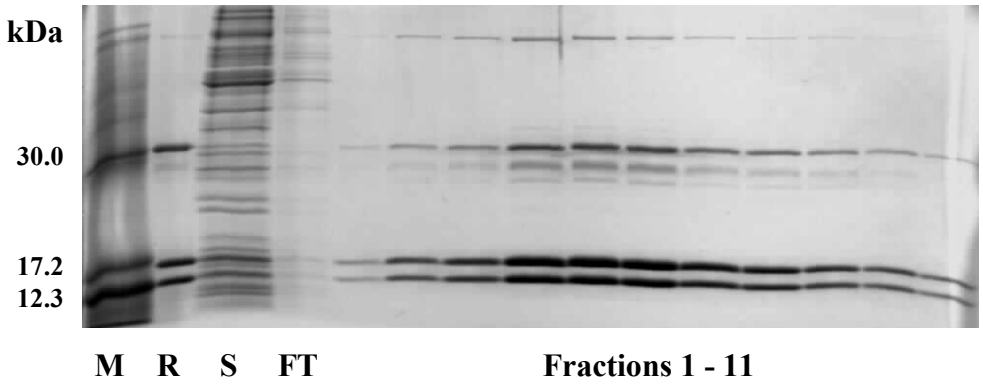

Figure 2.13 15 % SDS-PAGE analysis of DpnI purified from *E. coli* strain GM2929 without protease inhibitors. M = molecular weight marker, R = reference sample of DpnI, S = supernatant, FT = flow through.

SDS-PAGE analysis of the protein from the first purification showed that it was impure (Figure 2.13). Only a small amount of the protein eluted from the column had the expected molecular weight of DpnI (30,810 Da). The majority was in the form of two proteins, at similar concentration, with molecular masses of approximately 17 and 13 kDa. A hypothesis for this observation was that the two smaller proteins were the result of proteolytic degradation of DpnI. To test this, protease inhibitor tablets and PMSF, a serine protease inhibitor, were included in a second purification (Figure 2.14)

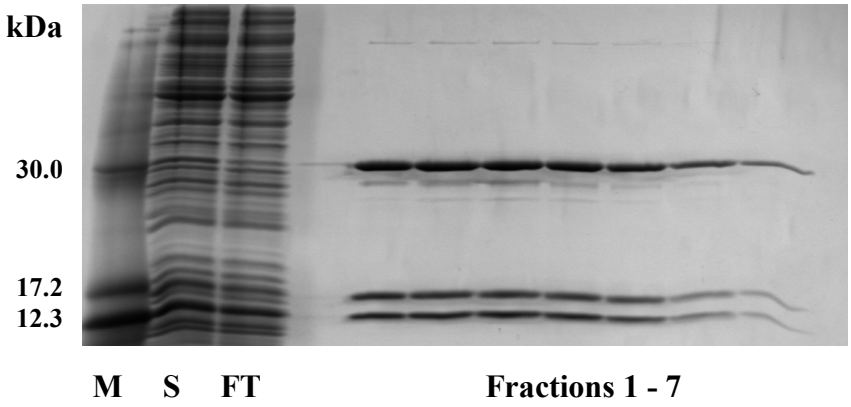

Figure 2.14 15 % SDS-PAGE analysis of DpnI purified from *E. coli* strain GM2929 with protease inhibitor tablets and PMSF. M = molecular weight marker, R = reference sample of DpnI, S = supernatant, FT = flow through.

The addition of protease inhibitors considerably improved the purification step. SDS-PAGE analysis of fractions eluted from the second column showed that they had a higher proportion of DpnI to impurity.

This DpnI was however still not considered pure enough and so different cell strains were investigated for its overexpression. *E. coli* strains GM33, 48, 124, 161 and 215 were all transformed with plasmid pMMS495859 and DpnI was expressed in 1 L cultures of each (Table 2.3, Table 2.1). Because DpnI cleaves DNA containing N6-methyladenine only Dam negative strains were tested.

E. coli *strain*	*Cell paste from growth (g)*	*Cell paste used in purification (g)*
GM33 #	23*	6*
GM48 #	2	2
GM124 ‡	3.8	3.8
GM161 ‡	6	6
GM215 ‡	1.4	1.4

Table 2.3 Cell paste yielded from 1 L growths of *E. coli* harbouring plasmid pMMS495859. # Cells cultured for 3 hours post induction. ‡ Cells cultured for 4 hours post induction. * Cells obtained as a watery slurry.

A nickel affinity purification, supplemented with protease inhibitors, was performed with cell paste from each of the strains. Samples of the protein fractions eluted from the nickel column were analysed by 15 % SDS-PAGE (Figure 2.15-Figure 2.19).

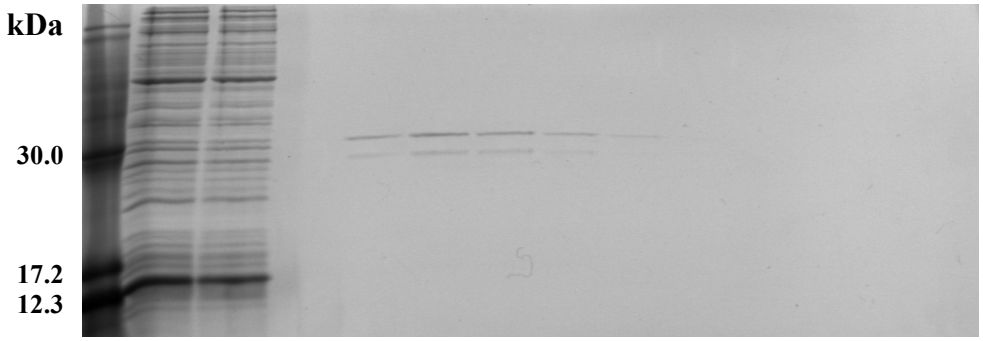

Figure 2.15 15 % SDS-PAGE analysis of DpnI purified from *E. coli* strain GM215 with protease inhibitor tablets and PMSF. M = molecular weight marker, S = supernatant, FT = flow through.

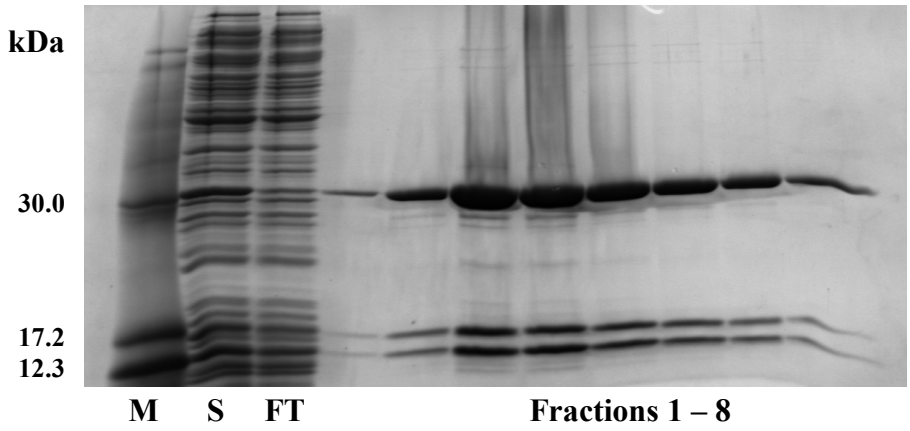

Figure 2.16 15 % SDS-PAGE analysis of DpnI purified from *E. coli* strain GM161 with protease inhibitor tablets and PMSF. M = molecular weight marker, S = supernatant, FT = flow through.

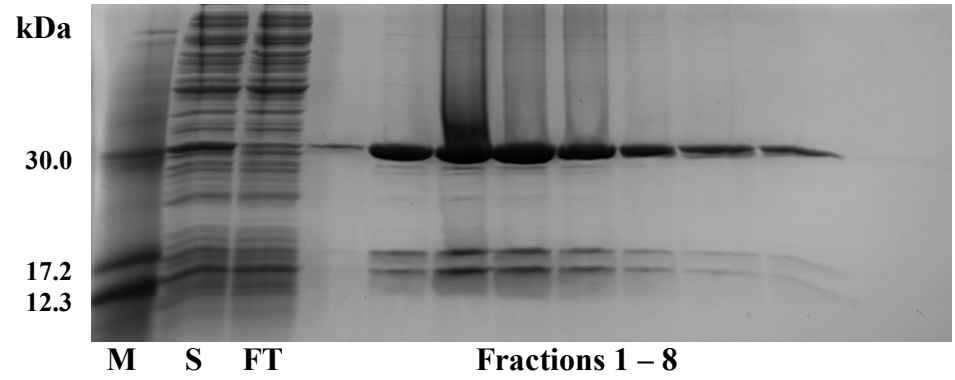

Figure 2.17 15 % SDS-PAGE analysis of DpnI purified from *E. coli* strain GM124 with protease inhibitor tablets and PMSF. M = molecular weight marker, S = supernatant, FT = flow through.

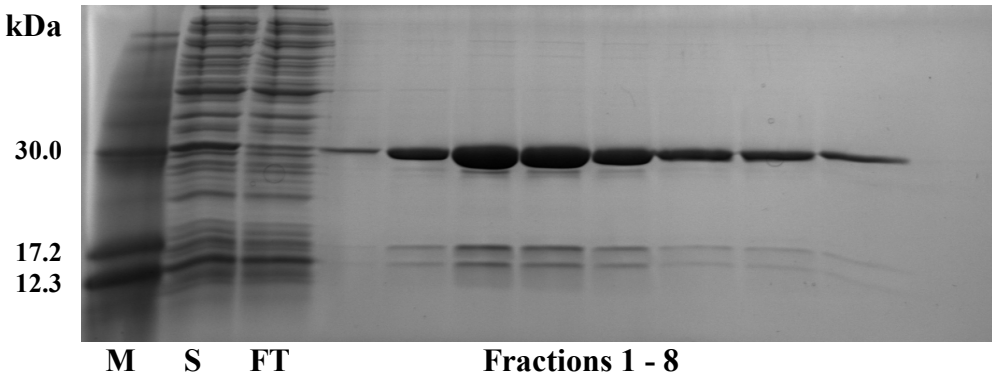

Figure 2.18 15 % SDS-PAGE analysis of DpnI purified from *E. coli* strain GM48 with protease inhibitor tablets and PMSF. M = molecular weight marker, S = supernatant, FT = flow through.

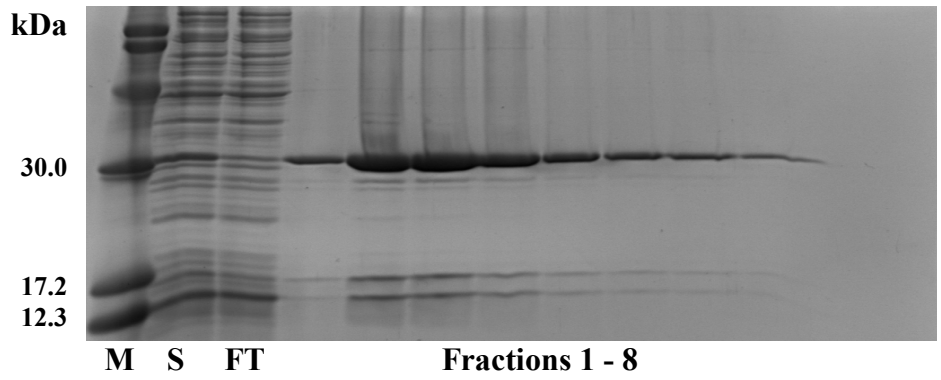

Figure 2.19 15 % SDS-PAGE analysis of DpnI purified from *E. coli* strain GM33 with protease inhibitor tablets and PMSF. M = molecular weight marker, S = supernatant, FT = flow through.

Expression in strain GM215 was poor, with little DpnI or impurity present. In the remaining strains, which all performed better than GM2929, a good quantity of DpnI was produced along with varying amounts of the two impurities. The two strains giving the highest proportion of intact DpnI were found to be GM33 and GM48. GM33 tended not to form a cohesive pellet upon centrifugation, instead remaining as a slurry which was difficult to manipulate. For this reason GM48 was chosen as the new preferred strain for DpnI overexpression. Typically 24 g of cell paste were obtained from a 5 L culture of *E. coli* strain GM48 harbouring plasmid pMMS495859. Approximately 25 mg of protein was obtained from a purification using 5 g of cell paste. After elution from the nickel column, DpnI was dialysed for two one hour periods into storage buffer containing 50 % glycerol and kept in frozen aliquots at a concentration of 2.3 mg ml $^{-1}$. The storage and purification buffers contained 400 mM sodium chloride. At lower salt concentrations the protein was observed to precipitate shortly after elution from the nickel column.

His_6-DpnI expressed in this way was incubated with unmethylated and methylated plasmid DNA as a rudimentary test of its activity. In parallel DpnI from a commercial source, New England Biolabs, was incubated with the same plasmids (Figure 2.20).

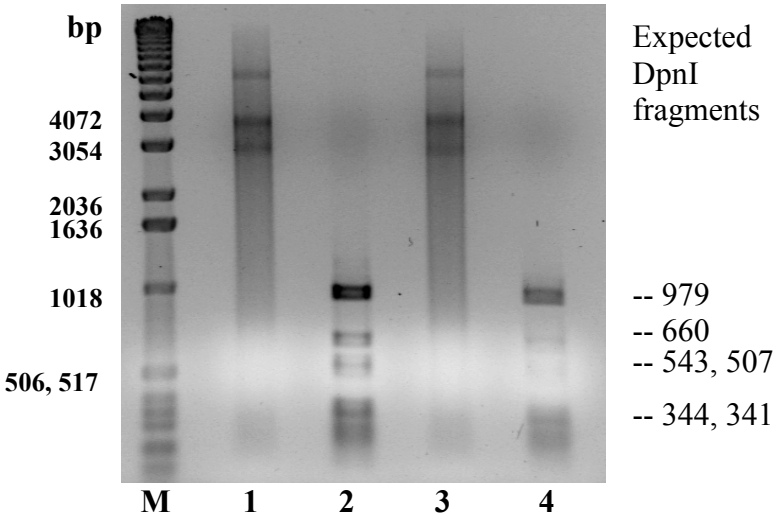

Figure 2.20 1 % AGE analysis of digests using commercial DpnI and His-DpnI expressed in GM48. M = DNA ladder, lanes 1 and 3 = Unmethylated plasmid pBadHisA (4102 bp) incubated with His_6-DpnI and commercial DpnI respectively. Lanes 2 and 4 = Methylated plasmid pMK171 (5114 bp) incubated with His_6-DpnI and commercial DpnI respectively, largest four expected fragments = 979, 660, 543, 507 bp.

His_6-DpnI displayed similar behaviour to its commercial counterpart, leaving the unmethylated plasmid intact but cleaving the methylated one into numerous fragments, the largest of which were of the expected sizes.

His_6-DpnI activity was measured as 0.38 ± 0.03 μmol mg^{-1} min^{-1}, which corresponds to a turnover of 12 ± 1 min^{-1} (J. McKelvie). Activity measurements were made using the optimised Dam methyltransferase assay principle which is discussed in the remaining part of this chapter (Figure 2.25). A fully methylated oligonucleotide substrate at a concentration of 30 nM was used. The His_6-DpnI was six times more active than commercial DpnI tested under the same conditions (0.06 ± 0.01 μmol mg^{-1} min^{-1}, J. McKelvie). Lacks and co-workers reported a specific activity of 0.03 μmol mg^{-1} min^{-1} for their DpnI (5). To make this measurement they used plasmid DNA, at a concentration of 4 nM, containing two fully methylated GATC sites. It is likely that the measured commercial DpnI activity was low because the enzyme had been stored for several weeks in solution at -20 °C. Whilst Lacks and co-workers stored their pure DpnI at -80 °C prior to use, their five step purification took three days to complete. This, along with the different substrates, may explain the lower activity of their DpnI compared to the His_6-DpnI which purified in just a few hours.

The unit definition of the commercial DpnI is the amount of the enzyme required to digest 1 µg of pBR322 DNA in 1 hour at 37 °C. One unit is equivalent to 0.12 pmol of commercial DpnI.

2.3 Design and optimisation of an assay for Dam activity

2.3.1 Oligonucleotide design 1

Early work on the optimisation of the Dam activity assay was carried out in collaboration with Dr R. Wood. Oligonucleotide 1 (ODN 1) was a 20 bp hairpin with an unmethylated GATC Dam recognition sequence in the middle and a fluorophore and quencher on opposite ends (Figure 2.21).

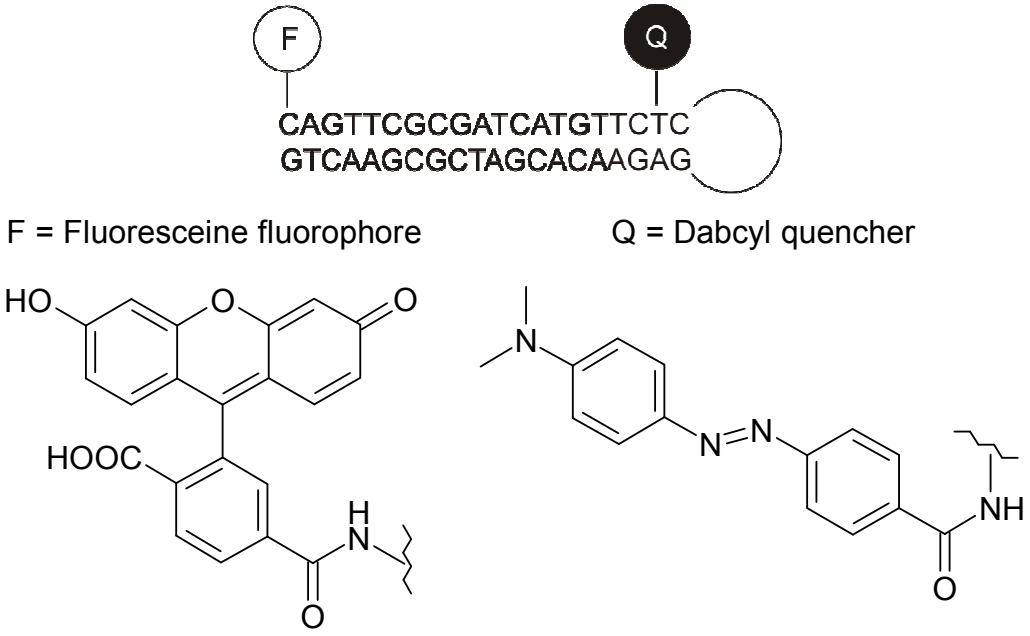

Figure 2.21 Oligonucleotide design 1. The fluorophore and quencher are attached to opposite ends of the same DNA strand containing the Dam recognition sequence. The hairpin loop is formed from a hexaethyleneglycol linker, denoted by a black curve.

The fluoresceine fluorophore has an absorption maxima at 494 nm and emission maxima at 517 nm. It exists predominantly as the dianion at the assay pH of 7.9 (18). The Dabcyl quencher has an absorption maxima at 475 nm but quenches effectively over a wide range of wavelengths including the 517 nm fluorescein emission maxima (19). Dabcyl is a dark quencher and returns to its ground electronic state through

nonradiative processes. FRET quenching efficiency for a fluorescein dabcyl pair has been measured as 80 % using a short oligonucleotide where the separation was 5 bases. When the fluorescein and dabcyl are in very close proximity static quenching is possible. The pair form a complex with altered absorption characteristics which can return to a ground electronic state without the emission of a photon. The efficiency of static quenching for a fluorescein dabcyl pair is 91 % (19).

Fluorescence timecourses of assays containing ODN 1, AdoMet, Dam and DpnI were measured in a plate reader (Figure 2.22). It was anticipated that methylation of ODN 1 by Dam and subsequent DpnI restriction would separate the FRET pair and give a measureable fluorescence increase.

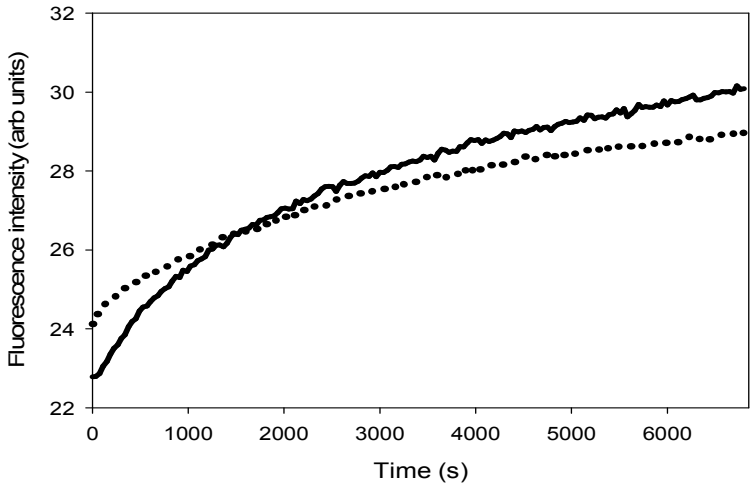

Figure 2.22 The fluorescence timecourse of Dam activity assays (triplicate averaged) using ODN 1. Assays contained AdoMet (500 µM), ODN 1 (25 nM), Dam (30 nM) and DpnI from a commercial source (2 µl, 40 Units (solid line), 0 Units (dotted line)).

A significant background fluorescence of 23-24 arb units was observed at the start of the assays and the signal increase specifically due to methyltransferase activity was small. The background increases in fluorescence may have been attributable to a contaminant in the Dam or changes in the meniscus of the assays throughout the experiment. During the course of the assays the meniscus developed a more pronounced upward curvature at the edges of the wells, which may have artificially changed the measured fluorescence of the solution.

The poor signal to background fluorescence was attributed to Dam instability and the remote positioning of fluorophore and quencher on opposite ends of ODN 1. A second oligonucleotide was designed to overcome the latter of these problems.

2.3.2 Oligonucleotide design 2

The fluorophore and quencher of oligonucleotide 2 (ODN 2) were positioned adjacent to one another on the same side of the Dam recognition sequence (Figure 2.23). Since FRET efficiency increases with decreasing distance and static quenching is more efficient than FRET it was reasoned that this would lower the background assay fluorescence, improving the signal to noise ratio. By necessity the oligonucleotide had to become much shorter. With the fluorophore and quencher on the same side of the DpnI cleavage site the assay was reliant on rapid melting of the cut oligonucleotide to separate them.

Figure 2.23 Oligonucleotide design 2. F and Q represent a fluorescein fluorophore and Dabcyl quencher respectively. The hairpin loop is formed by four unpaired thymine bases.

Assays containing AdoMet, Dam, DpnI and a range of ODN 2 concentrations were carried out. Background fluorescence was as expected much improved, as was the signal generated upon oligonucleotide cleavage (Figure 2.24).

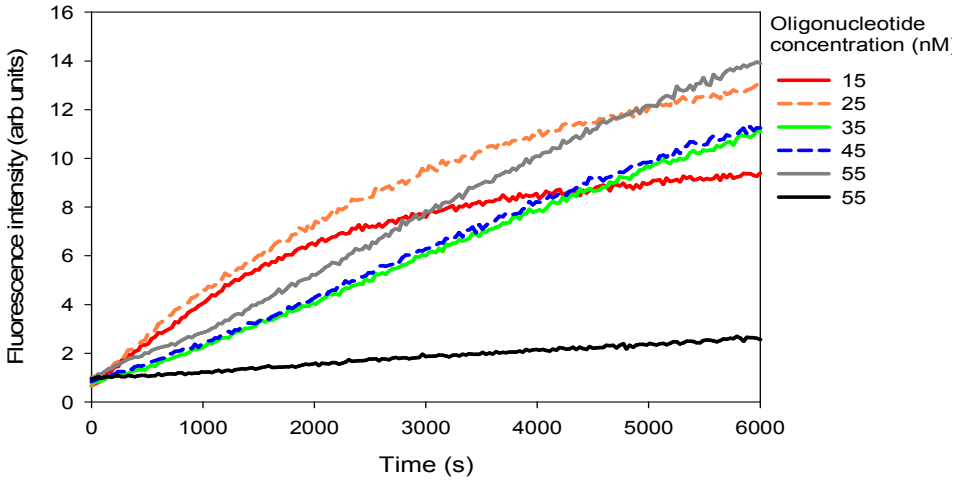

Figure 2.24 The fluorescence timecourse of Dam activity assays (triplicate averaged) using oligonucleotide design 2. Assays contained AdoMet (500 µM or 0 µM), ODN 2 15 nM (red), 25 nM (orange dash), 35 nM (green), 45 nM (blue dash), 55 nM (grey), 55 nM negative control (black), DpnI (1 µl, 20 U) and Dam (20 nM).

Fluorescence of the active assays was observed to increase significantly more than that of the negative controls. At low DNA concentrations, rates of fluorescence increase were highest at the start of the assay and then slowed, either as the substrate was exhausted or Dam inactivated. At higher DNA concentrations an unwanted phenomenon was observed. Rates of fluorescence increase were reduced and a lag phase appeared before the maximum rate was reached. An explanation for this lay in the fact that Dam had to methylate ODN 2 twice before it could be cut by DpnI and generate a fluorescence signal. Following the first methylation event, hemi-methylated ODN 2 was left in competition with the remaining unmethylated ODN 2 for Dam. The higher the starting ODN 2 concentration the less likely it was that the hemi-methylated oligonucleotide would find a free Dam active site. Li and co-workers developed an analogous Dam activity assay which used a DNA substrate requiring two methylations. It showed a similar phenomenon which they termed a ‘retention time’ (6). To overcome this drawback, and produce an assay that would permit in depth kinetic characterisation, a third oligonucleotide was designed.

2.3.3 Oligonucleotide design 3

The final version of the assay used oligonucleotide 3 (ODN 3), identical to its forerunner ODN 2 except for an extra methyl group on one of the central adenine bases (Figure 2.25).

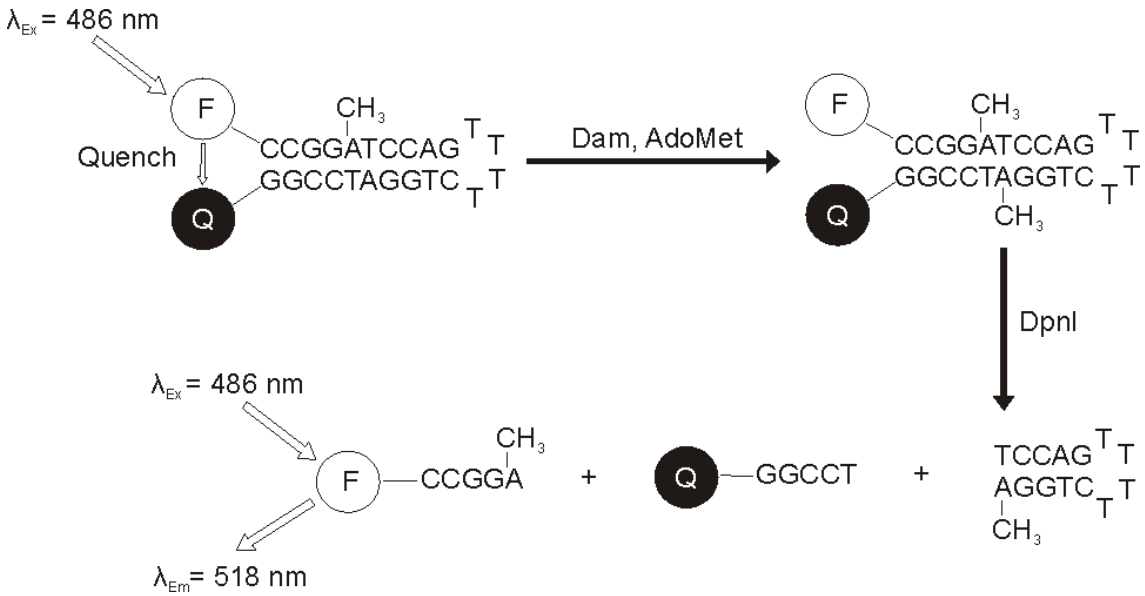

Figure 2.25 The real-time, fluorescence based, coupled enzyme assay for *Y. pestis* Dam activity.

It was reasoned that with a hemi-methylated DNA substrate, each turnover by Dam should lead to cleavage of the oligonucleotide by DpnI and an associated fluorescence increase.

Test assays at three Dam concentrations were carried out (Figure 2.26). Maximum rates of fluorescence increase occurred at the start of the timecourses despite the high DNA to Dam ratio which had caused a lag phase in the antecedent ODN 2 assay. Assay results suggested that the fluorescence signal generated was proportional to *Y. pestis* Dam activity. Doubling of the Dam concentration from 0.3 to 0.6 nM doubled the observed fluorescence increase over the first 180 s from 17.1 ± 2.1 to 34.7 ± 1.8 arb units s^{-1}. A background increase of 4.7 ± 1.7 arb units s^{-1} was measured in assays lacking Dam which was attributed to cleavage of the hemi-methylated oligonucleotide by DpnI.

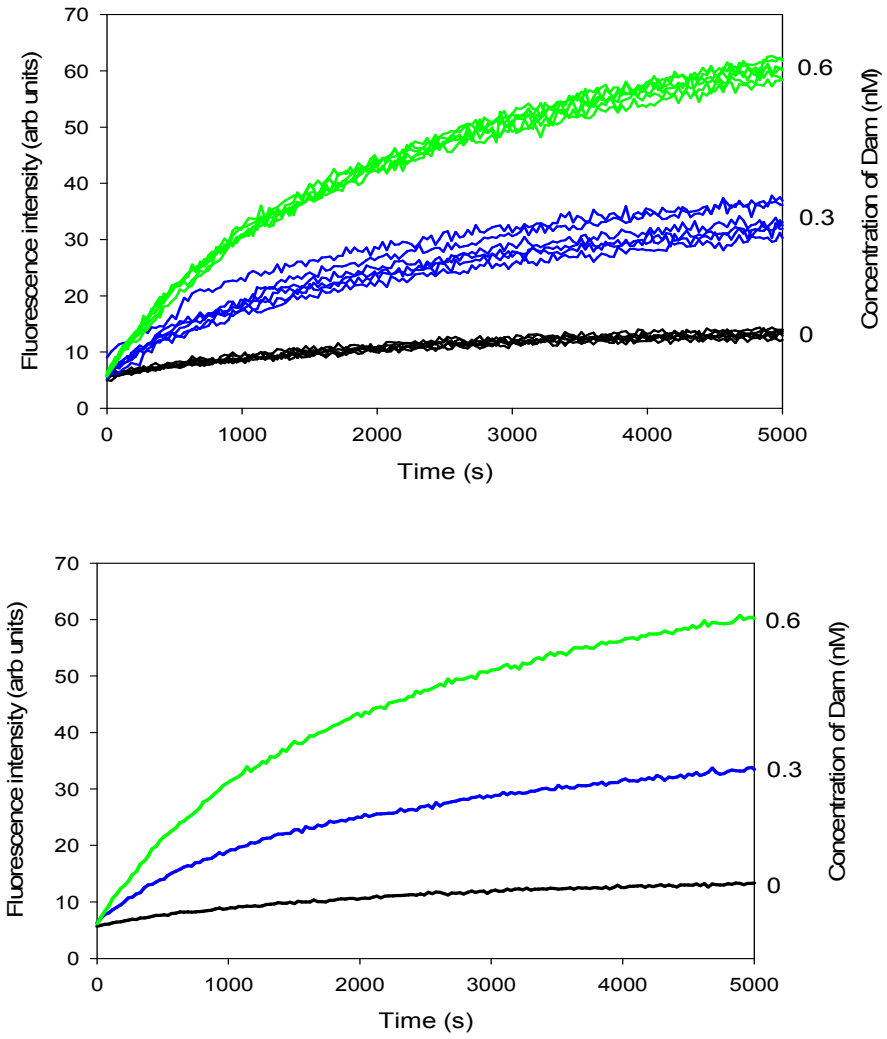

Figure 2.26 (Upper graph) Raw fluorescence timecourses of Dam activity assays using ODN 3. Assays contained DpnI (10 U), Dam (0 (black), 0.3 (blue) or 0.6 (green) nM), AdoMet (240 μM) and ODN 3 (33 nM). (Lower graph) Sextuplet averaged fluorescence timecourses. The instrument gain was 200, excitation and emission wavelengths were 486 and 518 nm respectively and the bandwidths were both 5 nm.

2.3.4 Optimisation of sodium chloride concentration

It is known that DpnI can cut hemi-methylated GATC sequences in DNA, but at a slower rate than fully methylated (20). Reports in the literature suggest that sodium chloride concentration plays a role in the specificity of DpnI for fully over hemi-methylated DNA (21,22). As sodium chloride concentration is increased DpnI must

compete with an increasing concentration of cations for binding sites on the DNA, reducing its binding affinity (23). Screening of the non-specific electrostatic attractive forces may have a more pronounced effect on hemi-methylated DNA binding since there are likely to be fewer specific hydrogen bonding and hydrophobic interactions with the DpnI (24).

To find the optimal salt concentrarion which would minimise background cleavage, without inhibiting *Y. pestis* Dam, a series of assays were set up. Assay buffer, which already contained 10 mM Mg^{2+} and 50 mM K^{+}, was supplemented with between 0 and 150 mM NaCl (Figure 2.27). For each set of activity assays at a particular sodium chloride concentration a set of negative controls without Dam was also run. Rates of fluorescence change caused by Dam activity were presumed to be the total rate of fluorescence change minus the DpnI background as determined in the negative control.

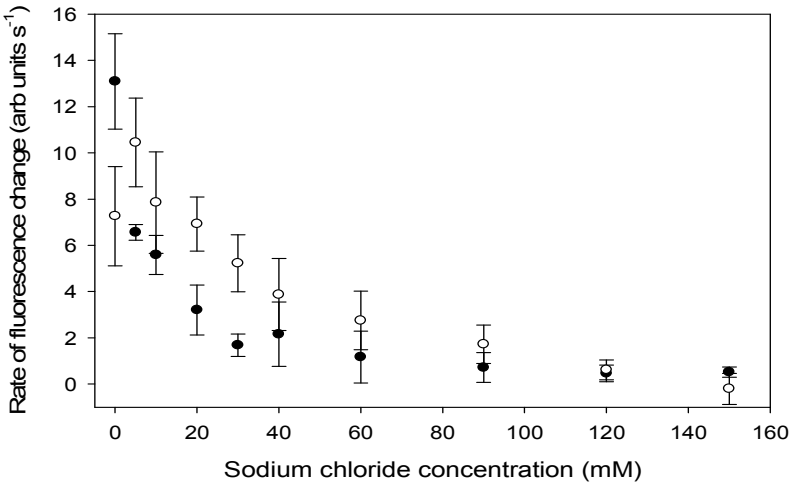

Figure 2.27 The effect of sodium chloride concentration on the apparent activity of Dam (○) and DpnI (●) (duplicate assays averaged). Assays (200 µl) contained Dam (0 or 0.6 nM), DpnI (10 U), AdoMet (30 µM), oligonucleotide 3 (30 nM) and were supplemented with the specified amount of sodium chloride.

As sodium chloride concentration increased, DpnI cleavage of the hemi-methylated DNA fell sharply. With 20 mM sodium chloride there was 75 % less background cleavage compared to unsupplemented assays. Unwanted DpnI activity continued to fall and was effectively absent at sodium chloride concentrations above 100 mM. Dam activity was also reduced by increased salt concentration but this effect was only

apparent above 20 mM sodium chloride. This concentration was therefore felt to be optimal for achieving the best signal to background ratio in the assay.

2.3.5 The effect of excess Dam or DpnI in the assay

Because this was a coupled enzyme assay, measurement of Dam activity relied on DpnI being present in excess, ensuring methylation was rate limiting. Fluorescence assays were conducted to examine the effect of varying the concentration of the two enzymes relative to each other. A set of assays containing 2 nM Dam and 0 – 10 U of DpnI were run, along with negative controls lacking Dam (Figure 2.28, upper graph).

Highest initial increases in fluorescence tended to be seen in the assays and negative controls with the most DpnI. At these high DpnI concentrations the fluorescence timecourses had the expected downward curvature attributable to progressive methyltransferase inactivation. By contrast, at low DpnI concentration the rate of fluorescence change increased as the assays progressed. This was due to the accumulation of fully methylated ODN 3 in the opening minutes of the assay, driving the DpnI active sites towards saturation point. The two types of curve were typified by the background subtracted fluorescence timecourses of the assays with 1 and 10 U of DpnI (Figure 2.28, lower graph).

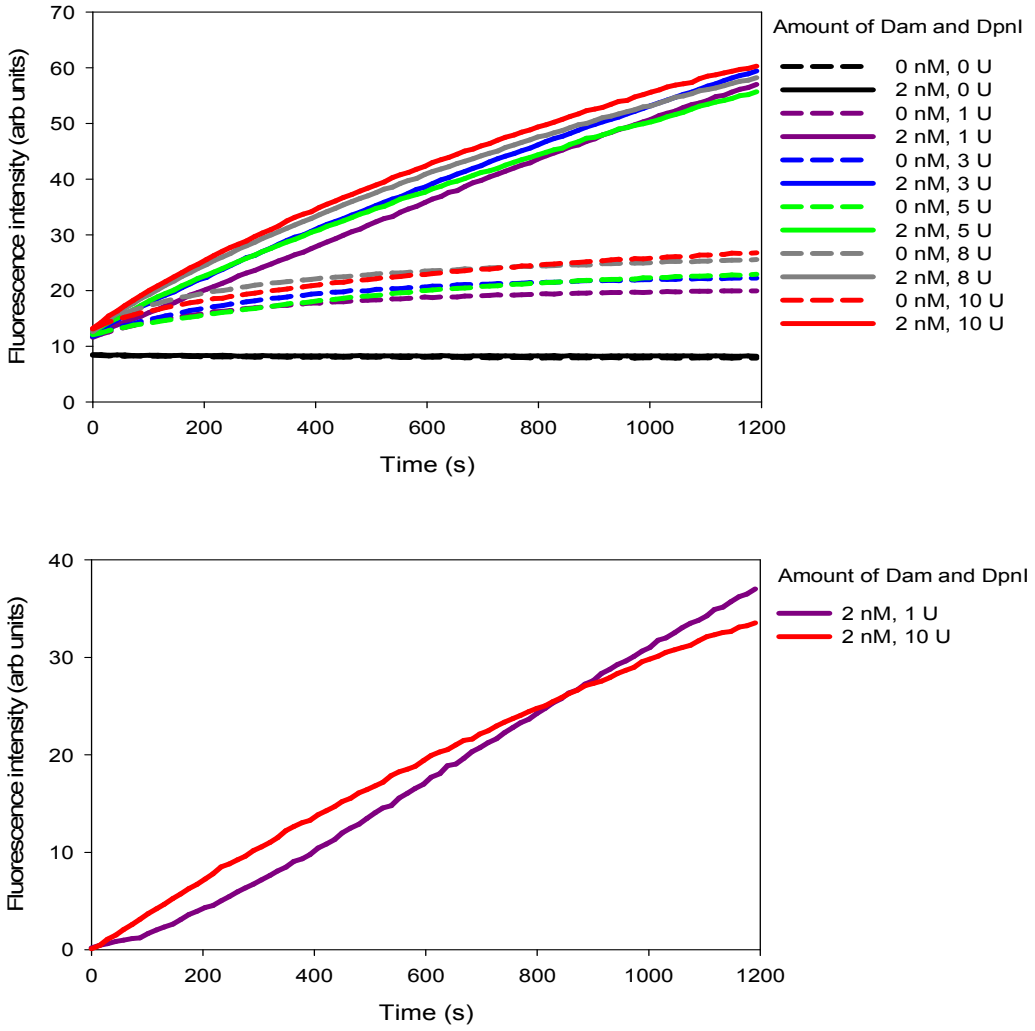

Figure 2.28 Fluorescence timecourses of Dam activity assays (triplicate averaged). (Upper Graph) Assays contained DpnI (0 (black), 1 (purple), 3 (blue), 5 (green), 8 (grey) or 10 U (red)), oligonucleotide 3 (33 nM), Dam 0 or 2 nM (dashed and solid lines respectively) and AdoMet (5 μM). (Lower Graph) Timecourses for assays containing 1 U (purple) and 10 U (red) of DpnI with background subtracted.

The complementary set of experiments with variable Dam and fixed DpnI concentration were carried out. DpnI was fixed at 1 U in all of the assays whilst the Dam concentration varied between 0 and 4 nM (Figure 2.29).

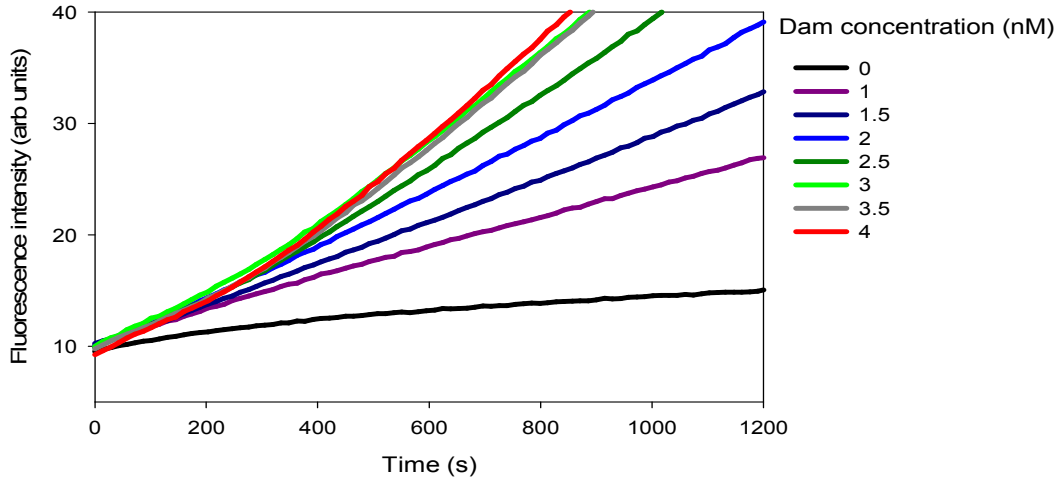

Figure 2.29 Fluorescence timecourses of Dam activity assays (triplicate averaged). Assays contained Dam (0 (black), 1 (purple), 1.5 (dark blue), 2 (light blue), 2.5 (dark green), 3 (light green), 3.5 (grey) or 4 nM (red)), DpnI (1 U), ODN 3 (33 nM), and AdoMet (5 μM).

Because the DpnI concentration was low, all of the Dam concentrations assayed yielded fluorescence timecourses with some upward curvature. At higher Dam concentrations the curvature became more pronounced. Raising the Dam concentration from 1 – 3 nM increased steady state concentrations of the fully methylated DpnI substrate leading to faster ODN 3 cleavage. Increasing Dam concentration above 3 nM had little effect on the assays, presumably because there was already enough to completely saturate the DpnI active sites with methylated oligonucleotide.

2.4 Summary and conclusions

Y. pestis Dam was expressed and purified from *E. coli* strain GM215 harbouring plasmid pRJW421307. Previous work by Dr. R. Wood had shown the enzyme to be unstable, even at 4 °C over long periods of time. This problem was surmounted by use of a short purification procedure in which the protein was kept as cold as possible. Enough Dam was obtained to permit development of the activity assay.

The restriction enzyme DpnI was expressed and purified from *E. coli* strain GM48 harbouring plasmid pMMS495859. Evidence had suggested that DpnI was subject to proteolytic degradation during purification. Choice of an appropriate expression strain and use of protease inhibitors were therefore necessary to ensure production of high quality restriction endonuclease.

A real-time, fluorescence based, coupled enzyme assay for *Yersinia pestis* Dam was successfully developed. Two design features of the oligonucleotide were found to be important for assay efficacy. Firstly, the position of the fluorophore and quencher pair adjacent to one another on the hairpin stem, which leads to a large fluorescence change upon oligonucleotide cleavage. Secondly, the methylation pattern, which ensures that only one methylation per oligonucleotide is necessary to form the substrate which is rapidly cleaved by DpnI. Other researchers developing a similar *E. coli* Dam activity assay did not make this final development (6).

Specificity of the DpnI restriction enzyme for fully methylated substrate was enhanced by optimisation of salt concentration. Provided that sufficient amounts of DpnI were used, the real-time fluorescence increases observed in the assay were found to be proportional to the amount of methyltransferase present. Fluorescence timecourses in which this was not the case and DpnI was rate limiting could be identified by a characteristic upward curvature.

2.5 References

1. Biggins, J. B., Prudent, J. R., Marshall, D. J., Ruppen, M., and Thorson, J. S. (2000) *Proc. Natl. Acad. Sci* **97**, 13537-13542
2. Lilley, D. M. J., and Wilson, T. J. (2000) *Curr Opin Chem Biol* **4**, 507-517
3. Gordon, G. W., Berry, G., Liang, X. H., Levine, B., and Herman, B. (1998) *Biophys J* **74**, 2702-2713
4. Lacks, S. A., and Greenberg, B. (1975) *J Biol Chem* **250**, 4060-4066
5. de la Campa, A. G., Springhorn, S. S., Kale, P., and Lacks, S. A. (1988) *J Biol Chem* **263**, 14696-14702
6. Li, J., Yan, H., Wang, K., Tan, W., and Zhou, X. (2007) *Anal Chem* **79**, 1050-1056
7. Roberts, R. J., Belfort, M., Bestor, T., Bhagwat, A. S., Bickle, T. A., Bitinaite, J., Blumenthal, R. M., Degtyarev, S., Dryden, D. T., Dybvig, K., Firman, K., Gromova, E. S., Gumport, R. I., Halford, S. E., Hattman, S., Heitman, J., Hornby, D. P., Janulaitis, A., Jeltsch, A., Josephsen, J., Kiss, A., Klaenhammer, T. R., Kobayashi, I., Kong, H., Kruger, D. H., Lacks, S., Marinus, M. G., Miyahara, M., Morgan, R. D., Murray, N. E., Nagaraja, V., Piekarowicz, A., Pingoud, A., Raleigh, E., Rao, D. N., Reich, N., Repin, V. E., Selker, E. U., Shaw, P. C., Stein, D. C., Stoddard, B. L., Szybalski, W., Trautner, T. A., Van Etten, J. L., Vitor, J. M., Wilson, G. G., and Xu, S. Y. (2003) *Nucleic Acids Res* **31**, 1805-1812
8. Hyman, H. C., and Honigman, A. (1986) *J Mol Biol* **189**, 131-141
9. Studier, F. W., and Moffatt, B. A. (1986) *J Mol Biol* **189**, 113-130
10. Marinus, M. G. (1973) *Mol Gen Genet* **127**, 47-55
11. Marinus, M. G., and Morris, N. R. (1973) *J Bacteriol* **114**, 1143-1150
12. Arraj, J. A., and Marinus, M. G. (1983) *J Bacteriol* **153**, 562-565
13. Yanisch-Perron, C., Vieira, J., and Messing, J. (1985) *Gene* **33**, 103-119
14. Durfee, T., Nelson, R., Baldwin, S., Plunkett, G., 3rd, Burland, V., Mau, B., Petrosino, J. F., Qin, X., Muzny, D. M., Ayele, M., Gibbs, R. A., Csorgo, B., Posfai, G., Weinstock, G. M., and Blattner, F. R. (2008) *J Bacteriol* **190**, 2597-2606
15. Herman, G. E., and Modrich, P. (1982) *J Biol Chem* **257**, 2605-2612
16. Lehman, I. R., Roussos, G. G., and Pratt, E. A. (1962) *J Biol Chem* **237**, 819-828
17. Lehman, I. R., Roussos, G. G., and Pratt, E. A. (1962) *J Biol Chem* **237**, 829-833
18. Margulies, D., Melman, G., and Shanzer, A. (2005) *Nat Mater* **4**, 768-771
19. Marras, S. A., Kramer, F. R., and Tyagi, S. (2002) *Nucleic Acids Res* **30**, e122
20. Hanish, J., and McClelland, M. (1991) *Nucleic Acids Res* **19**, 829-832
21. Wobbe, C. R., Dean, F., Weissbach, L., and Hurwitz, J. (1985) *Proc. Natl. Acad. Sci* **82**, 5710-5714
22. Sanchez, J. A., Marek, D., and Wangh, L. J. (1992) *J Cell Sci* **103**, 907-918
23. Dryden, D. T. F. (1999) Bacterial DNA Methyltransferases. In: Cheng, X., and Blumenthal, R. M. (eds). *S-Adenosylmethionine-Dependent Methyltransferases: Structures and Functions*, World Scientific, Singapore, New Jersey, London, Hong Kong
24. Horton, J. R., Liebert, K., Hattman, S., Jeltsch, A., and Cheng, X. (2005) *Cell* **121**, 349-361

Chapter 3:- Kinetic analysis of *Y. pestis* Dam and validation of the assay

3.1 Introduction

The fluorescence based assay which had been developed appeared to provide a real-time measure of Dam activity. To gain additional evidence for this and demonstrate functionality, the assay was used to perform a kinetic analysis of *Y. pestis* Dam with its two substrates. A study of the known Dam inhibitor, *S*-adenosylhomocysteine, was carried out to demonstrate that the assay was also useful for probing the kinetics of enzyme inhibition. Furthermore we sought to show that the assay was suitable for high throughput screening of compound libraries by validating it in 96-well format. This chapter describes the use of the assay to study the kinetics of methylation by *Y. pestis* Dam and its validation for high throughput screening.

3.2 Kinetic analysis of *Y. pestis* Dam

3.2.1 Calibration of oligonucleotide fluorescence

In order that fluorescence increases measured with the assay might be related to methylation rate, a calibration experiment was carried out. Known concentrations of oligonucleotide FM ODN 3, a fully methylated analogue of the DNA substrate used in the assay, were subjected to cleavage with DpnI. Fluorescence of the DNA solutions was measured before and after cleavage (Figure 3.1). Subtraction of the pre-cleavage from post-cleavage fluorescence gave the increase following restriction by DpnI (Figure 3.1, lower graph). A calibration plot of fluorescence increase against DNA concentration was fitted well by a straight line of gradient 9268 ± 294 arbitrary units nM^{-1} ($R^2 = 0.996$). This calculated gradient allowed the conversion of fluorescence increases, measured under the same conditions, into amount of substrate turned over.

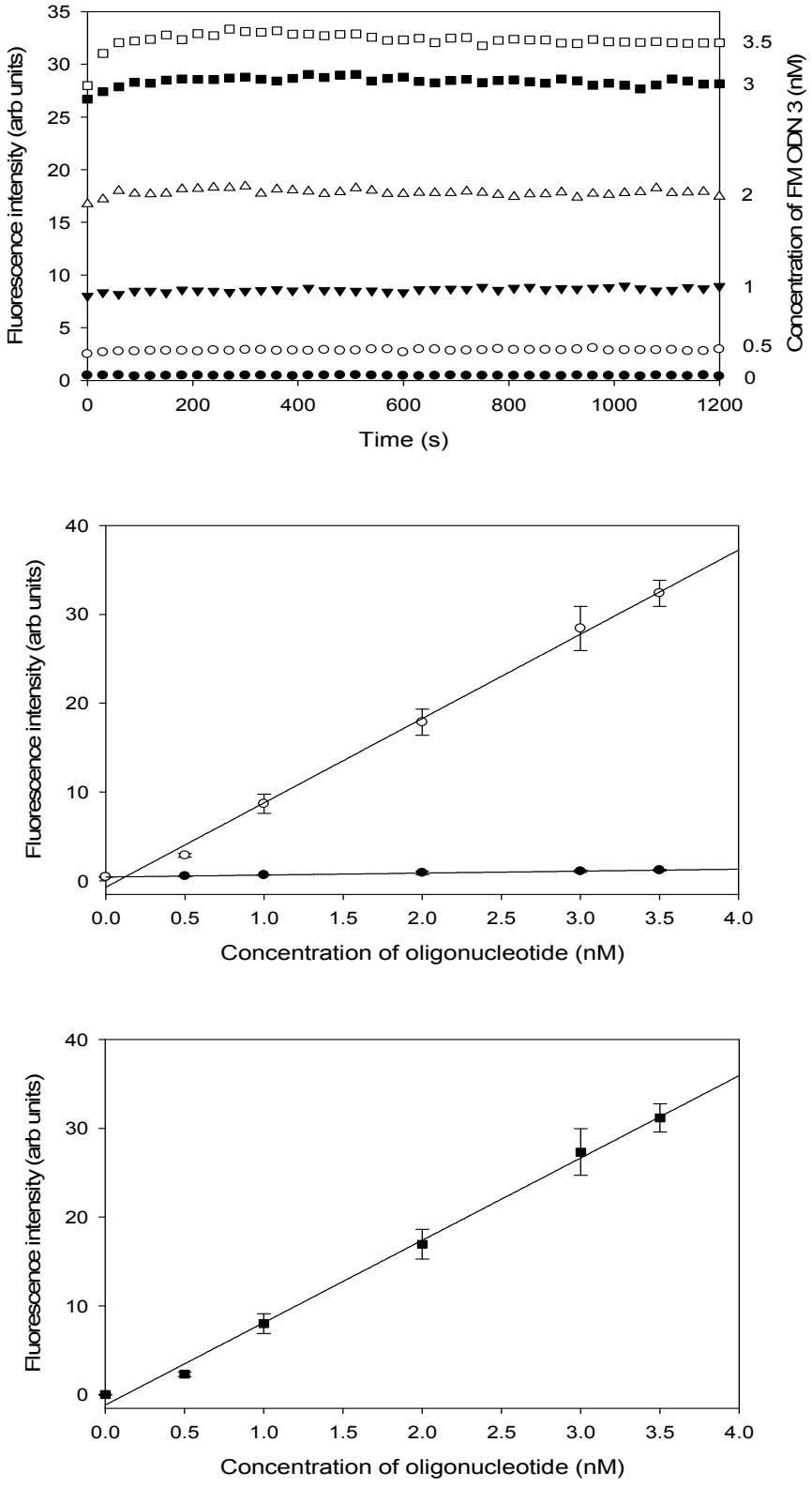

Figure 3.1 Calibration plots showing the relationship between fluorescein fluorescence and oligonucleotide concentration (gain 200, $\lambda_{excitation}$ = 486 nm, $\lambda_{emission}$ = 518 nm, bandwidths 5 nm). Solutions contained 0, 0.5, 1, 2, 3 and 3.5 nM FM ODN 3. (Upper

graph) averaged raw fluorescence data from wells containing FM ODN 3 exposed to 10 U of DpnI. (Middle graph) fluorescence of FM ODN 3 before (filled circles) and after (open circles) exposure to restriction enzyme DpnI. (Lower graph) Increase in FM ODN 3 fluorescence following exposure to DpnI.

Using the calibration plot and the standard deviation in the plate reader fluorescence measurements, the assay sensitivity was estimated. In each of the six assays containing 3.5 nM FM ODN 3, the standard deviation in the fluorescence measurements between 600 and 1200 s was on average 579 arbitrary units (three standard deviations = 1738 arbitrary units). It was assumed that DpnI had cleaved all of the oligonucleotide before 600 s and that variations in the fluorescence measurements were due to the imprecision of the plate reader (Figure 3.1, upper graph). Since three standard deviations represents a 99.73 % confidence limit it may be said that there is only a 0.27 % chance that a measured fluorescence change of 1738 arbitrary units in a single assay is due to plate reader imprecision. This fluorescence increase corresponds to cleavage of 37.5 fmol of oligonucleotide. Combining several replicate measurements increases the assay sensitivity. From the same data it was estimated that averaging measurements from six assays increases the sensitivity to 13.2 fmol. Roth and Jeltsch have reported a radioactive assay capable of measuring the incorporation of 0.8 fmol of methyl groups into DNA (1). In theory, the fluorescence based assay could be optimised in 384 well format to detect as little as 0.17 fmol of DNA methylation and cleavage. This theoretical limit is based on the typical sensitivity of modern plate readers (BMG POLARstar Omega 0.2 fmol / well fluorescein, Tecan Infinite M1000 0.17 fmol / well fluorescein).

3.2.2 Investigation of *Y. pestis* Dam stability

During purification, *Y. pestis* Dam was observed to readily inactivate so it was of interest to study the kinetics of this process and the effect of the substrates upon it. Dam was incubated at 30 °C for between 0 and 500 seconds under three sets of conditions; without substrates, with 30 nM ODN 3 or with 120 μM AdoMet. Aliquots of enzyme were taken periodically and assayed for activity. Activity data were fitted to a single, two parameter exponential decay, $y = ae^{-k_{inact}t}$, to obtain values for the rate of Dam inactivation (k_{inact}) and subsequently half-life, since $t_{1/2} = \ln 2 / k_{inact}$ (Figure 3.2).

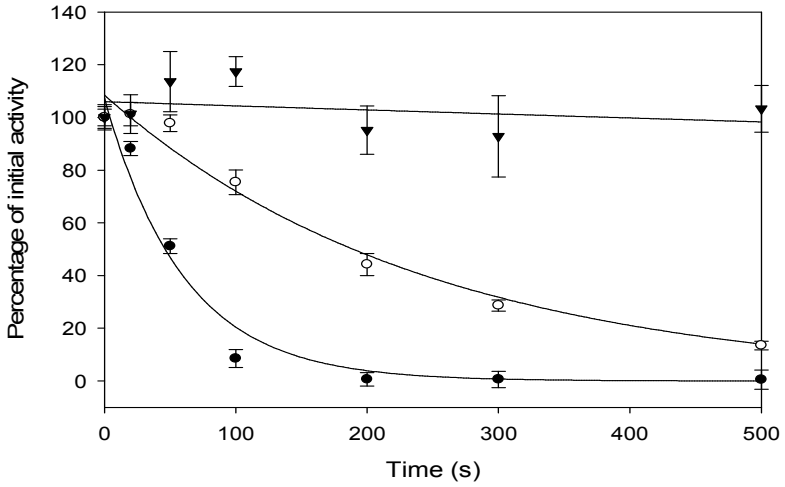

Figure 3.2. A plot showing the measured activity of *Y. pestis* Dam following pre-incubation at 30 °C for between 0 and 500 seconds. Dam was incubated without substrates (filled circles), with 120 μM AdoMet (open circles) and with 30 nM oligonucleotide (filled triangle). Activity is expressed as percentage activity of Dam which was not pre-incubated.

Dam was highly unstable when incubated alone at 30 °C, with a half-life of 42.5 ± 7.5 s (Figure 3.2). Protection of enzyme activity was afforded by both of the substrates in solution. AdoMet increased the half-life four fold to 170.5 ± 16.5 s but DNA had the greater effect giving a half-life of over 2300 s. Dam is not the first methyltransferase which has been observed to be unstable. The *Caulobacter crescentus* cell cycle regulated adenine MTase (CcrM) was found to have a half life of 300 s at 30 °C and was also stabilised by DNA (2). A truncated *S. typhimuirium* Dam mutant has also displayed temperature sensitivity (3).

3.2.3 The effect of *S*-adenosylmethionine concentration on Dam activity

The dependence of Dam activity on AdoMet concentration was measured in sets of assays at two different temperatures, 30 °C and 37 °C. Dam activity was measured at seven different concentrations in triplicate (Figure 3.3). For simplicity the DNA substrate was kept at a fixed concentration that was assumed to be saturating (33 nM).

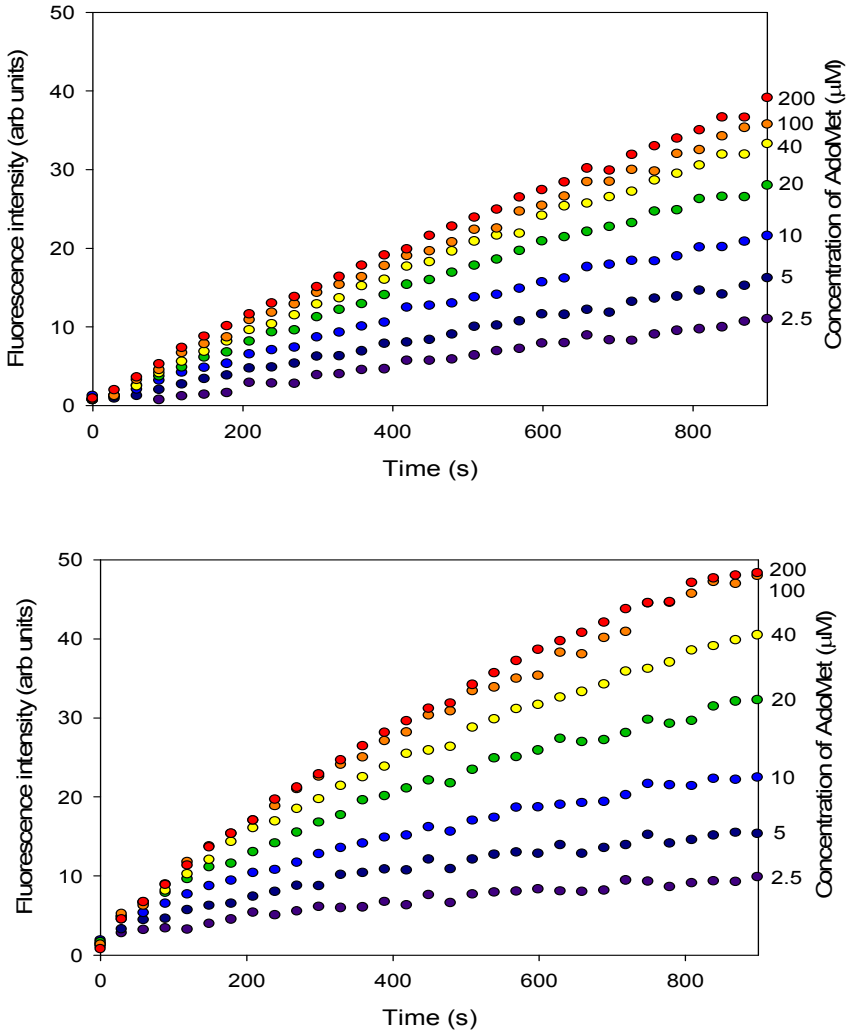

Figure 3.3 Fluorescence timecourses from Dam activity assays used to measure K_M ^{AdoMet}. Data shown is averaged from triplicate assays. Assays contained 33 nM ODN 3, 1 nM Dam, 10 U DpnI and 2.5, 5, 10, 20, 40, 100 and 200 µM AdoMet, (upper graph) 30 °C, (lower graph) 37 °C.

Fluorescence increases due to methylation were faster at 37 °C than 30 °C however the methylation rate was seen to reduce over the timecourse at the higher temperature, indicating a higher rate of enzyme inactivation. At both temperatures, methylation rates were increased by higher AdoMet concentrations. Plots of the methylation rate against AdoMet concentration were in accordance with a Michaelis-Menten mechanism of enzyme action, ignoring the effect of DNA concentration (Figure 3.4, Figure 3.5) (4).

$$\mathrm{E} + \mathrm{S} \underset{k_{-1}}{\overset{k_1}{\rightleftharpoons}} \mathrm{ES} \xrightarrow{k_2} \mathrm{P} \qquad (1)$$

$$v = k_2[\mathrm{ES}] \qquad (2)$$

$$\frac{\mathrm{d}[\mathrm{ES}]}{\mathrm{dt}} = k_1[\mathrm{E}][\mathrm{S}] - k_{-1}[\mathrm{ES}] - k_2[\mathrm{ES}] = 0 \qquad (3)$$

$$[\mathrm{ES}] = \left(\frac{k_1}{k_{-1} + k_2}\right)[\mathrm{E}][\mathrm{S}] \qquad (4)$$

$$[\mathrm{ES}] = \frac{[\mathrm{E}]_0}{1 + \left(\frac{k_{-1} + k_2}{k_1}\right)\frac{1}{[S]_0}} \qquad (5)$$

$$v = \frac{k_2[\mathrm{E}]_0}{1 + \left(\frac{k_{-1} + k_2}{k_1}\right)\frac{1}{[S]_0}} \qquad (6)$$

$$v = \frac{v_{\max}[\mathrm{S}]_0}{K_\mathrm{M} + [\mathrm{S}]_0} \qquad (7)$$

Figure 3.4 Derivation of the Michaelis-Menten equation from the Michaelis-Menten mechanism of enzyme action. In this mechanism an enzyme substrate complex is formed first. The substrate is either then released from the complex or converted into product. The rate of product formation is given by equation (2). Using the steady state approximation (3) it is possible to obtain equation (4) which gives the concentration of enzyme substrate complex in terms of the free enzyme and substrate concentrations. Using the assumptions that $[\mathrm{E}]_0 = [\mathrm{E}] + [\mathrm{ES}]$ and $[\mathrm{S}] \approx [\mathrm{S}]_0$ where a large excess of substrate over enzyme is used equation (5) may be obtained. Substituting this expression for [ES] into equation (2) gives equation (6), the Michaelis-Menten equation. Using the fact that $V_{max} = k_2[\mathrm{E}]_0$ and the Michaelis constant $K_\mathrm{M} = (k_{-1}+k_2)/k_1 = [\mathrm{E}][\mathrm{S}]/[\mathrm{ES}]$ the Michaelis-Menten equation may be re-written (7).

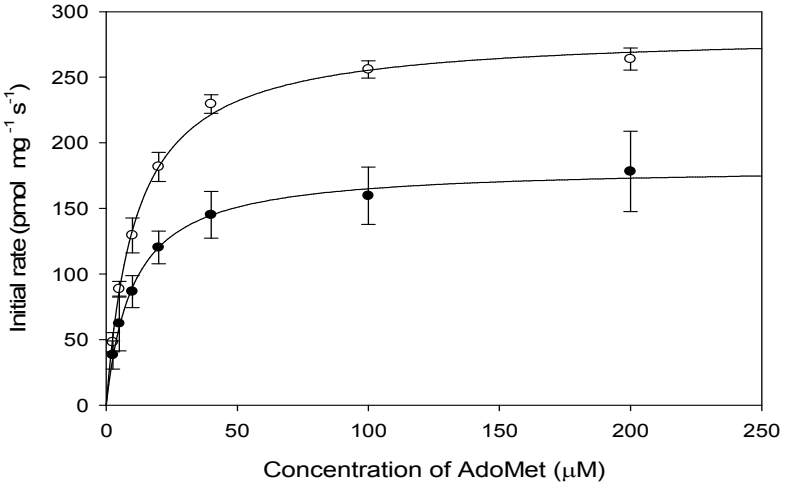

Figure 3.5 The dependence of Dam activity on AdoMet concentration at 30 °C (filled circles) and 37 °C (open circles). Initial rate measurements were based on the first 180 s of the fluorescence timecourses.

Data were fitted to the Michaelis-Menten equation ($v = V_{max}[\text{AdoMet}] / (K_M^{\text{AdoMet}} + [\text{AdoMet}])$) to obtain values for K_M^{AdoMet} and k_{cat}. At 37 °C, K_M^{AdoMet} and k_{cat} were found to be 11.3 ± 0.6 μM and 0.55 ± 0.01 min^{-1} (V_{max} = 284.3 ± 4.3 pmol mg^{-1} s^{-1}) respectively. At the lower temperature of 30 °C, K_M^{AdoMet} and k_{cat} were found to be 10.3 ± 0.7 μM and 0.35 ± 0.01 min^{-1} (V_{max} = 181.9 ± 3.3 pmol mg^{-1} s^{-1}) respectively.

This non-linear curve fitting method of K_M determination was used because it was simple and avoided the plotting of reciprocals which can bias data. The 37 °C rate data was however also analysed with Lineweaver-Burk, Eadie-Hofstee and Hanes-Woolf plots to allow a comparison of the respective K_M and V_{max} values (Figure 3.6, Figure 3.7, Figure 3.8). Within error all of these alternative plots yielded the same V_{max} and K_M^{AdoMet} as obtained from the fit of the Michaelis-Menten equation to the data. The Lineweaver-Burk and Hanes-Woolf plots gave the highest and lowest values for the K_M respectively. On both of these plots the data points were unevenly distributed and the K_M was derived from extrapolation of the data to the x-axis.

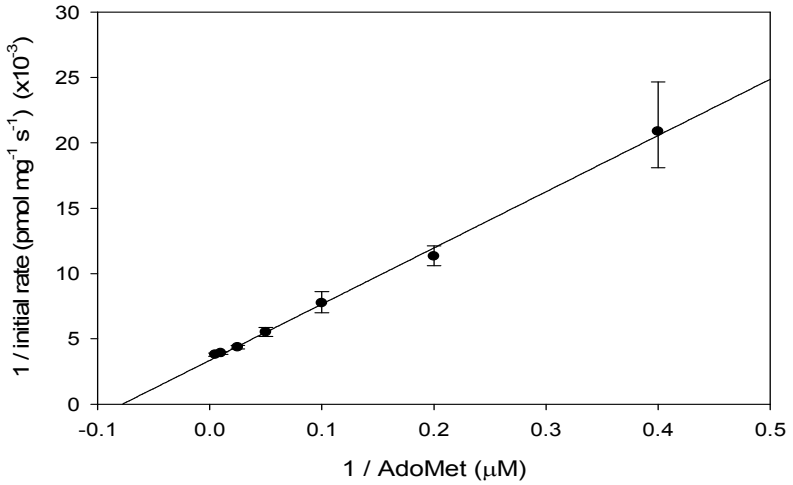

Figure 3.6 A Lineweaver-Burk plot of the Dam activity data used to determine K_M ^{AdoMet} at 37 °C (R^2 = 0.99). The x-axis intercept = -1 / K_M ^{AdoMet}. K_M ^{AdoMet} was determined as 12.6 ± 1.1 μM from this intercept. The y-axis intercept = 1 / V_{max}. From this intercept V_{max} was determined as 294.1 ± 18.4 pmol mg^{-1} s^{-1}.

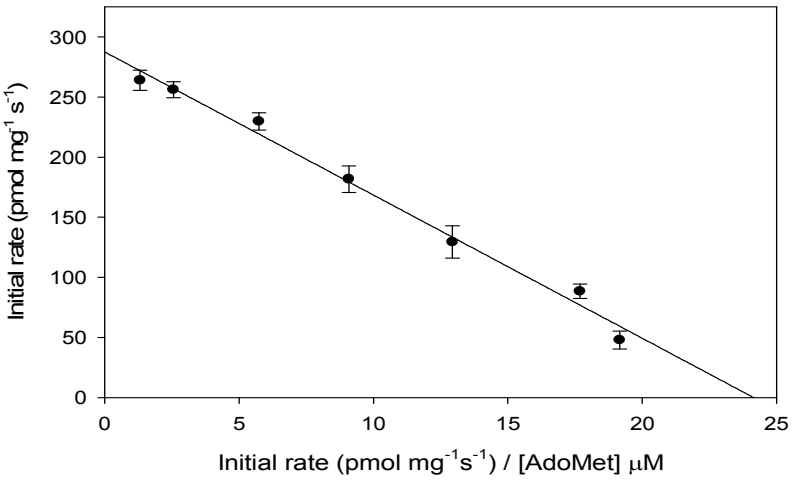

Figure 3.7 An Eadie-Hofstee plot of the Dam activity data used to determine K_M ^{AdoMet} at 37 °C (R^2 = 0.99). The gradient of the line = - K_M ^{AdoMet}. K_M ^{AdoMet} was determined as 11.9 ± 0.6 μM. The y-axis intercept is equal to V_{max} which was determined as 287.5 ± 6.5 pmol mg^{-1} s^{-1}.

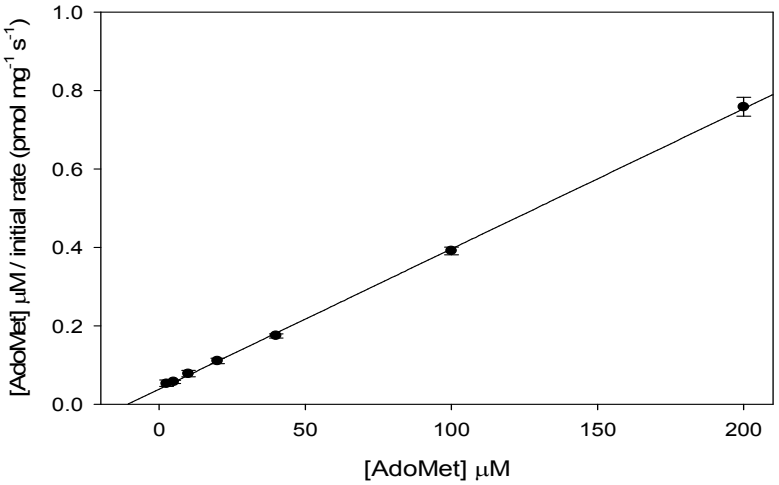

Figure 3.8 A Hanes-Woolf plot of the Dam activity data used to determine K_M ^{AdoMet} at 37 °C. The x-axis intercept = - K_M ^{AdoMet}. K_M ^{AdoMet} was determined as 10.6 ± 0.8 µM. The gradient of the line = 1 / V_{max}. From the gradient V_{max} was determined as 277.8 ± 2.3 pmol mg^{-1} s^{-1}.

3.2.4 The effect of DNA concentration on Dam activity

The dependence of Dam activity on oligonucleotide concentration was studied in a set of assays at 37 °C. Methylation rates were measured in triplicate at seven different oligonucleotide concentrations. For simplicity the AdoMet was kept at a fixed saturating concentration of 120 µM. Fluorescence increases obtained from the assays were small and quickly levelled off throughout the timecourse (Figure 3.9). This fits in with previous observations that the methyltransferase was unstable without DNA. Fluorescence increases were greatest in the assays which contained the highest concentrations of DNA.

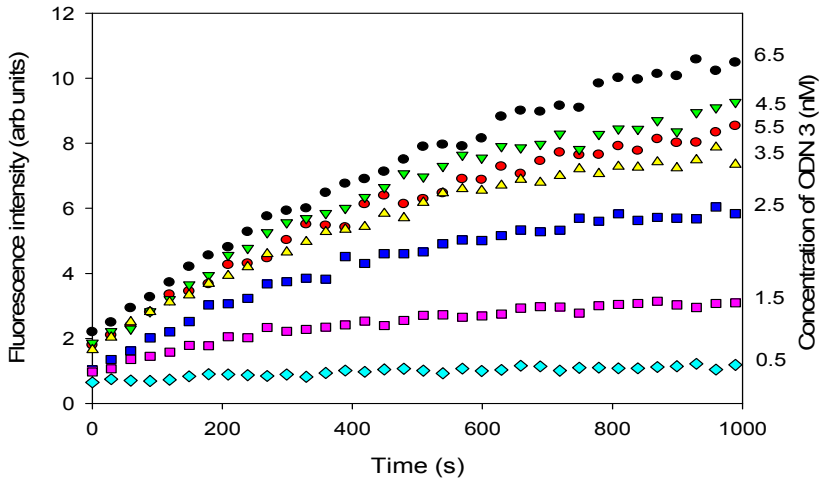

Figure 3.9 Fluorescence timecourses from Dam activity assays used to measure K_M DNA. Data shown is averaged from triplicate assays. Assays contained 0.31 nM Dam, 10 U DpnI, 120 µM AdoMet and 0.5, 1.5, 2.5, 3.5, 4.5, 5.5 and 6.5 nM ODN 3.

Methylation rate was plotted against concentration of ODN 3 (Figure 3.10). Data were fitted to the Michaelis-Menten equation to obtain a value for $K_M{}^{DNA}$ which was found to be 3.4 ± 1.8 nM. The large error in this value is due to the relatively poor fit of the data to the equation (R^2 = 0.91) which can be attributed to the instability of the enzyme under the assay conditions. At low DNA concentration the assay will tend to underestimate methyltransferase turnover.

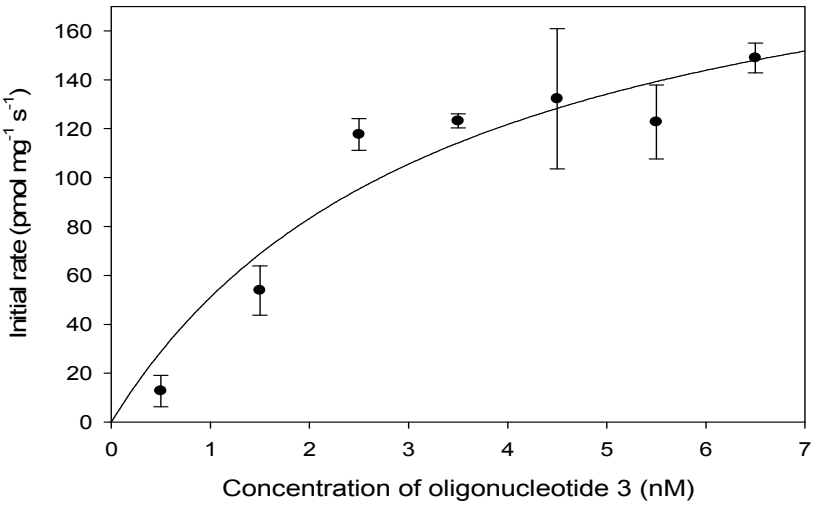

Figure 3.10 The dependence of Dam activity on DNA concentration at 37 °C. Initial rate measurements were based on the first 180 s of the fluorescence timecourses.

3.2.5 Inhibition of Dam by *S*-adenosylhomocysteine

To demonstrate the ability of the assay to probe the kinetics of enzyme inhibition, experiments were carried out using AdoHcy, a known Dam inhibitor. AdoHcy, an end product of the Dam catalysed reaction is competitive with the AdoMet substrate (Figure 3.11).

$$E + S \rightleftharpoons ES \longrightarrow P \qquad (1)$$

$$E + I \rightleftharpoons EI \qquad (2)$$

$$v = \frac{v_{max}[S]_0}{K_M\left(1+\frac{[I]}{K_i}\right)+[S]_0} \qquad (3)$$

Figure 3.11 Modification of the Michaelis-Menten mechanism of enzyme action by a competitive inhibitor. The enzyme can bind the substrate to form the enzyme substrate complex (1) or the inhibitor to form an unproductive enzyme inhibitor complex (2). An equilibrium exists between E, ES and EI. The apparent K_M of the enzyme and substrate = $K_M(1 +([I]/K_i))$.

With the goal of determining K_i^{AdoHcy}, assays were carried out with seven inhibitor concentrations at seven AdoMet concentrations (Figure 3.12). Initial rate data was used to produce a series of double reciprocal plots (Figure 3.12, upper graph) with gradient = $K_{M.app}$ / V_{max} and y-axis intercept = 1 / V_{max}. As expected for a series of double reciprocal plots at a range of competitive inhibitor concentrations, all of the lines fitted to the data intersected the y-axis at the same point (Figure 3.12, Table 3.1). Regardless of the AdoHcy concentration, the same V_{max} is reached as the AdoMet concentration rises towards infinity. Data derived from this graph was used to construct a plot of apparent K_M ($K_{M.app}$) against inhibitor concentration (Figure 3.12, lower graph). The negative of the x-axis intercept of this plot yielded K_i^{AdoHcy} which was found to be 6.93 ± 2.01μM.

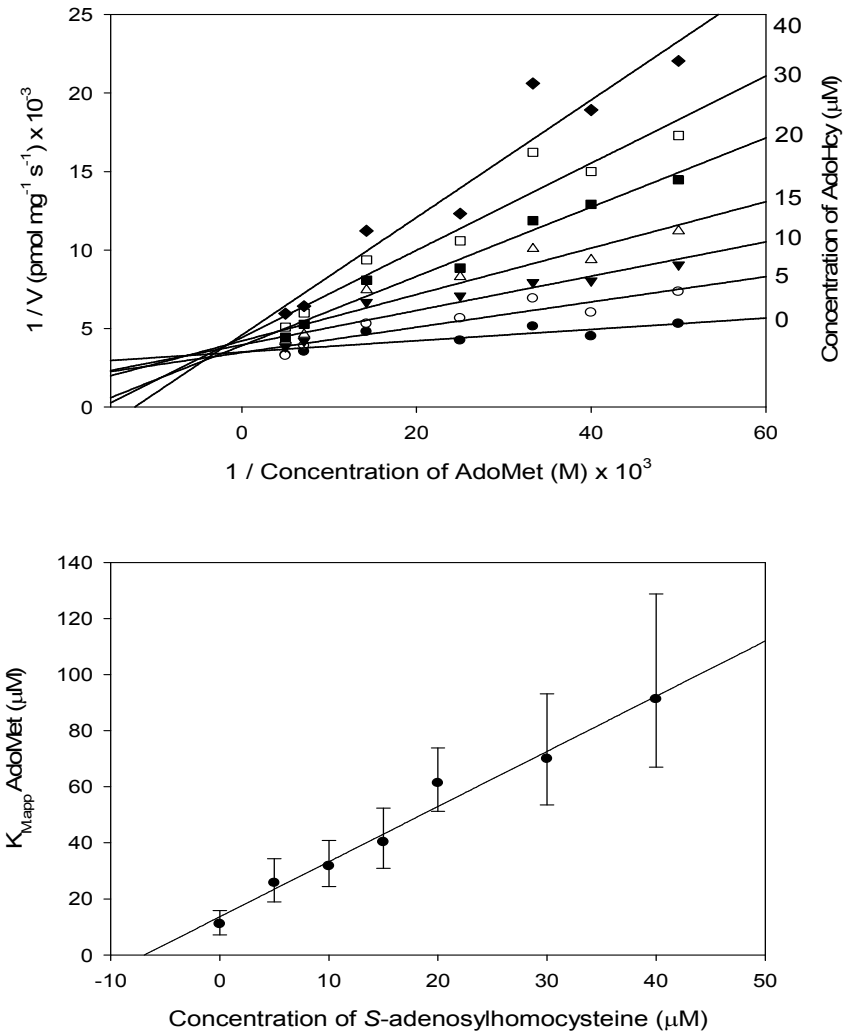

Figure 3.12 Inhibition of Dam by AdoHcy. (Upper graph) Double reciprocal plots of methylation rate against AdoMet concentration. Assays contained 1 nM Dam, 10 U DpnI and 33 nM ODN 3. AdoHcy concentrations were 0, 5, 10, 15, 20, 30 and 40 μM and AdoMet concentrations were 20, 25, 30, 40, 70, 140 and 200 μM. (Lower graph) Apparent K_M ^{AdoMet} plotted against concentration of AdoHcy.

[AdoHcy] μM	*y-axis intercept*	V_{max} *(pmol* mg^{-1} s^{-1}*)*
0	0.0034 ± 0.0003	294.1 ± 28.5
5	0.0033 ± 0.0004	303.0 ± 41.8
10	0.0037 ± 0.0004	270.3 ± 32.8
15	0.0039 ± 0.0005	256.4 ± 37.7
20	0.0037 ± 0.0004	270.3 ± 32.8
30	0.0041 ± 0.0007	243.9 ± 50.2
40	0.0042 ± 0.0009	238.1 ± 64.9

Table 3.1 The y-axis intercepts (= 1 / V_{max}) and corresponding V_{max} values derived from the double reciprocal plots used to determine K_i^{AdoHcy}.

Four kinetic parameters of *Y. pestis* Dam were measured using the coupled enzyme assay (Table 3.2). For comparison, the same kinetic parameters of eight other DNA methyltransferases are included in the table. *E. coli*, T4 and T2 Dam, also target adenine in the sequence G<u>A</u>TC. *C. crescentus* CcrM and M.EcoRV, methylate the underlined adenine within the sequences G<u>A</u>NTC and G<u>A</u>TATC respectively. M.HhaI and M.MspI are C5-cytosine MTases which target the first cytosine in the sequences G<u>C</u>GC and <u>C</u>CGG respectively. M.BamHI is an N4-cytosine MTase targeting the first cytosine in the sequence GGAT<u>C</u>C.

Enzyme (reference)	*Substrate*	k_{cat} *(min^{-1})*	K_M^{DNA} *(nM)*	K_M^{AdoMet} *(μM)*	K_i^{AdoHcy} *(μM)*
E. coli Dam					
(5)	ds20-mer	0.93 ± 0.06	17.4 ± 3.0	5.60 ± 1.1	41.6 ± 10.4
	16 bp hp UM	1.19 ± 0.33	28.6 ± 0.2	6.40 ± 1.2	-
(6) [a]	ds14-mer HM	1.25 ± 0.27	25.5 ± 5.2	1.5 ± 0.1	-
	ds14-mer HM	0.93 ± 0.52	44.8 ± 18.6	3.5 ± 0.2	-
(7)	plasmid DNA	3.6 [b]	-	6.5 ± 0.7 [b]	7.0 ± 0.5 [b]
	-	-	-	3.0 ± 1.5 [c]	2.5 ± 2 [c]
(8)	ColE1 DNA	19	3.6	12.2	-
T4 Dam					
(9)	T4 DNA	8.4	0.0011	0.1	2.4
(10)	ds24-mer UM	0.84 ± 0.18	7.7 ± 2.1	0.33	-
T2 Dam					
(11)	T4 DNA	18.6	0.0011	0.1	2.4
Y. pestis Dam					
(12)*	10 bp hp HM	0.55 ± 0.01	3.4 ± 1.8	11.3 ± 0.6	6.9 ± 2.0
M.EcoRV					
(13)	ds20-mer UM	0.065	300	12	-
CcrM					
(2) [b]	ds45/50-mer HM	0.02	-	-	-
M.HhaI					
(14)	polydGdC	1.3	2.3	0.015	0.002
M.MspI					
(15)	ds121-mer UM	3.36	7.69 ± 0.51	0.016 ± 0.004	0.016 ± 0.002
M.BamHI					
(16)	ds20-mer UM	3.18 ± 0.18	196 ± 50	1.22 ± 0.25	-

Table 3.2 Kinetic parameters of selected DNA methyltransferases. ds = double stranded, hp = hairpin, UM = unmethylated, HM = hemimethylated.[a] Measurements made at 6 °C. [b] Measurements made at 30 °C.[c] Measurements made at 8 °C.* This study.

Y. pestis Dam turnover was measured as 0.55 min^{-1} with the coupled enzyme assay. This is plausible based on a comparison with values reported for *E. coli* and T4 Dam with similar substrates (Table 3.2). Longer DNA substrates, containing several GATC sites, permit processive methylation which allows a higher rate of enzyme turnover (3.6 – 19 min^{-1}, *E. coli* Dam, Table 3.2). Due to its instability it is probable that not all of the *Y. pestis* Dam was active in the assays used to determine k_{cat}. The value of 0.55 min^{-1} would therefore be an underestimate, with the true value even closer to that of T4 and *E. coli* Dam. It has been shown that T4 Dam loses none of its activity when incubated at 37 °C for 30 minutes even without its substrates (11). *E. coli* Dam is probably also more stable than *Y. pestis* Dam. Both enzymes have a high degree of similarity to *S. typhimurium* Dam but *Y. pestis* Dam has a C-terminus which is shorter by nine amino acids (Table 3.3). It has been shown that truncation of the C-terminus of *S. typhimurium* Dam by ten amino acids renders the protein temperature sensitive (3). Interestingly a methyltransferase which has 95 % of the amino acids found in *Y. pestis* Dam and an additional seven amino acids on the C-terminus is encoded in *Yersinia rohdei* (Table 3.3).

MTase	*Sequence at C-Termini*
Wt *S. typhimurium* Dam	RKKVDELLALYQPGVATPARK
E. coli Dam	RKKVDELLALYKPGVVSPAKK
Y. rohdei Dam	RSKVNELLALYSCAETAAQ
Y. pestis Dam	RSKVNELLALYS
Ts *S. typhimurium* Dam	RKKVDELLALY

Table 3.3 A comparison of the C-termini of selected Dam MTases. Wt = wild type. Ts = temperature sensitive.

Y. pestis Dam turnover is considerably faster than that of regulatory MTase CcrM or M.EcoRV but six times slower than M.BamHI. At 10 bp, the *Y. pestis* Dam assay substrate is one of the shortest used to measure the activity of a methyltransferase. It is possible that a longer substrate, still containing just one GATC site, would allow faster *Y. pestis* Dam turnover. M.EcoRV turnover rates are strongly effected by DNA substrate length. Jeltsch and co-workers found that doubling the substrate length from 12 to 24 bp resulted in a fourfold increase in k_{cat} (13). They postulated that this rate

increase was due to altered electrostatic properties, the increased order of longer DNA duplexes and the influence of the DNA outside of the target sequence on the kinetic mechanism of the enzyme (13).

At 11.3 μM the *Y. pestis* Dam K_M ^{AdoMet} was within the range of values reported for *E. coli* Dam and very close to the measured value for M.EcoRV. By contrast T4 and T2 phage Dam have a K_M ^{AdoMet} which is 30-100 times lower (Table 3.2). Tight substrate binding may be particularly advantageous for the phage enzymes as it would help them compete for resources within the host cell. The two bacterial C5-cytosine MTases M.HhaI and M.MspI also have a very high affinity for AdoMet when compared to *Y. pestis* Dam.

At 3.4 nM the *Y. pestis* Dam K_M ^{DNA} was significantly lower than values reported for *E. coli* or T4 Dam with oligonucleotide substrates. The error on the measurement was high, but this was a reflection of enzyme instability rather than a weakness in the assay strategy. This instability may also account for the low K_M ^{DNA}. It was shown that the substrate DNA stabilises the enzyme by a factor of fifty (Figure 3.2). A high affinity for the genomic DNA would therefore help to preserve *Y. pestis* Dam. Use of a lower temperature in the *Y. pestis* Dam assay might serve to allow a more accurate determination of K_M ^{DNA}. Marzabal and co-workers have measured *E. coli* Dam activity at just 6 °C but the coupled assay is limited by the temperature needed to rapidly melt the DpnI digested substrate and separate the FRET pair (6).

The *Y. pestis* Dam K_i ^{AdoHcy} was measured as 6.9 μM with the assay, demonstrating its efficacy in probing the kinetics of *Y. pestis* Dam inhibition. The K_i is similar to those reported in the literature for *E. coli* Dam (Table 3.2). Because Dam is unstable at low oligonucleotide concentrations, the assay may not perform as well if used to study inhibitors which are competitive with DNA.

3.3 Assay validation in high throughput format

Before embarking on high throughput screening we sought to quantify the robustness of the assay in 96-well format. The Z' parameter, a simple statistical parameter developed

by Zhang and co-workers for the validation of high throughput screening assays, was used to this end (17). The Z' parameter takes into account the signal of the assay (μ_{C+} - μ_{C-}) and the standard deviation in the data generated ($3\sigma_{C+} + 3\sigma_{C-}$) (Equation 3.1). Scores between 0.5 and 1 indicate an excellent assay whilst scores less than 0 show the assay to be unsuitable for screening due to poor separation of positive and negative control signals.

$$Z' = 1 - \left[\frac{(3\sigma_{C+} + 3\sigma_{C-})}{(\mu_{C+} - \mu_{C-})} \right]$$

Equation 3.1 The equation for calculation of the Z' parameter. σ = standard deviation, μ = average, C+ = positive control signal, C- = negative control signal.

Ideally, high throughput screening conditions would have used both substrates at concentrations near to their respective K_M's (K_M^{AdoMet} = 10.3 ± 0.7 μM, K_M^{DNA} = 3.4 ± 1.8 nM). This minimises assay bias toward detection of competitive, uncompetitive or noncompetitive inhibitors and so helps identify lead compounds with a variety of modalities (18-21). *Y. pestis* Dam instability prohibited such a low DNA concentration and so 33 nM ODN 3 and 5 μM AdoMet were used. Consequently the assay was biased against compounds competitive with DNA and toward Adomet competitive or uncompetitive inhibitors binding the initial non-specific enzyme-DNA complex (5,22). Dam activity was measured with these substrate concentrations, at 30 °C, in three 96-well plates containing an even mixture of assays and negative controls lacking Dam. Initial rates of fluorescence increase were plotted against well number for each plate of assays (Figure 3.13). A temperature of 30 °C was used rather than 37 °C to minimise the amount of methylation and enzyme inactivation which occurred during the assay initiation period.

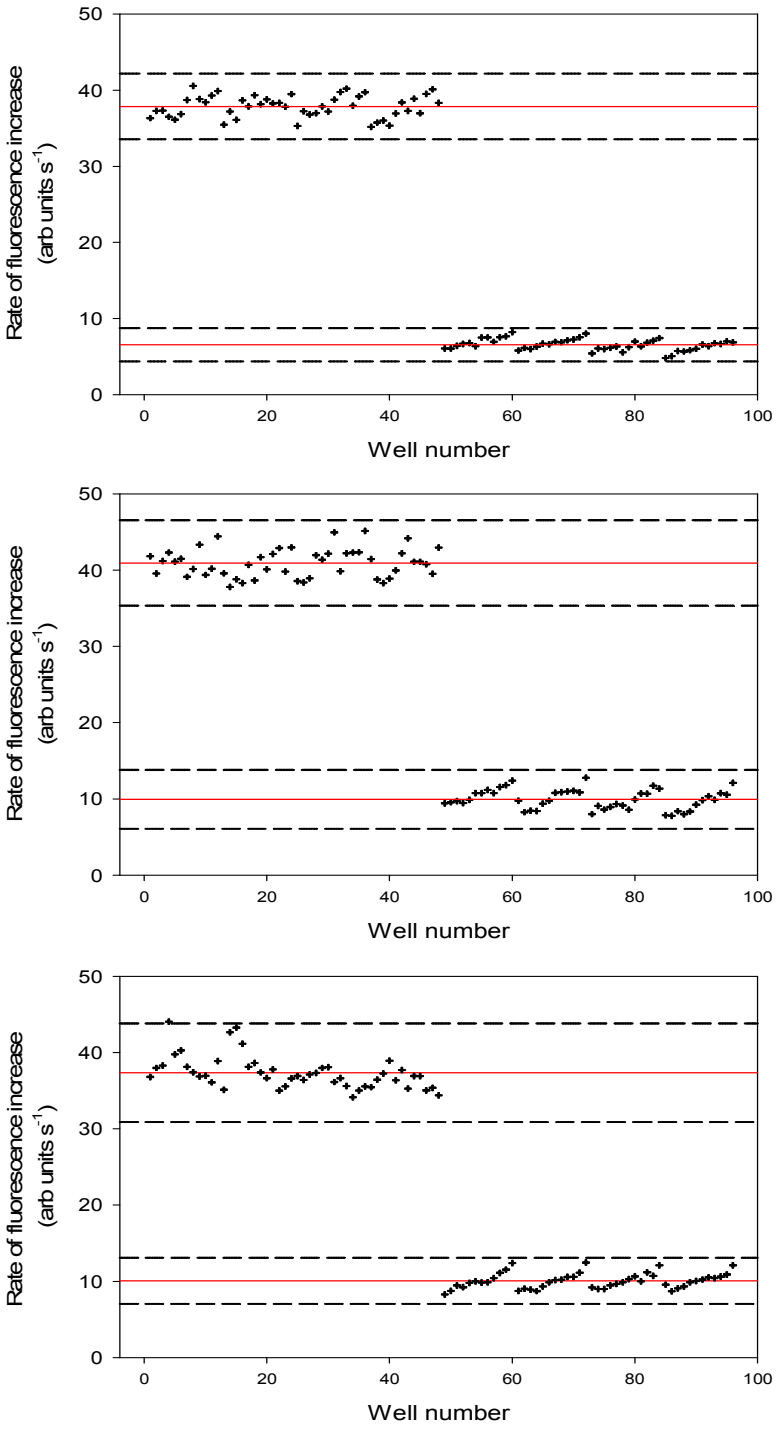

Figure 3.13 High throughput assay validation. Rates of fluorescence increase are shown plotted against well number for three 96-well plates. Solid red lines show the mean rates for positive and negative control datasets. Dashed lines indicate ± 3 standard deviations from the mean. Assays contained 33 nM ODN 3, 5 µM AdoMet, 5 U DpnI and 2 nM Dam except for negative controls, which lacked Dam.

Some clustering of assay data into sets of 12 wells was observed (Figure 3.13, upper graph, middle graph and lower graph negative controls). Within these sets, measured rate would increase with well number, the rate then dropped and the pattern repeated in the next set. Robotic initiation of the assays, column by column, with an eight channel pipette was the likely cause of this systematic trend. Assays initiated later produced faster rates because the enzymes were more active. This trend was however sometimes masked by other factors, possibly temperature variations across the assay plate (Figure 3.13, lower graph positive controls).

Data were used to calculate the Z' parameter for each of the assay plates according to equation 3.1 (Table 3.4). Based on an average of these values, the Z' parameter for the assay in 96-well format was found to be 0.71 ± 0.07. This indicated an excellent assay, suitable for high throughput screening.

Data Set (Figure 3.11)	μ_{C+}	μ_{C-}	$3\sigma_{C+}$	$3\sigma_{C-}$	*Z'*
Upper	37.86	6.57	4.32	2.20	0.79
Middle	40.95	9.95	5.62	3.86	0.69
Lower	37.36	10.07	6.46	3.03	0.65

Table 3.4 Data gathered for validation of the assay in high throughput format.

Mashhoon and co-workers have carried out the largest literature reported high throughput screen for Dam inhibitors (23). They do not detail a quantitative validation of the discontinuous assay which they used. Since it operates on a similar principle to the *Y. pestis* Dam assay and uses a FRET pair labelled oligonucleotide, it would be reasonable to expect it to have a similar Z' parameter.

3.4 Summary and conclusions

A calibration plot was produced to allow fluorescence signals to be converted into methylation rates. From this calibration data it was also estimated that the assay could detect as little as 37.5 fmol of methylation. Experimental results confirmed the previous

observation that *Y. pestis* Dam inactivated rapidly. This inactivation was slowed when Dam was incubated with substrate DNA. Consequently, the assay setup procedure was optimised to minimise the time which Dam spent in solution without DNA.

The K_M of both substrates, K_i^{AdoHcy} and the maximum rate of *Y. pestis* Dam turnover were determined using the assay and judged to be reasonable (Table 3.2). Enzyme instability resulted in a larger error on the K_M^{DNA} measurement at low oligonucleotide concentrations.

A validation of the *Y. pestis* Dam activity assay in 96-well format was carried out. The Z' parameter of 0.71 showed that it was an excellent assay, suitable for the high throughput screening of compound libraries for Dam inhibitors.

3.5 References

1. Roth, M., and Jeltsch, A. (2000) *Biol Chem* **381**, 269-272
2. Berdis, A. J., Lee, I., Coward, J. K., Stephens, C., Wright, R., Shapiro, L., and Benkovic, S. J. (1998) *Proc. Natl. Acad. Sci* **95**, 2874-2879
3. Brawer, R., Batista, F. D., Burrone, O. R., Sordelli, D. O., and Cerquetti, M. C. (1998) *Arch Microbiol* **169**, 530-533
4. Briggs, G. E., and Haldane, J. B. (1925) *Biochem J* **19**, 338-339
5. Mashhoon, N., Carroll, M., Pruss, C., Eberhard, J., Ishikawa, S., Estabrook, R. A., and Reich, N. (2004) *J Biol Chem* **279**, 52075-52081
6. Marzabal, S., Dubois, S., Thielking, V., Cano, A., Eritja, R., and Guschlbauer, W. (1995) *Nucleic Acids Res* **23**, 3648-3655
7. Bergerat, A., and Guschlbauer, W. (1990) *Nucleic Acids Res* **18**, 4369-4375
8. Herman, G. E., and Modrich, P. (1982) *J Biol Chem* **257**, 2605-2612
9. Kossykh, V. G., Schlagman, S. L., and Hattman, S. (1995) *J Biol Chem* **270**, 14389-14393
10. Malygin, E. G., Zinoviev, V. V., Petrov, N. A., Evdokimov, A. A., Jen-Jacobson, L., Kossykh, V. G., and Hattman, S. (1999) *Nucleic Acids Res* **27**, 1135-1144
11. Kossykh, V. G., Schlagman, S. L., and Hattman, S. (1997) *J Bacteriol* **179**, 3239-3243
12. Wood, R. J., Maynard-Smith, M. D., Robinson, V. L., Oyston, P. C., Titball, R. W., and Roach, P. L. (2007) *PLoS ONE* **2**, e801
13. Jeltsch, A., Friedrich, T., and Roth, M. (1998) *J Mol Biol* **275**, 747-758
14. Wu, J. C., and Santi, D. V. (1987) *J Biol Chem* **262**, 4778-4786
15. Bhattacharya, S. K., and Dubey, A. K. (1999) *J Biol Chem* **274**, 14743-14749
16. Lindstrom, W. M., Malygin, E. G., Ovechkina, L. G., Zinoviev, V. V., and Reich, N. O. (2003) *J Mol Biol* **325**, 711-720
17. Zhang, J. H., Chung, T. D., and Oldenburg, K. R. (1999) *J Biomol Screen* **4**, 67-73
18. Copeland, R. A. (2005) *Evaluation Of Enzyme Inhibitors In Drug Discovery*, Wiley-Interscience, Hoboken
19. Copeland, R. A. (2003) *Anal Biochem* **320**, 1-12
20. Dixon, M., Webb, E. C., Thorne, C. R. J., and Tipton, K. F. (1979) *Enzymes*, 3rd Ed., Longman, London
21. Segel, I. H. (1975) *Enzyme Kinetics*, Wiley Classics Library Ed., Wiley-Interscience, New York, Chichester, Brisbane, Toronto, Singapore
22. Liebert, K., Hermann, A., Schlickenrieder, M., and Jeltsch, A. (2004) *J Mol Biol* **341**, 443-454
23. Mashhoon, N., Pruss, C., Carroll, M., Johnson, P. H., and Reich, N. O. (2006) *J Biomol Screen* **11**, 497-510

Chapter 4:- High throughput screening for *Y. pestis* Dam inhibitors

4.1 Introduction

Following the successful assay development and validation in high throughput format the next objective was to screen a compound library and identify novel Dam inhibitors. Library 1 was a commercial collection of potential kinase inhibitors. Many kinase inhibitors target the adenine binding pocket and so might also hit the AdoMet or DNA base binding pockets of Dam. These compounds were screened, using the real-time fluorescence based assay, for activity against *Y. pestis* Dam. Identified inhibitors were to be synthesised in sufficient quantity to allow counter-screening against other DNA binding enzymes to assess selectivity. The initial tests for selectivity would involve a counter-screen against the restriction enzyme DpnI and measurement of the ability of the compounds to bind DNA. This chapter describes the screening process and subsequent synthesis and analysis of hit compounds.

4.2 High throughput screening of library 1

4.2.1 Data collection and analysis

Library compounds were each screened twice for activity against the *Y. pestis* DNA adenine methyltransferase. Compounds were assayed at 30 °C in batches of 80 in the middle columns of a 96-well plate at a concentration of 100 μM. This layout was a reflection of the typical storage format of library compounds in 96-well plates (1). The remaining 16 wells, in columns 1 and 12, contained 4 positive and negative controls with and without AdoMet and 8 controls having 100 μM of the known inhibitor AdoHcy. Average rates of fluorescence increase during the first 675 s of the assay were calculated based on the gradient of a straight line fitted to the raw data (Figure 4.1). This average was used for subsequent data analysis and hit evaluation. The period chosen

reflects the time it took fluorescence signals to span the measurement range of the instrument under the assay conditions used. At the end of this time *Y. pestis* Dam had typically carried out 1.5 – 2 turnovers and 10 – 15 % of the DNA substrate had been consumed. Most compounds from the library were successfully screened in this way, the exception being compounds with a large inherent fluorescence at the emission wavelength of fluorescein. These types of compound were however a rare occurrence with only 4 being prohibitively fluorescent in the 1000 tested. Details of which compounds were fluorescent and how data was manipulated to compensate are included as an appendix (appendix D).

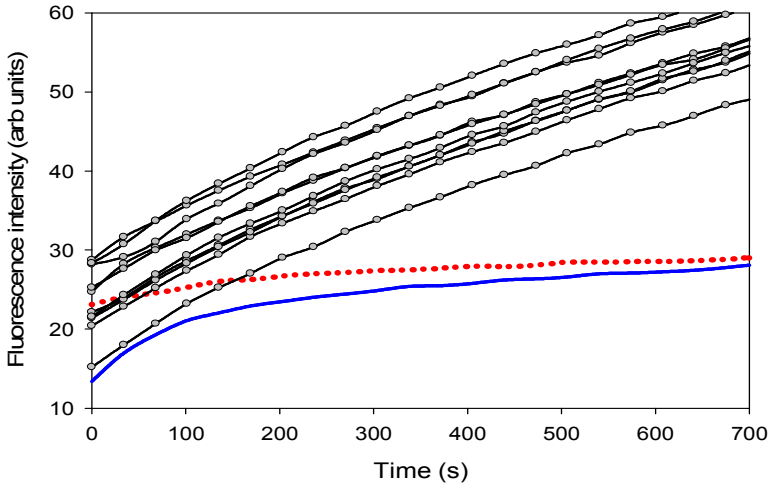

Figure 4.1 Example raw data obtained from one row of assays. Ten of the assays shown contained a library compound (grey circles joined by black lines), one lacked AdoMet (dotted red line) and one contained the known Dam inhibitor AdoHcy (solid blue line).

Initial rates derived from the raw data were tabulated to make them suitable for further analysis with the programme HTS corrector (Table 4.1) (2). Control assays were used to check assay performance but were omitted from the subsequent analysis and hit selection. Based on the four positive and negative controls the average Z'-parameter within a plate was 0.79 ± 0.12, indicative of an excellent assay. For the whole library screen, considering all 100 positive and negative controls together, the Z'-parameter was just 0.35 (Figure 4.2). These two Z'-parameters indicate that there was good reproducibility in the assay data within one row of one plate but large plate to plate variations.

6130	*2*	*3*	*4*	*5*	*6*	*7*	*8*	*9*	*10*	*11*
A	36.4	38.7	37.3	38.7	39.7	41.0	39.5	39.4	44.2	39.8
B	37.4	38.1	36.8	39.2	39.8	39.6	44.3	36.6	39.1	39.1
C	39.7	37.4	40.8	37.7	39.9	39.5	38.6	38.3	37.7	38.3
D	34.8	37.8	40.3	38.3	42.4	41.0	39.2	37.6	38.8	36.8
E	34.6	36.1	47.0	36.1	36.9	41.2	39.4	41.9	38.7	36.6
F	35.3	36.9	37.7	38.2	37.4	37.2	37.9	37.7	36.3	35.3
G	35.2	34.3	36.2	35.1	37.2	36.0	39.1	37.2	37.6	37.9
H	33.5	35.9	37.5	37.0	41.0	41.0	35.2	38.0	38.2	34.5

Table 4.1 Tabulated data obtained from a screen of compounds in library plate 6130. Each well position was assigned a single number based on the rate of fluorescence increase measured in the assay.

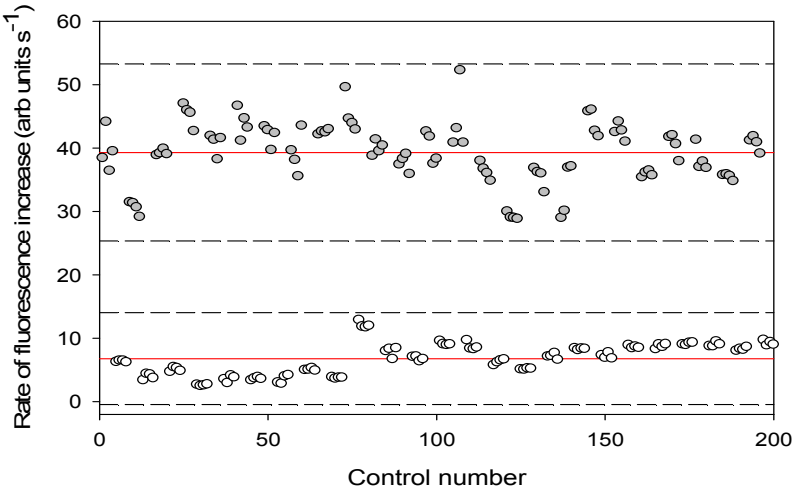

Figure 4.2 Measured rates of fluorescence increase in positive and negative controls carried out during the HTS. Positive and negative control assay data is denoted with grey and white circles respectively. The mean averages and 3 σ limits are shown with solid red and dashed black lines respectively.

Raw screening data for the compound containing assays appeared in distinct clusters (Figure 4.3). This arrangement of the data was caused by the inconsistencies between different batches of assay mix, different assay runs and different locations on the plate. The data as a whole was moderately well fitted by a normal distribution (R^2 = 0.979) (Figure 4.4). Deviation from this distribution was found to be due to the plate 6132 and 6134 repeat screening data (compound 160-240 and 320-400 green circles), which

contained atypically low rates. A frequency versus rate plot with this data removed was very well fitted by a normal distribution ($R^2 = 0.993$) (Figure 4.5).

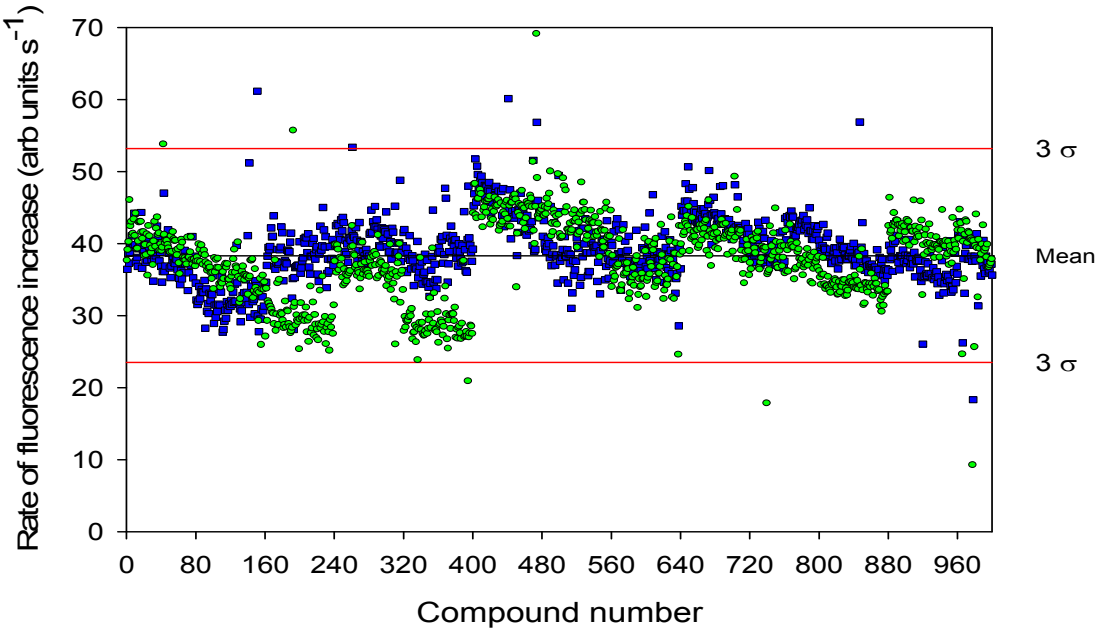

Figure 4.3 Unprocessed data from the duplicate screen of compound library 1. Measured rate of fluorescence increase is shown for each of the 1000 compounds. Data from the first and repeat round of screening are shown with blue squares and green circles respectively. The mean and 3 σ limit are denoted with horizontal black and red lines.

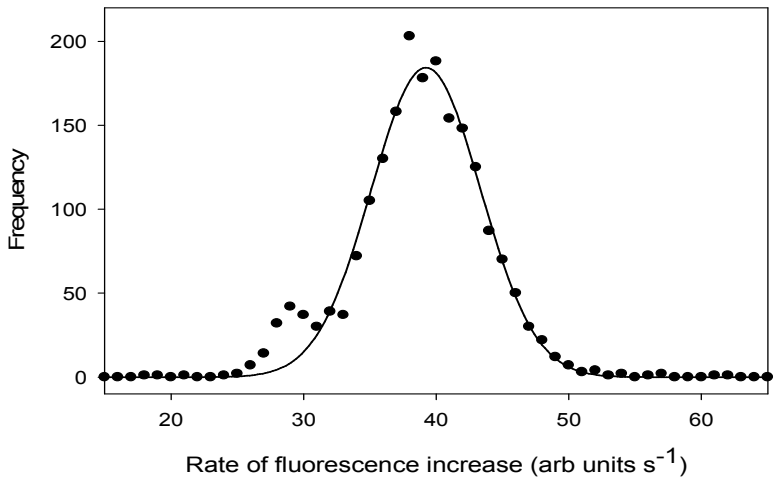

Figure 4.4 Distribution of unprocessed data from the duplicate screen of compound library 1. Data is shown by filled circles and the fit of a three parameter normal distribution by a black line.

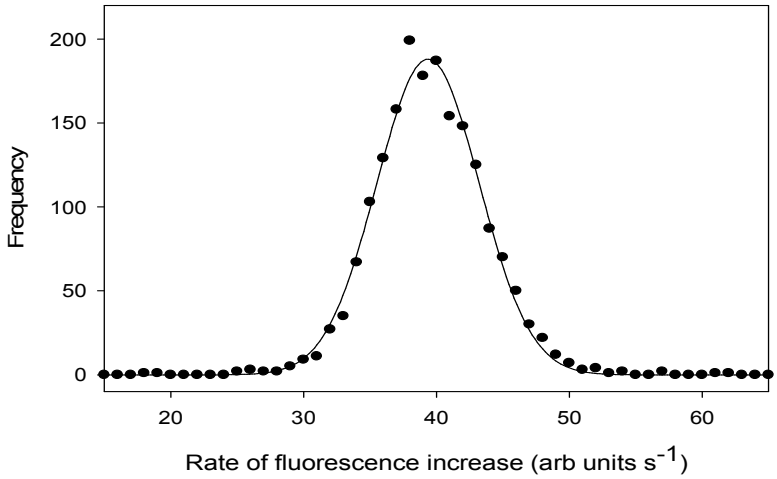

Figure 4.5 Distribution of unprocessed data from the duplicate screen of compound library 1 without data from plate 6132R (compounds 160-240) and 6134R (compounds 320-400). Data is shown by filled circles and the fit of a three parameter normal distribution by a black line.

The large standard deviation caused by patterns in the data masked the true effect of compounds on Dam activity. A simple 3 σ hit detection threshold represents the 99.73 % confidence level and is frequently used in HTS (3). To make the assay data suitable for hit selection in this manner it first had to be processed.

Compound-containing assays themselves provided the most abundant source of reference data for processing because the significant majority of compounds had no effect on the measured rates. It was felt to be imprudent to rely on the positive control assay data because it was comparatively sparse and all from one column of each plate. In retrospect, having only four positive controls in each assay plate was a mistake, typically eight positives are used and can be spread between columns 1 and 12 (1). Data processing methods which rely on control assay data were therefore not considered.

There are several ways HTS data can be normalised to account for inter-plate assay variations but one of the simplest methods, which was used to process this screening data, is Z-score standardisation (1) (Equation 4.1). Plate averages are subtracted from the individual rates and this residual divided by the standard deviation of the plate data.

$$Z = (X - \mu) / \sigma$$

Equation 4.1 The Z-score standardisation equation used by HTS corrector. Z = Z-score, X = rate of methylation measured in well, μ = average rate of methylation within plate, σ = standard deviation of measured rates.

HTS corrector was used to Z-score standardise the data and evaluate background trends according to well number (Figure 4.6). Outliers greater than 3 σ from the mean were discounted from this background evaluation on the basis that they most likely contained compounds having an effect on the rate.

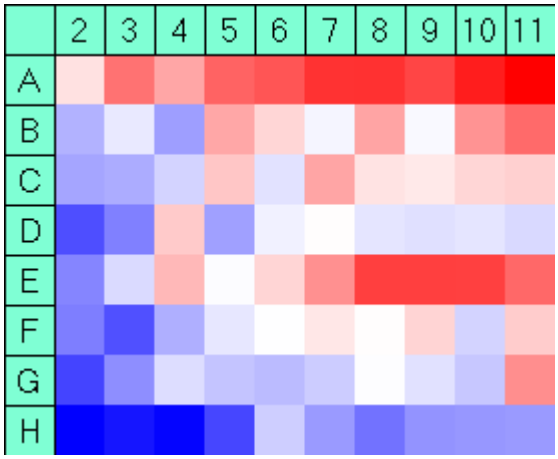

Figure 4.6 Observed background trends in the assay data for the screen of compound library 1. Blue wells tended to yield assays whose rates were below average whilst red ones on balance gave above average rates. Intensity of colour reflects the strength of the effect. Wells H02 and A11 typically gave respective rates 0.8 σ below and 1 σ above the averages in the normalised dataset.

As expected, based on the patterns in the HTS validation data discussed in chapter three, a column bias was observed in the data. Columns on the right of the plate, which were initiated later, tended to give higher rates (Figure 4.6). A row bias was also seen with rows nearest H giving the slowest rates of fluorescence increase. A speculative explanation for this is that wells nearest the front edge of the plate reader may have remained slightly colder than those at the back. Row E was an exception to this trend with a consistently higher average background than its neighbouring rows. A possible

explanation for this is that the multichannel pipette head of the robot may have introduced slightly more enzyme into row E assays.

Biases due to well position were removed by subtraction of this evaluated background to give processed data from which hit compounds were more readily identifiable (Figure 4.7)

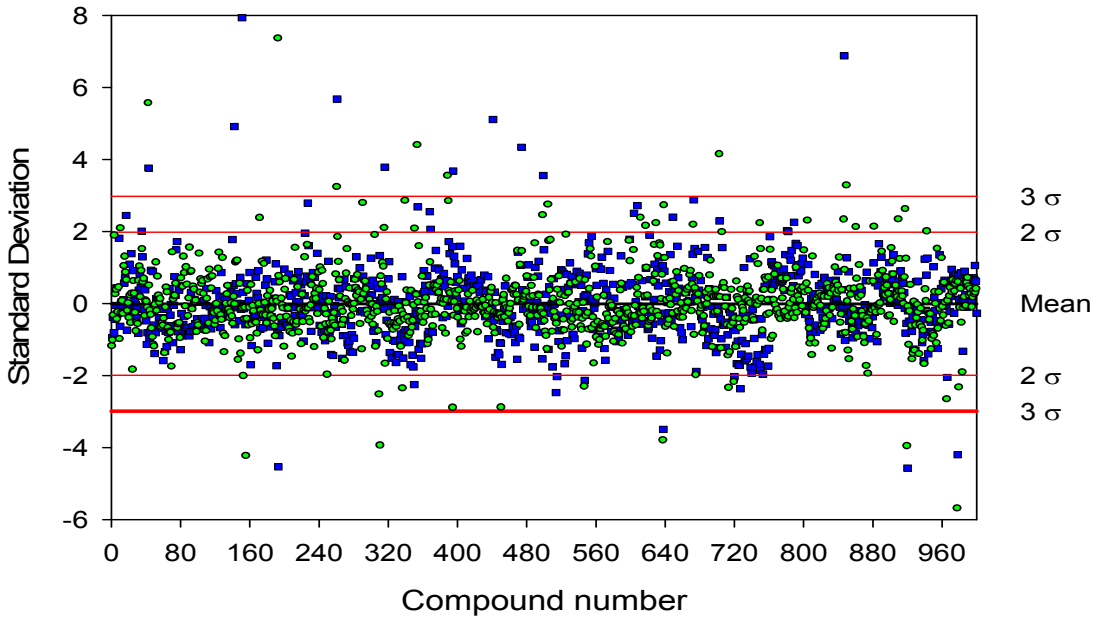

Figure 4.7 Processed data from the screen of compound library 1. Data was subjected to Z-score normalisation and background subtraction. Deviation of the rate of fluorescence increase from the mean is shown versus the compound number being tested. Data from the first and repeat round of screening are shown with blue squares and green circles respectively. Two and three standard deviations above and below the mean are denoted with horizontal red lines.

Three library compounds were identified as hits based on a 3 σ threshold (Figure 4.10). Assays containing compounds 638 (well H09, plate 6137), 920 (well D11, plate 6141) and 978 (well D04, plate 6142) all yielded rates below 3 σ in two separate assays (Figure 4.7, Figure 4.8). Values in σ for these compounds were -3.6 ± 0.2, -4.3 ± 0.4 and -4.9 ± 1 respectively. Additionally compound 966 (B02-6142) which yielded an average value of -2.4 ± 0.4 was deemed worthy of further study because of structural homology to two of the hits (Figure 4.10).

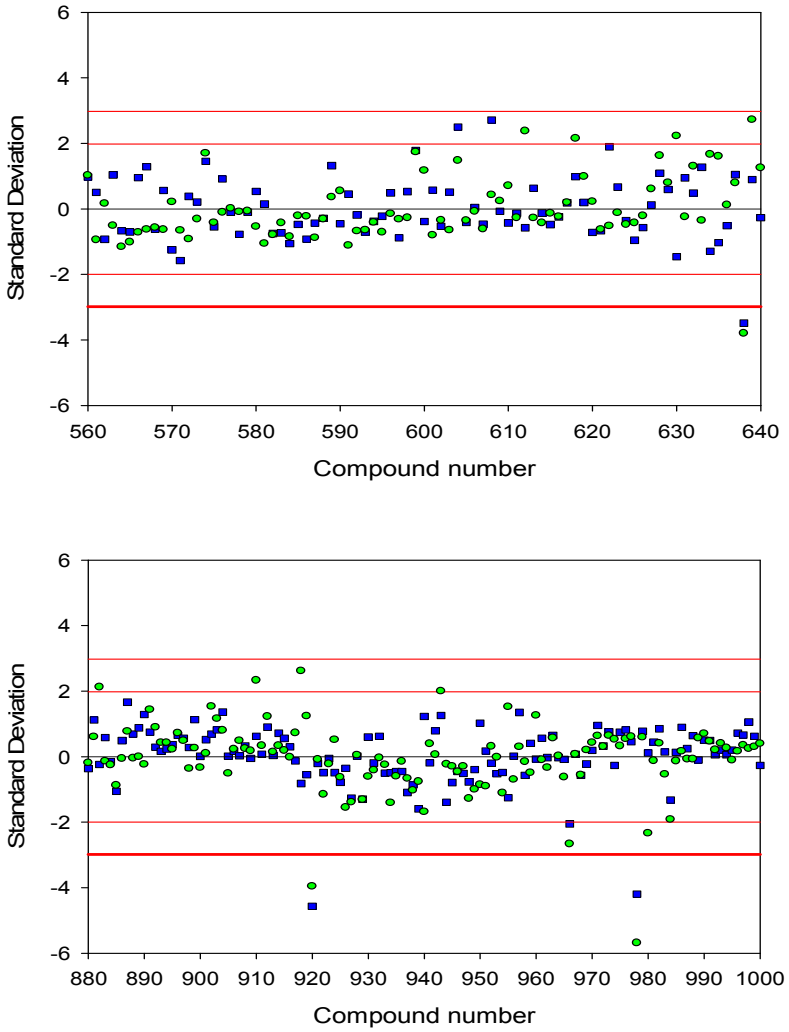

Figure 4.8 Selected processed data from the screen of compound library 1. Data was subjected to Z-score normalisation and background subtraction. Deviation of the rate of fluorescence increase from the mean is shown versus the compound number being tested. Data from the first and repeat round of screening are shown with blue squares and green circles respectively. Two and three standard deviations above and below the mean are denoted with horizontal red lines. (Upper Graph) Data from the screen of compounds in plate 6137 which contained one hit. (Lower Graph) Data from the screen of compounds in plate 6141 and 6142 which contained two hits and a compound of interest.

Despite normalisation and background subtraction, retrospective inspection of some processed data revealed small unwanted trends were still present. An example of this can be seen in assay data on compound numbers 880 – 960 (Figure 4.8, lower graph).

Rates for the first forty of these compounds sit mostly above the mean whilst rates from the second forty are disproportionately below.

An alternative, more complicated method for the processing of HTS data, which takes into account plate to plate and well to well variation, is B-scoring (4,5). Whilst this was not originally used to process data and select hits, it was of interest to carry out a retrospective B-score analysis as it has been described as a 'robust analogue of the Z-score' (1). B-scoring uses median average estimates to correct for row and column biases within a plate and then differences between plates in the screen. HTS corrector, the software originally used to analyse screening data is also equipped with a B-scoring function which was used to re-process the raw data (Figure 4.9)

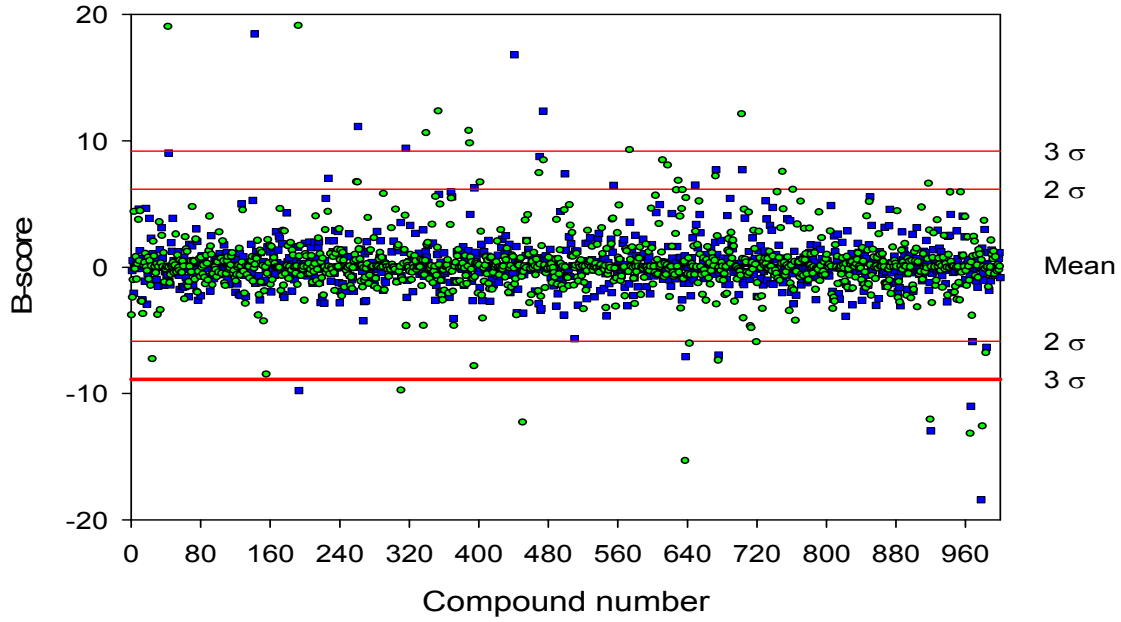

Figure 4.9 B-score processed data from the screen of compound library 1. B-scores are shown versus the compound number. Data from the first and repeat round of screening are shown with blue squares and green circles respectively. Two and three standard deviations above and below the mean are denoted with horizontal red lines.

Data processed in this way had no discernable residual trends so with hindsight B-scoring looks to be a superior processing method which is preferable to Z-scoring followed by background subtraction. Background subtraction from Z-score normalised data relies on the assumption that well to well trends remain constant throughout the

course of the whole screen, in reality this may not be the case. If a simple 3 σ hit detection threshold were applied to the B-scored data then compound 638 (H09-6137) would not have been classed as a hit. The remaining two hits and compound of interest, 966 (B02-6142), would all have been classified as hits by this method. Importantly therefore, failure to process data by B-score at the time of the screen did not result in compounds of interest being missed.

4.2.2 'Hit' structures

Four compounds which comprised three true 'hits' and a compound of interest were taken through to the next phase of the project. Structures of these molecules could be divided into two types. Compound 638 (H09-6137) was unique amongst the four, consisting of an imidazopyrazine core appended with pyridine and methylpiperazine rings. The three remaining compounds, 920 (D11-6141), 966 (B02-6142) and 978 (D04-6142) consisted of a pyrazine core attached directly to an aromatic ring and also to a bi-aryl amide or sulphonamide containing subunit (Figure 4.10).

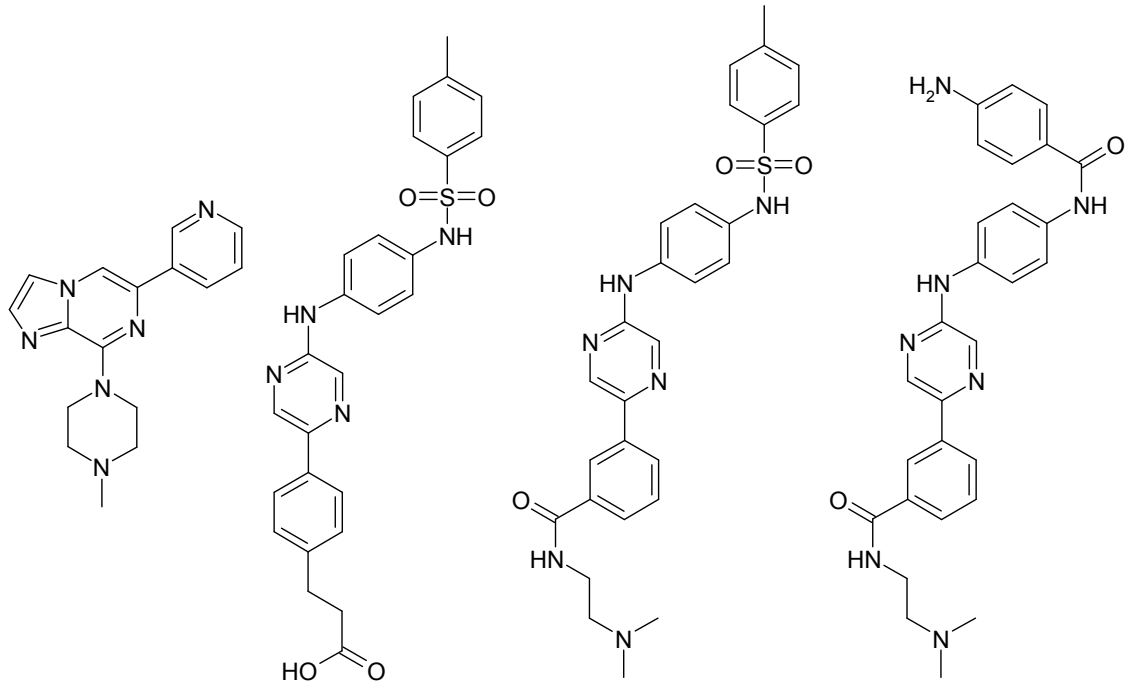

Figure 4.10 Compounds from library 1 identified as potential inhibitors of *Y. pestis* Dam. Structures 638 (H09-6137), 920 (D11-6141), 966 (B02-6142) and 978 (D04-6142) are shown from left to right respectively.

Three compounds were also identified in the library which consistently raised the measured rate of fluorescence increase above 3 σ. Compounds 43, 261 and 474 yielded average rates that were 4.7 ± 1.3, 4.5 ± 1.7 and 6.3 ± 2.7 σ above the mean respectively (Figure 4.11).

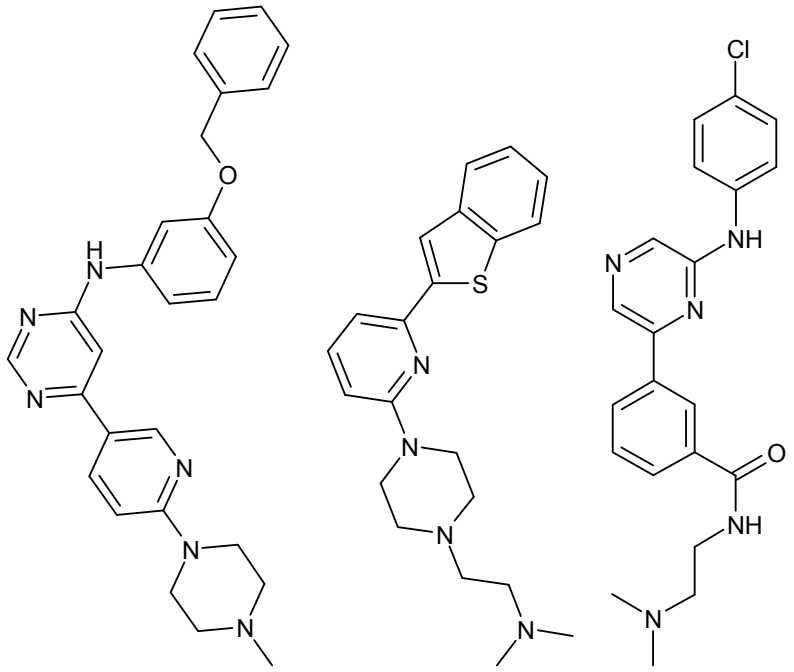

Figure 4.11 Structures of compounds identified as increasing the measured rates of fluorescence increase. Compounds 43 (E04-6130), 261 (C02-6133) and 474 (H05-6135) are shown from left to right respectively.

Apart from the fact that all of these compounds contained one or more tertiary amines and a heterocycle there were no conserved structural motifs in the group. It was unclear how such compounds illicit the abnormally high fluorescence increases observed. A slow intercalation of the compounds into DNA with an associated change in the absorbance and emission spectra was one possible explanation. Another was that the compounds were actually interacting with the methyltransferase. An AdoHcy analogue, 5'-*S*-(Propionic acid)5'-deoxy-9-(1'-β-D-ribofuranosyl)1,3-dideaza adenine, with a limited activating effect on *E. coli* Dam has been reported in the literature but such compounds are rare (6) (Figure 4.12). These compounds, whilst curious, were considered unlikely to be useful for the development of novel antibiotics and so were not studied any further.

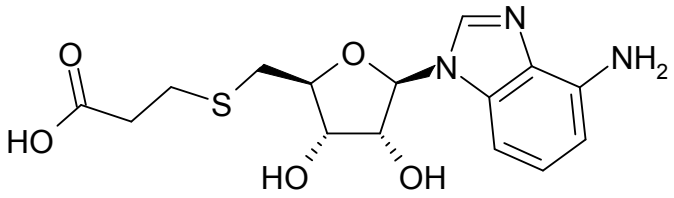

Figure 4.12 5'-*S*-(Propionic acid)5'-deoxy-9-(1'-β-D-ribofuranosyl)1,3-dideaza adenine.

4.3 Synthesis and testing of 'hits' from the library screen

4.3.1 Synthesis of compound H09-6137

Compound H09-6137 was synthesised using the two step procedure outlined below (Scheme 4.1).

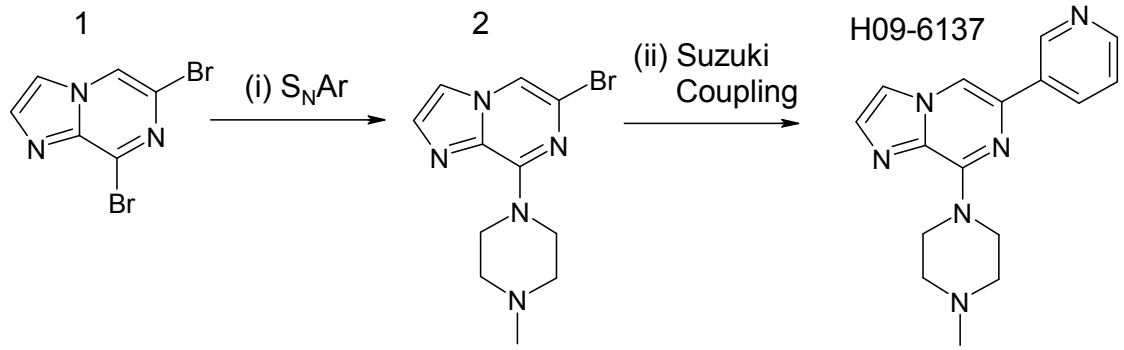

Scheme 4.1 Synthetic route to compound H09-6137. (i) Nucleophilic aromatic substitution: Compound **1** (6,8-dibromoimidazo-[1,2-a]pyrazine), 1-methylpiperazine (40 % v/v, aqueous), room temperature overnight under N_2. (ii). Suzuki Coupling: Compound **2** (6-bromoimidazo-8-(1-methylpiperazine)[1,2-a]pyrazine), pyridine-3-boronic acid (1 eq), tetrakis(triphenylphosphine)palladium(0) (3 mol %), sodium carbonate (3 eq), 1,2 dimethoxyethane / water (3:1 v/v), reflux 8 hours under nitrogen.

This approach was based on a patent covering the synthesis of certain kinase inhibitors (7). Compound **2** (Scheme 4.1) was formed by selective nucleophilic aromatic substitution of compound **1** with 1-methylpiperazine at the 8 position in a reaction similar to that used by Bonnet and co-workers (8). Recrystallisation from hot hexane

gave the pure product, a beige powder in a moderate 64 % yield. Compound **2** was taken on in a standard Suzuki-Miyaura cross coupling reaction with pyridine-3-boronic acid to give compound H09-6137, also a beige solid in 63 % yield (9-11). The yield for the two step synthesis of H09-6137 was therefore 40 %.

4.3.2 Synthesis of compounds D11-6141, B02-6142 and D04-6142

Initial attempts to form compound **5** (Scheme 4.3) from 2,5 dibromopyrazine, according to a patent covering the synthesis of potential kinase inhibitors, were unsuccessful (Scheme 4.2) (12). It remains unclear why the nucleophilic aromatic substitution failed to yield product.

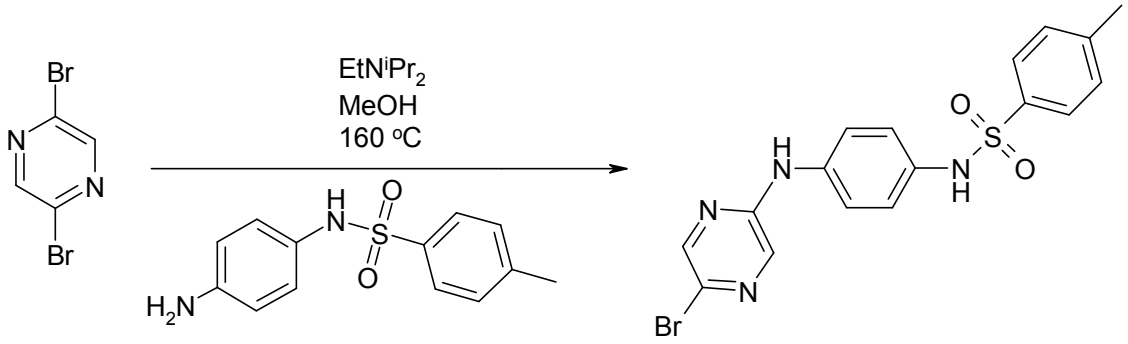

Scheme 4.2 Initial proposed first step in the synthetic route to compounds D11-6141 and B02-6142. Nucleophilic aromatic substitution: 2,5 Dibromopyrazine, *N*-(4-aminophenyl)-4-methylbenzenesulfonamide (1 eq), *N,N*-diisopropylethylamine (1 eq), MeOH, 160 °C, 10 minutes.

An alternative reaction considered for the formation of compound **5** was the Buchwald Hartwig amination (13,14) (Scheme 4.3). This palladium catalysed reaction can be used to form a C-N bond between an aryl halide and amine starting material in the presence of stoichiometric amounts of base (15). The reaction mechanism proceeds with oxidative addition of the aryl halide onto the Pd(0) centre, formation of an arylpalladium amido complex and finally reductive elimination to form the C-N bond (16,17). Developments have given the reaction a wide scope but its complexity means that a range of parameters must be optimised to achieve a satisfactory yield (16,18).

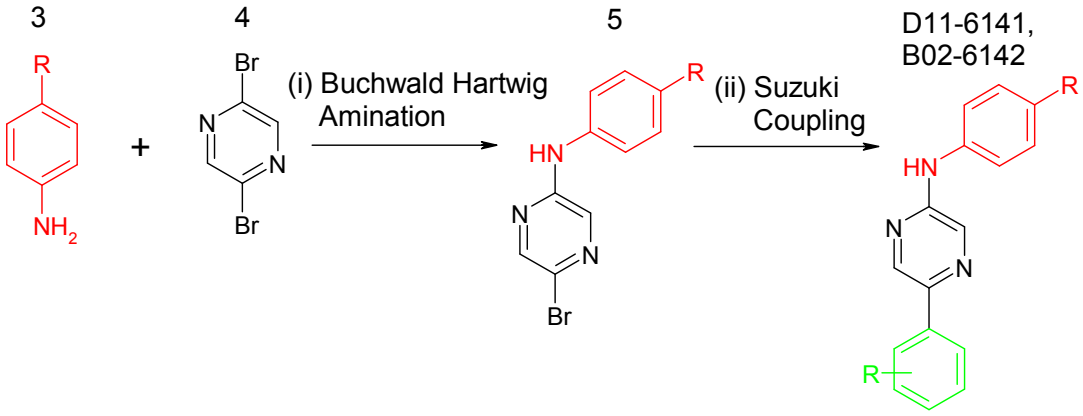

Scheme 4.3 Synthetic route to compounds D11-6141 and B02-6142. (i) Buchwald Hartwig Amination: Compound **4** (2,5-dibromopyrazine), *N*-(4-aminophenyl)-4-methylbenzenesulfonamide (1 eq), caesium carbonate (1.4 eq), tris(dibenzylideneacetone)dipalladium(0) (2.5 mol % Pd), 4,5-bis(diphenylphosphino)-9,9-dimethylxanthene (5 mol %), 18-crown-6 (10 mol %), 1,4 dioxane at 90 °C under N_2 overnight. (ii) Suzuki Coupling: Compound **5,** boronic acid (1.1 eq), caesium carbonate (4 eq), tetrakis(triphenylphosphine)palladium(0) (10 mol %), 1,2 dimethoxyethane / water (3:1) reflux under nitrogen overnight.

Following a search for optimal conditions by a project student under my supervision, the pyrazine ring of compound **4** was aminated with *N*-(4-Aminophenyl)-4-methylbenzenesulfonamide in sufficient yield (Scheme 4.3) (19). Compound **5** a pale yellow solid was obtained after an aqueous work up and purification by column chromatography in 50 % yield.

The yield of the reaction was particularly sensitive to the ligand and solvent used. Effective amination was achieved in 1,4-dioxane with 4,5-bis(diphenylphosphino)-9,9-dimethylxanthene (xantphos) as the ligand and a weak caesium carbonate base (20,21). Dioxane is a more polar solvent than toluene, the other commonly used solvent in Buchwald Hartwig aminations, and dioxane facilitated the dissolution of the sulfonamide start material (17). A test reaction between *N*-(4-aminophenyl)-4-methylbenzenesulfonamide and 2-bromopyridine conducted in toluene, with a weak caesium carbonate base and a bidentate 2,2'-bis(diphenylphosphino)-1,1'-binapthyl (BINAP) ligand, had given a low 8 % yield. By contrast aniline had been able to aminate 2-bromopyridine in 50 % yield in toluene with

a bidentate phosphine ligand and strong sodium tert-butoxide base. 1,4-Dioxane was Yin and Buchwalds choice of solvent when arylating a sulphonamide-containing start material (22). Xantphos is bidentate, such ligands are known to be good for reactions involving aryl amines and also suppress the formation of bis-pyridine complexes which terminate the catalytic cycle (16,23-25). When the reaction was instead carried out with BINAP, another bidentate phosphine ligand, the required amination product was given with a 20 % yield. The noteable differences between Xantphos and other bidentate ligands are its large P-Pd-P 'bite angle' and the presence of a heteroatom (oxygen) which alters the electronic properties of the Pd centre (26,27) (Figure 4.13). Xantphos has previously been reported as an effective ligand for aminations involving anilines (28). Before use, the caesium carbonate base was ground in a pestle and mortar as there was literature evidence to suggest smaller particle size improves reaction rates (29). Research has also suggested that addition of a crown ether, 18-crown-6, may increase rates of amination by interaction with the Cs and Pd ions (30,31). Reactions with and without a crown ether were both observed to have yielded product based on TLC results. Precise yields of these test reactions were not measured.

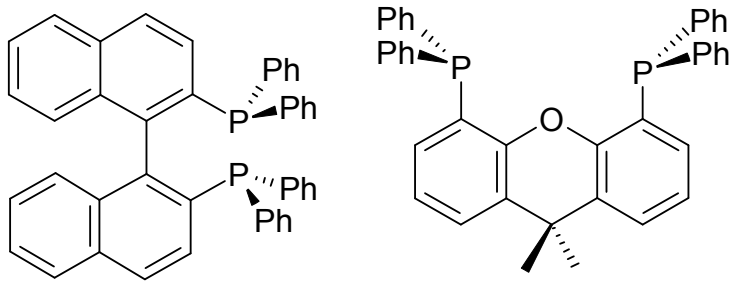

Figure 4.13 Structures of the two bidentate phosphine ligands used in the amination of compound 4.

A yield of 50 % from the final amination reaction conditions was fit for purpose. Time could have been spent trying to enhance yields further but this would have slowed down the screening process. That said, a modification to the reaction conditions which was overlooked and should have been tried was the addition of a triethylamine co-solvent which Buchwald and Ali say provided 'significant rate enhancements when running reactions with caesium carbonate' (28).

Buchwald Hartwig amination was also to be used in the first step of compound D04-6142 synthesis (Scheme 4.4).

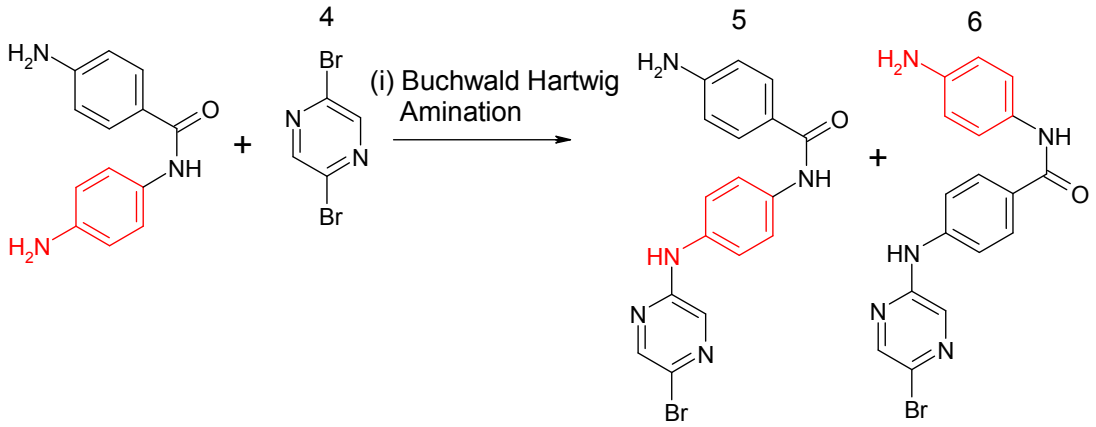

Scheme 4.4 First step of the synthetic route to compound D04-6142. (i) Buchwald Hartwig Amination: Compound **4** (2,5-dibromopyrazine), 4,4'-diaminobenzanilide (1 eq), caesium carbonate (1.4 eq), tris(dibenzylideneacetone)dipalladium(0) (2.5 mol % Pd), 4,5-bis(diphenylphosphino)-9,9-dimethylxanthene (5 mol %), 18-crown-6 (10 mol %), 1,4 dioxane, 90 °C, under nitrogen overnight.

TLC analysis of this reaction showed that a new ninhydrin active compound had been formed. This material was isolated by a combination of normal and reversed phase chromatography and analysed by electrospray mass spectrometry. Mass ions of 384, 386 and 406, 408 were consistent with $[M + H]^+$ or $[M + Na]^+$ respectively for either product **5** or **6**. To differentiate between these potential products, samples were sent for analysis by electrospray mass spectrometry at increased cone voltage (50 V) (J. Herniman). This led to the formation of two new mass ions at 276 and 278 which were consistent with a breakdown of product **6** at the amide bond within the mass spectrometer. On this basis the identified product was attributed to reaction at the unwanted end of the 4,4'-diaminobenzanilide. The yield of this product was, at 28 %, low. An alternative route to D04-6142 was considered, but it was felt that optimising this strategy, particularly the amination step, so as to achieve an acceptable yield would prove time consuming. Analysis of the two very similar compounds to D04-6142 had shown that they were not selective Dam inhibitors and therefore further efforts to complete its synthesis were discontinued.

4.3.3. Counter-screening of compounds for selective inhibition of Dam

The three successfully synthesised compounds of interest were re-tested to determine their effect in the Dam activity assay. As a counter screen their effect in a DpnI activity assay was also measured. This DpnI assay operated on the same principle as the Dam assay but used FM ODN3, a fully methylated analogue of ODN 3. Compound H09-6137 was tested in both assays at eleven concentrations between 0 and 2 mM (Figure 4.14).

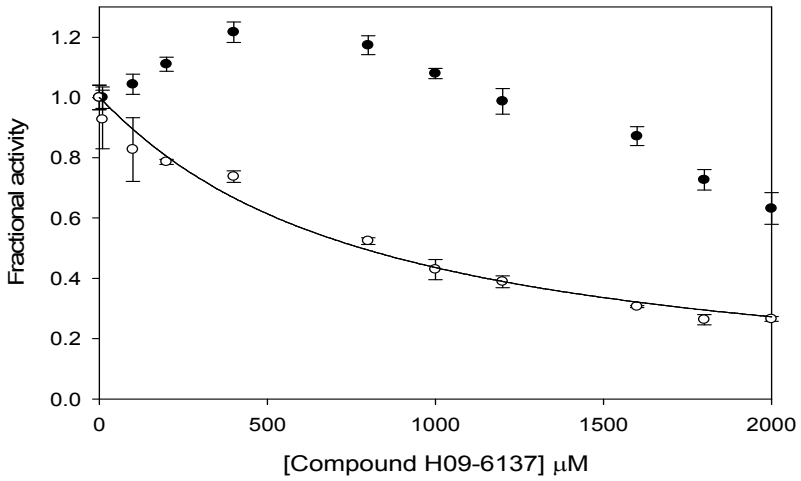

Figure 4.14 Compound H09-6137 concentration-response curve for apparent Dam (filled circles) and DpnI (open circles) activity. The fractional activity in the Dam or the DpnI assay is plotted against the compound concentration. DpnI data were fit to a 3 parameter logistic sigmoid to obtain the IC_{50} and the Hill coefficient (solid line).

In the Dam assay H09-6137 caused an increase in measured activity up to a concentration of approximately 400 μM. Above this a steady decrease in activity was seen with 60 % remaining at a compound concentration of 2 mM. DpnI activity was reduced by the compound at much lower concentrations than those required in the Dam assay. DpnI activity dropped to less than 50 % at a compound concentration of 1 mM and continued to fall to ~ 25 % with 2 mM H09-6137. The IC_{50} for the inhibition of DpnI was calculated as 781 ± 83 μM from the fit of a 3 parameter logistic sigmoid to the data (R^2 = 0.98) (Equation 4.2). A poor fit of the Dam concentration response plot data to this sigmoid made it unsuitable for the determination of an IC_{50} (R^2 = 0.69).

$$Fractional\ activity = \frac{1}{1 + ([I]/IC_{50})^h}$$

Equation 4.2 The 3 parameter logistic sigmoid used to derive the IC_{50} and Hill coefficients from the concentration-response assay data. [*I*] is the compound concentration and *h* is the Hill coefficient.

The Hill coefficient for the inhibition of DpnI by H09-6137 was determined as 1.0 ± 0.1. This indicates that the inhibition of enzyme activity was the result of stoichiometric binding of one inhibitor molecule to one component of the assay (3).

Compound H09-6137 was only weakly inhibitory in the Dam activity assay. These repeat results are inconsistent with the compound being identified as a hit in the initial screen at a concentration of 100 μM. An explanation could be that the original library sample was contaminated with a small amount of a more potent inhibitor. Compound H09-6137 was not selective for *Y. pestis* Dam as it was found to inhibit the restriction enzyme DpnI.

Compound D11-6141 was tested at several concentrations between 0 and 500 μM in the Dam activity assays and between 0 and 200 μM in the DpnI assay (Figure 4.15).

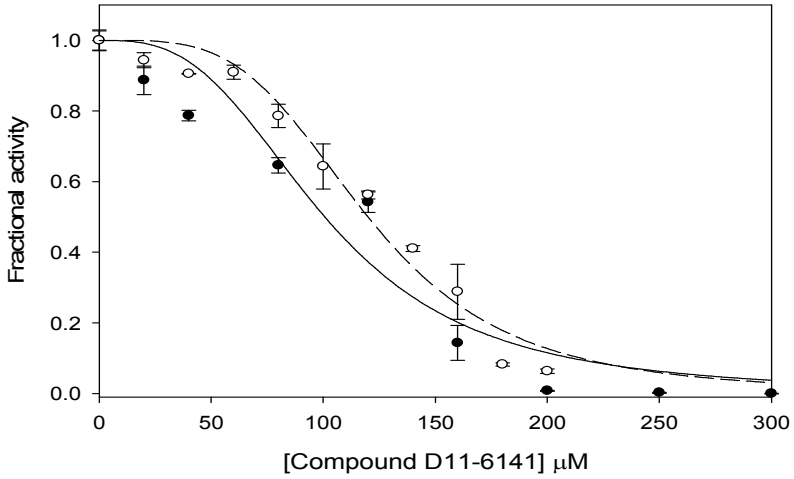

Figure 4.15 Compound D11-6141 concentration-response curve for apparent Dam (filled circles) and DpnI (open circles) activity. The fractional activity in the Dam or the DpnI assay is plotted against the compound concentration. Dam and DpnI data were fit

to a 3 parameter logistic sigmoid to obtain the IC_{50} and the Hill coefficient (solid (R^2 = 0.95) and dashed (R^2 = 0.97) lines respectively).

A very similar inhibitory effect was observed with compound D11-6141 in both types of activity assay. Between 0 and 200 μM the compound steadily reduced measured rates to nothing. The IC_{50}s in the Dam and DpnI assays were 101 ± 12 μM and 120 ± 5 μM respectively. Results from these assays are consistent with the compounds identification as a hit in the initial screen. These results also suggest that D11-6141 was not selective for *Y. pestis* Dam. The Hill coefficients from the fits of the Dam and DpnI data were 2.9 ± 0.8 and 3.8 ± 0.5 respectively. These high Hill coefficients, greater than one, provide additional evidence that D11-6141 is non-selective in its mode of action (3). Where an inhibitor was targeting a specific site in an enzyme a Hill coefficient of one would be expected. Coefficients above one can indicate cooperativity in the inhibitor binding, the targeting of multiple equivalent binding sites or other non-ideal behaviour by the inhibitor. Non-ideal inhibition can result from compound aggregation or protein denaturation by the inhibitor (3).

Compound B02-6142 was tested at several concentrations between 0 and 150 μM in the Dam and DpnI assays (Figure 4.16).

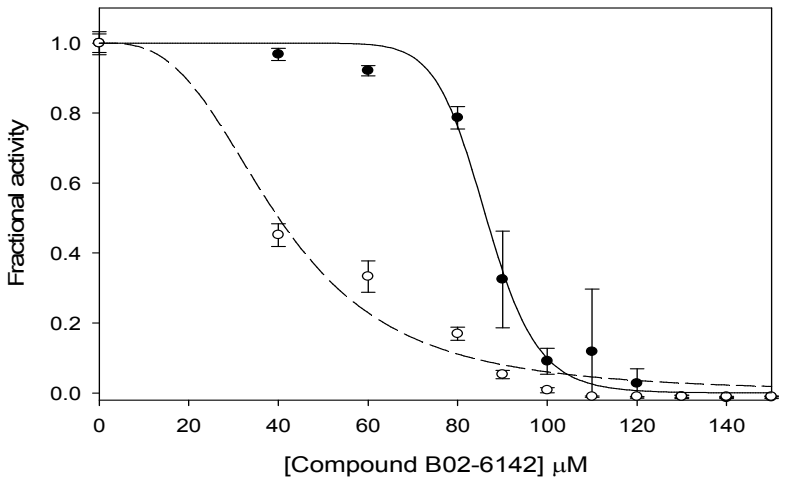

Figure 4.16 Compound B02-6142 concentration-response curve for apparent Dam (filled circles) and DpnI (open circles) activity. The fractional activity in the Dam or the DpnI assay is plotted against the compound concentration. Dam and DpnI data were fit to a 3 parameter logistic sigmoid to obtain the IC_{50} and the Hill coefficient (solid (R^2 = 0.99) and dashed (R^2 = 0.97) lines respectively).

Compound B02-6142 was only weakly inhibitory in the Dam activity assay up to a concentration of 60 μM. Measured activity then dropped by 80 % as the compound concentration was raised further from 60 to 100 μM. At a concentration of 150 μM no measurable activity remained. By contrast the effect of the compound on DpnI activity was pronounced even at low concentrations, with enzyme activity halving at 40 μM B02-6142. No DpnI activity remained in assays with a compound concentration of 110 μM. The IC_{50}s in the Dam and DpnI assays were 86 ± 1 μM and 40 ± 3 μM respectively. These results are consistent with the classification of the compound as a hit in the initial screen but also show it to be non-specific in its mode of action. The Hill coefficients from the fits of the Dam and DpnI data were 15.1 ± 2.2 and 3.0 ± 0.5 respectively. As discussed for compound D11-6141 these high coefficients provide additional evidence that B02-6142 was a non-specific inhibitor.

Tests on the synthesised compounds H09-6137, D11-6141 and B02-6142 showed that they were all acting non-specifically. DNA binding or intercalation was one possible mechanism by which the hit compounds elicited their non-specific effect in the assays. Mashoon and co-workers identified several such false hits in their HTS for *E. coli* Dam inhibitors (32). These DNA binding or intercalating compounds were identified with a 'Fluorescent Intercalator Displacement' (FID) assay (33,34).

A FID assay was used to test compounds H09-6137, D11-6141 and B02-6142. Thiazole orange is a molecule whose fluorescence is significantly higher when it is intercalated into DNA (35) (Figure 4.17). The K_d for thiazole orange with the DNA used in this assay is most likely in the range 3 – 15 μM, based on literature reports detailing its affinity for other oligonucleotides (33,35). Thiazole orange was used in the FID assays at a concentration of 0.75 μM, with 1.5 μM of dsDNA base pairs, ensuring it could be effectively displaced by a rival DNA binding molecule. Test compounds were added to solutions containing thiazole orange and DNA at the concentration needed for ~ 50 % DpnI inhibition. The fluorescence of these solutions was compared to a control containing no test compound (Figure 4.18).

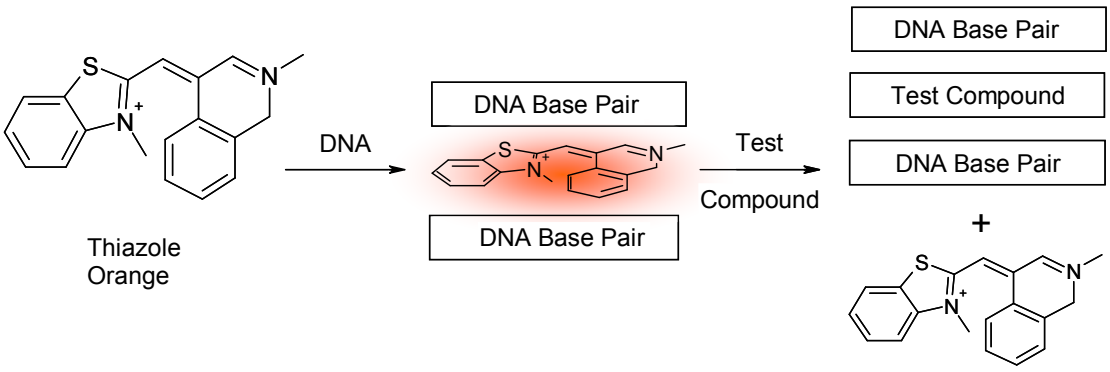

Figure 4.17 Principle of the FID assay. Thiazole orange has a low fluorescence in solution. Upon intercalation into a DNA double helix the fluorescence of thiazole orange is enhanced. Test compounds interacting with DNA in such a way as to displace thiazole orange cause a decrease in fluorescence.

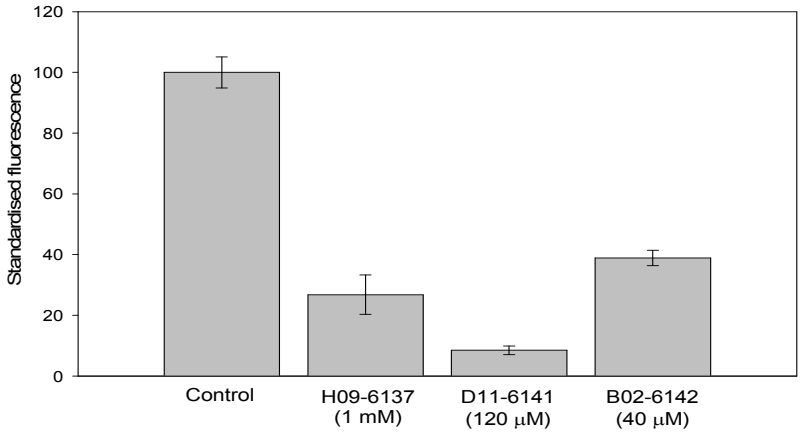

Figure 4.18 FID assay results for compounds H09-6137, D11-6141 and B02-6142. Fluorescence of assays containing test compounds is shown relative to a negative control.

Addition of compounds H09-6137, D11-6141 and B02-6142 led to falls in assay fluorescence of 73, 92 and 61 % respectively. These decreases are consistent with the compounds binding or intercalating with the DNA causing an associated displacement of thiazole orange.

4.4 Summary and conclusions

A 1000 compound library was screened in duplicate for activity against *Y. pestis* Dam using the real-time, fluorescence based, coupled enzyme assay. Raw data from this screen was processed by Z-score standardisation followed by background subtraction to negate plate and well biases. B-scoring appeared to be a better method of data processing on the basis that it removed some of the background patterns in the data which Z-scoring did not (Figure 4.8). Three hits and a compound of interest were identified from the screen and synthetic routes to them were devised. H09-6137 was made by a nucleophilic aromatic substitution followed by a Suzuki-Miyaura coupling. D11-6141 and B02-6142 were synthesised in a two step process involving a Buchwald-Hartwig amination followed by a Suzuki-Miyaura coupling. Disappointingly, all three of the synthesised compounds inhibited DpnI as well as Dam, showing that they were non-specific. Further testing with an FID assay revealed that the hits had elicited their inhibitory effects by binding to the DNA substrates rather than the enzymes.

Whilst disappointing, it should not have been surprising that a small compound library yielded only a few hits which subsequently turned out to be false positives. There are several ways in which compounds can inhibit enzyme activity assays without specifically targeting the enzyme of interest. These include reaction with the protein, optical interference, compound aggregation and DNA intercalation (36-38). Mashoon and co-workers screened a library of 50,000 compounds for activity against *E.coli* Dam. Their hit rates for compounds with an IC_{50} below 400 and 25 μM were 0.7 and 0.1 % respectively. About one third of the most potent inhibitors identified were found to have some interaction with DNA (32). It is worth noting that compared to other screens against different antibacterial targets this ranks as one of the more favourable outcomes. Mashoon and co-workers felt it validated a HTS strategy for this class of enzymes. Between 1995 and 2001 GlaxoSmithKline ran 67 HTS campaigns on antibacterial targets, none of which were DNA MTases, using a library containing hundreds of thousands of compounds. Only 16 of these resulted in hits and just 5 progressed to give leads (39). This scenario is typical of the worse than expected success rate which often accompanies HTS against a specific antibacterial target (40). Consequently some have

even suggested that HTS on a selected target is an unsuitable paradigm for discovery of novel antibacterials (39,40).

One drawback of the real-time, fluorescence based assay, which was apparent during the screen, was its inherent reliance on two enzymes. For compounds inhibiting DpnI it was impossible to deconstruct data from the whole assay to determine how much they affected the Dam-DNA interaction. A counter-screen against the restriction enzyme allowed the effect on the DNA-DpnI interaction to be measured. A direct assay for Dam activity would prevent false hits by DpnI inhibitors and also allow the study of the effect of compounds purely on the Dam-DNA interaction. With such an assay a true IC_{50} for Dam could be measured and compared with the IC_{50} for other enzymes like DpnI.

4.5 References

1. Malo, N., Hanley, J. A., Cerquozzi, S., Pelletier, J., and Nadon, R. (2006) *Nat Biotechnol* **24**, 167-175
2. Makarenkov, V., Kevorkov, D., Zentilli, P., Gagarin, A., Malo, N., and Nadon, R. (2006) *Bioinformatics* **22**, 1408-1409
3. Copeland, R. A. (2005) *Evaluation Of Enzyme Inhibitors In Drug Discovery*, Wiley-Interscience, Hoboken
4. Brideau, C., Gunter, B., Pikounis, B., and Liaw, A. (2003) *J Biomol Screen* **8**, 634-647
5. Inglese, J., Shamu, C. E., and Guy, R. K. (2007) *Nat Chem Biol* **3**, 438-441
6. Kumar, R., Srivastava, R., Singh, R. K., Surolia, A., and Rao, D. N. (2008) *Bioorg Med Chem* **16**, 2276-2285
7. Burns, C. J., and Wilks, A. F. (2002) *World Intellectual Property Organization. International publication number WO 02/060492*
8. Bonnet, P. A., Michel, A., Laurent, F., Sablayrolles, C., Rechencq, E., Mani, J. C., Boucard, M., and Chapat, J. P. (1992) *J Med Chem* **35**, 3353-3358
9. Miyaura, N., Yanagi, T., and Suzuki, A. (1981) *Synth Comm* **11**, 513-519
10. Miyaura, N., and Suzuki, A. (1995) *Chemical Reviews* **95**, 2457-2483
11. Bromidge, S. M., Dabbs, S., Davies, D. T., Davies, S., Duckworth, D. M., Forbes, I. T., Gaster, L. M., Ham, P., Jones, G. E., King, F. D., Mulholland, K. R., Saunders, D. V., Wyman, P. A., Blaney, F. E., Clarke, S. E., Blackburn, T. P., Holland, V., Kennett, G. A., Lightowler, S., Middlemiss, D. N., Trail, B., Riley, G. J., and Wood, M. D. (2000) *J Med Chem* **43**, 1123-1134
12. Harris, J., Church, N., Proud, A., Kling, M., and Vickery, B. D. (2004) *World Intellectual Property Organization. International publication number WO 2004/085409 A2*
13. Paul, F., Patt, J., and Hartwig, J. F. (1994) *J Am Chem Soc* **116**, 5969-5970
14. Guram, A. S., and Buchwald, S. L. (1994) *J Am Chem Soc* **116**, 7901-7902
15. Li, J. J., and Gribble, G. W. (2000) *Palladium in Heterocyclic Chemistry*, Pergamon, Amsterdam
16. Hartwig, J. F. (2002) Palladium-Catalyzed Amination of Aryl Halides and Related Reactions. In: Negishi, E. (ed). *Handbook of Organopalladium Chemistry for Organic Synthesis*, John Wiley and Sons, New York
17. Muci, A. R., and Buchwald, S. L. (2002) Practical Palladium Catalysis for C-N and C-O Bond Formation. In: Miyaura, N. (ed). *Cross-Coupling Reactions*, Springer-Verlag, Berlin
18. Guram, A. S., Rennels, R. A., and Buchwald, S. L. (1995) *Angew Chem Int Ed Engl* **34**, 1348-1350
19. Shelbourne, M. (2008) 4th Year Project Report. In., University Of Southampton
20. Kranenburg, M., Vanderburgt, Y. E. M., Kamer, P. C. J., Vanleeuwen, P., Goubitz, K., and Fraanje, J. (1995) *Organometallics* **14**, 3081-3089
21. Wolfe, J. P., and Buchwald, S. L. (1997) *Tetrahedron Lett* **38**, 6359-6362
22. Yin, J. J., and Buchwald, S. L. (2000) *Org Lett* **2**, 1101-1104
23. Driver, M. S., and Hartwig, J. F. (1996) *J Am Chem Soc* **118**, 7217-7218
24. Wolfe, J. P., Wagaw, S., and Buchwald, S. L. (1996) *J Am Chem Soc* **118**, 7215-7216
25. Wagaw, S., and Buchwald, S. L. (1996) *J Org Chem* **61**, 7240-7241
26. Guari, Y., van Es, D. S., Reek, J. N. H., Kamer, P. C. J., and van Leeuwen, P. (1999) *Tetrahedron Lett* **40**, 3789-3790

27. Kamer, P. C. J., van Leeuwen, P. W. N., and Reek, J. N. H. (2001) *Acc Chem Res* **34**, 895-904
28. Ali, M. H., and Buchwald, S. L. (2001) *J Org Chem* **66**, 2560-2565
29. Meyers, C., Maes, B. U., Loones, K. T., Bal, G., Lemiere, G. L., and Dommisse, R. A. (2004) *J Org Chem* **69**, 6010-6017
30. Torisawa, Y., Nishi, T., and Minamikawa, J. (2000) *Bioorg Med Chem Lett* **10**, 2489-2491
31. Wolfe, J. P., and Buchwald, S. L. (1997) *J Org Chem* **62**, 6066-6068
32. Mashhoon, N., Pruss, C., Carroll, M., Johnson, P. H., and Reich, N. O. (2006) *J Biomol Screen* **11**, 497-510
33. Boger, D. L., and Tse, W. C. (2001) *Bioorg Med Chem* **9**, 2511-2518
34. Tse, W. C., and Boger, D. L. (2004) *Acc Chem Res* **37**, 61-69
35. Nygren, J., Svanvik, N., and Kubista, M. (1998) *Biopolymers* **46**, 39-51
36. Rishton, G. M. (2003) *Drug Discov Today* **8**, 86-96
37. Shoichet, B. K. (2006) *Drug Discov Today* **11**, 607-615
38. Ostrov, D. A., Hernandez Prada, J. A., Corsino, P. E., Finton, K. A., Le, N., and Rowe, T. C. (2007) *Antimicrob Agents Chemother* **51**, 3688-3698
39. Payne, D. J., Gwynn, M. N., Holmes, D. J., and Pompliano, D. L. (2007) *Nat Rev Drug Discov* **6**, 29-40
40. Chan, P. F., Holmes, D. J., and Payne, D. J. (2004) *Drug Discovery Today* **1**, 519-524

Chapter 5:- A novel and direct assay for Dam activity

5.1 Introduction

In our original Dam assay, measurement of N6-adenine methyltransferase activity relied on coupling of methylation to oligonucleotide cleavage by DpnI (1). As a consequence the observed *Y. pestis* Dam activity measurements could have been distorted by DpnI inhibitors. Such compounds might give the appearance of Dam inhibition via DpnI inhibition. We sought to produce a real time, fluorescence based, direct assay for Dam activity to overcome this weakness. The direct assay used the known destabilising effect of adenine methylation to partially melt a DNA duplex labelled with a FRET pair (2).

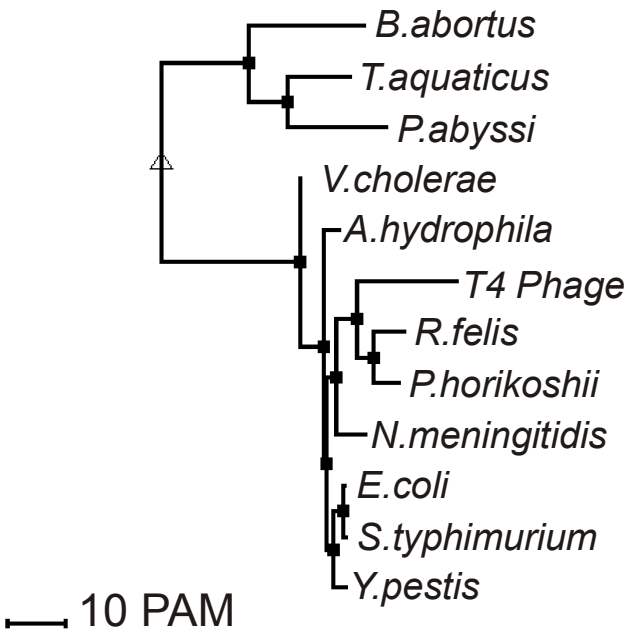

Figure 5.1 Phenogram showing the sequence similarity of selected N6-adenine methyltransferases from various organisms (3). Differences between methyltransferase sequences are shown in Point Accepted Mutation (PAM) (4).

For development purposes it was desirable to use a highly stable methyltransferase, which would allow long assay times at a wide range of temperatures. It was also

preferable for the methyltransferase to retain a high sequence similarity to the original enzyme of interest, *Y. pestis* Dam. A homology search identified *Pyroccocus horikoshii* Dam (M. PhoDam) as a suitable candidate (Figure 5.1).

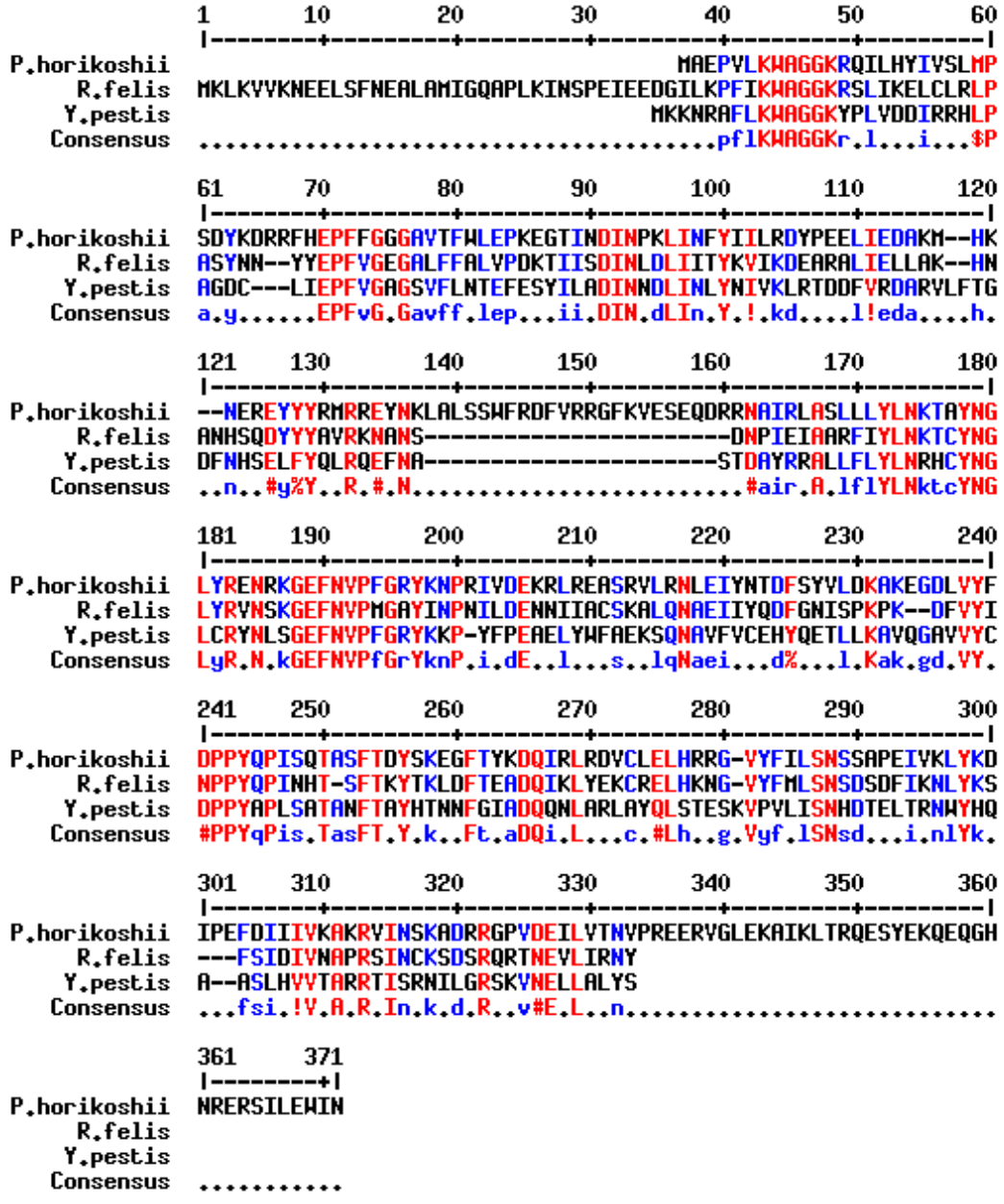

Figure 5.2 An alignment of the *P. horikoshii, R.felis and Y. pestis* Dam amino acid sequences carried out using the program Multialign (3). Sequences with high and low consensuses are shown in red and blue respectively. In the consensus sequence, symbols are used to show the conservation of particular sets of amino acids; # = D, E, N or Q, ! = I or V, $ = L or M and % = F or Y. For comparison an alignment of *Y. pestis* Dam with that of *E. coil* and T4 phage may be found in appendix G.

Pyroccocus horikoshii is a hyperthermophillic archaeon and, with an optimal growth temperature of 98 ^{o}C, its proteins are by necessity thermally stable (5). *P. horikoshii* Dam shows a high degree of sequence similarity to the adenine MTases of pathogenic bacteria such as *Y. pestis* and *R. felis* (Figure 5.2). *P. horikoshii* Dam is 330 amino acids long and when aligned has 93 and 125 amino acids identical to *Y. pestis* and *R. felis* Dam respectively.

This chapter describes the production of *P. horikoshii* Dam and its application in a novel and direct real-time fluorescence based N6-adenine methyltransferase activity assay.

5.2 Cloning, expression and purification of *P. horikoshii* Dam

5.2.1 Cloning of the *P. horikoshii dam* gene

PCR reactions were set up using *P. horikoshii* genomic DNA as a template and primers designed to copy the *dam* gene adding NcoI and XhoI restriction sites at the start and end respectively. The reverse primer encoded a His_6-tag which would be appended to the C-terminus of the protein upon translation.

Primer	*Sequence 5' to 3'*
PhoCfo	GATCGA*CCATGG*CAGAACCCGTTTTA
PhoCre	GACTC**CTCGAG**TTAATGATGATGATGATGATGATTAATCCACTC AAGTATTGATCTC

Table 5.1 Sequences of the forward (PhoCfo) and reverse (PhoCre) primers used to amplify the *P. horikoshii dam* gene. The NcoI and XhoI restriction sites are shown in italics and bold respectively. The sequence encoding the His_6-tag is underlined.

Previous work had been carried out within the group by Dr. R. J. Wood, J. McKelvie, C. Williams, D. Coomber and A. Stares in which N-terminally His_6-tagged *P. horikoshii* Dam was expressed and purified. A shorter protein was observed to co-purify with this full length Dam (6). It was thought that this contaminant may have been a product of

premature termination of translation. Since translation proceeds from the N to C termini, it was reasoned that a C-terminal His_6-tag would permit the isolation of pure full length Dam.

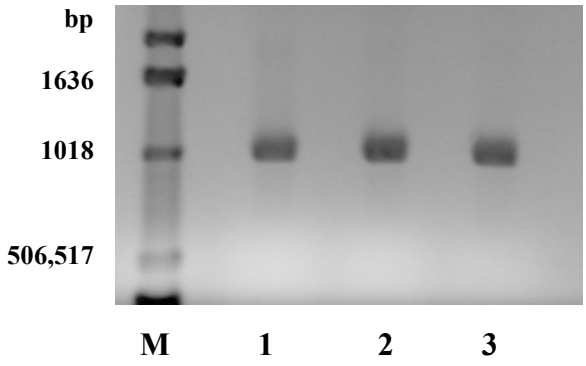

Figure 5.3 1 % AGE analysis of PCR reactions to amplify the *P. horikoshii dam* gene. Lane M = DNA ladder. Lanes 1-3 = PCR reactions containing 10, 1 and 0.1 ng μl^{-1} template DNA respectively, expected size = 1030 bp.

Analysis of the PCR reactions by agarose gel electrophoresis showed that at each template DNA dilution a fragment consistent with the *dam* gene had been formed (Figure 5.3)

The purified *dam* gene was digested with restriction enzymes XhoI and NcoI to form sticky ends. A second fragment, with complementary sticky ends and an ampicillin resistance marker, was made by digestion of plasmid pBadHisA with the same enzymes. Both gene and vector were purified with agarose gel electrophoresis before analysis by 1 % AGE (Figure 5.4).

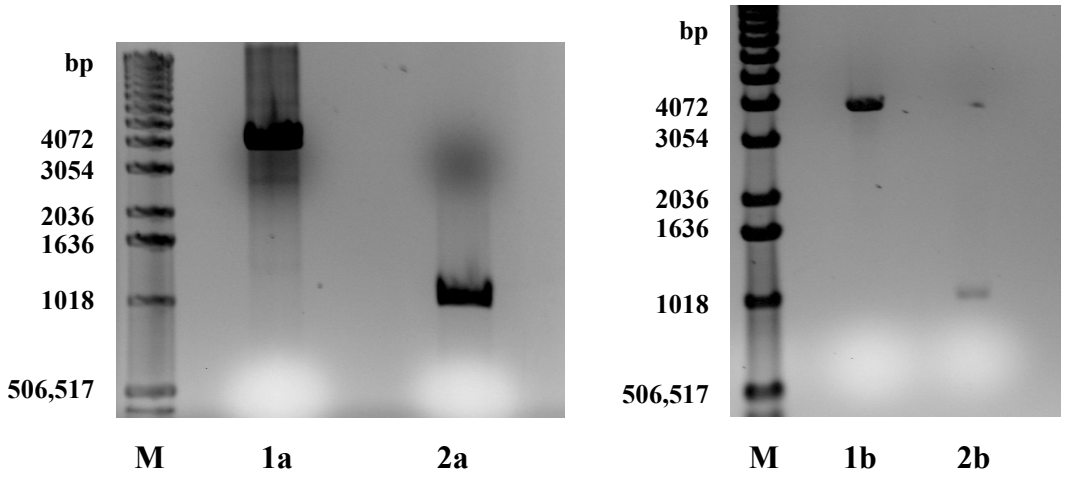

Figure 5.4 (Left) 1 % agarose gel purification of digests of pBadHisA and the cloned *P. horikoshii dam* gene. Lane M = DNA ladder, 1a = digested pBadHisA, expected size = 3989 bp, 2a = *dam* gene, expected size 1013 bp. (Right) 1 % AGE analysis of pBadHisA vector and the *dam* gene after gel purification. M = DNA ladder. Lane 1b = digested pBadHisA, 2b = *dam* gene.

Both gene and vector appeared as single bands of the expected sizes. Overnight ligation reactions were carried out at two different insert to vector ratios, 3:2 and 6:2. A negative control without any insert was also prepared. Competent *E. coli* TOP10 cells were transformed with these ligations. High and low insert to vector ratio ligations yielded thirty and forty five colonies per plate respectively whilst the vector only negative control plate had eleven colonies. Transformants which contained a copy of the *dam* gene were identified by colony PCR (Figure 5.5).

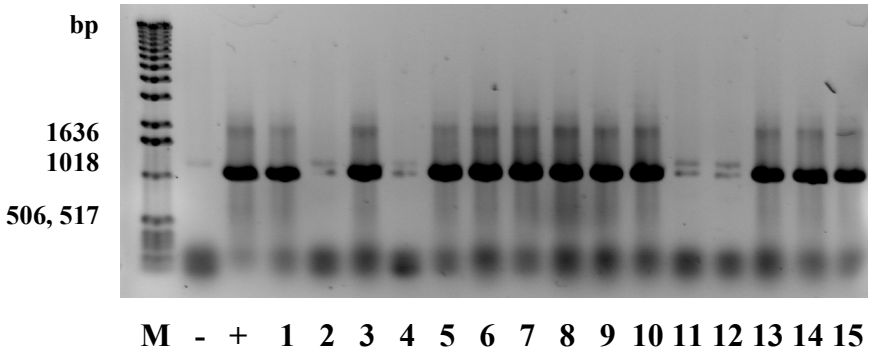

Figure 5.5 1 % AGE analysis of colony PCR reactions. Lane M = DNA Ladder. - = negative control (colony containing pBadHisA). + = positive control (*P. horikoshii* genomic DNA), expected size 1030 bp. Lanes 1 – 15 represent PCR reactions set up using colonies assigned numbers 1 - 15.

Of the fifteen colonies screened, eleven were found to contain a copy of the *P. horikoshii dam* gene. Plasmid was extracted from overnight cultures of colonies numbered 9, 10, 13 and 14, and subjected to analytical digestion (Figure 5.6).

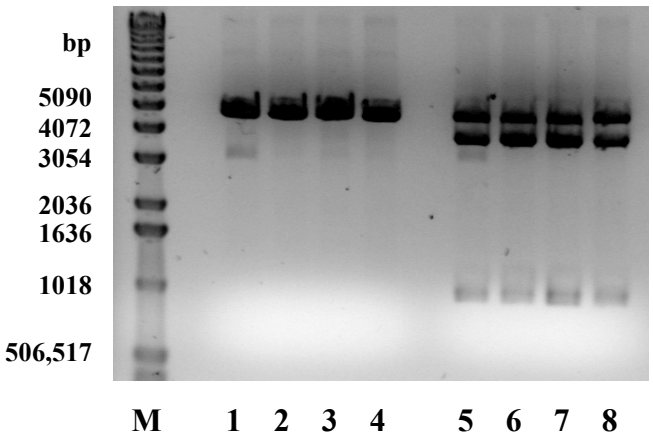

Figure 5.6 1 % AGE analysis of digests of plasmid extracted from transformants containing the *dam* gene. Lane M = DNA Ladder. Lanes 1-4 = plasmid from colonies 9, 10, 13 and 14 linearised with NcoI, expected size = 5002 bp. Lanes 5-8 = plasmid from colonies 9, 10, 13 and 14 digested with NcoI and XhoI, expected sizes 1013, 3989 bp.

Linearised plasmids appeared to be of the correct size as did the excised *dam* gene and vector. Some DNA was not cut twice in the double digestion reactions leading to the observation of a third band the size of linearised plasmid (Figure 5.6, lanes 5-8). Plasmid from one of the colonies was subjected to further restriction mapping with a selection of restriction enzymes (Figure 5.7).

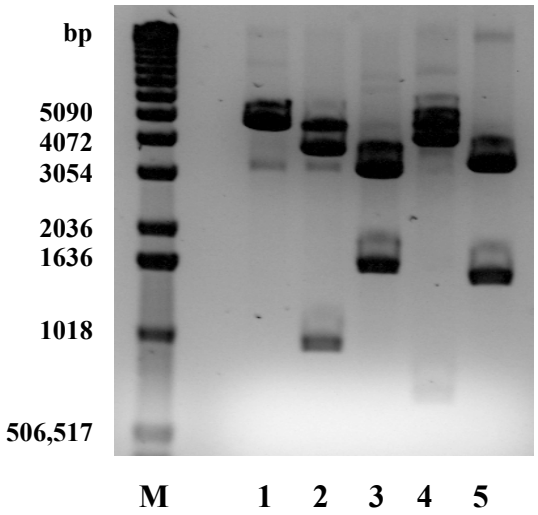

Figure 5.7 1 % AGE analysis of digests of plasmid extracted from colony 9. Lane 1: NcoI, expected = 5002 bp, observed ~ 5000 bp. Lane 2: NcoI, XhoI, expected = 1013, 3989 bp, observed ~ 1000, 4000, 5000 bp (linearised plasmid). Lane 3: BamHI, PciI, expected = 1677, 3325 bp, observed ~ 1600, 3300 bp. Lane 4: BamHI, NheI, expected = 710, 4292 bp, observed ~ 700 (faint), 4000, 5000 bp (linearised plasmid). Lane 5: NsiI = 1551, 3451 bp, observed ~ 1500, 3400 bp.

Plasmid from colony 9 digested in a manner consistent with the expected structure. Competent *E. coli* BL21 pLysS Rosetta 2 cells were transformed with this plasmid. The Rosetta 2 strain, which supplies additional tRNA for seven rare codons, had proved the most successful for expression of the N-terminally His_6-tagged Dam (6,7). The plasmid, which contained the *P. horikoshii dam* gene under the control of an arabinose inducible promoter, was designated pMMS511811.

5.2.2 Expression of C-His_6-*P. horikoshii* Dam

2YT media supplemented with ampicillin and chloramphenicol was inoculated from an overnight culture of BL21 pLysS Rosetta 2 harbouring pMMS511811. The culture was grown at 27 °C for two hours after induction with arabinose at an absorbance of 0.6 at 600 nm. Approximately 12 g of cell paste was harvested from the 4 L culture, of which 5 g were subsequently used for a nickel affinity purification of *P. horikoshii* Dam. Fractions from the chromatography column were analysed by SDS-PAGE (Figure 5.8).

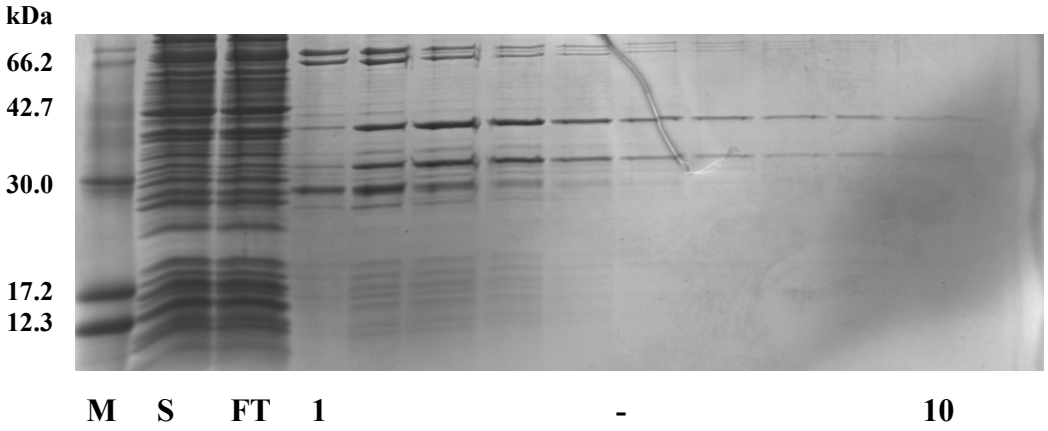

Figure 5.8 15 % SDS-PAGE analysis of C-His_6-tagged *P. horikoshii* Dam expressed in BL21 pLysS Rosetta 2. M = molecular weight marker. S = supernatant. FT = column flow through. 1 - 10 = eluted fractions, expected size = 40,171 Da.

The full length C-His_6-tagged *P. horikoshii* Dam was not observed to be any purer than the N-His_6-tagged enzyme which had been prepared previously. In the purer fractions eluted from the nickel column an impurity, approximately 10 kDa smaller than the full length Dam, was still observed. Expression was therefore also tested in three other *E. coli* cell strains, GM161, GM124 and JW3351-1 from the Keio collection of knockouts (8) (Figure 5.9, Figure 5.10, Figure 5.11).

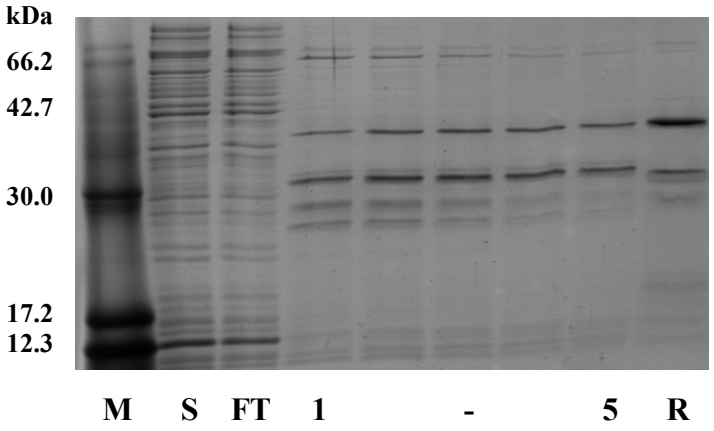

Figure 5.9 15 % SDS-PAGE analysis of C-His_6-*P. horikoshii* Dam expressed in strain JW3351-1. M = molecular weight marker. S = supernatant. FT = column flow through. 1 - 7 = eluted fractions, expected size = 40,171 Da. R = N-His_6-*P. horikoshii* Dam.

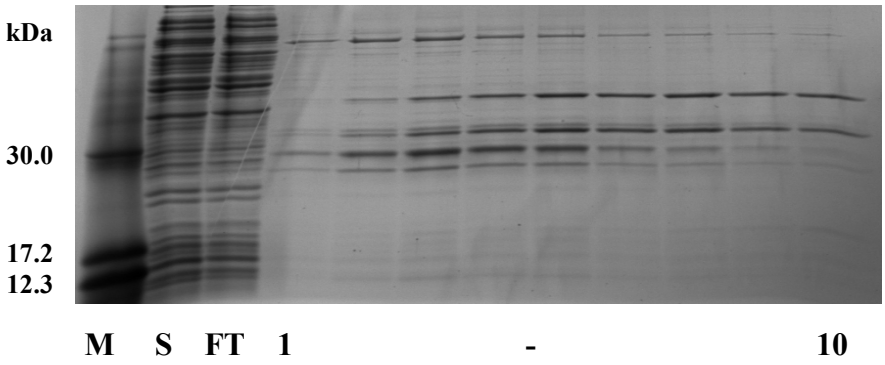

Figure 5.10 15 % SDS-PAGE analysis of C-His$_6$-*P. horikoshii* Dam expressed in GM161. M = molecular weight marker. S = supernatant. FT = column flow through. 1 - 10 = eluted fractions, expected size = 40,171 Da.

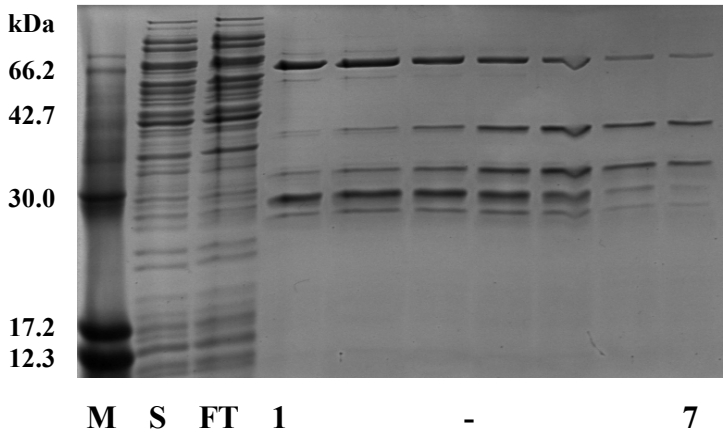

Figure 5.11 15 % SDS-PAGE analysis of C-His$_6$-*P. horikoshii* Dam expressed in GM124. M = molecular weight marker. S = supernatant. FT = column flow through. 1 - 7 = eluted fractions, expected size = 40,171 Da.

These alternative expression strains afforded no enhancement in Dam purity. C-His$_6$-tagged *P. horikoshii* Dam was consistently judged to be more contaminated than the N-terminally tagged enzyme on 15 % polyacrylamide gels (Lane R, Figure 5.9). This assessment was supported by high resolution polyacrylamide gel analysis of samples from the purification of each protein expressed in BL21 pLysS Rosetta 2 (Figure 5.12).

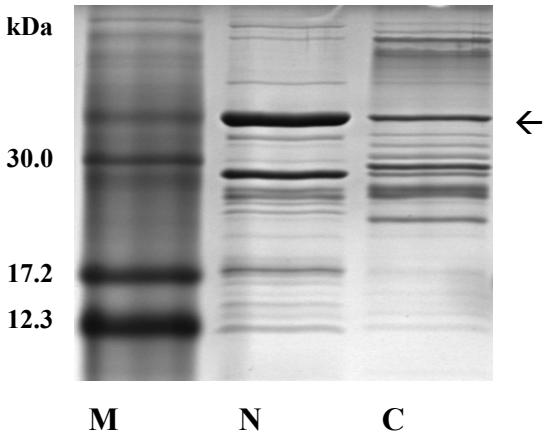

Figure 5.12. High Resolution 16 % Tricine SDS-PAGE analysis of N and C-terminally His_6-tagged *P. horikoshii* Dam. M = marker, N / C = termini to which the His_6-tag was attached. Expected mass of the full length protein was 40 kDa (see arrow).

The ratio of *P. horikoshii* Dam to truncated impurity was clearly lower with the C-terminal affinity tag. It was also noted that the impurity appeared slightly larger with the tag on the C-terminus. Both of these observations were inconsistent with the hypothesis of premature termination of translation.

To provide a definitive identification, the contaminating protein was isolated by SDS-PAGE, electroblotted onto a PVDF membrane and sent for N-terminal sequencing at Cambridge Peptides (appendix E). The six N-terminal amino acids were found to be M - - E Y N, were – represents an unidentified amino acid. This amino acid sequence, MRREYN, was found in the middle of *P. horikoshii* Dam. The contaminant was therefore attributed to a mis-initiation of translation at this internal methionine residue. This explanation also accounted for the observation that a C-terminal His_6-tag made the contamination worse and slightly increased the mass of the impurity.

To eliminate this contaminant, directed mutagenesis of N-His_6-M.PhoDam was undertaken. The methionine amino acid, where mis-initiation of translation began, was to be replaced with an alanine residue. Alanine was chosen because it is a small and comparatively inert amino acid which was unlikely to have deleterious effects on the methyltransferase activity.

5.2.3 Directed mutagenesis of *P. horikoshii* Dam

Plasmid pCLW469397, encoding N-His_6-Dam, was isolated from *E. coli* strain TOP10 and used as template DNA in PCR reactions containing two mutagenic primers. These primers each contained a mismatch which replaced the troublesome methionine codon with an alanine one (Table 5.2).

Primer	*Sequence 5' to 3'*
PhofM98A	GGGAGTACTACTATAGAGCGCGAAGAGAATACAATAAACTTGCCC
PhorM98A	GGGCAAGTTTATTGTATTCTCTTCGCGCTCTATAGTAGTACTCCC
Wild type sequence: GAGTACTACTATAGA***ATG***CGAAGAGAATACAATAAAC	

Table 5.2 Sequences of the primers used to mutate the *P. horikoshii dam* gene. The mismatched codons are underlined. The methionine codon which was replaced is shown in bold italics in the wild type sequence.

PCR reactions were analysed by AGE, subjected to incubation with DpnI to destroy any original template DNA and re-analysed by AGE (Figure 5.13).

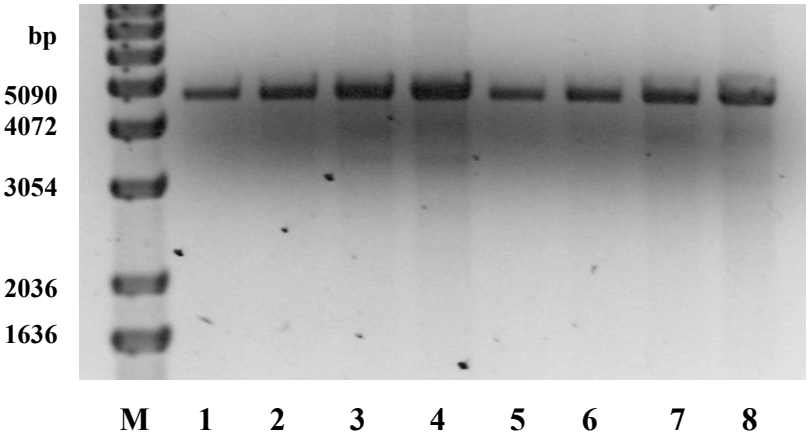

Figure 5.13. 1 % AGE analysis of PCR reactions used to mutate the *P. horikoshii dam* gene in plasmid pCLW469397. M = DNA ladder, lanes 1-4 = samples from PCR reactions containing 5, 10, 20 and 40 ng of template DNA respectively, expected size = 5007 bp. lanes 5-8 = DNA from lanes 1-4 after incubation with DpnI, expected size = 5007 bp.

The PCR reactions all gave a product of the expected length but those with more template appeared to be higher yielding. Since DpnI is specific for methylated DNA it degraded the bacterially synthesised pCLW469397 plasmid but left the new PCR product intact (Figure 5.13).

E. coli strain TOP10 was transformed with this newly formed mutated DNA. Staggered strand breaks in the DNA will have been ligated by repair enzymes within the bacteria. The resultant plasmid encoding N-His_6-M98A-*P. horikoshii* Dam was designated pMMS528431. Plasmid DNA was isolated from overnight bacterial cultures and subjected to analytical digestion (Figure 5.14).

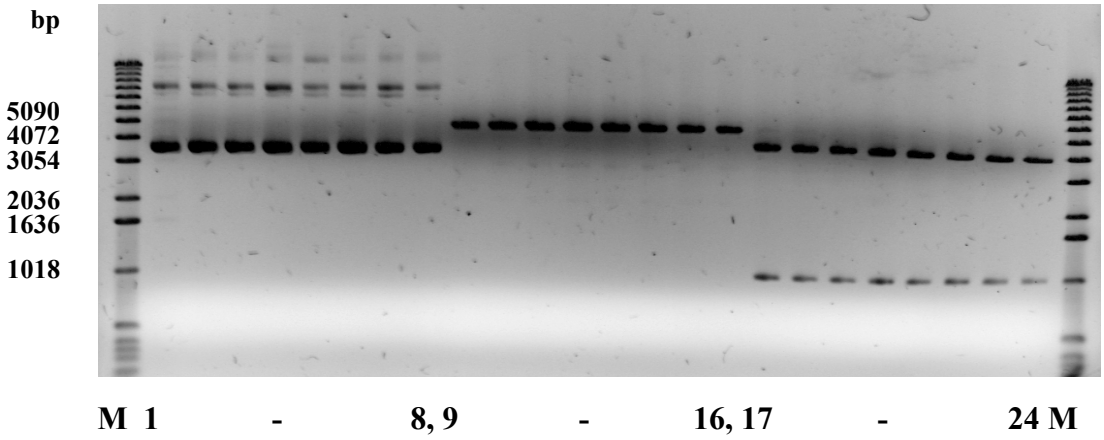

Figure 5.14. 1 % AGE analysis of plasmid pMMS528431 isolated from *E. coli* TOP10. M = DNA Ladder, lanes 1/2, 3/4, 5/6, 7/8 = plasmid isolated from two separate colonies of bacteria transformed with PCR reactions 1 to 4 respectively, lanes 9 – 16 = plasmid as for lanes 1 – 8 but linearised with NcoI, expected size = 5007 bp, lanes 17 – 24 = plasmid as for lanes 1- 8 but digested with NcoI and XhoI, expected sizes = 1016 and 3991 bp.

All of the plasmids examined were of the expected length and contained a XhoI, NcoI excisable insert of the expected size. Plasmid DNA, from a couple of the colonies, was sent for sequencing using two primers which extended towards the centre of the gene from a region beyond each of its ends (pBad forward and reverse, appendix B). In both plasmids the gene was found to contain the specific mutation which would exchange methionine ninety eight with alanine in the expressed protein (appendix F).

Plasmid pMMS528431 was transformed into *E. coli* strain BL21 pLysS Rosetta 2 and Dam expression carried out under conditions optimised for the wild type enzyme (7). After induction, a 5 litre culture was maintained at 16 °C overnight and yielded 66 g of cell paste upon centrifugation. A nickel affinity purification was carried out on 10 g of cell paste. Fractions eluted from the column were analysed by SDS-PAGE (Figure 5.15)

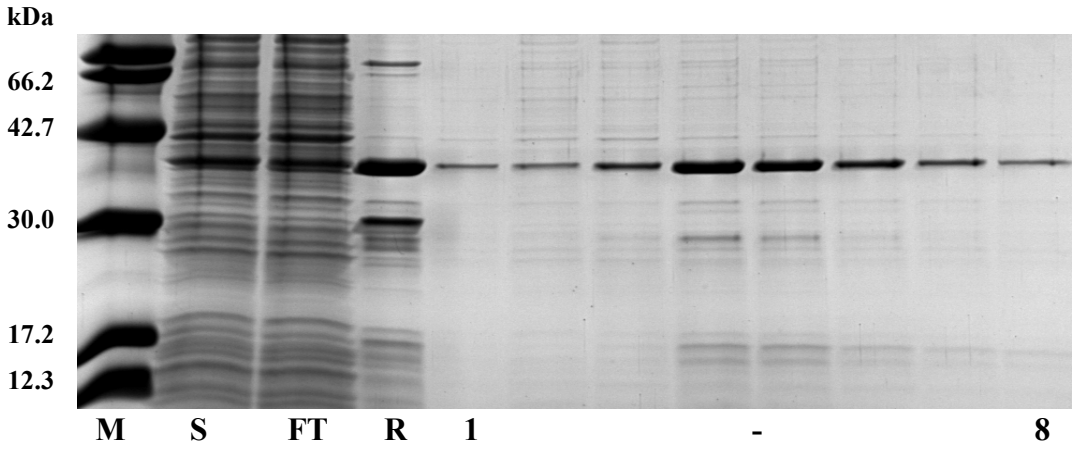

Figure 5.15. 15 % SDS-PAGE analysis of N-His_6-M98A-*P. horikoshii* Dam expressed in BL21 pLysS Rosetta 2. M = molecular weight marker, S = supernatant, FT = flow through, R = wild type Dam reference, lanes 1 – 8 = eluted fractions, expected 40,228 Da.

A protein with the mass of *P. horikoshii* Dam was observed and found to be free from the product of mis-translation, clearly visible in the reference sample of wild type enzyme (Figure 5.15, lane R). From 10 g of cell paste, 3.5 mg of the mutant hyperthermophilic N6-adenine methyltransferase was isolated. This enzyme was dialysed into a storage buffer containing 20 % glycerol and frozen in 0.2 mg ml^{-1} aliquots at – 80 °C until needed.

5.3 A direct assay for N6-adenine methyltransferase activity

5.3.1 A preliminary test of the assay principle

The direct assay was designed to use the destabilising effect that adenine methylation has on double helical DNA to increase the mean separation of a FRET pair attached to an oligonucleotide. To test the feasibility of measuring the real-time fluorescence increases associated with this process, a preliminary experiment, using *P. horikoshii* Dam and the hairpin oligonucleotide from the coupled assay, was carried out (Figure 5.16, Figure 5.17).

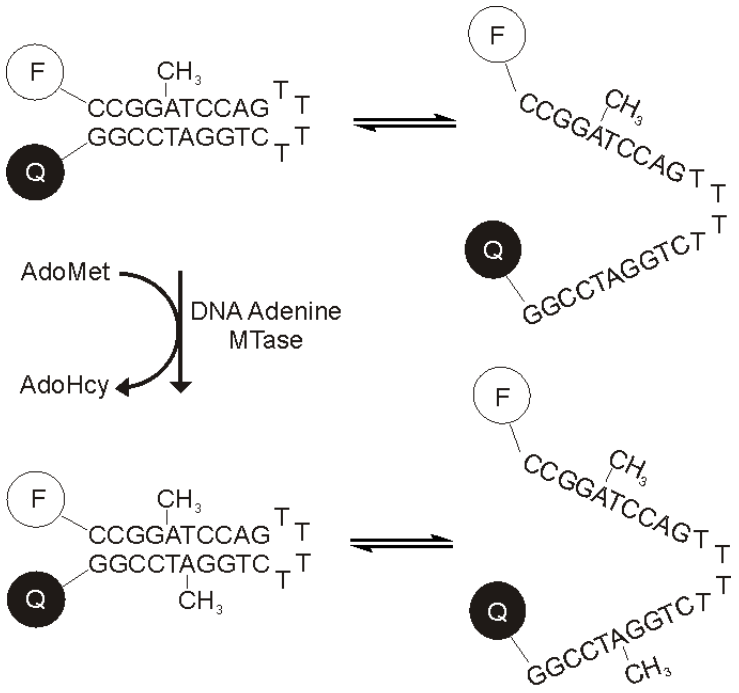

Figure 5.16 High temperature Fluorescence Equilibrium Perturbation (FEP) assay scheme. At temperatures near to the T_m, methylation shifts the equilibrium between closed and open ODN 3 towards the more fluorescent open form.

Four different concentrations of *P. horikoshii* Dam were added to duplicate buffered solutions of ODN 3 and AdoMet. Fluorescence timecourses of the solutions were measured in a Roche lightcycler at 78 °C (Figure 5.17).

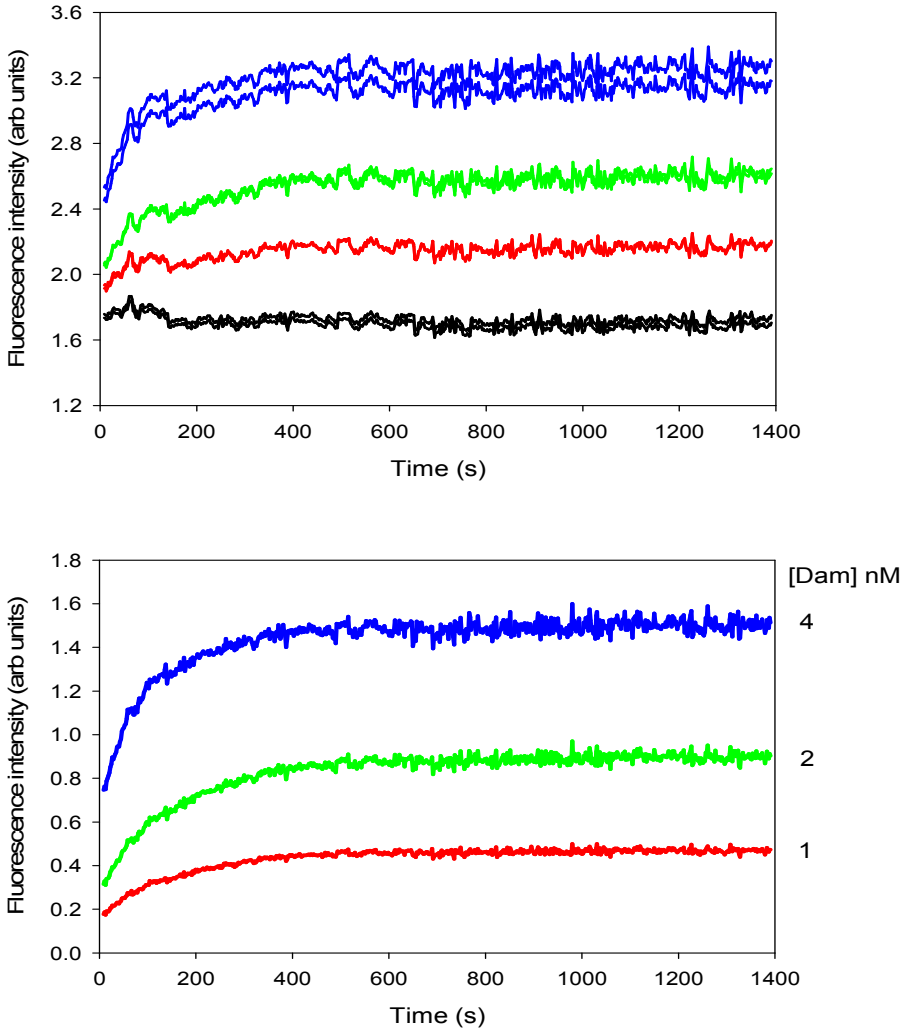

Figure 5.17 (Upper graph) Raw duplicate fluorescence timecourses of direct Dam activity assays performed at 78 °C. Assays (20 µl) contained 20 mM potassium phosphate buffer (pH 7.8), 200 mM NaCl, 1 mM $MgCl_2$, 1 mM DTT, 0.1 mg ml^{-1} BSA, 25 µM AdoMet, 100 nM ODN 3 and 0 nM (black), 1 nM (red), 2 nM (green) or 4 nM (blue) *P. horikoshii* Dam. (Lower graph) Averaged fluorescence timecourses for assays containing 1, 2 and 4 nM Dam with the background fluorescence (0 nM Dam) subtracted.

Real-time fluorescence increases were observed in all of the Dam containing assays (Figure 5.17). The greatest increases in fluorescence were seen in the assays which contained the most Dam. This effect was attributed to incomplete substrate turnover caused by enzyme inactivation at the high assay temperature. Complete turnover would have resulted in the same fluorescence endpoints being reached in each of the assays

regardless of methyltransferase concentration. Initial rates of fluorescence increase in the Dam containing assays, after background subtraction, were determined as 1.8 x 10^{-3} ± 0.1 x 10^{-3} (1 nM Dam), 3.8 x 10^{-3} ± 0.1 x 10^{-3} (2 nM Dam) and 6.9 x 10^{-3} ± 0.2 x 10^{-3} arb units s^{-1} (4 nM Dam). The initial rates of fluorescence increase were almost directly proportional to Dam concentration.

Once the fluorescence increases had ceased, the thermal melting profile of the DNA in each of the eight duplicate assays was measured (Figure 5.18). The melting temperatures of the DNA in the assays containing 0 and 4 nM Dam were determined by the fit of a 4 parameter sigmoid, $f = f_0 + (a / 1 + e^{-(T - Tm / b)})$, to the profiles. In this equation fluorescence and fluorescence at a low temperature are denoted with f and f_0, temperature and the melting temperature are denoted with T and T_m.

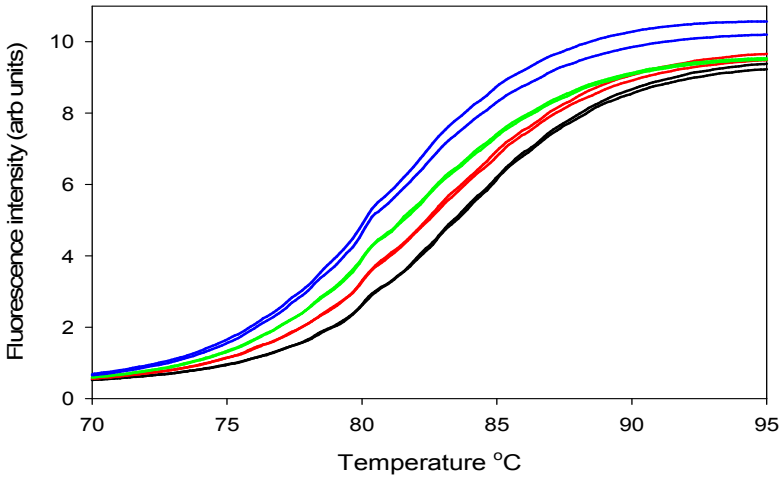

Figure 5.18 Thermal melting profiles of the eight duplicate Dam activity assays. Profiles are of assays containing 0 nM (black), 1 nM (red), 2 nM (green) and 4 nM (blue) Dam.

The oligonucleotides in the 0 and 4 nM Dam assays had melting temperatures of 83.3 ± 0.1 and 80.8 ± 0.1 °C respectively. This reduction of the melting temperature in the assays containing Dam could be accounted for by methylation of the oligonucleotide.

On the basis of these encouraging results, oligonucleotides were designed to allow the assay to be conducted at a lower temperature, permitting the use of a microplate reader

to collection the experimental data. This was also necessary to make the assay applicable to the study of non-thermophilic adenine MTases from pathogenic bacteria.

5.3.2 Proof of the assay principle at lower temperatures

The lower temperature assay would rely on using enzymatic DNA methylation to perturb the equilibrium between intermolecular single and double stranded DNA and cause a fluorescence increase (Figure 5.19).

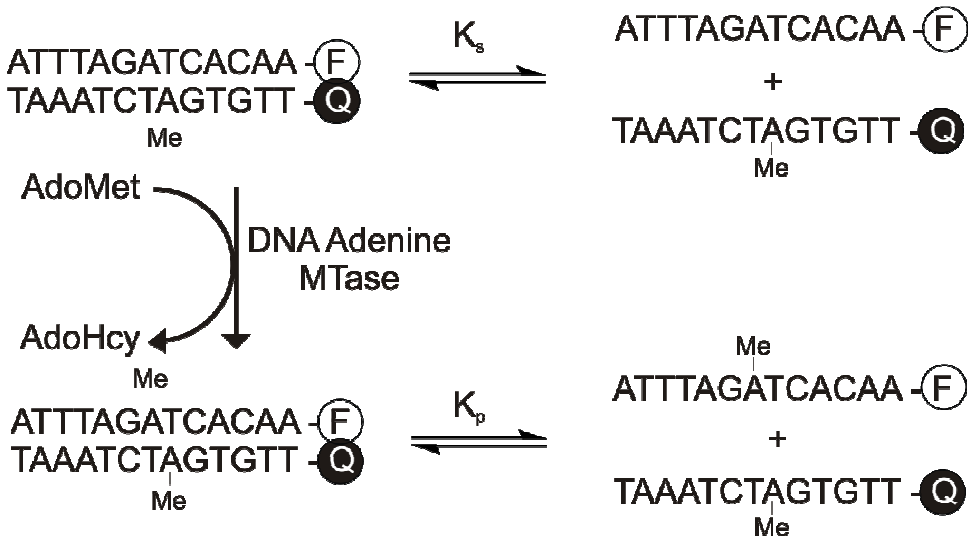

Figure 5.19 Fluorescence Equilibrium Perturbation (FEP) assay scheme. ODN 4 and M ODN 7 were annealed to form the initial double stranded, hemi-methylated MTase substrate (upper left). K_s and K_p are the substrate and product equilibrium constants respectively.

The assay was to be conducted a few degrees below the melting temperature of the initial hemi-methylated duplex, labelled on opposite strands with a FRET pair. The equilibrium between double and single stranded DNA would at the start of the assay be governed by equilibrium constant K_s. Upon methylation this equilibrium would instead be governed by constant K_p. Since equilibrium K_p lies more in favour of single stranded DNA, methylation would be accompanied by an increases in the mean distance between the FRET pair. A measurable increase in fluorescence would result.

A gel based assay was used to confirm that the mutant hyperthermophilic adenine MTase was active at the intended assay temperature of 33 °C. Hemi-methylated oligonucleotide (1 μM), formed from ODN 4 and M ODN 7, was incubated with 100 nM *P. horikoshii* Dam for between 0 and 80 minutes before exposure to DpnI which cut any fully methylated duplex. The resulting mixture of uncut and cut DNA was analysed by short oligonucleotide gel electrophoresis with visualisation under UV light (Figure 5.20).

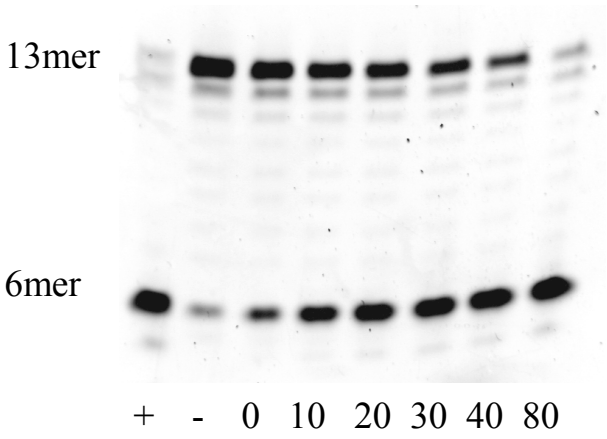

Figure 5.20 20 % PAGE analysis of fluorescently labelled DNA, digested with DpnI, following incubation with *P. horikoshii* Dam for between 0 and 80 minutes. Lanes + and – contained synthetic fully and hemi-methylated DNA exposed to DpnI. Numbered lanes were incubated with Dam, for the indicated time in minutes, prior to digestion with DpnI.

Without staining, only the full length (13 mer) or digested (6 mer) ODN 4 with its fluorescent label were visible on the gel. Results indicated that the methyltransferase was active, with longer incubation times producing a higher proportion of DpnI susceptible DNA. Relative intensities of the bands from this and a repeat short oligonucleotide gel were quantified and plotted on a graph (Figure 5.21).

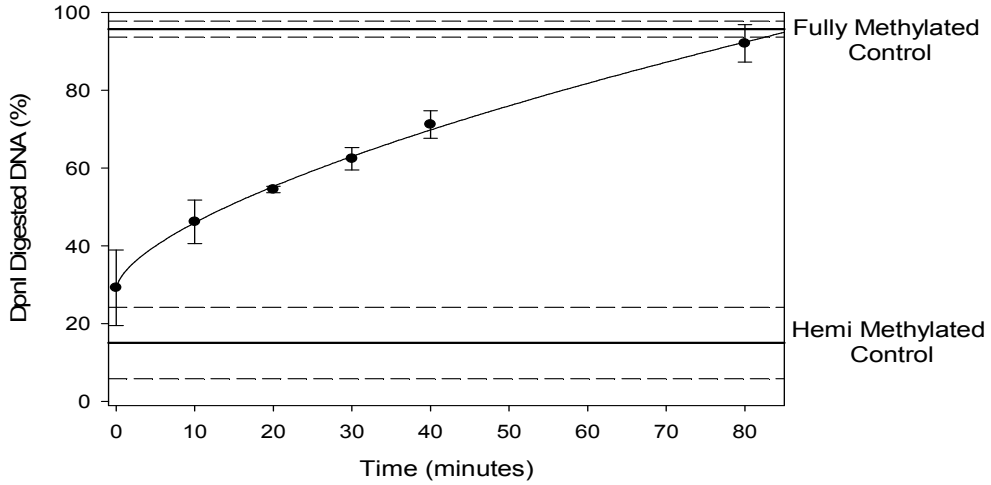

Figure 5.21 Quantification of the gel electrophoresis analysis of fluorescently labelled duplex DNA, digested with DpnI, following incubation with *P. horikoshii* Dam. The percentage of the DNA susceptible to DpnI cleavage versus the time for which the DNA had previously been incubated with *P. horikoshii* Dam is shown.

Methyltransferase activity looked to be near linear for at least 40 minutes and methylation of the substrate appears to approach completion after 80 minutes. Turnover of the methyltransferase was estimated to be 0.10 ± 0.03 min^{-1} from the quantification of the gel.

The gel based assay was carried out in the same phosphate buffer which was to be used for the direct assay. A phosphate based buffer was chosen instead of Tris because its pH is less affected by temperature changes. Work by J. Mckelvie and A. Stares had shown that greater fluorescence increases were observed upon oligonucleotide melting in phosphate buffer (7). A sodium chloride concentration of 200 mM was chosen based on Watanabe and co-workers study of a hyperthermophilic adenine MTase from an archaeon of the same genus (9).

DNA melting profiles of hemi and enzymatically fully-methylated duplex were carried out in this buffer to demonstrate that there would be a clear fluorescence increase upon oligonucleotide methylation (Figure 5.22)

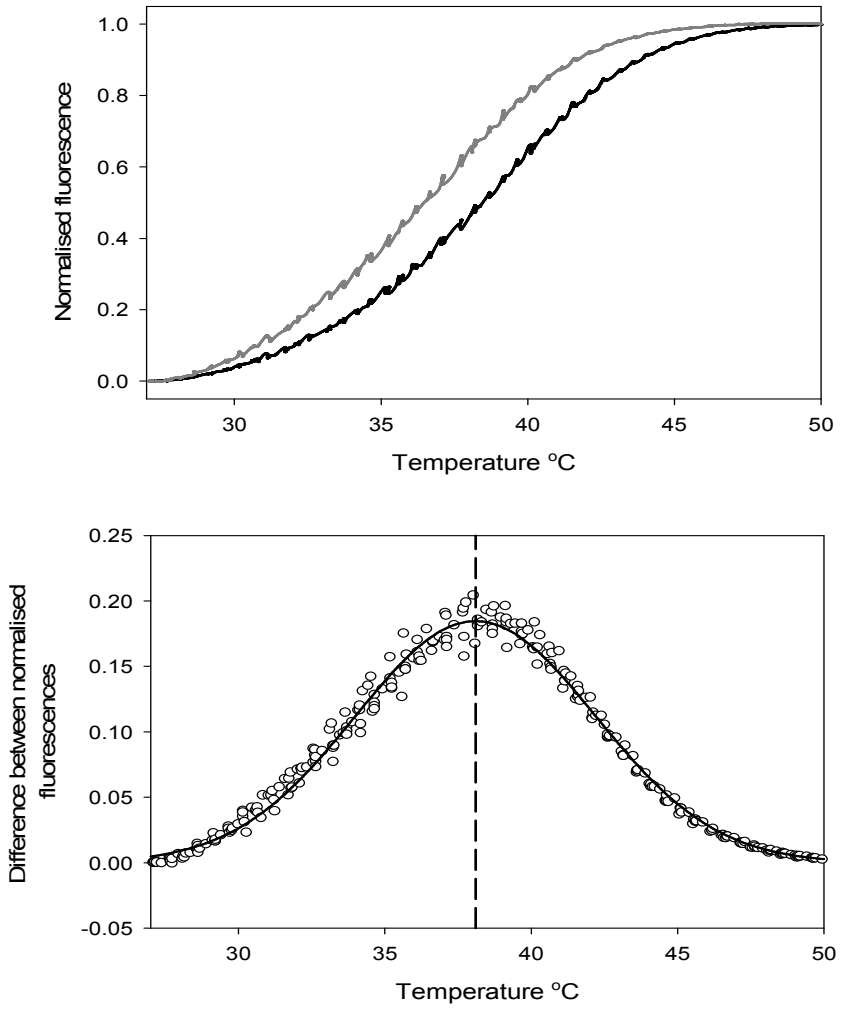

Figure 5.22 (Upper graph) Melting curves (duplicate averaged) for hemi (black) and enzymatically fully methylated (grey) ODN 4 / M ODN 7. Solutions contained 20 mM potassium phosphate buffer pH 7.8, 200 mM sodium chloride and 50 nM oligonucleotide. Melting temperatures were 38.37 ± 0.02 and 36.26 ± 0.02 °C for hemi and fully methylated oligonucleotide respectively as determined by a fit of a 4 parameter sigmoid to the data. (Lower graph) The difference between hemi and fully methylated duplex fluorescence at a range of temperatures. The maximum difference in fluorescence between the fully and hemi-methylated duplex was found to occur at 38.10 ± 0.02 °C, based on the fit of a Gaussian 3 parameter peak, $f = ae^{(-0.5 (T - T_{max\ difference}) / b)^2)}$, to the data.

The normalised fluorescence melting profiles showed that at a fixed temperature the fluorescence of the fully methylated duplex was higher, as predicted. Under the conditions used the melting temperature of the fully methylated oligonucleotide was

2.1 °C lower than its hemi-methylated analogue. Fluorescence increases upon methylation were highest near to the hemi-methylated duplex melting temperature.

In the coupled enzyme assay it had been important to prove that DpnI activity was not constraining measurements. Similarly with the direct assay it was important to know when the kinetics of oligonucleotide melting would be rate limiting. The kinetics of oligonucleotide melting were therefore studied with a series of temperature jump experiments similar to those used by James, Brown and Fox (10).

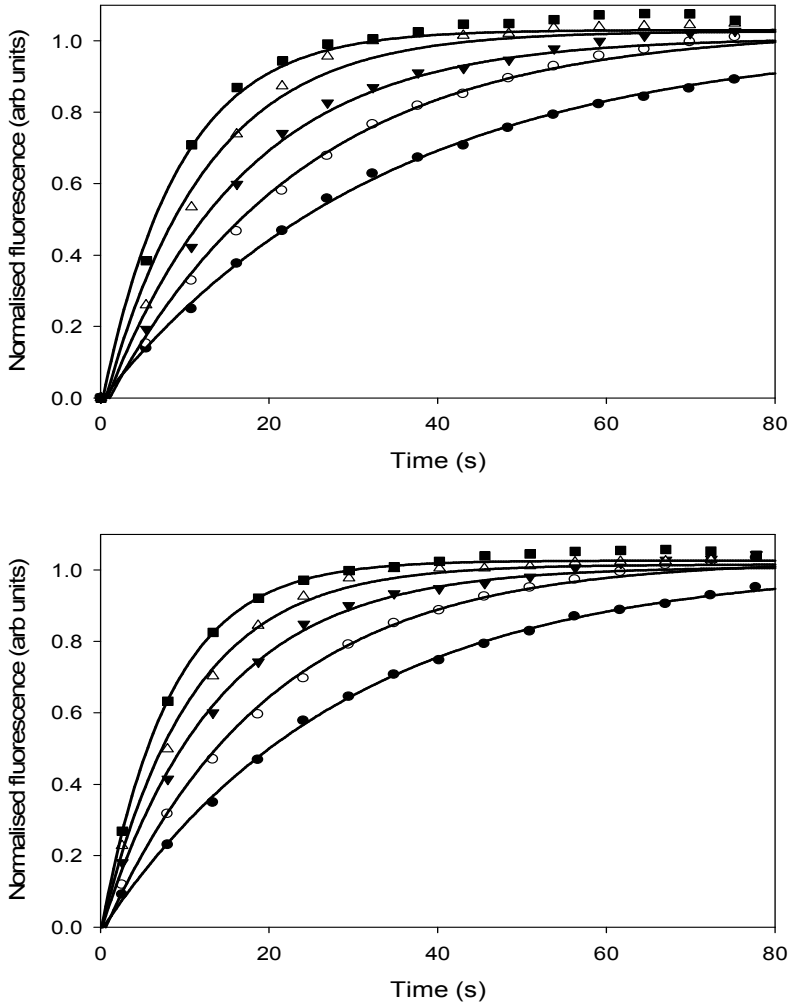

Figure 5.23 Example temperature jump relaxtion profiles for hemi (upper graph) and enzymatically fully methylated oligonucleotide (lower graph) for T-jumps from 28 to 30 °C (filled circles), 30 to 32 °C (open circles), 32 to 34 °C (filled triangles), 34 to 36 °C (open triangles) and 36 to 38 °C (filled squares). Relaxation profiles shown were obtained using 50nM duplex ODN 4 / M ODN 7.

Several buffered solutions containing a range of DNA concentrations were exposed to a series of 2 °C temperature jumps and the fluorescence relaxation profiles monitored (Figure 5.23).

As expected, the fluorescence of the solutions showed an exponential rise to a new maximum, reflecting the new equilibrium between single and double stranded DNA. Data were fitted to the equation $F_t = F_f \times (1\text{-}e^{-bt}) + F_0$ where F_0, F_t and F_f are the initial, time t and final fluorescences. From this fit the rate constant b for the relaxation at each DNA concentration and temperature was obtained. These rate constants were plotted against the single stranded DNA concentration, derived from melting curves which had been carried out previously (Figure 5.24).

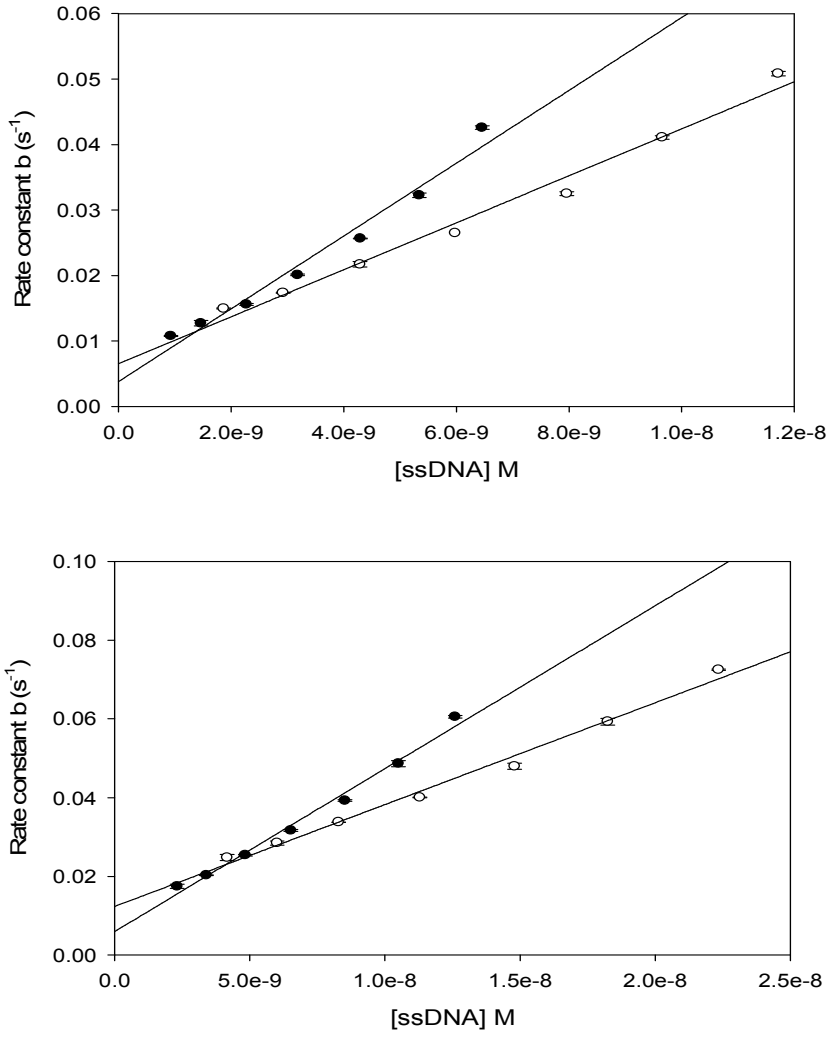

Figure 5.24 Plots of rate constant b versus total concentration of single stranded DNA in solution for hemi (filled circles) and fully (open circles) methylated oligonucleotide. Upper and lower graphs show T-jumps from 30 – 32 °C and 32 – 34 °C respectively.

Data on this second plot were fitted to the equation b = k_1[ssDNA] + k_{-1} to obtain values of k_1 and k_{-1}, the rate constants for the association and dissociation of the DNA duplex respectively (11). The calculated values appear reasonable when compared with the literature (Table 5.3) (11).

Duplex	*Length*	*GC base pairs*	k_1 (M^{-1} min^{-1})	k_{-1} (min^{-1})
$A_9.U_9$	9	0	32 x 10^6	38400
$A_{10}.U_{10}$	10	0	37 x 10^6	10500
$A_{11}.U_{11}$	11	0	30 x 10^6	1680
$A_{14}.U_{14}$	14	0	43 x 10^6	60
$A_4U_4.A_4U_4$	8	0	60 x 10^6	180000
$A_5U_5.A_5U_5$	10	0	108 x 10^6	9000
$A_6U_6.A_6U_6$	12	0	90 x 10^6	480
$A_7U_7.A_7U_7$	14	0	48 x 10^6	48
$A_2GCU_2.A_2GCU_2$	6	2	96 x 10^6	27000
$A_3GCU_3.A_3GCU_3$	8	2	45 x 10^6	180
$A_4GCU_4.A_4GCU_4$	10	2	7.8 x 10^6	90
$A_5G_2.C_2U_5$	7	2	264 x 10^6	20400
$A_4G_3.C_3U_4$	7	3	252 x 10^6	300
ODN 4/M ODN 7 (HM, 28-30 °C)	13	3	405 x 10^6	0.30
ODN 4/M ODN 7 (FM, 28-30 °C)	13	3	287 x 10^6	0.27
ODN 4/M ODN 7 (HM, 30-32 °C)	13	3	334 x 10^6	0.23
ODN 4/M ODN 7 (FM, 30-32 °C)	13	3	215 x 10^6	0.39
ODN 4/M ODN 7 (HM, 32-34 °C)	13	3	248 x 10^6	0.35
ODN 4/M ODN 7 (FM, 32-34 °C)	13	3	155 x 10^6	0.74
ODN 4/M ODN 7 (HM, 34-36 °C)	13	3	164 x 10^6	1.11
ODN 4/M ODN 7 (FM, 34-36 °C)	13	3	97 x 10^6	1.94
ODN 4/M ODN 7 (HM, 36-38 °C)	13	3	99 x 10^6	2.77
ODN 4/M ODN 7 (FM, 36-38 °C)	13	3	60 x 10^6	4.01

Table 5.3 Relaxation kinetics of oligonucleotide duplexes (21 to 23 °C) (11). ODN 4 / M ODN 7 values measured in this study, average standard error on k_1 = 6 % and k_{-1} = 17 %.

It was noted that since Dam was by necessity a DNA binding protein it could potentially affect the equilibrium between single and double stranded DNA by stabilising the duplex. To test this hypothesis a rudimentary experiment was conducted in which a fixed concentration of DNA was incubated with increasing amounts of the enzyme, in the absence of AdoMet. This would allow binding of Dam to the DNA whilst prohibiting methylation.

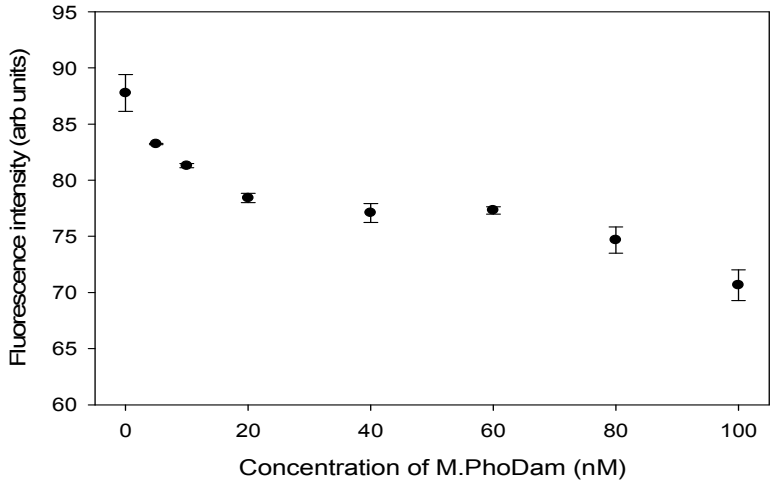

Figure 5.25 The relationship between *P. horikoshii* Dam concentration and DNA fluorescence in solution. Solutions contained 20 mM potassium phosphate buffer pH 7.8, 200 mM sodium chloride, 5 nM ODN 4 / M ODN 7 and *P. horikoshii* Dam 0, 5, 10, 20, 40, 60, 80, 100 nM.

A reduction in fluorescence intensity of about 20 % was observed as the Dam concentration was increased from 0 to 100 nM. Fluorescence reduction was not linearly proportional to methyltransferase concentration but rather had three apparent phases. An initial steep decrease up to 20 nM was seen, followed by relatively little change between 20 and 60 nM and another sharper decrease above 60 nM. A speculative explanation for this behaviour is that two Dam molecules could be binding to the DNA above 60 nM. Whatever the complexities, results suggested that the hypothesised effect existed but was relatively weak. Any potential problems would be avoided simply by keeping the Dam concentration significantly lower than that of the DNA substrate.

Proof of principle assays were set up with 50 nM hemi-methylated duplex in phosphate buffer at 33 °C in a 96-well plate. These direct activity assays were initiated with the

addition of 0, 1.25, 2.5 or 5 nM Dam, to demonstrate that measured fluorescence increases were proportional to the rate of methylation (Figure 5.26). Negative controls which lacked Dam were prepared in wells interspersed with these assays, which was important to negate the effect of small temperature differences across the plate. The temperature at which assays were maintained, 33 °C, reflected a compromise between wanting the DNA in duplex form so it could be recognised by Dam and the desire to maximise the fluorescence signal, which was greatest near the T_m.

Gratifyingly, fluorescence increases appeared to be directly proportional to the Dam concentration (Figure 5.26). Initial rates of fluorescence increase over the first 1000 s were determined as 22.7 ± 3.0, 9.6 ± 1.5, 5.9 ± 1.5 and 0.7 ± 3.1 for assays with 5, 2.5, 1.25 and 0 nM Dam respectively. At each *P. horikoshii* Dam concentration the same endpoint fluorescence was reached. The observation is consistent with full turnover of the substrate by the highly stable MTase and is in contrast to the early coupled assay experiments with the inactivation prone *Y. pestis* Dam. Fluorescence increases in the assays were calibrated from this endpoint and the rate of Dam turnover, k_{cat}, was determined as 0.26 ± 0.03 min^{-1} at 33 °C.

For the real-time fluorescence increases measured with the assay to be proportional to Dam concentration the rates of duplex association and dissociation must have been non-limiting and therefore fast compared to the methylation rate. This can be demonstrated from the rate constants derived from the temperature jump experiments (Table 5.3). Hemi-methylated DNA jumped from 32 - 34 °C had k_1 and k_{-1} values of 248 x 10^6 ± 12 x 10^6 $M^{-1}min^{-1}$ and 0.354 ± 0.090 min^{-1} respectively. Fully methylated DNA jumped from 32 - 34 °C had k_1 and k_{-1} values of 155 x 10^6 ± 7 x 10^6 $M^{-1}min^{-1}$ and 0.738 ± 0.096 min^{-1} respectively. Rates of strand association, dissociation and methylation are equal to k_1[strand 1][strand 2], k_{-1}[duplex] and k_{cat}[Dam] respectively. Copasi, a simulator for biochemical networks was used to calculate the concentrations of each of the DNA species at several different assay timepoints. From this data the rates of DNA association, dissociation and methylation were calculated (Table 5.4).

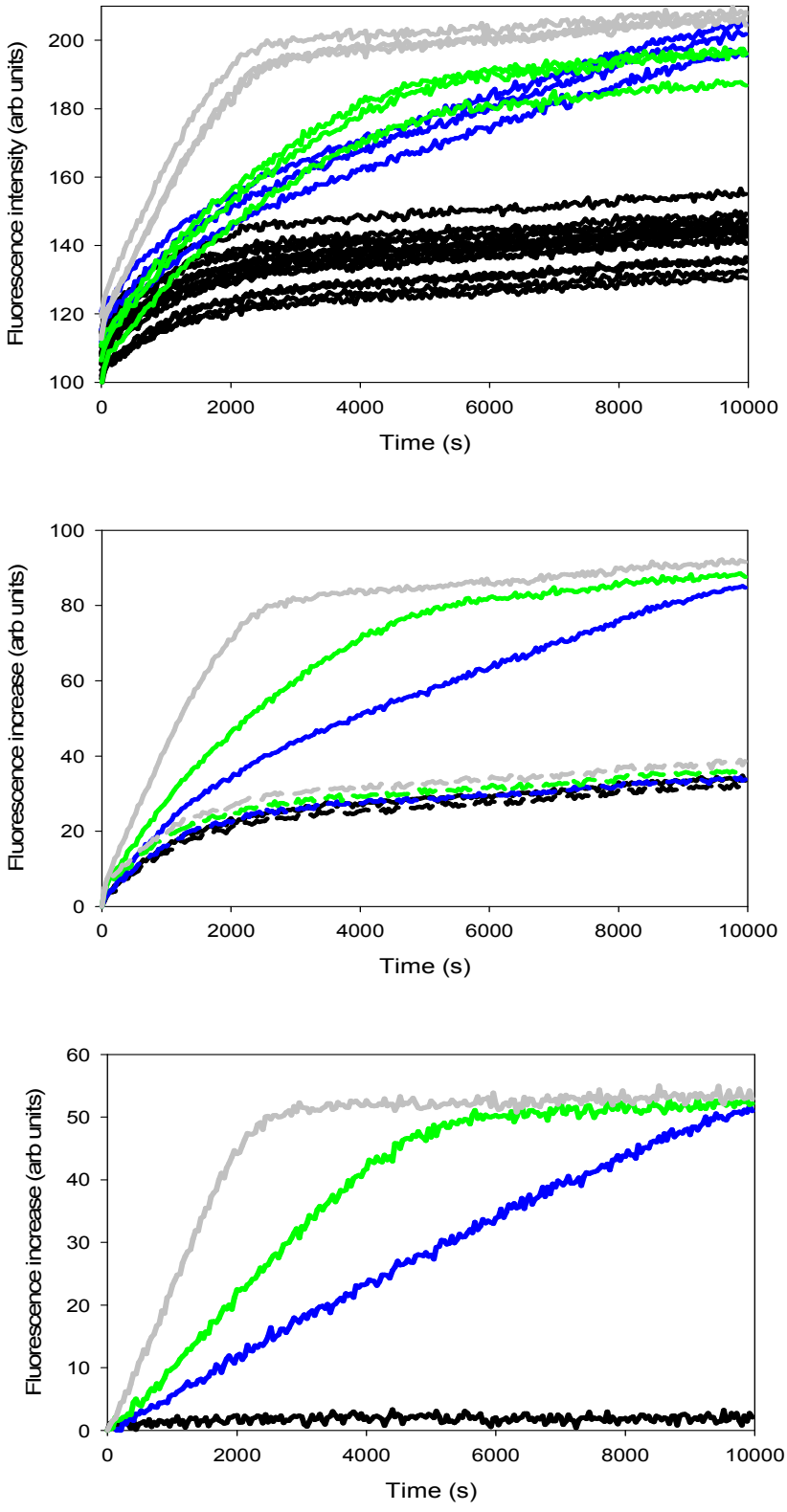

Figure 5.26 (Upper graph) Raw fluorescence timecourses for activity assays containing 5 (grey), 2.5 (green), 1.25 (blue) and 0 (black) nM *P. horikoshii* Dam. (Middle graph) Fluorescence increases (triplicate averaged) for activity assays (solid lines, 5 – 0 nM Dam) and their negative controls (dashed lines, 0 nM Dam). (Lower graph)

Fluorescence increases (triplicate averaged) after subtraction of their respective negative controls.

Time (min)	*assoc HM duplex*	*dissoc HM duplex*	*Methylation*	*assoc FM duplex*	*dissoc FM duplex*
1	1.47×10^{-8}	1.44×10^{-8}	1.3×10^{-9}	3.20×10^{-10}	7.25×10^{-10}
2	1.44×10^{-8}	1.41×10^{-8}	1.3×10^{-9}	8.67×10^{-10}	1.32×10^{-9}
3	1.41×10^{-8}	1.38×10^{-8}	1.3×10^{-9}	1.45×10^{-9}	1.90×10^{-9}

Table 5.4 Rates of processes occurring in the proof of principle FEP assays containing 5 nM Dam. All rates are in moles L^{-1} min^{-1}. Assoc and dissoc refer to association and dissociation of the duplex respectively. HM and FM refer to fully or hemi-methylated.

The rate of methylation is ten times slower than the rate of hemi-methylated duplex association and dissociation at the beginning of the assay. There is however a period of two to three minutes at the start of the assay during which methylation of the duplex is faster than the rate of fully methylated duplex association and disscociation. Theoretically this should result in a small lag phase at the start of the fluorescence timecourses. In practice this lag is not noticeable because of the initiation time and the FEP assay sensitivity.

An estimate of FEP assay sensitivity was made from the standard deviation in the averaged 5 nM *P. horikoshii* Dam activity data between 4000 and 10,000 s (Figure 5.26, lower graph, grey line). The standard deviation in the fluorescence measurement during this time, due to temperature fluctuations and the imprecision of the plate reader, was 780 arbitrary units (three standard deviations = 2339 arbitrary units). Therefore there is a 99.73 % likelihood that a measured fluorescence increase of 2339 arbitrary units is statistically significant. This corresponds to methylation of 222 fmol of oligonucleotide. The direct FEP assay is an order of magnitude less sensitive than the coupled assay used to measure *Y. pestis* Dam activity (13 – 38 fmol sensitivity). The theoretical maximum FEP assay sensitivity, assuming it could be carried out in 384 well format, is 2 fmol of methylation. This limit is based on the sensitivity of modern plate readers (BMG POLARstar Omega 0.2 fmol / well fluorescein) and the fact that methylation causes a fluorescence increase equal to around 10 % of the free fluorophore fluorescence (Figure

5.22, lower graph). FEP assays carried out in smaller volumes may however be subject to larger errors in the fluorescence measurements due to increased temperature fluctuations.

To further substantiate the new assay principle it was used to characterise the kinetics of *P. horikoshii* Dam methylation.

5.3.3 Kinetic characterisation of *P. horikoshii* Dam

5.3.3.1 The effect of AdoMet concentration on *P. horikoshii* Dam activity

The dependence of Dam activity on AdoMet concentration was measured in a set of 100 µl assays at 33 °C. Duplicate assays contained nine AdoMet concentrations and the DNA duplex was kept at a fixed saturating concentration (Figure 5.27). Fluorescence increases in these assays were calibrated by comparison with the endpoint fluorescence increase in the assays whose fluorescence had reached a plateau. Levelling off of the fluorescence timecourses was assumed to be due to complete DNA methylation. The gel based assay had demonstrated that, given enough time, *P. horikoshii* Dam methylated the significant majority of substrate in solution.

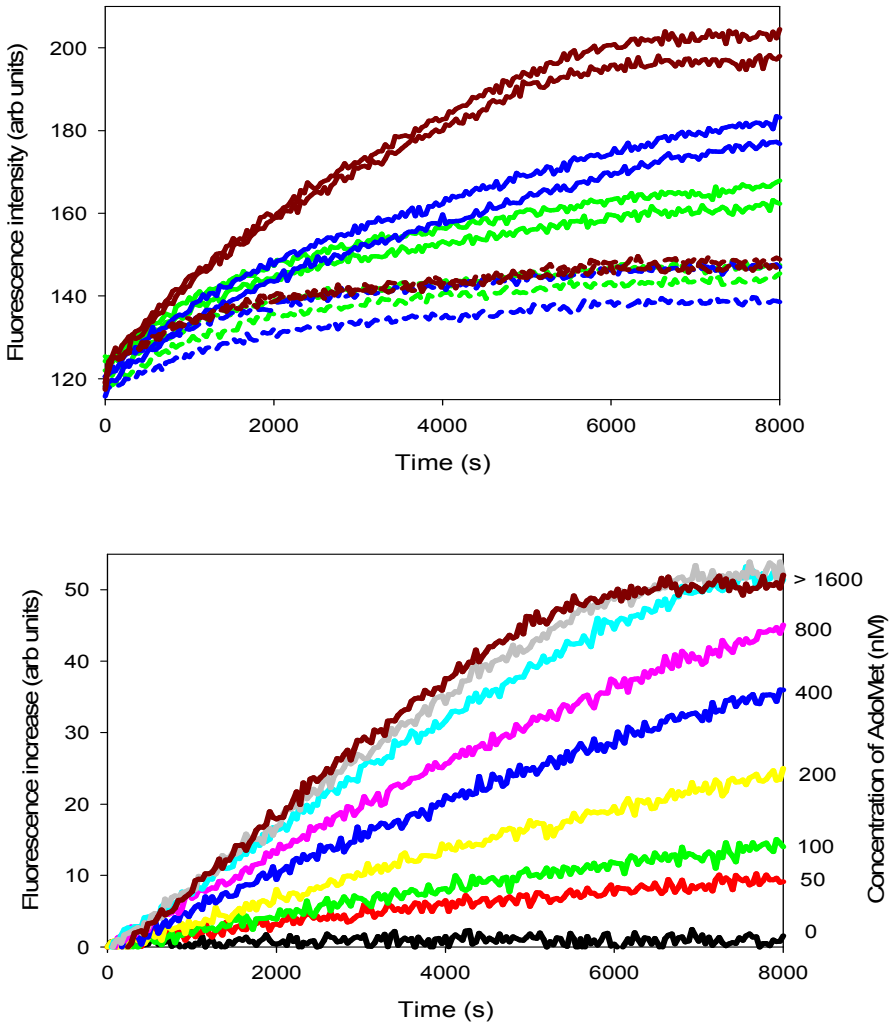

Figure 5.27 (Upper graph) Example raw fluorescence timecourses containing 100 (green), 400 (blue) or 6400 (brown) nM AdoMet and 0 (dashed) or 2.5 (solid) nM *P. horikoshii* Dam. (Lower graph) Fluorescence timecourses of Dam activity assays used to measure K_M ^{AdoMet}. Data shown is averaged from duplicate assays, background fluorescence changes have been subtracted. Assays contained 2.5 nM Dam, 50 nM ODN 4 / M ODN 7 and 0 (black), 50 (red), 100 (green), 200 (yellow), 400 (blue), 800 (pink), 1600 (cyan), 3200 (grey) and 6400 (brown) nM AdoMet.

Measured methylation rates increased as the AdoMet concentration was raised from 0 to 6.4 µM. Plots of the initial methylation rate, calculated from the first 3000 s of data, against AdoMet concentration showed this relationship was in accordance with a Michaelis-Menten mechanism of enzyme action, ignoring the effect of DNA concentration (Figure 5.28).

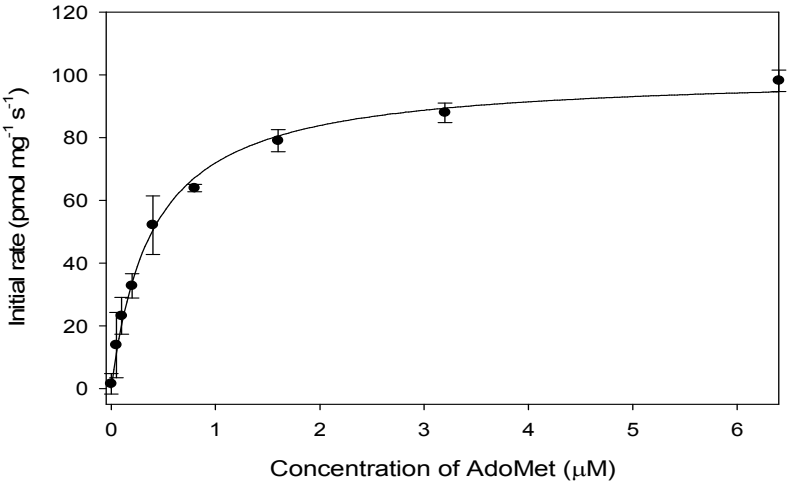

Figure 5.28 The dependence of *P. horikoshii* Dam activity on AdoMet concentration. Initial rate measurements were based on the first 3000 s of data.

Data were fitted to the Michaelis-Menten equation ($v = V_{max}$ [AdoMet] / (K_M ^{AdoMet} + [AdoMet]) to obtain values for K_M ^{AdoMet} and k_{cat}. The R^2 value of the fit was 0.99. At 33 °C, K_M ^{AdoMet} and k_{cat} were found to be 396 ± 33 nM and 0.24 ± 0.01 min^{-1} (100 ± 2 pmol mg^{-1} s^{-1}) respectively.

5.3.3.2 The effect of DNA concentration on *P. horikoshii* Dam activity

The dependence of Dam activity on DNA concentration was measured in a set of 100 µl assays at 32 °C. This was one degree lower than for the AdoMet assays, a reflection of the lower melting temperatures seen when DNA concentrations were reduced. Duplicate assays were run at nine different DNA concentrations whilst the AdoMet was kept at a fixed saturating concentration.

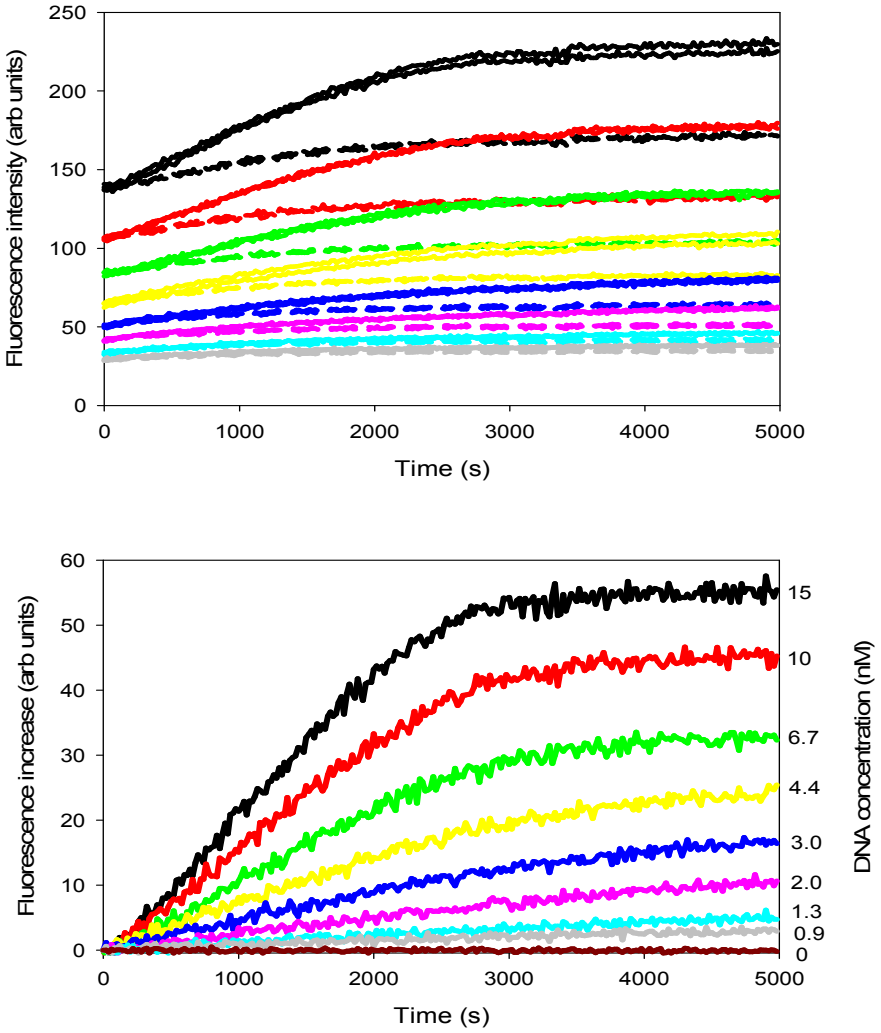

Figure 5.29 (Upper graph) Raw fluorescence timecourses of Dam activity assays used to measure K_M ^{DNA}. Solid and dashed lines represent activity assays and negative controls respectively. Colour scheme is as for lower graph. (Lower graph) Fluorescence timecourses of Dam activity assays used to measure K_M ^{DNA}. Data shown is averaged from duplicate assays, background fluorescence changes have been subtracted. Assays contained 20 µM AdoMet, Dam at 10 % of the DNA concentration and 15 (black), 10 (red), 6.7 (green), 4.4 (yellow), 3.0 (blue), 2.0 (pink), 1.3 (cyan), 0.9 (grey) and 0 (brown) nM duplex oligonucleotide ODN 4 / M ODN 7.

Rates of fluorescence increase became larger as the DNA concentration was increased from 0 to 15 nM. A calibration plot was constructed from the endpoint fluorescence increases measured at each DNA concentration to allow the determination of methylation rates (Figure 5.30). As expected, the endpoint fluorescence increases were

not quite linearly dependent on the DNA concentration. Deviation from a linear relationship was attributable to the changes in T_m experienced by intermolecular duplexes as their concentrations are changed. At higher DNA concentrations the system is operating further below the T_m and so the fluorescence increase upon methylation is proportionally smaller.

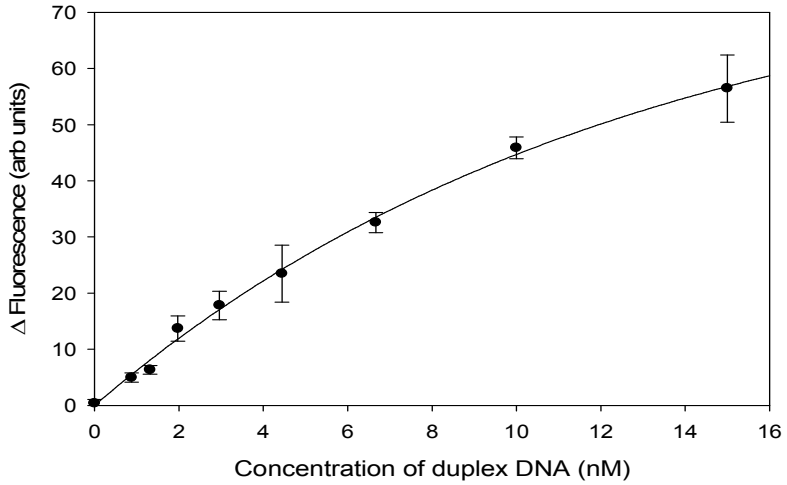

Figure 5.30 The relationship between fluorescence increase upon full methylation and DNA concentration at 32 °C.

An equation of the form $\Delta F = a(1-e^{-b[DNA]})$, where ΔF is the fluorescence increase upon methylation and a and b are constants, accurately described the relationship between the variables on the calibration plot ($R^2 = 0.997$) (Figure 5.30). This plot was used to determine the expected endpoint fluorescence increases due to complete methylation in each of the assays, allowing methylation rates to be determined. Using all of the measured endpoints to make a calibration plot was preferable to individual calibration of the assays using their own endpoints. There was concern that at the lowest DNA concentrations full turnover would not be achieved because of the slow methylation rates. By using all of the available data to calibrate these assays the effect of any incomplete turnover on the apparent initial rates was minimised.

Plots of initial methylation rates, calculated from the first 1500 s of data, versus DNA concentration showed the relationship to be in accordance with a Michaelis-Menten model of enzyme substrate interaction, ignoring the effect of AdoMet concentration (Figure 5.31).

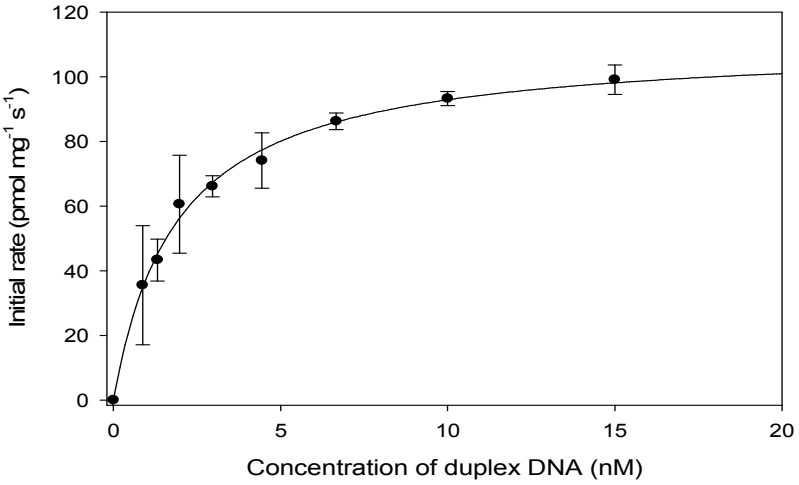

Figure 5.31 Dependence of *P. horikoshii* Dam activity on oligonucleotide concentration.

Data were fitted to the Michaelis-Menten equation ($v = V_{max}[DNA] / (K_M^{DNA} + [DNA])$ with an R^2 of 0.99 to obtain values for K_M^{DNA} and k_{cat}. Values for these parameters were determined as 1.91 ± 0.14 nM and 0.25 ± 0.01 min $^{-1}$ (106 ± 2 pmol mg^{-1} s^{-1}) respectively. The errors are higher for the data points at low DNA concentrations because assays contained Dam at 10 % of the DNA concentration. Correction factors were used in the analysis to standardise the rates so they appeared to be for the same amounts of Dam.

Over half of the measurements used to determine K_M^{DNA} relied on an amount of methylation below the previously estimated 222 fmol limit of FEP assay sensitivity (Table 5.5). Despite this, the data did fit the Michaelis-Menten model of enzyme activity very well. The assay is probably more sensitive than the previous estimate because initial rate measurements are based on the fit of a trend line to seventy five successive data points, which has an averaging effect. By contrast the initial rate measurements used to determine K_M^{DNA} for *Y. pestis* Dam, measured with the coupled assay, were based on the fit of a trend line to just seven data points. This was because the *Y. pestis* Dam quickly inactivated, leaving a short initial period when the fluorescence timecourses were linear.

DNA concentration in assay (nM)	*Dam concentration in assay (nM)*	*Amount of methylation used to determine rate (fmol)*
15.0	1.50	894
10.0	1.00	561
6.7	0.67	346
4.4	0.44	198
3.0	0.30	118
2.0	0.20	72
1.3	0.13	34
0.9	0.09	19

Table 5.5 Amount of methylation used to determine the rates in assays for the measurement of K_M ^{DNA}.

It is also relevant that the sensitivity of 222 fmol was calculated with a background fluorescence from 50 nM duplex DNA. At lower DNA concentrations the assay sensitivity is increased. Estimating assay sensitivity from the standard deviation in the measurements on the linear portion of the 15, 10, 6.7 and 0.9 nM DNA assay fluorescence timecourses gives values of 74, 55, 42 and 24 fmol (Figure 5.29, lower graph, black, red, green and grey lines).

The K_M values for both of the *P. horikoshii* Dam substrates appear reasonable when compared to literature values for similar enzymes (Table 5.6). The K_M for AdoMet was 396 ± 33 nM, lower than the 11.3 μM calculated for *Y. pestis* Dam with the coupled enzyme assay or literature values for *E. coli* Dam (Table 5.6) (1). The value is closer to that of MTases from the thermophiles *T. thermophilus and P. abyssi*. AdoMet is known to be unstable in solution and it may well be that the higher affinity of the thermophilic MTases for AdoMet is a reflection of its relative paucity within the cell (12,13). The thermophilic methyltransferases may derive a beneficial stabilisation from binding to their substrates. DNA and AdoMet did stabilise Dam from the mesophile *Y. pestis* and substrate stabilisation of thermophilic enzymes is well known (1,14-16). If this were true then a high affinity for AdoMet would help to preserve the enzymes at elevated temperatures.

MTase Source	*Target sequence*	*DNA Substrate*	K_M^{DNA} *(nM)*	K_M^{AdoMet} *(μM)*	k_{cat} *(min $^{-1}$)*
E. coli (17)	GATC	20 bp Duplex	17.4 ± 3.0	5.60 ± 1.10	0.93 ± 0.06
T. aquaticus (18) [b]	TCGA	36 bp Duplex	600 ± 200	3.7 ± 1.1	44 ± 7
T. thermophilus (19)	TCGA	λ-DNA	-	0.8	0.25
P. abyssi (9) [c]	GTAC	40 bp Duplex	159	1.28	2.46
P. horikoshii [a]	GATC	13 bp Duplex	1.9 ± 0.1	0.40 ± 0.03	0.24 ± 0.06

Table 5.6 A comparison of the kinetic parameters of N6-adenine MTases found in *E. coli* and four thermophilic organisms.[a] Results from this study at 32-33 °C.[b] Values obtained at 60 °C.[c] Values obtained at 75 °C.

The K_M^{DNA} of *P. horikoshii* Dam was, at 1.9 nM, lower than any of the values for the mesophilic MTases listed in table 3.2 with oligonucleotide substrates. This observation can be explained in the same way as the tight AdoMet binding. If the DNA substrate stabilises the enzyme then a high affinity will serve to protect the thermophilic methyltransferase from inactivation. The high temperatures at which the *T. aquaticus* and *P. abyssi* MTases were assayed might account for the comparatively high K_M^{DNA} they both possess.

At 0.24 min^{-1} the k_{cat} was lower than the value of 0.55 min^{-1} measured for *Y. pestis* Dam and reported rates for *E. coli* and T4 Dam at 37 °C (table 3.2). Thermophilic enzymes are often slower than their mesophilic counterparts if assayed at low temperatures because of their higher structural rigidity (14). The thermophilic adenine MTase of *T. thermophilus*, which was assayed at 37 °C, had a value of k_{cat} similar to *P. horikoshii* Dam (Table 5.6). This value was not measured with an oligonucleotide substrate.

The effect of the 200 mM sodium chloride concentration on the measured methylation rate was not investigated. This value had been chosen, for expediency, based on the

salinity under which a *Pyrococcus abyssi* adenine MTase was active (9). It also gave convenient melting temperatures for the DNA duplex substrate. At this salinity the *Y. pestis* enzyme would have appeared inactive, based on observations from the coupled enzyme assay. *E. coli* Dam is reported to retain 35 % activity in tris buffer supplemented with 200 mM sodium chloride (20).

5.3.4 Application of the FEP assay principle to another DNA modifying enzyme

Uracil-DNA glycosylases catalyse the excision of uracil bases from DNA. A direct real-time fluorescence based assay for the activity of this enzyme has been reported in the literature (21). This assay uses the removal of four uracil bases to cause complete melting of a 14 bp duplex labelled with a FRET pair.

A proof of principle experiment was carried out to determine if it was possible to monitor the excision of single uracil bases from a 13 bp duplex in real-time with the FEP assay. For simplicity, these assays were prepared in the same way as the *P. horikoshii* Dam assays but without AdoMet. The DNA duplex used consisted of ODN 4, also used in the Dam assay, and ODN 5, a complementary uracil containing strand labelled with a dabcyl quencher (Table 5.7).

Strand	*DNA Sequence 5' to 3'*
ODN 4	ATTTAGATCACAA
ODN 5	TTGTGAUCTAAAT

Table 5.7 Sequences of oligonucleotides used in the uracil-DNA glycosylase assay.

Triplicate assays containing 50 nM duplex were initiated with 0, 63, 125 and 250 pM of commercially available *Archaeolobus fulgidis* uracil-DNA glycosylase. An equal number of negative controls were initiated without uracil-DNA glycosylase. The fluorescence timecourses of the assays were measured at 31 °C (Figure 5.32).

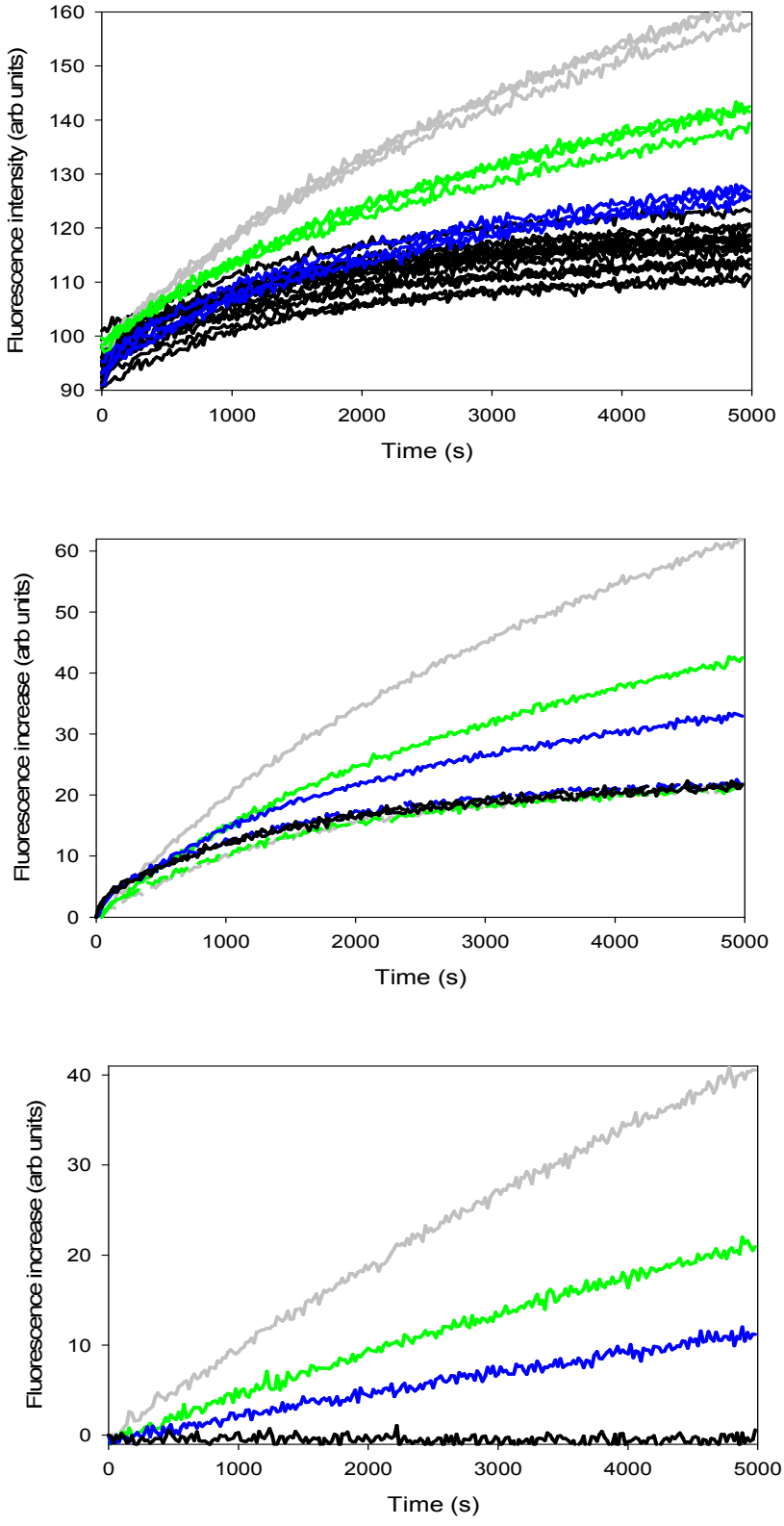

Figure 5.32 (Upper graph) Raw fluorescence timecourses for activity assays containing 250 (grey), 125 (green), 63 (blue) and 0 (black) pM *Afu*-UDG. (Middle graph) Fluorescence increases (triplicate averaged) for activity assays (solid lines, 0 – 250 pM

Afu-UDG) and their negative controls (dashed lines, 0 nM *Afu*-UDG). (Lower graph) Fluorescence increases (triplicate averaged) after subtraction of their respective negative controls.

Initial rates of fluorescence increase in the assays containing 0, 63, 125 and 250 pM *Afu*-UDG were 0.1 ± 0.6, 2.7 ± 0.7, 5.3 ± 1.0 and 9.7 ± 0.8 respectively. The initial rates of fluorescence increase were therefore proportional to the amount of uracil-DNA glycosylase in the assays. This result provides evidence that the FEP assay could be used to study enzymes besides Dam which also catalyse a destabilising DNA modification.

5.4 Summary and conclusions

The Dam gene from the hyperthermophilic archaeon *Pyrococcus horikoshii* was cloned and placed in an expression plasmid, pMMS511811, under the control of an arabinose inducible promoter. Expression and purification of the C-terminally His_6-tagged Dam by immobilised nickel affinity chromatography yielded not only the full length protein but a shorter contaminant. Sequencing showed that the 28,556 Da contaminant was due to mis-initiation of translation beginning at what should have been an internal methionine residue. SDS-PAGE carried out by Koike and co-workers on *P. horikoshii* Dam which they expressed in *E. coli* BL21 (DE3) also shows the presence of a 28 kDa protein (22). It may be that they too were seeing the same product of mis-translation. Mutagenesis of the *dam* gene to replace the problematic codon with that of alanine facilitated isolation of purer N-His_6-*P. horikoshii* Dam.

The thermophilic methyltransferase was shown to be active with a gel based assay and subsequently used in a novel Fluorescence Equilibrium Perturbation (FEP) activity assay. It was demonstrated that in the FEP assay the measurements of the methylation rate were not limited by the kinetics of the duplex association and dissociation. Fluorescence increases in the assay reflected methyltransferase activity. This was the first example of a direct, fluorescence based, real-time assay suitable for studying subtle base modifications. The assay was successfully used to measure some kinetic parameters for *P. horikoshii* Dam. The K_M of both substrates and the maximum rate of

Dam catalysis, k_{cat}, were determined and judged to be reasonable on the basis of literature reports on other methyltransferases. The FEP assay was estimated to be at least ten fold less sensitive than the coupled enzyme assay under similar conditions. This lower sensitivity was compensated for by the stability of *P. horikoshii* Dam which allowed reliable kinetic measurements to be made at a wide range of substrate concentrations.

The FEP assay principle was used in conjunction with another enzyme, *Archaeolobus fulgidis* uracil-DNA glycosylase, to demonstrate its possible application beyond the study of Dam.

5.5 References

1. Wood, R. J., Maynard-Smith, M. D., Robinson, V. L., Oyston, P. C., Titball, R. W., and Roach, P. L. (2007) *PLoS ONE* **2**, e801
2. Guo, Q., Lu, M., and Kallenbach, N. R. (1995) *Biochemistry* **34**, 16359-16364
3. Corpet, F. (1988) *Nucleic Acids Res* **16**, 10881-10890
4. Xu, W., and Miranker, D. P. (2004) *Bioinformatics* **20**, 1214-1221
5. Gonzalez, J. M., Masuchi, Y., Robb, F. T., Ammerman, J. W., Maeder, D. L., Yanagibayashi, M., Tamaoka, J., and Kato, C. (1998) *Extremophiles* **2**, 123-130
6. Wood, R. J. (2008) *Personal communication*
7. Mckelvie, J., and Stares, A. (2008) *Personal communication*
8. Baba, T., Ara, T., Hasegawa, M., Takai, Y., Okumura, Y., Baba, M., Datsenko, K. A., Tomita, M., Wanner, B. L., and Mori, H. (2006) *Mol Syst Biol* **2**, 2006 0008
9. Watanabe, M., Yuzawa, H., Handa, N., and Kobayashi, I. (2006) *Appl Environ Microbiol* **72**, 5367-5375
10. James, P. L., Brown, T., and Fox, K. R. (2003) *Nucleic Acids Res* **31**, 5598-5606
11. Cantor, C. R., and Schimmel, P. R. (1980) *Biophysical Chemistry. Part III: The behavior of biological macromolecules*, Freeman, San Francisco
12. Parks, L. W., and Schlenk, F. (1958) *J Biol Chem* **230**, 295-305
13. Iwig, D. F., and Booker, S. J. (2004) *Biochemistry* **43**, 13496-13509
14. Vieille, C., and Zeikus, G. J. (2001) *Microbiol Mol Biol Rev* **65**, 1-43
15. Wilquet, V., Gaspar, J., Van de Lande, M., Van de Casteele, M., Legrain, C., Meiering, E., and Glansdorff, N. (1998) *Eur J Biochem* **255**, 628-637
16. Takai, K., Sako, Y., Uchida, A., and Ishida, Y. (1997) *J Biochem* **122**, 32-40
17. Mashhoon, N., Carroll, M., Pruss, C., Eberhard, J., Ishikawa, S., Estabrook, R. A., and Reich, N. (2004) *J Biol Chem* **279**, 52075-52081
18. Pues, H., Bleimling, N., Holz, B., Wolcke, J., and Weinhold, E. (1999) *Biochemistry* **38**, 1426-1434
19. Sato, S., Nakazawa, K., and Shinomiya, T. (1980) *J. Biochem.* **88**, 737-747
20. Herman, G. E., and Modrich, P. (1982) *J Biol Chem* **257**, 2605-2612
21. Liu, B., Yang, X., Wang, K., Tan, W., Li, H., and Tang, H. (2007) *Anal Biochem* **366**, 237-243
22. Koike, H., Katsushi, Y., Tsuyoshi, K., Tomoko, Y., Shin-ichi, M., Lester, C., and Masashi, S. (2005) *Proc Jpn Acad Ser B Phys Biol Sci* **81**, 278-290

Chapter 6:- Overall conclusions and future work

6.1 *Y. pestis*, Dam and the need for novel antibacterial compounds

Thousands of cases of bubonic plague occur annually and MDR-strains of *Y. pestis,* the causative agent, have been isolated (1,2). There is concern that *Y. pestis* could be used as a biological weapon (3).

Dam is an enzyme with a regulatory role in *Y. pestis* and has a proven link to virulence. This has led to the suggestion that Dam inhibitors could provide a novel source of antibiotics (4).

With the aim of identifying and characterising such inhibitors, two new assays for Dam activity were developed. The first, a coupled enzyme assay, was used to characterise *Y. pestis* Dam and screen a library of compounds for inhibitors. The other, a direct assay, was demonstrated with the hyperthermophilic *P. horikoshii* Dam.

6.2 Development of an assay for Dam activity

Y. pestis Dam was expressed from plasmid pRJW421307 in *E. coli* strain GM215. The protein had an N-terminal His_6-tag which facilitated purification by immobilised nickel affinity chromatography. To maximise activity of this unstable enzyme the purification procedure and dialysis were carried out at 4 °C and kept as short as possible.

The DpnI restriction endonuclease was expressed from plasmid pMMS495859 in *E. coli* strain GM48. The protein had an N-terminal His_6-tag which permitted purification by immobilised nickel affinity chromatography. DpnI was observed to be subject to degradation and so selection of an appropriate expression strain and use of protease inhibitors were essential to maximise enzyme quality.

A fluorescence based coupled enzyme assay for *Y. pestis* Dam activity was developed. Assay efficacy relied on a well designed oligonucleotide substrate. It was important that the FRET pair were in close proximity and that the oligonucleotide had an 'n-1' methylation pattern, where n is the number of methyl groups recognised by the restriction enzyme in the assay. The signal to background noise ratio of the assay was improved by optimisation of the salt concentration.

Future work could include trying to expand the range of MTases which can be assayed with the real-time coupled enzyme approach. To some extent this process has begun with the development of a coupled enzyme assay for Dnmt1 activity within the Roach group (5). This assay came about after it was noticed that restriction enzyme GlaI had the appropriate recognition sequence to complement Dnmt1 (M. Maynard-Smith). A potentially important restriction enzyme which could be used in a similar manner is Mrr (methylated adenine recognition and restriction) which is part of the restriction system of *E. coli* responsible for recognising foreign DNA. Mrr appears to recognise not just one but a variety of m6A and m5C containing sequences including (m5C)G and G(m6A)NTC, the sequences formed by Dnmt1 and CcrM respectively (6-9). It is however unclear if the enzyme is specific for the fully or hemi-methylated sequences. If Mrr could be substituted for GlaI in a Dnmt1 activity assay it would be advantageous because the *mrr* gene could be cloned from *E. coli* DNA and the enzyme overexpressed.

6.3 Kinetic characterisation of *Y. pestis* Dam and validation of the assay

The fluorescence signals of the real-time, coupled enzyme, assay were quantified with a set of calibration experiments. Activity measurements made with the assay showed that *Y. pestis* Dam inactivated rapidly in solution without either of its substrates present. This inactivation was significantly reduced when Dam was incubated with its DNA substrate.

The affinity of Dam for both of its substrates was determined with the assay. Whilst the K_M ^{AdoMet} was similar to literature reported values the measured K_M DNA was somewhat lower and subject to a large error. This large error in the value was attributed to enzyme

instability and not an inherent weakness in the assay strategy. The measured rate of *Y. pestis* Dam turnover was considered plausible in view of the range of values reported for other DNA MTases.

The ability of the assay to characterise Dam inhibitors was proven by using it to measure the K_i of AdoHcy. This known inhibitor is competitive with AdoMet and so low DNA concentrations, where the assay appears least effective, were not necessary. Future work could include use of the assay to characterise different inhibitors with other known modalities of action. Benkovic's borinic esters or some of the compounds discovered by Mashoon and co-workers could be used for such purposes (10,11).

It would be interesting to determine if certain dsDNA mimicking proteins could act as inhibitors of Dam. Protein HI145 found in *H. influenzae* has homologues in *E. coli*, *P. multocida*, *S. typhimurium*, *V. cholerae* and *Y. pestis* and might be a good initial dsDNA mimic to study since its target is unknown (12,13). It is conceivable that a protein mimic could be found or designed specifically to inhibit Dam (14-16). The DNA mimicking protein Ugi inhibits the enzyme Uracil DNA glycosylase which, like Dam, flips a base out from the DNA double helix (17).

It would be relatively easy to characterise *E. coli* Dam with the coupled enzyme assay since it is now being expressed and purified within the Roach group (J. Mckelvie and J. Harmer). This would allow comparison of measured kinetic parameters with ones for the identical enzyme reported in the literature.

6.4 High throughput screening for *Y. pestis* Dam inhibitors

A 1000 compound library was screened for Dam inhibitors using the fluorescence based, coupled enzyme assay. Following reprocessing of the data, four compounds were identified as potential Dam inhibitors. Three of these compounds of interest were successfully synthesised and subjected to a counter-screen against DpnI and a fluorescence intercalation displacement assay for DNA binding. Results suggested that all three of the synthesised compounds were non-selective Dam inhibitors exerting their effects through interaction with the DNA substrate. The remaining compound showed

considerable homology to two of the compounds which had been synthesised and so would most likely have been a non-selective inhibitor.

One drawback of the coupled assay was its reliance on two enzymes, Dam and DpnI. Where compounds were identified which inhibited both enzymes it was not possible to obtain an accurate IC_{50} for Dam, with the measured value merely being an apparent IC_{50}. Values for the DpnI IC_{50} could be determined from the counter screen data. This highlighted the need for a direct fluorescence based Dam activity assay.

Since this initial screen of 1000 compounds the coupled assay has been successfully employed in 384 well format and used to screen a library of 3000 compounds in duplicate (J. Mckelvie). Future work should and will include use of the coupled enzyme assay to screen additional compound libraries and to study the potential inhibitors which have been logically designed (Dr. G. Hobley).

6.5 A novel and direct assay for Dam activity

P. horikoshii Dam was expressed in *E. coli* strain BL21 pLysS Rosetta 2 with a C-terminal His_6-tag and when purified by immobilised nickel affinity chromatography found to be contaminated with a shorter protein. N-terminal amino acid sequencing revealed this protein to be a fragment of the full length enzyme formed by mis-initiation of translation at an internal methionine residue. The sequence 5' to this methionine / start codon, GAAAGGGAGTACTACTATAGA[ATG], happens to encode a Shine-Dalgarno sequence 13 bp upstream (underlined) (18-20). This observation could explain why translation began at this internal methionine whilst it was not observed at others. Pure N-His_6-*P. horikoshii* Dam was obtained following mutagenesis of the Dam gene to replace the problematic internal methionine residue with alanine. A superior approach to this problem may have been to mutate the sequence upstream of the methionine to decrease the mRNA affinity for the 16s rRNA. In this way, because of the degeneracy in the genetic code, the contaminant protein expression could have been eliminated whilst the wild type protein sequence was retained. Optimising this region of the Dam gene to retain the wild phenotype and stop unwanted translation could form the basis of future work for a summer placement student.

Mutant thermophilic Dam was successfully used in a novel and direct fluorescence based assay for adenine MTase activity. This Fluorescence Equilibrium Perturbation assay used the inherent destabilising effect of adenine methylation to increase the mean distance between an adjacent FRET pair on an oligonucleotide substrate. The K_M of both substrates and the maximum rate of methylation were measured with this assay.

The 200 mM sodium chloride concentration in the assay was, for expediency, simply based upon the conditions under which another thermophilic adenine MTase was known to function (21). Future work could include an investigation into the relationship between salt concentration and *P. horikoshii* Dam activity. Collection and analysis of FEP assay data at a range of sodium chloride concentrations would not necessarily be straight forward due to changes in DNA melting kinetics and temperature with salinity. With proper calibration experiments it should however be possible and the results would help assess the limits of the assay.

The FEP assay provided a way to measure DNA methylation without the need for DpnI but it had disadvantages as well as advantages over the coupled assay. It was estimated that under similar conditions the FEP assay would be ten times less sensitive than the coupled enzyme assay. It also required a large number of negative controls interspersed with the activity assays. Tight temperature control in a BMG plate reader and the stability of *P. horikoshii* Dam compensated for this lower sensitivity and allowed good experimental results to be obtained. The specific oligonucleotide duplex limited the temperatures and salt concentrations which could be used in the FEP assay but DpnI places similar constraints on the coupled assay. DpnI based assays are limited to temperatures below ~ 40 °C, sodium chloride concentrations under ~ 150 mM and the recognition sequence GATC. With an appropriate set of oligonucleotides the FEP assay could be operated at a much wider range of temperatures, salinities and recognition sequences. Any *Y. pestis* Dam inhibitors identified from a high throughput screen could be tested with the FEP assay against adenine MTases with non-GATC recognition sequences. One such MTase is CcrM which recognises the sequence GANTC and is essential for viability in the pathogen *Brucella abortus* (22,23).

Future work could include evaluation of the FEP assay in high throughput format and its use with the less stable *Y. pestis* Dam. For high throughput screening a stopped

version of the assay, in which methylation is carried out at a low temperature before the fluorescence is measured near the T_m, may be appropriate. It seems likely that with its higher sensitivity and need for fewer negative controls the coupled assay will still be the best method to initially screen for *Y. pestis* Dam inhibitors. The FEP assay could then be used as part of the counter screening process and to identify the mode of inhibition.

Coupled enzyme assay results could be improved by the use of a thermally stable enzyme, but it would not be appropriate to simply substitute *P. horikoshii* for *Y. pestis* Dam in a library screen. Future work could involve engineering of a hybrid methyltransferase which retains the majority of the *Y. pestis* Dam amino acids but has improved thermostability (24,25).

6.6 References

1. Anker, M., and Schaaf, D. (2000) *WHO Report on Global Surveillance of Epidemic-prone Infectious Diseases*, World Health Organization, Geneva
2. Galimand, M., Guiyoule, A., Gerbaud, G., Rasoamanana, B., Chanteau, S., Carniel, E., and Courvalin, P. (1997) *N Engl J Med* **337**, 677-680
3. Health_Protection_Agency. (2008) *Deliberate Release of Plague: Information for the Public. Available at* *http://www.hpa.org.uk/webw/HPAweb&HPAwebStandard/HPAweb_C/1203084387130?p=1191942145702*
4. Heithoff, D. M., Sinsheimer, R. L., Low, D. A., and Mahan, M. J. (1999) *Science* **284**, 967-970
5. Wood, R. J. (2008) *Personal communication*
6. Heitman, J., and Model, P. (1987) *J Bacteriol* **169**, 3243-3250
7. Kelleher, J. E., and Raleigh, E. A. (1991) *J Bacteriol* **173**, 5220-5223
8. Waite-Rees, P. A., Keating, C. J., Moran, L. S., Slatko, B. E., Hornstra, L. J., and Benner, J. S. (1991) *J Bacteriol* **173**, 5207-5219
9. Bujnicki, J. M., and Rychlewski, L. (2001) *Gene* **267**, 183-191
10. Benkovic, S. J., Baker, S. J., Alley, M. R. K., Woo, Y. H., Zhang, Y. K., Akama, T., Mao, W. M., Baboval, J., Rajagopalan, P. T. R., Wall, M., Kahng, L. S., Tavassoli, A., and Shapiro, L. (2005) *J Med Chem* **48**, 7468-7476
11. Mashhoon, N., Pruss, C., Carroll, M., Johnson, P. H., and Reich, N. O. (2006) *J Biomol Screen* **11**, 497-510
12. Parsons, L. M., Yeh, D. C., and Orban, J. (2004) *Proteins* **54**, 375-383
13. Parsons, L. M., Liu, F., and Orban, J. (2005) *Protein Sci* **14**, 1684-1687
14. Kennaway, C. K., Obarska-Kosinska, A., White, J. H., Tuszynska, I., Cooper, L. P., Bujnicki, J. M., Trinick, J., and Dryden, D. T. (2009) *Nucleic Acids Res* **37**, 762-770
15. Dryden, D. T., and Tock, M. R. (2006) *Biochem Soc Trans* **34**, 317-319
16. Putnam, C. D., and Tainer, J. A. (2005) *DNA Repair (Amst)* **4**, 1410-1420
17. Putnam, C. D., Shroyer, M. J., Lundquist, A. J., Mol, C. D., Arvai, A. S., Mosbaugh, D. W., and Tainer, J. A. (1999) *J Mol Biol* **287**, 331-346
18. Shine, J., and Dalgarno, L. (1974) *Proc. Natl. Acad. Sci* **71**, 1342-1346
19. Schurr, T., Nadir, E., and Margalit, H. (1993) *Nucleic Acids Res* **21**, 4019-4023
20. Ma, J., Campbell, A., and Karlin, S. (2002) *J Bacteriol* **184**, 5733-5745
21. Watanabe, M., Yuzawa, H., Handa, N., and Kobayashi, I. (2006) *Appl Environ Microbiol* **72**, 5367-5375
22. Stephens, C., Reisenauer, A., Wright, R., and Shapiro, L. (1996) *Proc. Natl. Acad. Sci* **93**, 1210-1214
23. Robertson, G. T., Reisenauer, A., Wright, R., Jensen, R. B., Jensen, A., Shapiro, L., and Roop, R. M. (2000) *J Bacteriol* **182**, 3482-3489
24. Vieille, C., and Zeikus, G. J. (2001) *Microbiol Mol Biol Rev* **65**, 1-43
25. Li, W. F., Zhou, X. X., and Lu, P. (2005) *Biotechnol Adv* **23**, 271-281

Chapter 7:- Experimental

7.1 Materials and general methods

7.1.1 Materials

PfuTurbo® DNA polymerase and dNTPs were purchased from Stratagene. BioXACT Short® and Mango Taq® DNA polymerases were purchased from Bioline along with their associated reaction buffers. PCR primers were purchased from Sigma-Genosys. Restriction enzymes were purchased from New England Biolabs and used with the manufacturer's recommended buffer. New England Biolabs buffer compositions are given in appendix H. T4 DNA Ligase and Wizard® SV minipreps were purchased from Promega. QIAquick® PCR cleanup and gel extraction kits were purchased from Qiagen. Electrophoresis grade agarose was purchased from Sigma Aldrich.

Plasmids pRJW421307 (created by Dr. R. J. Wood), pCLW469397 (created by Dr. R. J. Wood and Miss C. Williams) and pMK171 (created by Dr. M. Kriek) were kept in frozen stocks at the University of Southampton. Plasmid pBADHisA was originally obtained from Invitrogen and kept in stocks at the University of Southampton. Plasmid pLS251, containing the *dpnI* gene, was a kind gift from Professor Sanford Lacks of Brookhaven National Laboratory. *Pyrococcus horikoshii* genomic DNA was obtained from the NITE Institute. DNA sequencing was carried out by Eurofins MWG Operon.

E. coli strains beginning with GM were obtained from the Yale *E. coli* genetic stock centre. *E. coli* strain TOP10 was originally obtained from Invitrogen and, with all other strains used, kept in frozen stocks at the University of Southampton.

Bacto tryptone and yeast extract were obtained from Oxoid. Ampicillin and DTT were obtained from Melford Laboratories Ltd. Bacto agar and SDS were purchased from Fisher Scientific. Complete, mini, EDTA free, protease inhibitor cocktail tablets were from Roche. Chelating fast flow resin was from Pharmacia and acrylamide / bis-

acrylamide solution was from Amresco. N-terminal protein sequencing was carried out by Cambridge Peptides.

Microplates used to conduct assays were purchased from Greiner Bio-One Ltd. Bovine serum albumin was from Advanced Protein Products Ltd. *S*-adenosylmethionine chloride and *S*-adenosylhomocysteine were purchased from Sigma Aldrich. All fluorescently labelled oligonucleotides used in assays were obtained from ATD Bio.

1-Methylpiperazine, tris(dibenzylideneacetone)diplladium(0), 4,5-bis(diphenylphosphino)-9,9-dimethylxanthene and tetrakis(triphenylphosphine)palladium(0) were purchased from Sigma Aldrich. [3-(2-N,N-dimethylaminoethylaminocarbonyl)phenyl] boronic acid was purchased from Combi-Blocks. Pyridine-3-boronic acid was purchased from Alfa Aesar. 2,5-Dibromopyrazine and 6,8-dibromoimidazo[1,2-a]pyrazine were purchased from Rihachem. All other chemicals were purchased from Sigma Aldrich.

PCR

PCR reactions were carried out in an Eppendorf Mastercycler Gradient thermal cycler.

Electrophoresis

Agarose gel electrophoresis was carried out in a Bio-Rad mini-sub cell. SDS-PAGE was carried out in a Bio-Rad mini-PROTEAN® cell. Electroblotting was carried out in a Bio-Rad mini trans-blot® electrophoretic transfer cell. Short oligonucleotide gel electrophoresis was carried out in a Hoefer SE410 sturdier vertical slab gel electrophoresis unit.

Centrifugation

Centrifugation was typically carried out at 4 °C in a Sorval Evolution RC centrifuge (Thermo Scientific) with an SLC-6000 (8000 g), SLA-1500 (17,500 g) or SS-34 (25,000 g) fixed angle rotor. Centrifugation of small overnight cultures (< 10 ml) was

carried out at 4 °C in a Heraeus Contifuge Stratos centrifuge with rotor #3057 (3000 g). Microcentrifugation was carried out in an Eppendorf 5415D microcentrifuge (16,000 g).

pH determination

pH measurements were determined using an Inolab level 3 bench pH meter with Sentix 22 combination electrode. The instrument was calibrated at pH 4.0, 7.0 and 10.0 prior to use.

Incubation

Liquid cultures were incubated in a New Brunswick Innova 44R shaker with orbital shaking, typically at 180 rpm. Cultures on solid media were incubated in a Heraeus Function Line incubator at 37 °C.

Enzyme activity assays

The activities of *Y. pestis* Dam and DpnI were measured in a Tecan Safire II microplate reader. For high throughput experiments *Y. pestis* Dam assays were prepared and initiated using a Beckmann Coulter Biomek 3000 liquid handling system. Assays of *P. horikoshii* Dam activity were carried out in a BMG PolarStar Omega microplate reader.

DNA melting analysis

DNA melting profiles were measured in a Roche Lightcycler (ex 488 nm, em 520 nm).

7.1.2 General experimental methods

Standard sterile techniques were used during microbiological manipulations. Growth media, glassware and plastic pipette tips were sterilised in an autoclave and heat labile materials such as ampicillin and arabinose were filter sterilised through Millipore 0.22 μm filters. Plastic tubes for bacterial cell culture were pre-sterilised by gamma irradiation.

SOC and 2YT bacterial growth media was prepared as described by Sambrook *et al* (1). Antibiotics were typically used to supplement media at the following concentrations: ampicillin, 100 μg ml^{-1}; chloramphenicol, 30 μg ml^{-1}; kanamycin, 10 μg ml^{-1}. Plasmids and their antibiotic resistance markers are shown in appendix A. Protein expression from these pBad derived plasmids was induced by the addition of 0.2 % w/v arabinose to the growth media. Protein samples were manipulated at 4 °C or on ice unless otherwise stated.

Method 1. Agarose gel electrophoresis

Powdered agarose was added to 1 x TAE buffer (40 mM tris base, 20 mM acetic acid, 1 mM EDTA) to give a 1 % w/v suspension. The mixture was heated with microwave irradiation and gently swirled to achieve complete dissolution of the agarose. Once partially cooled the solution was poured into the gel mould and allowed to solidify around a comb. DNA samples were mixed with 6 x loading buffer (water, 20 % glycerol, 0.05 % bromophenol blue) and added to gel wells formed by removal of the comb. Gels were run at 4 - 5 V cm^{-1} for 40 – 80 minutes and visualised under UV light following staining with ethidium bromide.

Method 2. Miniprep isolation of plasmid DNA

Plasmid DNA was isolated using a Wizard® *Plus* SV Minipreps DNA Purification System according to the manufacturer's instructions. Plasmid DNA was eluted in filter sterilised water.

Method 3. Agarose gel purification of DNA

DNA samples were separated by electrophoresis on a 1 % agarose gel as described in general method 1. Bands containing DNA of interest were excised and the DNA isolated using a QIAquick® gel extraction kit according to the manufacturer's instructions.

Method 4. Glycerol freeze preparation

Frozen stocks of bacterial cell strains were prepared by gently mixing 125 µl of sterile glycerol with 500 µl of bacterial culture in a 1.5 ml microcentrifuge tube. These stocks were stored at -80 °C until required.

Method 5. Determination of protein concentration

Protein concentration was determined with the method of Bradford (2). Protein solution of unknown concentration (20 µl) was mixed with 1 ml of Bradford reagent in a cuvette. The absorbance at 595 nm was measured after the spectrophotometer had been reset using a negative control containing 1 ml Bradford reagent and 20 µl of water. This absorbance was compared to a 20 µl sample of 1 mg ml $^{-1}$ BSA. Calibration curves were prepared for each batch of Bradford reagent to ensure that the relationship between protein concentration and absorbance was linear between an absorbance of 0 and 1.

Method 6. Preparation of competent cells

Solutions TBF I and II were prepared according to the table (Table 7.1). Overnight cultures of *E. coli* were used as a 1 % inoculum for 100 ml of 2YT media. Cultures were maintained at 37 ^{o}C with orbital shaking at 180 rpm until an absorbance of 0.6 at 600 nm was reached. Cultures were then cooled on ice for ten minutes and separated into 50 ml aliquots. Cells were pelleted by centrifugation for 10 minutes at 4 °C (Heraeus Contifuge Stratos, rotor #3057, 4000 rpm) and the supernatant decanted off. The tubes were inverted on paper towel for 1 minute.

Solutions for competent cell preparation	
TBF I (pH 5.8)	Potassium acetate (30 mM)
	Rubidium chloride (100 mM)
	Calcium chloride (10 mM)
	Manganese chloride (50 mM)
	Glycerol 15 % v/v
TBF II (pH 6.5)	MOPS (10 mM)
	Calcium chloride (75 mM)
	Rubidium chloride (10 mM)
	Glycerol 15 % v/v

Table 7.1

Each pellet was resuspended in 5 ml of TBF I solution and stored on ice. Cells were recovered by centrifugation as before. Each pellet was resuspended in 2 ml of TBF II solution. Aliquots of 100 µl were quick frozen on dry ice and stored at -80 ^{o}C.

Method 7. SDS-PAGE

7a. Buffer preparation

SDS-PAGE was carried out using the stock solutions and buffers described in the table below (Table 7.2).

Buffers and stock solutions for SDS-PAGE	
1 x SDS-PAGE loading buffer	Tris.HCl (50 mM, pH 6.8)
	Dithiothreitol (100 μM)
	SDS (2 %)
	Bromophenol blue (0.1 %)
	Glycerol (10 %)
1 x Tris-glycine electrophoresis buffer	Tris (25 mM)
	Glycine (250 mM, pH 8.3)
	SDS (0.1 %)
Gel stain (100 ml)	Coomassie brilliant blue R250 (0.25 g)
	Methanol (45 ml)
	Water (45 ml)
	Glacial acetic acid (10 ml)
Gel destain	Water (87.5 %)
	Methanol (5 %)
	Acetic acid (7.5 %)

Table 7.2

7b. Preparation of 15 % polyacrylamide gels

Polyacrylamide gels contained the components listed in the table (Table 7.3). Components were gently mixed together in the order shown, poured into glass moulds and allowed to set. Whilst the 5 ml main gels were setting they were overlaid with 50 % aqueous isopropanol. Once set, the aqueous isopropanol was removed and 1 ml of stacking gel and a comb were added to the mould. When solidified, gels were stored in moist tissue at 4 ºC until required.

Polyacrylamide gel components (ml)		
	15 % Main Gel (5 ml)	5 % Stacking Gel (5 ml)
Water	1.1	3.4
Acrylamide / bis-acrylamide solution (30 % w/v, 37.5:1)	2.5	0.83
Tris (1.5 M, pH 8.8) and (1 M, pH 6.8) respectively	1.3	0.63
SDS (10 % w/v)	0.05	0.05
APS (10 % w/v)	0.05	0.05
TEMED	0.002	0.005

Table 7.3

7c. Sample analysis

Samples were mixed 1:1 with 2 x SDS-PAGE loading buffer and heated at 95 ^{o}C for 2 minutes. Alternatively, in the case of expression studies, 100 µl of sample loading buffer was added to cells harvested from 1 ml of culture and heated. The wells of the gel were filled with 20 µl, or 2 µl in the case of expression studies, of sample in loading buffer. Electrophoresis was carried out at 200 V in 1 x tris-glycine electrophoresis buffer for 40 – 60 minutes. Gels were stained with coomassie blue and photographed following agitation in gel destain for 12-48 hours.

Method 8. Tricine SDS-PAGE

8a. Buffer preparation

Tricine-SDS-PAGE was carried out using the stock solutions and buffers described in the table below, based on a protocol by Schägger (Table 7.4) (3).

Tricine-SDS-PAGE buffers and stock solutions	
AB-3 stock	Acrylamide (48 g)
	Bisacrylamide (1.5 g)
	Water (bring to 100 ml)
Gel buffer (3 x) pH 8.45	Tris (3 M)
	HCl (1 M)
	SDS (0.3 %)
Anode buffer (10 x) pH 8.9	Tris (1 M)
	HCl (0.225 M)
Cathode buffer (10 x) pH 8.25	Tris (1 M)
	Tricine (1 M)
	SDS (1 %)
Sample loading buffer pH 7.0	SDS (12 % w/v)
	2-Mercaptoethanol (6 % v/v)
	Glycerol (30 % w/v)
	Coomasie blue G-250 (0.05 %)
	Tris.HCl (150 mM)

Table 7.4

8 b. Preparation of 16 % polyacrylamide gels

Gels contained components listed in the table below (Table 7.5) and were prepared as described for normal SDS-PAGE.

Gel components		
Component	16 % Main Gel (30 ml)	4 % Stacking Gel (12 ml)
AB-3 (ml)	10	1
Gel Buffer (3 x) (ml)	10	3
Glycerol (g)	3	-
Water to volume (ml)	30	12
10 % w/v APS (µl)	100	90
TEMED (µl)	10	9

Table 7.5

8 c. Sample analysis

Protein samples were mixed 3:1 with sample loading buffer and incubated at 37 °C for 15 minutes. The gel electrophoresis apparatus was assembled with the gel and electrode buffers filling the appropriate sections. Samples of 50 µl were loaded and the gel run at 30 V until samples had entered the stacking gel. The voltage was then maintained for 3 – 4 hours at 200 V. Protein bands on the gel were visualized with coomassie staining as for SDS-PAGE (general method 7).

Method 9. Preparation of 20 % polyacrylamide gels for the resolution of oligonucleotides

Components listed in the table were mixed and sonicated in a conical flask until no particulate material remained (Table 7.6).

Component	*Quantity*
Acrylamide / bis-acrylamide (40 % w/v, 19:1)	35 ml
TBE buffer (10 x) [890 mM tris base, 890 mM boric acid, 200 mM EDTA]	7 ml
Urea	29.4 g
Water	5 ml

Table 7.6

To initiate polymerisation, 49 µl of TEMED and 490 µl of a 10 % APS solution were added to the solution. This mixture was immediately transferred into the 14 x 24 cm gel mould containing an appropriate comb. Once solidified, the gel was pre-run at a constant 20 W for 2-3 hours in 1 x TBE buffer and then used for sample analysis.

Method 10. Recharging of the nickel affinity column

The 5 ml bed volume nickel column was stripped with a solution of 50 mM EDTA in 50 mM tris until no blue colouration was observed on the column. The column was then sequentially washed with the solutions listed in the table below (Table 7.7).

Solution	*Quantity (ml)*
1. Water	100
2. $NiSO_4$ (0.2 M)	10
3. Water	50
4. Low imidazole buffer*	50
5. High imidazole buffer*	50
6. Low imidazole buffer	100

Table 7.7 * Buffer composition varied depending on the subsequent protein to be purified. Low and High imidazole buffers typically contained 50 mM and 500 mM imidazole respectively.

Method 11. Dam activity assays for the kinetic analysis of *Y. pestis* Dam

Buffers listed in the table below were used in the preparation of Dam activity assays (Table 7.8).

Dam activity assay buffers	
Buffer A (pH 7.9)	Tris-acetate (22.4 mM)
	Sodium chloride (23.5 mM)
	Potassium acetate (56 mM)
	Magnesium acetate (11.2 mM)
	Dithiothreitol (1.12 mM)
	BSA (0.12 mg ml^{-1})
	S-adenosylmethionine (0 – 235 μM)
	Oligonucleotide (0 – 35 μM)
Buffer B (pH 7.9)	Tris-acetate (20 mM)
	Potassium acetate (50 mM)
	Magnesium acetate (10 mM)
	Dithiothreitol (1 mM)
Buffer C (pH 7.4)	Tris.HCl (48 mM)
	EDTA (9.6 mM)
	2-Mercaptoethanol (4.8 mM)
	BSA (0.4 mg ml^{-1})
	Oligonucleotide (30 nM)

Table 7.8

Fluorescence changes were monitored in a microplate reader using 10 reads per well, 0.5 s delay between movement and reading, 1 s of shaking between data collections and 7 s of post shake settling time. Excitation and emission wavelengths were 486 nm and 518 nm respectively with bandwidths of 5 nm. The gain was 200, the Z-position 9300 μm and the integration time 40 μs.

Dam activity was measured in triplicate in black, flat bottomed, 96-well microplates with a total assay volume of 200 μl, maintained at 37 ºC unless otherwise stated.

Wells of a microplate were filled with 170 μl of buffer A and overlaid with 3 drops of mineral oil. The plate was equilibrated at 37 ºC for 15 minutes and initiated by the addition of a mixture containing 10 μl of dilute DpnI solution and 20 μl of dilute Dam solution to each well. Dilute DpnI solution was prepared by diluting the stock solution

to 1 U μl^{-1} in buffer B. Dilute *Y. pestis* Dam solution was prepared by defrosting an aliquot of 0.2 mg ml^{-1} Dam stock on ice for 10 minutes and diluting it with the required amount of buffer C.

Following initiation, the plate was returned to the microplate reader and the fluorescence timecourses recorded. Methylation rates were calculated from the initial rate of fluorescence change and a calibration plot which linked these changes to DNA substrate turnover. Background increases in fluorescence were accounted for by subtraction of a negative control lacking Dam. Data were fitted with the programme 'SigmaPlot'.

Method 12. High throughput format *Y. pestis* Dam activity assays

Fluorescence changes were monitored in a microplate reader using 10 reads per well without orbital shaking between sets of reads. Excitation and emission wavelengths were 486 nm and 518 nm with bandwidths of 9 nm and 20 nm respectively. The gain was 130, the Z-position 9300 µm and the integration time 40 µs. Preparation and initiation of the assays was performed using an automated liquid handling system.

Dam activity was measured in triplicate in black, flat bottomed, 96-well half area microplates with a total assay volume of 100 µl maintained at 30 °C. Three buffers were used for the setup of the assay: Buffer A containing 5.9 µM AdoMet and 35 nM ODN 3, buffer B and buffer C. The composition of these buffers is shown in the table above (Table 7.8, general method 11).

An 85 µl aliquot of Buffer A was added to each of the wells of a microplate and incubated at 30 °C for 15 minutes. Assays were initiated, whilst sat on a Peltier temperature controlled block at 30 °C, by the addition of 5 µl of dilute DpnI solution and 10 µl of dilute Dam solution to each well. Dilute DpnI solution was prepared by diluting the DpnI stock solution to 1 U μl^{-1} in buffer B. Dilute *Y. pestis* Dam solution was prepared by dilution of the stock to 20 nM in buffer C.

Following initiation, the plate was returned to the microplate reader and the fluorescence timecourses recorded. Initial rates of fluorescence increase were based on a linear trend-line fitted to the first 675 s of data. Data from library screen 1 was evaluated with 'HTS-Corrector'software (4).

Method 13. Fluorescence Equilibrium Perturbation (FEP) assays for Dam activity

Fluorescence changes were recorded in a microplate reader with excitation at 490 nm, an emission wavelength of 520 nm and bandwidths of 10 nm. The recorded internal temperature variation of the plate reader was typically < 0.1 °C during experiments. Equal amounts of ODN 4 and M ODN 7 (appendix C) were annealed in a hot block overnight to form duplex ODN 4 / M ODN 7 used in the assay. Assays were prepared in black, flat bottomed, 96-well, half area microplates. Spaces around the wells were filled with 75 % aqueous glycerol to act as a thermal buffer.

Dam activity was measured in duplicate or triplicate 100 µl assays, overlaid with two drops of mineral oil, maintained at a constant temperature.

FEP assays were prepared in buffer D (20 mM potassium phosphate (pH 7.8), 200 mM sodium chloride, 0.1 mg ml^{-1} BSA) supplemented with ODN 4 / M ODN 7, AdoMet and *P. horikoshii* Dam. All components except the AdoMet were added to the microplate and incubated for 30 minutes to allow the temperature to equilibrate. Assays and negative controls were initiated by the addition of 10 µl of a solution of AdoMet or water. Assays and negative controls were interspersed on the plate in equal number.

7.2 Experimental for chapter 2: Development of an assay for *Y. pestis* Dam activity

7.2.1 Cloning, expression and purification of His_6-M.YpeDam

7.2.1.1 His_6-M.YpeDam expression studies

Y. pestis Dam was expressed in *E. coli* strains BL21(DE3), JM110 and GM215 harbouring plasmid pRJW421307. Each 10 ml overnight starter culture, grown from a

glycerol freeze, was used as a 1 % inoculum for 100 ml of 2YT media supplemented with 100 μg ml^{-1} ampicillin. Cultures were maintained at 37 ºC with orbital shaking until an absorbance of 0.6 at 600 nm was reached. Cells were induced with the addition of arabinose and maintained at 37 ºC with orbital shaking for a further four hours. Cell culture aliquots of 1.5 ml were harvested every hour after induction and the crude lysate analysed by 15 % SDS-PAGE with coomasie staining.

7.2.1.2 Large scale expression of His_6-M.YpeDam in GM215

Y. pestis Dam was expressed in *E. coli* strain GM215 harbouring plasmid pRJW421307. All purification steps were carried out at 4 ºC to preserve methyltransferase activity. Overnight cultures grown from glycerol freezes were used as a 1 % inoculum for 5 L of 2YT media supplemented with 100 μg ml^{-1} ampicillin. Cultures were maintained at 37 ºC with orbital shaking until an absorbance of 0.6 at 600 nm was reached. Protein expression was induced by the addition of arabinose and the culture maintained for a further hour at 37 °C. Cells, typically 20 g, were collected by centrifugation (Sorval SLC-6000 rotor, 8000 rpm, 4 ºC, 12 min) and frozen at -80 ºC.

7.2.1.3 Nickel affinity purification of His_6-M.YpeDam

Purification buffers were prepared according to the table below (Table 7.9).

Buffers for Y. pestis Dam purification	
Low imidazole buffer (pH 9)	Tris.HCl (50 mM)
	Sodium chloride (300 mM)
	Imidazole (50 mM)
	Glycerol (10 % w/v)
	2-Mercaptoethanol (10 mM)
	Triton X-100 (0.05 % v/v)
High imidazole buffer (pH 9)	Tris.HCl (50 mM)
	Sodium chloride (300 mM)
	Imidazole (500 mM)
	Glycerol (10 % w/v)
	2-Mercaptoethanol (10 mM)
	Triton X-100 (0.05 % v/v)
Dam methyltransferase storage buffer (pH 7.5)	Tris.HCl (50 mM)
	Sodium chloride (200 mM)
	Glycerol (20 % w/v)
	DTT (2 mM)
	EDTA (0.2 mM)

Table 7.9

Cell paste, typically 10 g, was resuspended in 30 ml of low imidazole buffer at room temperature with stirring. A 0.3 ml aliquot of 10 mg ml $^{-1}$ lysozyme solution was added and the mixture stirred for 20 min at 4 ºC. The solution was put on ice and sonicated twenty five times with rest intervals of 5 s. The resultant lysate was cleared by centrifugation for 30 minutes at 4 °C (15,000 rpm, JA 25.5 rotor, Beckmann Avanti J-25 centrifuge). The resultant supernatant was applied to a nickel column with a bed volume of 5 ml. The column was washed with 150 – 200 ml of low imidazole buffer and *Y. pestis* Dam was then eluted with a gradient of 0 – 100 % high imidazole buffer. Fractions containing Dam were identified by SDS-PAGE, pooled, dialysed for two half hour periods into Dam methyltransferase storage buffer and frozen at -80 ºC. Protein concentration was determined as 0.2 mg ml $^{-1}$ by Bradford assay. Approximately 1.5 mg of *Y. pestis* Dam was obtained from 10 g of cell paste.

7.2.2 Subcloning, expression and purification of His_6-DpnI

7.2.2.1 PCR amplification of the *dpnI* gene

PCR reactions with a volume of 50 µl were set up in sterile PCR tubes with components listed in the table below (Table 7.10).

Component	*Quantity (µl)*
Optimax buffer* (10 x)	5
$MgCl_2$ (50 mM)	2
dNTP's (2 mM each)	1
Primers (DpnIf and DpnIr 100 µM)	0.5 each
Template plasmid DNA[#] (10 – 1000 x dilution)	1
Sterile water	39
BioXACT short polymerase mix	1

Table 7.10 * For colony PCR, MangoTaq DNA polymerase and buffer were used. Template DNA was substituted with whole cells picked into the mixture. The temperature programme was also preceeded with 10 minutes at 95°C. [#] Template DNA was obtained from a Wizard® *Plus* SV Miniprep of a 10 ml overnight culture of GM33 harbouring plasmid pLS251.

PCR reactions were cycled through the temperature programme outlined below (Table 7.11).

Temperature programme	
30 x	1 x
95 °C, 90 seconds	68 °C 10 minutes
47 °C, 90 second	Hold 4 °C
68 °C, 90 seconds	

Table 7.11

Samples of 5 µl taken from the PCR reactions were analysed by 1 % gel electrophoresis and the reactions purified using a QIAquick gel extraction kit according to the manufacturer's instructions.

7.2.2.2 Digestion of the *dpnI* gene

Digests with a volume of 50 µl were prepared in 1.5 ml microcentrifuge tubes and contained the components listed in the table below (Table 7.12).

Component	*Quantity (µl)*
PCR product or plasmid pMK171 *	25
Sterile water	11
Buffer 2 (10 x)	5
BSA (1mg ml^{-1})	5
NcoI (10 U μl^{-1})	2
XhoI (20 U μl^{-1})	2

Table 7.12 * pMK171 was harvested from a 10 ml overnight culture of *E.coli* TOP10 using a Wizard ® *Plus* SV Miniprep.

Digests were incubated for 2 hours at 37 °C in a water bath. Digested DNA was run on a 1 % agarose gel and purified using a QIAquick gel extraction kit according to the manufacturer's instructions. Samples of the purified digested *dpnI* gene and pBad vector from pMK171 were analysed by 1 % agarose gel electrophoresis.

7.2.2.3 Ligation of the *dpnI* gene into a pBad vector

Ligation reactions contained three different vector to insert ratios and were prepared in PCR tubes. DNA was used as purified after digestion. Ligation reactions contained the components listed in the table (Table 7.13).

Component	*Quantity (µl)*		
Digested *dpnI* gene	6	3	0
Digested vector	2	2	2
Sterile water	0	3	6
T4 DNA ligase buffer (10 x)	1	1	1
T4 DNA ligase (1-3 U μl^{-1})	1	1	1

Table 7.13

Reactions were incubated at room temperature for two hours or overnight at 4 °C.

7.2.2.4 Transformation of *E. coli* with the DpnI expression plasmid

Ligation reactions were added to a 100 µl aliquot of GM2929 competent cells previously thawed on ice for 15 minutes. Cells were kept on ice for a further 30 minutes and heat shocked in a water bath at 42 °C for 45 seconds. The cells were returned to the ice for 2 minutes and 250 µl of SOC media added. Following incubation at 37 °C with orbital shaking for one hour, 150 µl of cell culture was plated out onto 2YT agar supplemented with 10 µg ml^{-1} chloramphenicol and 100 µg ml^{-1} ampicillin. Transformants yielded colonies following incubation at 37 °C overnight. The newly formed DpnI expression plasmid was designated pMMS495859.

7.2.2.5 Analytical digestion of pMMS495859

Plasmid pMMS495859 was harvested from 10 ml overnight cultures of GM2929 supplemented with 100 µg ml^{-1} ampicillin and 10 µg ml^{-1} chloramphenicol using minipreps. Double and single digests were set up containing components listed in the table below and incubated for 1 hour at 37 °C (Table 7.14).

Component	*Quantity (µl)*	
Plasmid DNA	5	5
Sterile water	3.5	2.5
Buffer 4 (10 x)	1	1
BSA (1 mg ml^{-1})	1	1
NcoI (10 U μl^{-1})	0	1
XhoI (20 U μl^{-1})	1	1

Table 7.14

Digestions were analysed by 1 % agarose gel electrophoresis.

7.2.2.6 His_6-DpnI expression studies

Overnight cultures of GM2929 harbouring pBad or pMMS495859 were used as a 1 % inoculum for 100 ml 2YT media supplemented with 100 µg ml^{-1} ampicillin and 10 µg ml^{-1} chloramphenicol. Cultures were maintained at 37 °C with orbital shaking until an absorbance of 0.6 at 600 nm was reached. Expression was induced with the addition of arabinose. Cultures were maintained as before and 1.5 ml samples taken after 1 and 2 hours. Cells from the samples were collected by microcentrifugation, re-suspended in 100 µl of 2 x SDS-PAGE loading buffer and heated at 95 °C for 10 minutes. The protein content of 5 µl samples was analysed by 15 % SDS-PAGE with coomasie staining.

7.2.2.7 Large scale expression of His_6-DpnI in *E. coli* strain GM2929

An overnight culture of *E.coli* GM2929 harbouring plasmid pMMS495859 was grown from a glycerol stock in 2YT media supplemented with 100 µg ml^{-1} ampicillin and 10 µg ml^{-1} chloramphenicol. The culture was used as a 1 % inoculum for 5 L of 2YT media supplemented with 100 µg ml^{-1} ampicillin. The culture was maintained at 37 °C with orbital shaking. At an absorbance of 0.6 at 600 nm, expression was induced by addition of arabinose. The culture was maintained for a further 3 hours at 27 °C and 23 g of cell paste was harvested by centrifugation (Sorval Evolution, SLC-6000 rotor, 6800 rpm, 4 °C).

7.2.2.8 Selection of a strain for His_6-DpnI expression

Overnight cultures of GM33, GM48, GM124, GM161 and GM215 harbouring plasmid pMMS495859 were grown in 2YT media supplemented with 100 μg ml^{-1} ampicillin. Overnight growths were each used as a 1 % inoculum for 1 L of 2YT media supplemented with 100 μg ml^{-1} ampicillin. All 1 L cultures were maintained at 37 °C with orbital shaking. Cultures of GM124, GM161 and GM215 were induced by addition of arabinose after 2 ½ hours, when they had an absorbance of 0.6 at 600 nm. Cultures of GM33 and GM48 were induced after 3 ½ hours when they had reached absorbances of 0.57 and 0.2 at 600 nm respectively. All cell cultures were harvested by centrifugation 6 ½ hours after inoculation (Sorval Evolution, SLC-6000 rotor, 6800 rpm, 4 °C). Strain GM33 did not pellet efficiently and gave 23 g of mobile slurry upon centrifugation. Strains GM48, GM124, GM161 and GM215 yielded 2, 3.8, 6 and 1.4 g of cell paste respectively.

7.2.2.9 Nickel affinity purification of His_6-DpnI

Buffers were prepared as outlined in the table below (Table 7.15).

Buffers for the purification of His_6-DpnI	
Low imidazole buffer (pH 7.4)	Tris.HCl (50 mM)
	Sodium chloride (400 mM)
	Imidazole (50 mM)
	Glycerol (10 % w/v)
	2-Mercaptoethanol (5 mM)
High imidazole buffer (pH 7.4)	Tris.HCl (50 mM)
	Sodium chloride (400 mM)
	Imidazole (500 mM)
	Glycerol (10 % w/v)
	2-Mercaptoethanol (5 mM)
DpnI storage buffer (pH 7.4)	Tris.HCl (10 mM)
	Sodium chloride (400 mM)
	EDTA (0.1 mM)
	DTT (1 mM)
	Glycerol (50 % w/v)

Table 7.15

Depending on the cell strain between 1 and 6 g of cell paste was resuspended in 30 ml of ice cold low imidazole buffer, supplemented with 1 mM PMSF and a Roche protease inhibitor tablet. Lysozyme, 10 mg, was added and the mixture stirred over ice for 15 minutes. The PMSF was replenished and the solution sonicated for ten 25 s periods whilst over ice. The resultant lysate was centrifuged for 25 minutes at 4 °C to precipitate cell debris (Sorvall Evolution centrifuge, SLA-1500 rotor, 14,000 rpm). The supernatant was applied to a nickel affinity column with a bed volume of 10 ml at a flow rate of 4 ml min^{-1}. The column was washed with 150 ml of low imidazole buffer after which His_6-DpnI was eluted with a step from 0-100 % high imidazole buffer. Fractions containing protein were identified by Bradford assay and analysed by 15 % SDS-PAGE. The remaining protein was frozen at -80 ^{o}C without dialysis into storage buffer.

7.2.2.10 Large scale expression of His_6-DpnI in GM48

An overnight culture of GM48 harbouring pMMS495859 was used to inoculate 5 L of 2YT media supplemented with 100 μg ml^{-1} ampicillin. The culture was maintained at 37 °C with orbital shaking. Once the absorbance at 600 nm reached 0.6, DpnI expression was induced with the addition of arabinose. The culture was maintained for a further 3 hours at 37 °C and 24 g of cells were harvested by centrifugation (Sorval evolution, SLC-6000 rotor, 6800 rpm, 4 °C).

7.2.2.11 Nickel affinity purification of His_6-DpnI from *E. coli* GM48

Purification was carried out using 5 g of cell paste as described in section 7.2.2.9. DpnI was eluted from the column with a 30 ml gradient from low to high imidazole buffer rather than a step. Protein was pooled and dialysed into 'DpnI storage buffer' for two one hour periods. Approximately 25 mg of protein was obtained at a concentration of 2.3 mg ml^{-1}.

7.2.2.12 Digests using His_6-DpnI

Digests were set up in 1.5 ml microcentrifuge tubes and incubated at 37 °C for 30 minutes. Digests contained components listed in the table below (Table 7.16).

Component	*Quantity (μl)*
Plasmid DNA*	5
Sterile water	1
Buffer 4 (10 x)	1
BSA (1 mg ml^{-1})	1
DpnI (Commercial (2 U μl^{-1}) or His_6-DpnI (300 nM))	2

Table 7.16 * Unmethylated pBadHisA from GM2929 or Methylated pMK171 from *E.coli* TOP10

.

Digestions with the His_6-DpnI and the commercially available restriction enzyme were analysed by 1 % agarose gel electrophoresis with ethidium bromide staining.

7.2.3 Development of an assay for *Y. pestis* Dam activity

7.2.3.1 Assays using the first and second oligonucleotide designs

Assays were not carried out as described in the general experimental methods. Dam used in early assay development with ODN 1 and 2 (appendix C) was of a low quality due to its instability. The stabilising effect of DNA on the enzyme was not discovered until after the initial period of assay development.

Fluorescence changes were monitored in a microplate reader using 100 reads per well, 0.5 s delay between movement and reading, 3 s of shaking between data collections and 5 s of post shake settling time. Excitation and emission wavelengths were 486 nm and 518 nm respectively with bandwidths of 5 nm. The gain was 170, the Z-position 9300 μm and the integration time 40 μs.

Dam activity was measured in black, flat bottomed, 96-well microplates with a total assay volume of 200 μl maintained at 37 °C.

Two buffers were used for the preparation of the assay: Buffer 4 (appendix H) and Dam methyltransferase buffer (50 mM Tris-HCl (pH 7.5), 10 mM EDTA, 5 mM 2-mercaptoethanol and 0.4 mg ml^{-1} BSA).

Assays using ODN 1 were prepared as follows: Buffer 4 (180 μl, 1.1 x) supplemented with 4 U DpnI, 0.1 mg ml^{-1} BSA, 550 μM AdoMet and 27.5 nM ODN 1 was added to the wells of a microplate, overlaid with mineral oil, and incubated at 37 °C for 30 minutes. Assays were initiated by the addition of 20 μl of 300 nM Dam diluted in Dam methyltransferase buffer. The plate was returned to the microplate reader and the fluorescence timecourses were monitored. Final concentrations of assay components were: 500 μM AdoMet, 25 nM ODN 1**,** 30 nM *Y. pestis* Dam and 0.2 U μl^{-1} DpnI.

Assays using ODN 2 were set up as described for ODN 1 except that final concentrations of assay components were: 15, 25, 35, 45, 55 nM ODN 2, 250 μM AdoMet, 20 nM *Y. pestis* Dam and 0.1 U μl^{-1} DpnI.

7.2.3.2 Proof of principle assays using oligonucleotide design 3

The principle of the real-time coupled enzyme assay was demonstrated in a series of assays containing 33 nM ODN 3, 240 μM AdoMet and 0, 0.3 or 0.6 nM Dam. Assays were prepared as described in the general experimental methods section (method 11).

7.2.3.3 Optimisation of the sodium chloride concentration in Dam activity assays

Assays were prepared as described in general experimental method 11 except that buffer A contained various amounts of sodium chloride to give concentrations between 0 and 150 mM in the final assay.

7.3 Experimental for chapter 3: Kinetic analysis of *Y. pestis* Dam and validation of the coupled enzyme assay

7.3.1 Kinetic analysis of *Y. pestis* Dam

7.3.1.1 Calibration of oligonucleotide fluorescence

Calibration assays were carried out as described in general experimental method 11 with some exceptions. Assays contained the fully methylated oligonucleotide FM ODN 3 in place of ODN 3, at concentrations of 0, 0.5, 1, 2, 3, 3.5 nM. AdoMet was present in the assays at 25 μM but buffer C was added instead of 'dilute Dam solution' at the initiation step. Endpoint fluorescence was measured in duplicate on three separate occasions for each concentration of DNA.

7.3.1.2 Measurement of the stabilisation of *Y. pestis* Dam by its substrates

Enzyme inactivation was studied under three conditions, without either substrate, in the presence of 30 nM ODN 3 or with 120 μM AdoMet in solution. Dilute Dam solutions were prepared at a concentration of 24 nM in buffer C**,** with or without the appropriate substrates. Dilute Dam solutions were mixed 2:1 with dilute DpnI solution and

incubated at 30 °C in a PCR machine. Aliquots of this enzyme mix were withdrawn periodically and rapidly cooled on ice. These aliquots were used to initiate Dam activity assays containing 120 μM AdoMet and 33 nM ODN 3 in the usual manner. Resultant fluorescence timecourses were used to determine the relative activity of the Dam in the aliquots.

7.3.1.3 Dependence of *Y. pestis* Dam activity on substrate concentrations

The dependence of *Y. pestis* Dam activity on AdoMet concentration was determined with two sets of assays both containing 1 nM Dam, 33 nM ODN 3 and 2.5, 5, 10, 20, 40, 100 and 200 μM AdoMet. The first set of assays was incubated at 37 °C and the other at 30 °C. The dependence of Dam activity on ODN 3 concentration was measured in a series of assays containing 0.31 nM Dam, 120 μM AdoMet and 0.5, 1.5, 2.5, 3.5, 3.5, 4.5, 5.5 and 6.5 nM ODN 3. Assays were carried out as described in general experimental method 11.

7.3.1.4 Inhibition of Dam by *S*-adenosylhomocysteine

Inhibition of Dam by *S*-adenosylhomocysteine was investigated with several sets of assays containing 1 nM Dam, 33 nM ODN 3 and 20, 25, 30, 40, 70, 140 and 200 μM AdoMet. One set of assays was conducted at each of the following AdoHcy concentrations; 0, 5, 10, 15, 20, 30 and 40 μM. The K_i AdoHcy was determined using two plots constructed from the assay data. Straight lines were fitted to double reciprocal plots of 1 / methylation rate against 1 / [AdoMet] at each AdoHcy concentration. These lines had a gradient = $K_{M.app}$ / V_{max}, a y-axis intercept = 1 / V_{max} and were used to obtain values for the $K_{M.app}$ (the apparent K_M ^{AdoMet}). These values were plotted against AdoHcy concentration. A straight line fitted to this second plot had an intercept of -K_i AdoHcy on the x-axis.

7.3.2 Assay validation in high throughput format

Three 96-well plates containing positive and negative control assays were prepared as described in general experimental method 12. Negative controls were performed by

replacing the 'dilute Dam solution' with buffer C in the initiation step. Z' values derived from the three plates of data were averaged to give an estimated Z' for the assay.

7.4 Experimental for chapter 4: High throughput screening for *Y. pestis* Dam inhibitors

7.4.1. HTS of a compound library

Assays were prepared as described in general experimental method 12. Buffer A was however modified by the addition of 1 μl of a 10 mM test compound solution in DMSO. The final concentration of the test compounds in the assays was 100 μM.

7.4.2 Synthesis of potential Dam inhibitors

7.4.2.1 Synthesis of 6-bromoimidazo-8-(1-methylpiperazine)[1,2-a]pyrazine

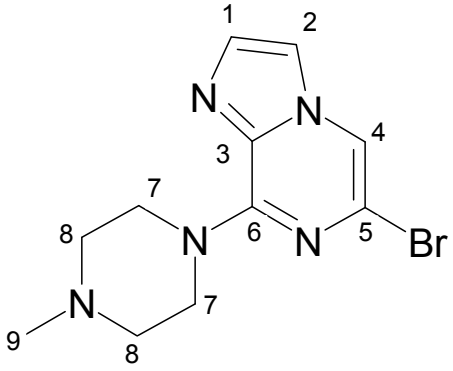

A mixture of 6,8-dibromoimidazo[1,2-a]pyrazine (300 mg, 1.08 mmol) in 40 % v/v aqueous 1-methylpiperazine (3 ml) was stirred under nitrogen at room temperature overnight. Water (5 ml) was added to the reaction and the product extracted into dichloromethane (2 x 20 ml). The organic phase was dried over magnesium sulphate and the solvent removed *in vacuo* to afford a brown gum. After recrystallisation from hot hexane the product, an off white solid, was obtained in 64 % yield (204 mg, 0.69 mmol). R.f. (10 % MeOH : DCM) = 0.4; mp 85-87 °C. ^{1}H NMR (300 MHz, $CDCl_3$) δ: 7.59 (1H, s) H4, 7.50 (1H, d, J = 0.9 Hz) and 7.43 (1H, d, J = 0.9 Hz) H1 and H2, 4.37 (4H, t, unresolved) H7, 2.57 (4H, t, J = 5.1 Hz) H8, 2.35 (3H, s) H9; ^{13}C NMR (75 MHz, $CDCl_3$) δ: 132.2 C4, 122.4 C3 or C5, 114.6 and 109.8 C1 and C2, 55.5 C8, 46.3 and 46.3 C7 and C9; LRMS (ES^+) *m/z* 296 / 298 ($[M + H]^+$).

7.4.2.2 Synthesis of Compound H09-6137

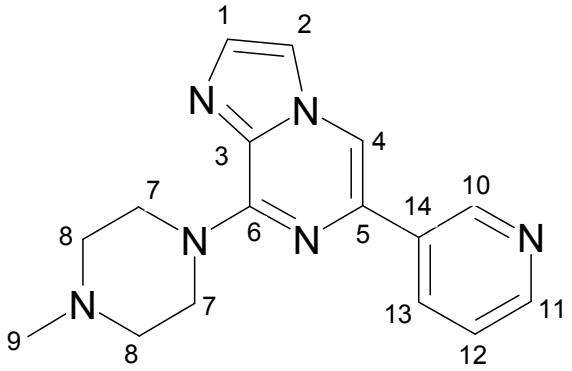

A mixture of 6-bromoimidazo-8-(1-methylpiperazine)[1,2-a]pyrazine (80 mg, 0.27 mmol), pyridine-3-boronic acid (33.2 mg, 0.27 mmol), sodium carbonate (86 mg, 0.81 mmol), tetrakis(triphenylphosphine)palladium(0) (10 mg, 8.6 μM) in 1,2 dimethoxyethane (6 ml) and water (2 ml) was refluxed under nitrogen for 6-8 hours until TLC analysis showed the reaction had gone to completion. The majority of the solvent was removed *in vacuo* and the cooled concentrated reaction partitioned between dilute brine (30 ml) and ethyl acetate (3 x 25 ml). The organic extracts were combined, dried over magnesium sulphate and evaporated to give the crude product. Chromatography on a silica gel column with 10 % methanol : dichloromethane afforded the pure product, a pale yellow solid, in 63 % yield (49 mg, 0.17 mmol). R.f. (10 % MeOH : DCM) = 0.15; mp 128 – 130 °C; ^{1}H NMR (300 MHz, $CDCl_3$) δ: 9.12 (1H, br s) H10, 8.58 (1H, br s) H11, 8.21 (1H, d, J = 7.9 Hz) H13, 7.95 (1H, s) H4, 7.56 (2H, 2 x d) H1 and H2, 7.36 (1H, dd, J = 4.9, 7.4 Hz) H12, 4.43 (4H, t, J = 4.5 Hz) H7, 2.61 (4H, t, J = 5.0 Hz) H8, 2.37 (3H, s) H9; ^{13}C NMR (75 MHz, $CDCl_3$) δ: 149.2 C11, 148.4, 147.3 C10, 135.1, 133.6, 133.4 C13, 133.1, 131.9 C1 or C2, 123.4 C12, 114.8 C1 or C2, 107.2 C4, 55.2 C8, 46.2 C7, 46.0 C9.

HMQC (400 MHz, $CDCl_3$).

	2.37	2.61	4.43	7.36	7.56	7.95	8.21	8.58	9.12
46.0	X								
46.2			X						
55.2		X							
107.2						X			
114.8					X				
123.4				X					
131.9					X				
133.4							X		
147.3									X
149.2								X	

MS-(ES^+) *m/z* 295 ($[M + H]^+$); HRMS (ES) $C_{16}H_{19}N_6^+$ calcd 295.1666, found 295.1664; IR (neat) 2985, 2889, 2831, 2417, 2299, 2128, 2000, 1583, 1493, 1430, 1250, 1097, 972, 819 cm^{-1}; UV-Vis (MeOH) 242 nm (ε = 19,500 L mol^{-1} cm^{-1}), 316 nm (ε = 9,700 L mol^{-1} cm^{-1}); Fluorescence (MeOH, $\lambda_{excitation}$ = 244 nm) $\lambda_{emission}$ = 395 nm.

7.4.2.3 Synthesis of compound 5 (scheme 4.3, chapter 4)

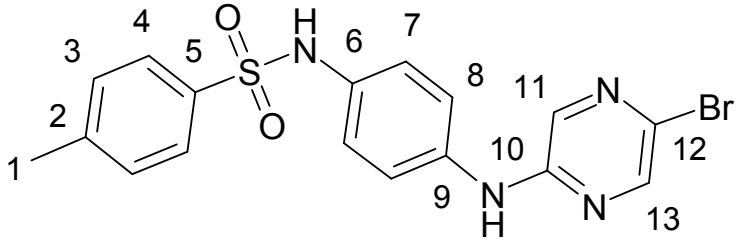

Tris(dibenzylideneacetone)dipalladium(0) (7.2 mg, 7.86 µmol, 2.5 mol % Pd), 4,5-bis(diphenylphosphino)-9,9-dimethylxanthene (18.2 mg, 31.52 µmol, 5 mol %), *N*-(4-aminophenyl)-4-methylbenzenesulfonamide (165.0 mg, 630.50 µmol, 1 eq), caesium carbonate (287.6 mg, 882.79 µmol, 1.4 eq) and 18-crown-6 (16.6 mg, 62.80 µmol, 10 %) were stirred and heated in 1,4-dioxane (3 ml) under a nitrogen atmosphere for 15 minutes at 50 °C. 2,5-dibromopyrazine (150 mg, 630.50 µmol, 1 eq) was dissolved in 1,4-dioxane (1 ml) and added to the mixture, via a septum, which was

then heated and stirred overnight at 90 °C. The solvent was removed *in vacuo* and the residue partitioned between dilute brine (50 ml) and ethyl acetate (3 x 50 ml). The organic extracts were combined, dried over magnesium sulphate and evaporated to give the crude product. Chromatography on a silica gel column with 1 % methanol : dichloromethane afforded the pure product, a pale solid, in 53 % yield (139 mg, 333 µmol). Any product containing fractions, from the first column, found to be contaminated with *N*-(4-aminophenyl)-4-methylbenzenesulfonamide were purified by RP-column chromatography in 50 % MeCN : H_2O. R.f. (3 % MeOH : DCM) = 0.21, (RP, 50 % MeCN : H_2O) = 0.11; mp 173 – 175 °C; ^{1}H NMR (300 MHz, MeOD) δ: 8.15 (1H , d, J = 1.7 Hz) and 7.88 (1H, d, J = 1.7 Hz) H11 and H13, 7.53 (4H, 2 x dd, J = 3.0, 7.6 and 3.0 and 8.9 Hz) H4 and H7, 7.27 (2H, d, J = 6.2 Hz) H3, 6.99 (2H, dd, J = 3.1 and 9.0 Hz) H8, 2.36 (3H, d, J = 2.5 Hz) H1; ^{13}C NMR (75 MHz, MeOD) δ: 153.1 C10, 144.9 and 144.4 C11 and C13, 138.8, 138.1, 135.3, 133.1, 130.5, 128.3, 127.2, 124.3, 120.6, 21.4 C1; LRMS (ES^-) *m/z* 417 / 419 ($[M-H]^-$).

7.4.2.4 Synthesis of compound D11:6141

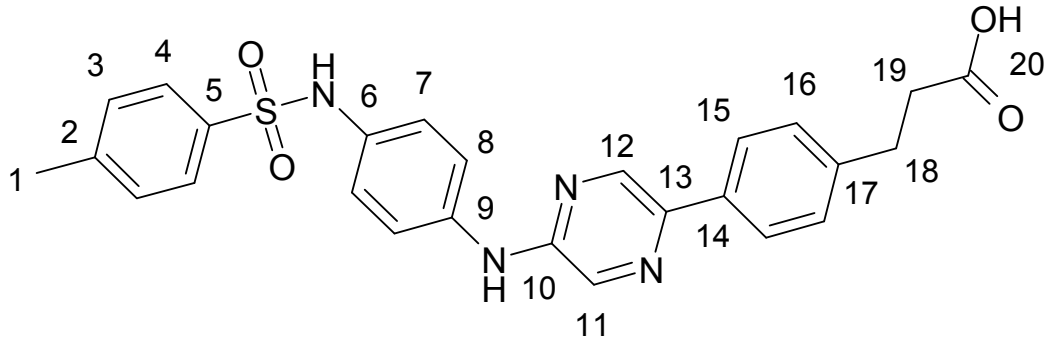

A mixture of compound 5 (60.0 mg, 143.50 µmol, 1 eq), 4-(2-carboxyethyl)benzeneboronic acid (30.6 mg, 157.70 µmol, 1.1 eq), caesium carbonate (186.0 mg, 572.30 µmol, 4 eq), tetrakis(triphenylphosphine)palladium(0) (16.6 mg, 14.37 µmol, 10 mol %) in 1,2 dimethoxyethane (3 ml) and water (1 ml) was refluxed under nitrogen overnight. The solvent was removed *in vacuo* and the product purified by RP-column chromatography using a 10 - 15 % MeCN gradient in 0.03 % aqueous ammonia. Removal of the MeCN *in vacuo* and the remaining water by freeze drying afforded the product, D11:6141, as a white powder in 87 % yield (60.8 mg, 124.79 µmol). R.f. (RP, 25 % MeCN : 0.03 % aqueous NH_3) = 0.32; mp > 270 °C dec. ^{1}H NMR (300 MHz, DMSO / D_2O 75 : 25) δ: 8.55 (1H, s) and 8.16 (1H, s) H11 and H12, 7.79 (2H, d, J = 7.7 Hz), 7.54 (4H, 2 x d, J = 8.5 and 8.5 Hz), 7.28 (4H, 2 x d, J =

7.9 and 7.7 Hz), 6.98 (2H, d, J= 8.5 Hz), 2.80 (2H, t, J = 7.2 Hz) H18, 2.45 (t, J = 7.2 Hz) H19, 2.29 (3H, s) H1; ^{13}C NMR (75 MHz, MeCN / D_2O) δ: 175.9 C20, 150.7 C10, 143.9 C13, 141.6 and 141.2 C11 and C12, 137.9, 137.5, 135.6, 134.3, 133.3, 130.7, 129.3, 128.6, 126.8, 125.3, 122.7, 119.2, 35.4 C18, 30.1 C19, 20.2 C1; LRMS (ES^-) *m/z* 487 ($[M-H]^-$); HRMS (ES) $C_{26}H_{25}N_4O_4S^+$ calcd 489.1591, found 489.1583; IR (neat) 3387, 3279, 3034, 2926, 2895, 2359, 2325, 1716, 1614, 1530, 1508, 1316, 1153, 1088, 838, 815, 617 cm^{-1}; UV-Vis (MeOH) 310 nm (ε = 19,700 L mol^{-1} cm^{-1}), 369 nm (ε = 10,200 L mol^{-1} cm^{-1}); Fluorescence (MeOH, $\lambda_{excitation}$ = 310 nm) $\lambda_{emission}$ = 436, 497 nm.

7.4.2.5 Synthesis of compound B02:6142

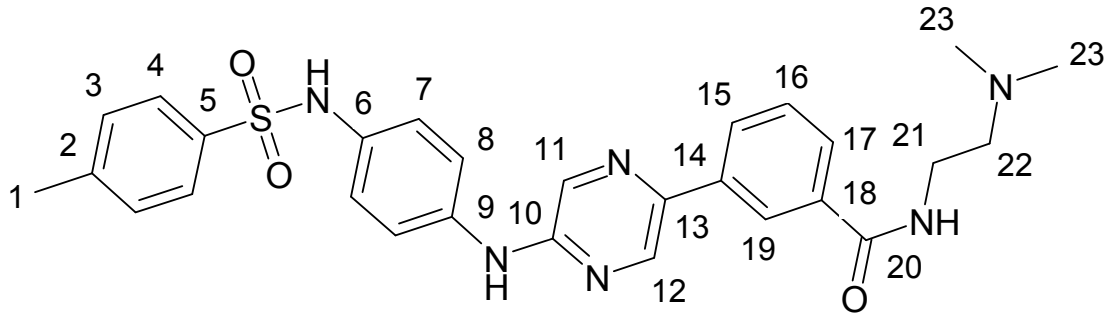

A mixture of compound 5 (50.0 mg, 119.60 µmol, 1 eq), [3-(2-*N,N*-dimethylaminoethylaminocarbonyl)phenyl] boronic acid (31.0 mg, 131.56 µmol, 1.1 eq), caesium carbonate (155 mg, 478.92 µmol, 4 eq), tetrakis(triphenylphosphine)palladium(0) (13.8 mg, 11.94 µmol, 10 mol %) in 1,2 dimethoxyethane (3 ml) and water (1 ml) was refluxed under nitrogen overnight. The solvent was removed and the product purified by RP-column chromatography using a 10 – 50 % MeCN : H_2O gradient with or without 0.1 % acetic acid. Removal of the MeCN *in vacuo* and remaining water by freeze drying afforded the product, B02:6142, as a pale orange powder in 65 % yield (41 mg, 77.43 µmol). R.f. (RP, 50 % MeCN : H_2O) = 0.32; mp 123 - 127 °C; ^{1}H NMR (300 MHz, DMSO / D_2O 75 : 25) δ: 8.65 (1H, s) and 8.36 (1H, s) H11 and H12, 8.21 (1H, s) H19, 8.09 (1H, d, J = 7.9 Hz) and 7.79 (1H, d, J = 7.9 Hz) H15 and H17, 7.56 (5H, m (2 x d + t), J = 8.1, 8.7 Hz) includes H16, 7.30 (2H, d, J = 8.5 Hz), 6.99 (2H, d, J = 8.9 Hz), 3.79 (0.43H, s) H21, 3.63 (1.7H, t, J = 5.84 Hz) H21, 3.46 (0.65H, s) H22, 3.26 (1.8H, t, J = 5.94 Hz) H22, 2.82 (5.5H, s) H23, 2.29 (3H, s) H1; ^{13}C NMR (75 MHz, MeOD) δ: 170.9 C20, 153.0 C10, 145.0 C13, 142.0, 139.6, 139.2, 138.8, 138.0, 135.3, 135.1, 132.8, 130.6, 130.2, 130.0, 128.3,

128.0, 125.6, 124.4, 120.6, 58.8 C21, 44.0 C23, 36.5 C22, 21.5 C1; LRMS (ES^+) *m/z* 531 ($[M + H]^+$), 277 ($[M + H + Na]^{2+}$), 185 ($[M + 2H + Na]^{3+}$); HRMS (ES) $C_{28}H_{31}N_6O_3S^+$ calcd 531.2173. found 531.2169; IR (neat) 3440, 3067, 2956, 2931, 2850, 1668, 1644, 1507, 1326, 1200, 1154, 834, 814, 799, 720, 662 cm^{-1}; UV-Vis (MeCN) 255 nm (ε = 7,500 L mol^{-1} cm^{-1}), 316 nm (ε = 14,500 L mol^{-1} cm^{-1}), 360 nm (ε = 11,400 L mol^{-1} cm^{-1}); Fluorescence (MeCN, $\lambda_{excitation}$ = 255 nm) $\lambda_{emission}$ = 452, 498 nm.

7.4.3 Analysis of hit compounds

7.4.3.1 Assays to determine the effect of hit compounds on Dam activity

The activity of Dam, in assays containing a range of compound concentrations, was measured in triplicate using general experimental method 12.

7.4.3.2 Assays to determine the effect of hits on DpnI activity

DpnI activity was measured in duplicate assays, with a volume of 100 µl maintained at 30 °C in black 96-well half area microplates. Assays contained buffer B (Table 7.8) supplemented with 20 mM sodium chloride, 0.1 mg ml^{-1} BSA, 30 nM FM ODN 3 and 0.2 nM DpnI. Rates were determined from the first 175 s of data using the same plate reader parameters as for the library screen.

7.4.3.3 Fluorescence intercalation displacement assays

DNA binding of compounds was measured in triplicate assays, with a volume of 100 µl in black 96-well half-area microplates. Assays contained buffer B (Table 7.8) supplemented with 20 mM sodium chloride, 0 or 1.5 µM UL ODN 2 (appendix C), 0.75 µM thiazole orange and test compounds at the specified concentrations. Fluorescence intensity was measured in a Tecan Safire II microplate reader with excitation at 504 nm, emission at 527 nm and bandwidths of 10 nm.

7.5 Experimental for chapter 5: A novel and direct assay for Dam activity

7.5.1 Cloning, expression and purification of His_6-M.PhoDam

7.5.1.1 Cloning of the *P. horikoshii dam* gene

The *P. horikoshii dam* gene was amplified in 50 µl PCR reactions. Reactions contained components listed in the table below (Table 7.17).

Component	*Quantity (µl)*
DMSO	5
Pfu DNA polymerase reaction buffer # (10 x)	5
dNTPs (2 mM each)	1
Primers (PhoCfo and PhoCre 100 µM)	0.5 each
P. horikoshii genomic DNA (10 – 0.1 ng μl^{-1})	1
Sterile water	32
Pfu DNA polymerase mix*	5

Table 7.17 *Pfu polymerase mix contained Pfu turbo polymerase (4 µl), Pfu DNA polymerase reaction buffer (2 µl), water (14 µl) and was added to the reactions at 80 °C.# For colony PCR MangoTaq polymerase and buffer were used and the template DNA was substituted with whole cells picked into the mixture. The temperature programme was preceded with 10 minutes at 95°C and the step at 80 °C was removed.

Reactions were cycled through the temperature programme outlined below (Table 7.18).

Temperature programme		
1 x	30 x	1 x
95 °C, 60 seconds	95 °C, 60 seconds	72 °C 10 minutes
80 °C, 180 seconds	49 °C, 60 seconds	Hold 4 °C
	72 °C, 150 seconds	

Table 7.18

Samples of 5 µl taken from the PCR reactions were analysed by 1 % agarose gel electrophoresis with ethidium bromide staining and the successful reactions purified using a QIAquick® PCR clean up kit according to the manufacturer's instructions.

7.5.1.2 Digestion of the *P. horikoshii dam* gene

Digests were prepared in 1.5 ml microcentrifuge tubes and contained components listed in the table below (Table 7.19).

Component	*Quantity (µl)*
PCR product as purified or pBad *	25
Sterile water	12
NEB buffer 3 (10 x)	5
BSA (1mg ml^{-1})	5
NcoI (10 U μl^{-1})	1.5
XhoI (20 U μl^{-1})	1.5

Table 7.19 *pBad was sourced from a 10 ml overnight culture of *E. coli* TOP10 and purified using Promega Wizard® SV Minipreps.

Digests were incubated for 2 hours at 37 °C. Products were run on a 1 % agarose gel and purified using a QIAquick gel extraction kit according to the manufacturer's instructions.

7.5.1.3 Ligation of the *P. horikoshii dam* gene into a pBad vector

Ligation reactions containing three different vector to insert ratios were prepared in 200 µl PCR tubes. The reactions contained components listed in the table below (Table 7.20).

Component	*Quantity (µl)*		
Digested *dam* gene (as purified)	6	3	0
Digested vector (pBad derived, as purified)	2	2	2
Sterile water	0	3	6
T4 DNA ligase buffer (10 x)	1	1	1
T4 DNA ligase	1	1	1

Table 7.20

The components were gently mixed with pipetting and incubated at 4 °C overnight.

7.5.1.4. Transformation of *E. coli* strain TOP10 with the C-His$_6$-M.PhoDam expression plasmid

Ligation reactions were added to a 50 µl aliquot of TOP10 competent cells previously thawed on ice for 15 minutes. Cells were kept on ice for a further 30 minutes and heat shocked in a water bath at 42 °C for 45 seconds. Cells were returned to the ice for 2 minutes and 250 µl of SOC media added. Following incubation with orbital shaking at 37 °C for one hour, 150 µl of culture was plated out onto 2YT agar supplemented with 100 µg ml^{-1} ampicillin. Plates yielded colonies following incubation at 37 °C overnight. The plasmid formed was designated pMMS511811.

7.5.1.5 Analytical digests of pMMS511811 harvested from *E. coli* strain TOP10

Plasmid was harvested from 10 ml overnight cultures of *E. coli* TOP10 supplemented with 100 µg ml^{-1} ampicillin using minipreps. Double and single digests with NcoI, NcoI / XhoI, BamHI / PciI, BamHI / Nhe and NsiI were prepared and incubated for 1 hour at 37 °C. Digests contained the components listed in the table below (Table 7.21).

Component	*Quantity (µl)*	
	Single digest	Double digest
Plasmid DNA	5	5
Sterile Water	2.5	2
NEB buffer 3 (10 x)	1	1
BSA (1mg ml^{-1})	1	1
Restriction enzyme 1*	0.5	0.5
Restriction enzyme 2*	0	0.5

Table 7.21 * Restriction enzymes were used at the standard concentrations supplied by New England Biolabs. None of the enzyme stocks were of the high concentration (HC) enzyme.

Digests were analysed using 1 % agarose gel electrophoresis with ethidium bromide staining.

7.5.1.6 Transformation of *E.coli* BL21 pLysS Rosetta 2 with plasmid pMMS511811

E. coli BL21 pLysS Rosetta 2 competent cells were transformed with pMMS511811 plasmid as described in section 7.5.1.4. In addition to ampicillin the 2YT agar plates used were supplemented with 30 µg ml^{-1} chloramphenicol.

7.5.1.7 Large scale expression of C-His_6-M.PhoDam

An overnight culture of BL21 pLysS Rosetta 2 harbouring plasmid pMMS511811 was grown in 2YT media supplemented with 100 µg ml^{-1} ampicillin and 10 µg ml^{-1} chloramphenicol. This overnight growth was used as a 1 % inoculum for 4 L of 2YT media supplemented with the same antibiotics. The culture was maintained at 37 °C with orbital shaking to an absorbance of 0.6 at 600 nm. Expression was induced by the addition of arabinose. The culture was maintained for a further 2 hours at 27 °C and 12 g of cell paste was harvested by centrifugation (Sorval Evolution, SLC-6000 rotor, 6800 rpm, 4 °C). Cell paste was stored at -80 °C until required.

7.5.1.8 Small scale expression of C-His$_6$-M.PhoDam in GM124, GM161 and JW3351-1

Each strain was cultured in 1 L of 2YT media in a similar manner to the large scale BL21 growth (section 7.5.1.7), with some exceptions. Chloramphenicol was not used to supplement growth media and post-induction cultures were maintained at 37 °C for $3^1/_2$ hours before harvest. GM124, GM161 and JW3351-1 yielded 6.7, 7 and 2.8 g of cell paste respectively.

7.5.1.9 Nickel affinity purification of C-His$_6$-M.PhoDam

Buffers were prepared according to the table below (Table 7.22).

Buffer composition for the purification of C-His$_6$-M.PhoDam	
Low imidazole buffer (pH 7.5)	Tris.HCl (50 mM)
	Sodium chloride (300 mM)
	Imidazole (50 mM)
	Glycerol (10 %)
	Triton X-100 (0.05 % v/v)
	2-Mercaptoethanol (5 mM)
High imidazole buffer (pH 7.5)	Tris.HCl (50 mM)
	Sodium chloride (300 mM)
	Imidazole (500 mM)
	Glycerol (10 %)
	Triton X-100 (0.05 % v/v)
	2-Mercaptoethanol (5 mM)
Dam storage buffer (pH 7.5)	Tris.HCl (50 mM)
	Sodium chloride (200 mM)
	EDTA (0.2 mM)
	Glycerol (20 %)
	DTT (1 mM)

Table 7.22

Depending on the cell strain, between 2.8 and 7 g of cell paste was resuspended in 30 ml of ice cold low imidazole buffer, supplemented with 1 mM PMSF and a roche protease inhibitor tablet. Lysozyme, 10 mg, was added and the mixture stirred over ice for 15 minutes. The PMSF was replenished and the solution sonicated for ten 25 s periods whilst over ice. The resultant lysate was centrifuged for 25 minutes at 4 °C to precipitate cell debris (Sorvall Evolution centrifuge, SLA-1500 rotor, 14,000 rpm). The supernatant was applied to a nickel column with a bed volume of 10 ml at a flow rate of 4 ml min^{-1}. The column was washed with 150 ml of low imidazole buffer after which C-His_6-M.PhoDam was eluted with a 30 ml gradient from 0 - 100 % high imidazole buffer. Fractions containing protein were identified by Bradford assay, analysed by 15 % SDS-PAGE, pooled, dialysed into Dam storage buffer and frozen at -80 ^{o}C.

7.5.1.10 Electroblotting of protein onto a PVDF membrane

Electroblotting was carried out in a Bio-Rad Mini Trans-Blot® Electrophoretic Transfer Cell. Samples, each containing 200 pmoles of the protein of interest, were applied to a standard 15 % SDS-polyacrylamide gel. A PVDF membrane and two filter papers were cut to the size of the gel. The PVDF membrane was soaked in methanol for 10 minutes after which it was, along with the gel, filter papers and fibre pads equilibrated for 15 minutes in transfer buffer (25 mM tris pH 8.3, 192 mM glycine, 10 % MeOH, 0.025 % SDS). The equilibrated components were sandwiched inside a plastic cassette according to the manufacturer's instructions. The cassette was inserted into the electrophoretic tank along with ice cold transfer buffer and a magnetic stirrer bar. Transfer of the protein sample onto the membrane was carried out at 30 V and 4 °C with stirring overnight. Protein bands on the membrane were visualised with coomassie staining. The membrane was air dried and stored between two filter papers.

7.5.1.11 Site directed mutagenesis of the *P. horikoshii dam* gene

Mutagenic PCR reactions were prepared in 200 µl PCR tubes. Reactions contained the components listed in the table below (Table 7.23).

Component	*Quantity (µl)*
Pfu DNA polymerase reaction buffer (10 x)	5
dNTPs (2 mM each)	2
Primers (PhofM98A and PhorM98A 10 µM)	1 each
Plasmid pCLW469397* (10 ng μl^{-1})	1
Sterile water	39
Pfu Turbo DNA polymerase#	1

Table 7.23 * Isolated from *E. coli* TOP10 and so full methylated at GATC sites and susceptible to DpnI.# Added at 80 °C.

Reactions were cycled through the temperature programme outlined in the table below (Table 7.24).

Temperature programme		
1 x	16 x	1 x
95 °C, 60 seconds	95 °C, 30 seconds	4 °C, 180 seconds
80 °C, 180 seconds	55 °C, 60 seconds	
	68 °C, 300 seconds	

Table 7.24

Samples of 5 µl taken from the PCR reactions were analysed by 1 % agarose gel electrophoresis with ethidium bromide staining. PCR reactions were then incubated at 37 °C for 1 hour following the addition of 10 U of DpnI. Samples of 5 µl taken from the DpnI incubations were analysed by 1 % agarose gel electrophoresis. A 1 µl aliquot from the DpnI incubations was used to transform competent *E. coli* TOP10 and so produce the plasmid designated pMMS528431.

7.5.1.12 Analytical digests of plasmid pMMS528431

Analytical digests were carried out on pMMS528431 isolated from *E. coli* TOP10 as described for pMMS511811. NcoI was used to linearise the plasmid and a double NcoI / XhoI digest was used to excise the *P. horikoshii dam* gene. Digests and the uncut plasmid were analysed by 1 % agarose gel electrophoresis.

7.5.1.13 Transformation of *E. coli* BL21 pLysS Rosetta 2 with plasmid pMMS528431

E. coli BL21 pLysS Rosetta 2 competent cells were transformed with pMMS528431 plasmid as described in section 7.5.1.4. In addition to ampicillin, the 2YT agar plates used were supplemented with 30 μg ml^{-1} chloramphenicol.

7.5.1.14 Large scale expression of N-His_6-M.PhoDam mutant M98A

An overnight culture of BL21 pLysS Rosetta 2 supplemented with 10 μg ml^{-1} chloramphenicol and 100 μg ml^{-1} ampicillin was used as a 1 % inoculum for 5 L of 2YT media supplemented with 100 μg ml^{-1} ampicillin. The culture was maintained at 37 °C with orbital shaking until an absorbance of 0.6 at 600 nm was reached. Expression was induced by the addition of arabinose. The culture was maintained overnight at 16 °C with orbital shaking and yielded 66 g of cell paste upon centrifugation for 25 minutes at 4 °C (Sorval Evolution, SLC-6000 rotor, 6800 rpm). Cell paste was stored at -80 °C until required.

7.5.1.15 Nickel affinity purification of N-His_6-M.PhoDam

Purification by nickel affinity chromatography was carried out as described for the C-terminally His_6-tagged protein (section 7.5.1.9). Typically 10 g of cell paste yielded 3.5 mg of N-His_6-M.PhoDam.

7.5.2 Fluorescence Equilibrium Perturbation assay development

7.5.2.1 Gel based assays for Dam activity

ODN 4 / M ODN 7 at a concentration of 1 μM was incubated with 100 nM mutant M98A N-His_6-M.PhoDam and 20 μM AdoMet in buffer D at 33 °C. At regular timepoints 100 μl aliquots of assay mixture were taken and heated at 90 °C for 15 minutes to terminate methylation. Terminated assays were diluted 1:1 with DpnI solution (20 mM potassium phosphate pH 7.8, 0.1 mg ml^{-1} BSA, 1 mM magnesium

chloride, 200 nM DpnI) and incubated for 40 minutes at 30 °C. Samples of these digests were taken, mixed 2:1 with formamide, heated at 90 °C for 5 minutes and kept on ice. The DNA content of the samples was analysed with denaturing short oligonucleotide gel electrophoresis. This analysis was performed on 20 % polyacrylamide gels, made as described in general experimental method 9, run at a constant 20 W for 3 – 4 hours. Fluorescently labelled DNA in the gels was visualised under UV light. Relative intensities of the DNA bands were quantified using GeneTools software from Syngene.

7.5.2.2 Measurement of thermal melting profiles

Thermal melting curves for hemi and enzymatically fully methylated ODN 4 / M ODN 7 were measured in a Lightcycler. Duplicate melting curves were recorded at 4.4, 6.6, 9.9, 14.8, 22.2, 33.3 and 50.0 nM ODN 4 / M ODN 7 in 10 µl of buffer D. The excitation wavelength was 488 nm and fluorescence changes were recorded as a function of temperature at an emission wavelength of 520 nm. Melting profiles were fitted to the 4 parameter sigmoid $F = F_0 + a / (1 + e^{- (T - T_0) / b})$ using Sigmaplot 11 to obtain values for the melting temperatures. In the equation F_0 is fluorescence of the solution at temperature far below the melting temperature, F is the measured fluorescence, a is the maximum increase in fluorescence due to melting, T is the temperature, T_0 is the melting temperature and b is a constant.

7.5.2.3 Oligonucleotide temperature jump kinetics

Kinetics of oligonucleotide melting were studied by measuring the rate of change in ODN 4 / 7 fluorescence following a rapid increase in temperature in a Lightcycler. Duplicated solutions of 4.4, 6.6, 9.9, 14.8, 22.2, 33.3 and 50.0 nM ODN 4 / 7 in 10 µl of buffer D were exposed to a rapid temperature increase from 32 to 34 °C (20 °C s^{-1}). Fluorescence timecourses were recorded for 5 minutes thereafter with excitation and emission wavelengths of 488 nm and 520 nm respectively. Time dependant changes in fluorescence were fitted to the equation $F_t = F_f \times (1 - e^{-bt}) + F_0$ using Sigmaplot 11. In the equation F_0 is initial fluorescence, F_f is the maximum increase in fluorescence and F_t is the fluorescence at time t. The relaxation rate constant b obtained from these fits is related to the rates of association (k_1) and dissociation (k_{-1}) of the two single strands by the equation $b = k_1$ [ODN 4 + M ODN 7] + k_{-1} (5). Relaxation rates were plotted against

the total ssDNA concentrations which were calculated from the melting curves assuming an all or nothing model of DNA hybridisation. Straight lines were fitted to these plots using Sigmaplot 11 to yield the association and dissociation rate constants given by the gradients and y-axis intercepts respectively.

7.5.2.4 Proof of FEP assay principle

Dependence of the rate of fluorescence increase on M98A N-His_6-M.PhoDam concentration was measured at 33 °C in triplicate assays containing 50 nM ODN 4 / M ODN 7, 20 mM AdoMet and 0, 1.25, 2.5 and 5 nM Dam. Assays were set up as described in general experimental method 13.

7.5.2.5 The effect of Dam concentration on the inherent fluorescence of ODN 4 / M ODN 7

The influence of M98A N-His_6-M.PhoDam concentration, in the absence of turnover, on the equilibrium between single and double stranded ODN 4 / M ODN 7 was investigated in a series of 100 µl duplicate solutions. Solutions contained 5 nM ODN 4 / M ODN 7 and 0, 5, 10, 20, 40, 60, 80 and 100 nM Dam in buffer D (general method 13). They were equilibrated to 33 °C and the fluorescence measured as for the normal FEP assays.

7.5.2.6 Kinetic analysis of M98A N-His_6-M.PhoDam

The dependence of M98A N-His_6-M.PhoDam activity on AdoMet concentration was measured in a series of duplicate assays at 33 °C containing 50 nM ODN 4 / M ODN 7, 2.5 nM Dam and 0, 0.05, 0.1, 0.2, 0.4, 0.8, 1.6, 3.2 and 6.4 µM AdoMet. The dependence of Dam activity on DNA concentration was measured in a series of duplicate assays at 32 °C containing 20 µM AdoMet and 0, 0.9, 1.3, 2.0, 3.0, 4.4, 6.7, 10, 15 nM ODN 4 / M ODN 7. The Dam concentration was equal to 10 % of the DNA concentration.

Fluorescence changes were calibrated based on the endpoint fluorescence increases in assays, which were assumed to be due to complete methylation. A two parameter exponential rise to a maximum, Δ Fluorescence = $a(1 - e^{-b[\text{ODN 4 / M ODN 7}]})$, fitted to a plot of ODN 4 / M ODN 7 concentration against endpoint fluorescence increase was used to convert fluorescence increases into methylation rates.

7.6 References

1. Sambrook, J., Russell, D. W., Irwin, N., and Jansen, K. A. (2001) *Molecular Cloning A Laboratory Manual*, Third Ed., Cold Spring Harbor Laboratory Press, New York
2. Bradford, M. M. (1976) *Anal Biochem* **72**, 248-254
3. Schagger, H. (2006) *Nat Protoc* **1**, 16-22
4. Makarenkov, V., Kevorkov, D., Zentilli, P., Gagarin, A., Malo, N., and Nadon, R. (2006) *Bioinformatics* **22**, 1408-1409
5. Cantor, C. R., and Schimmel, P. R. (1980) *Biophysical Chemistry. Part III: The behavior of biological macromolecules*, Freeman, San Francisco

Appendix A: Plasmid maps

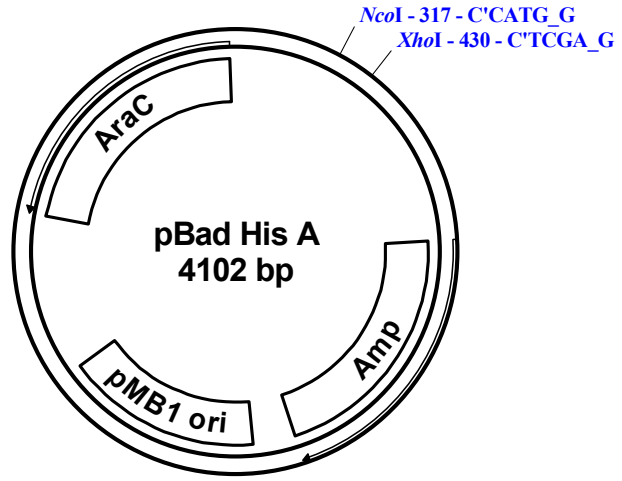

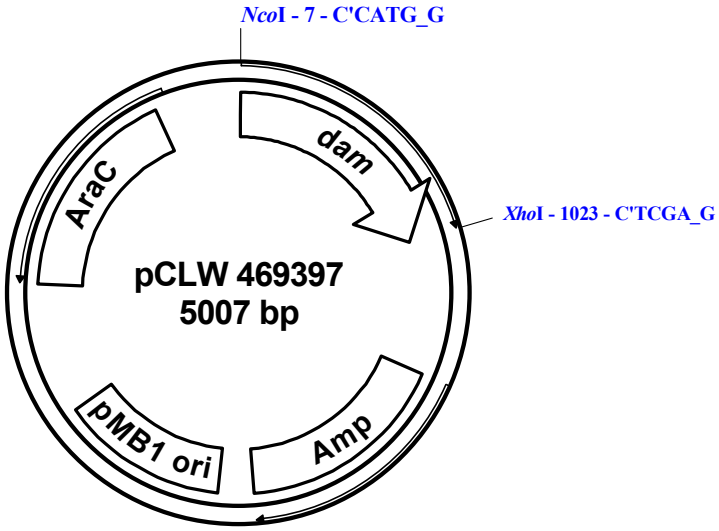

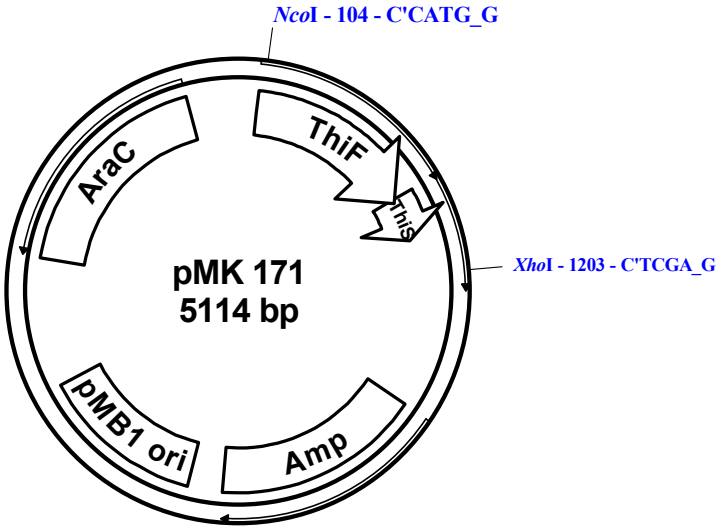

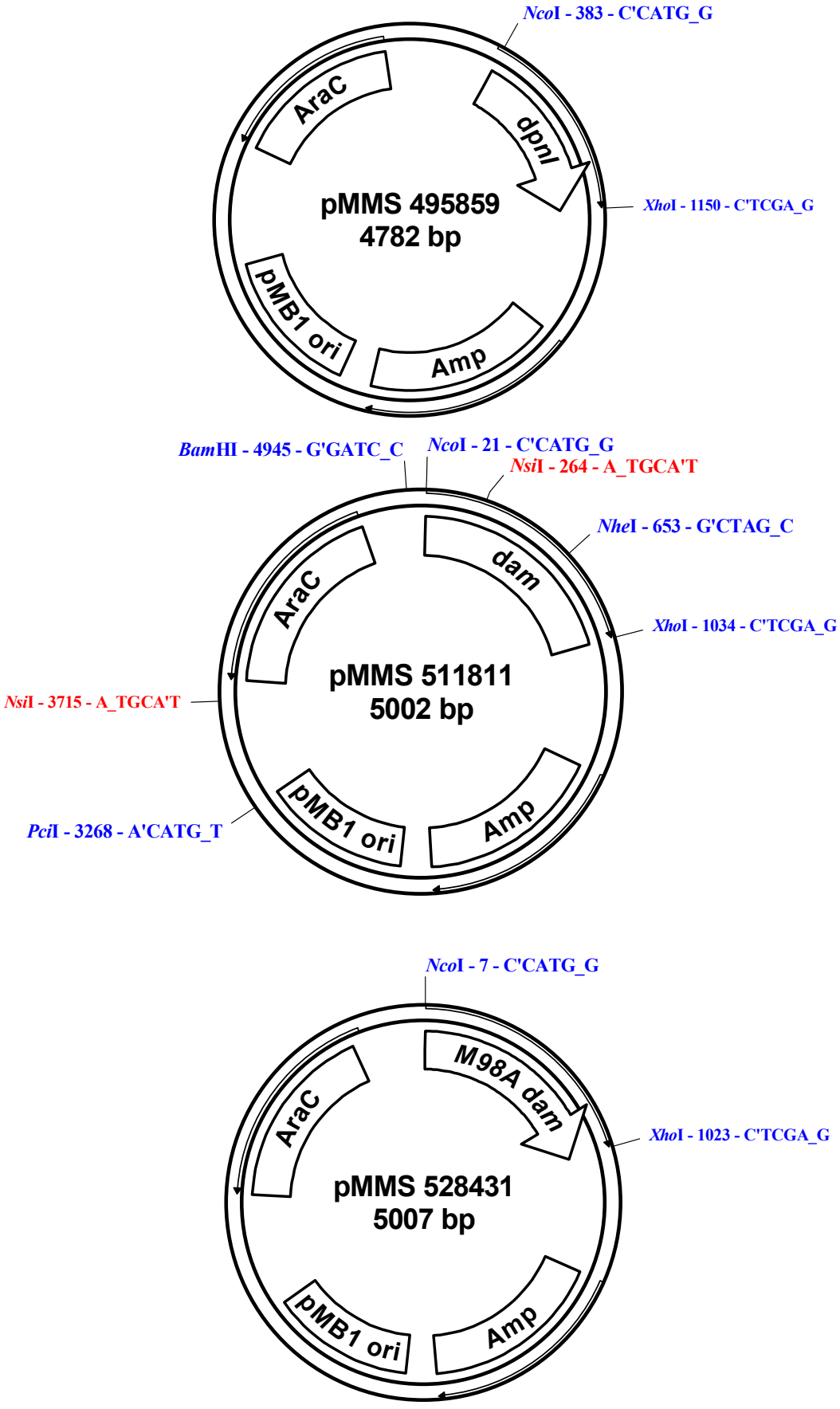
NcoI - 383 - C'CATG_G
AraC
dpnI
pMMS 495859
4782 bp
XhoI - 1150 - C'TCGA_G
pMB1 ori
Amp
BamHI - 4945 - G'GATC_C
NcoI - 21 - C'CATG_G
NsiI - 264 - A_TGCA'T
NheI - 653 - G'CTAG_C
dam
AraC
XhoI - 1034 - C'TCGA_G
pMMS 511811
5002 bp
NsiI - 3715 - A_TGCA'T
pMB1 ori
Amp
PciI - 3268 - A'CATG_T
NcoI - 7 - C'CATG_G
M98A dam
AraC
XhoI - 1023 - C'TCGA_G
pMMS 528431
5007 bp
pMB1 ori
Amp

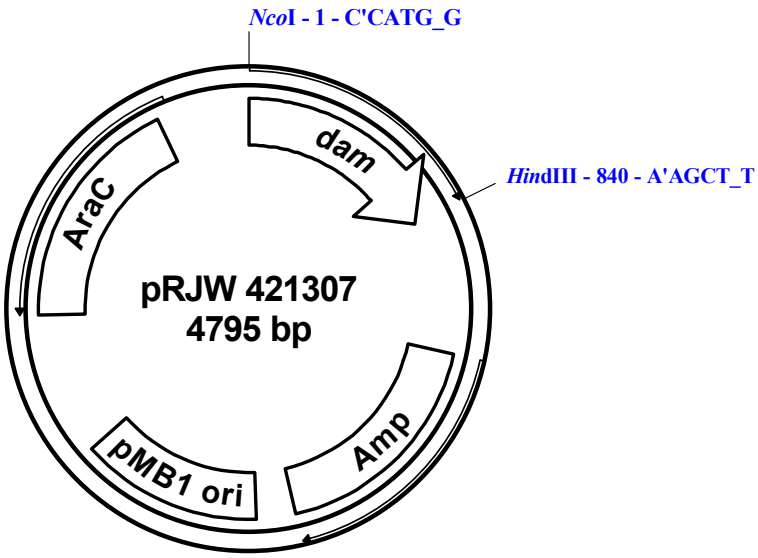
NcoI - 1 - C'CATG_G
HindIII - 840 - A'AGCT_T
dam
AraC
pRJW 421307
4795 bp
pMB1 ori
Amp

Appendix B: Primer sequences

DpnIf: 5’ CCCCCCATGGAATTACACTTTAATTTAGAATTAGTA 3’

DpnIr: 5’ CCCCCTCGAGTCATAATTTCCGATACTTTCC 3’

PhoCfo: 5’ GATCGACCATGGCAGAACCCGTTTTA 3’

PhoCre:
5’ GACTCCTCGAGTTAATGATGATGATGATGATGATTAATCCACTCAAGTAT
TGATCTC 3’

PhofM98A :
5’ GGGAGTACTACTATAGAGCGCGAAGAGAATACAATAAACTTGCCC 3’

PhorM98A:
5’ GGGCAAGTTTATTGTATTCTCTTCGCGCTCTATAGTAGTACTCCC 3’

pBad Forward: 5’ ATGCCATAGCATTTTTATCC 3’

pBad Reverse: 5’ CTGATTTAATCTGTATCAGGCTG 3’

Appendix C: Dam activity assay oligonucleotide sequences

Oligonucleotide name and structure abbreviations:

FAM – Fluorescein

D – Dabcyl

HEG – Hexaethyleneglycol

m6A – N6-methyladenine

UL – Unlabelled

M – Methylated

FM – Fully methylated

Sequences:

ODN 1: 5’ (FAM)CAGTTCGCGATCATGTTC(TD)C(HEG)
GAGAACATGATCGCGAACTG 3’

ODN 2: 5’ (FAM)CCGGATCCAGTTTTCTGGATCCGG(D) 3’

UL ODN 2: 5’ CCGGATCCAGTTTTCTGGATCCGG 3’

ODN 3: 5’ (FAM)CCGG(m6A)TCCAGTTTTCTGGATCCGG(D) 3’

FM ODN 3: 5’ (FAM)CCGG(m6A)TCCAGTTTTCTGG(m6A)TCCGG(D) 3’

ODN 4: 5’ ATTTAGATCACAA(FAM) 3’

ODN 5: 5’ (D)TTGTGAUCTAAAT 3’

M ODN 7: 5’ (D)TTGTG(m6A)TCTAAAT 3’

Appendix D: Adjustments made to high throughput screening data

Plate	*Well*	*Observations*	*Result replaced with plate average*
6130	E04	High rate	No
6130 R	E04	High rate	No
6131	H02	High fluorescence, high rate, fewer data points available as above machine limit.	No
6131 R	-	-	No
6132	D04	Low rate	No
6132 R	D04	High rate	No
6133	C02	High rate	No
6133 R	C02	High rate	No
6134	-	-	No
6134 R	-	-	No
6135	B02, E02, G04, H04, H05.	B02, E02 fluorescence increased above machine maximum so fewer data points available. G04 inherently fluorescent, fewer data points available. H04 very fluorescent, no data. H05 high rate.	B02, E02, G04 no. H04 yes. H05 no.
6135 R	G04, H04, H05	G04, H04 as above. H05 high rate, fluorescence increased above machine maximum so fewer data points available	As above.
6136	F02, F07	F02 and F07 inherently fluorescent	F02 and F07 yes
6136 R	F02, F07	F02 and F07 inherently fluorescent	F02 and F07 yes
6137	H09	Significantly reduced rate	No
6137 R	H09	Significantly reduced rate	No
6138	-	-	No
6138 R	-	-	No
6139	E03, H03	E03 fluorescence increased above machine maximum so fewer data points available. H03 inherently fluorescent.	E03 no. H03 yes
6139 R	E03, H03	E03, H03 as above.	E03 and H03 as above
6140	E11	Fluorescence increased above machine maximum so fewer data points available	E11 no
6140R	E11	As for E11 6140	E11 no
6141	D11	Significantly reduced rate	No
6141R	D11	As for D11 6141	No
6142 including replicates	D06 / D11 E05 / E10 B02 / B07 D04 / D09	D06 and duplicate were fluorescent, fewer data points available. E05 and duplicate were fluorescent, fewer data points were available. B02 / B07, D04 / D09 showed significantly reduced rates.	No

Appendix E: Results of N-terminal amino acid sequencing of the wild type *P. horikoshii* Dam contaminant

Cambridge Peptides
Leading the way in quality custom synthesis

Protein sequence report

Cambridge Peptides Order: **CPO27574**

Customer sample code: **27kDa band**

Created on: **4th August 2008**

N terminus

Residue	
1	M
2	---
3	---
4	E
5	Y
6	N

Comments:

Notes on the presentation of the data:

? most probable assignment.

--- nothing detected at this position

xxx unknown component

Where several sequences are observed, an attempt is made to arrange them in descending order of abundance at each residue. However because of difficulties inherent in the sequencing process, this should be treated as a guide only.

Appendix F: Results of the sequencing of mutant N-His$_6$-M.PhoDam genes in expression plasmids from *E. coli* TOP10 colonies 1 and 3

Colony 1 plasmid: Reverse

Colony 1 plasmid: Forward

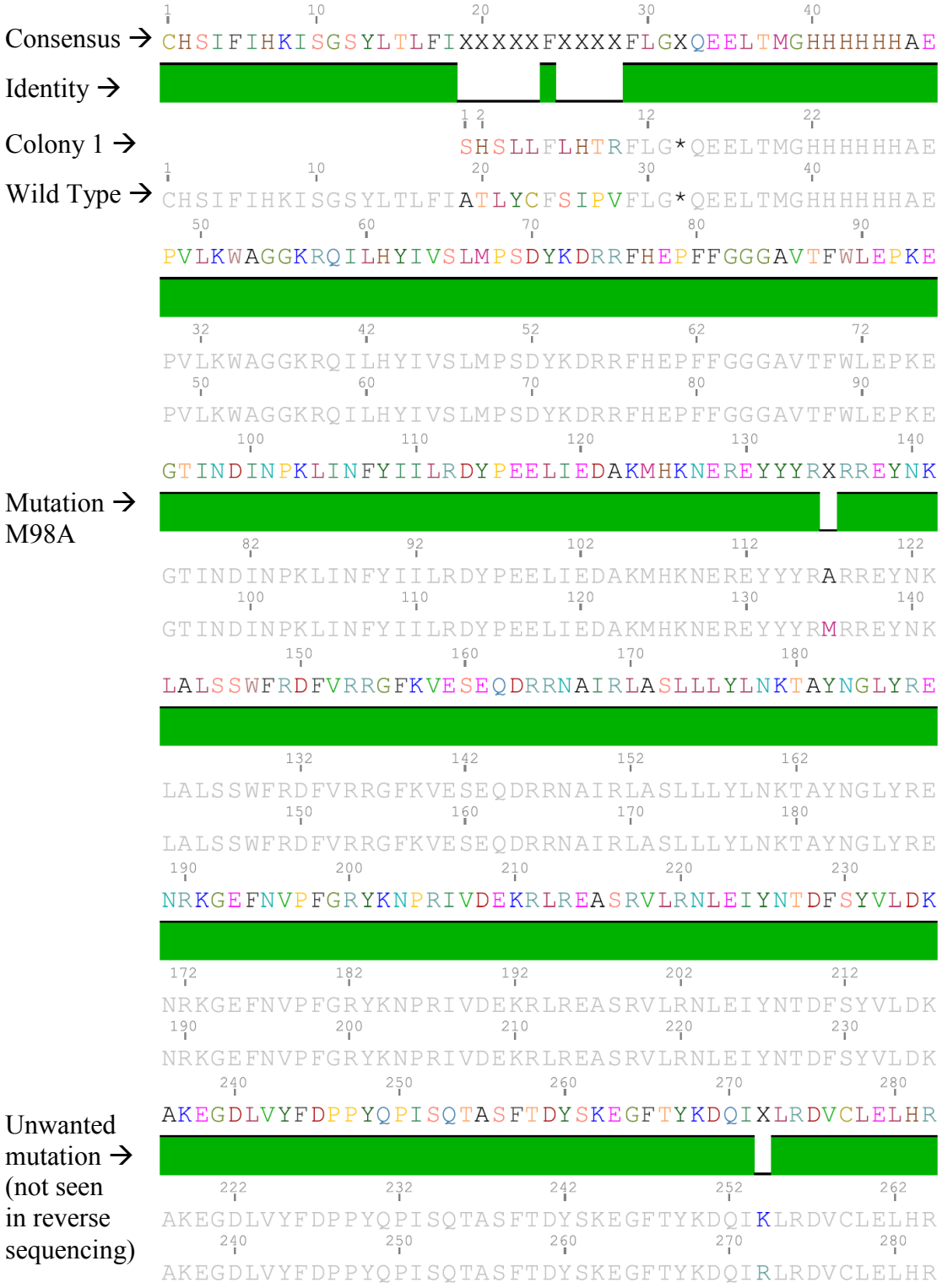

Colony 3 plasmid: Reverse

Colony 3 plasmid: Forward

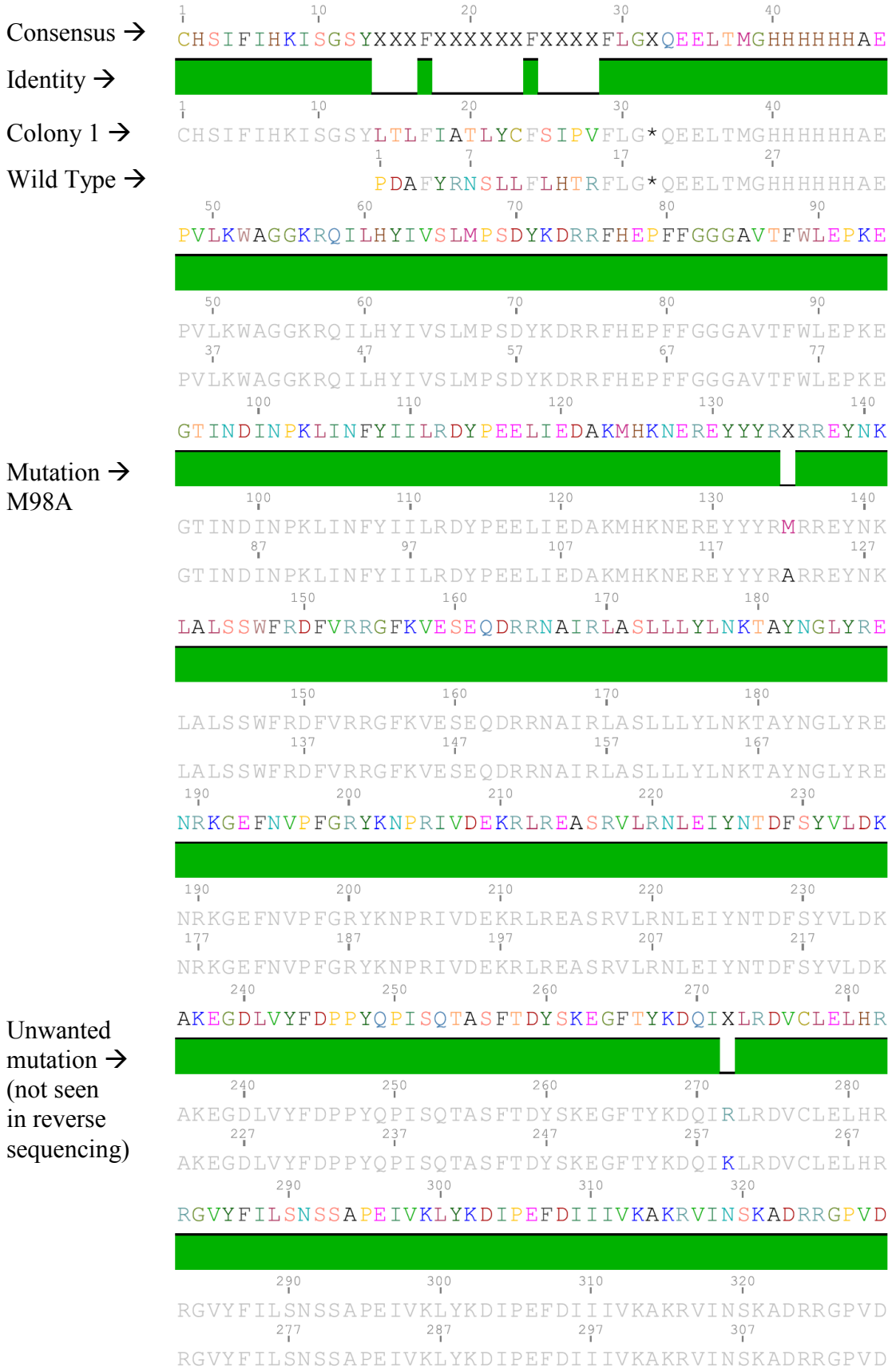

Appendix G: A sequence alignment of the *Y. pestis*, *E. coli* and *T4 phage* Dam MTases.

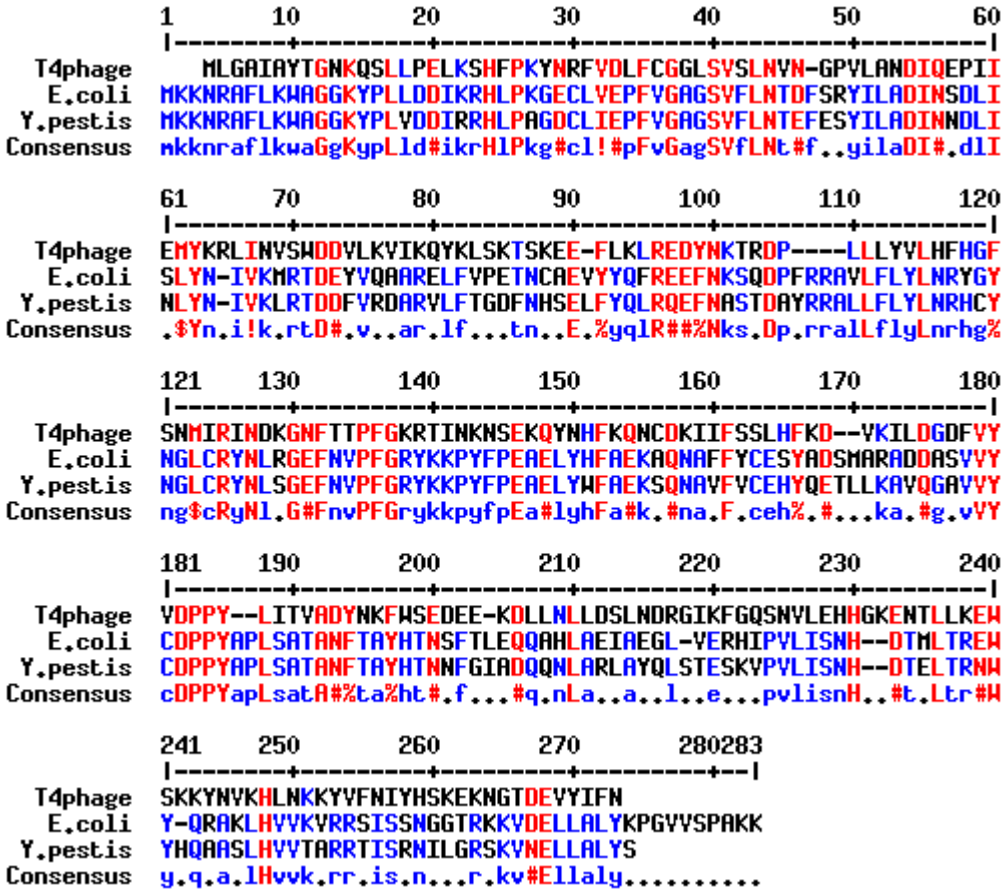

Sequences with high and low consensuses are shown in red and blue respectively. In the consensus sequence, symbols are used to show the conservation of particular sets of amino acids; # = D, E, N or Q, ! = I or V, $ = L or M and % = F or Y. All of the MTases shown recognise the sequence GATC. When aligned *E.coli* Dam (278 amino acids) shares 193 amino acids with *Y. pestis* Dam (271 amino acids) and 61 with T4 phage Dam (259 amino acids).

Appendix H: Commonly used commercial buffers

New England Biolabs buffer composition (1 x)	
Buffer 1 (pH 7.0)	10 mM Bis-tris-propane.HCl 10 mM Magnesium chloride 1 mM Dithiothreitol
Buffer 2 (pH 7.9)	50 mM Sodium chloride 10 mM Tris.HCl 10 mM Magnesium chloride 1 mM Dithiothreitol
Buffer 3 (pH 7.9)	100 mM Sodium chloride 50 mM Tris.HCl 10 mM Magnesium chloride 1 mM Dithiothreitol
Buffer 4 (pH 7.9)	50 mM Potassium acetate 20 mM Tris acetate 10 mM Magnesium acetate 1 mM Dithiothreitol